D C Meena

thesis-2

Journal Paper

Document Details

Submission ID
trn:oid:::27535:142293373

Submission Date
Jun 9, 2026, 3:52 PM GMT+5:30

Download Date
Jun 9, 2026, 4:25 PM GMT+5:30

File Name
thesis-2.pdf

File Size
42.5 MB

198 Pages

47,134 Words

234,412 Characters

7% Overall Similarity

The combined total of all matches, including overlapping sources, for each database.

Filtered from the Report

- Bibliography
- Small Matches (less than 10 words)

Exclusions

- 260 Excluded Matches

Match Groups

170 Not Cited or Quoted 5%
Matches with neither in-text citation nor quotation marks

40 Missing Quotations 2%
Matches that are still very similar to source material

1 Missing Citation 0%
Matches that have quotation marks, but no in-text citation

0 Cited and Quoted 0%
Matches with in-text citation present, but no quotation marks

Top Sources

2% Internet sources
5% Publications
4% Submitted works (Student Papers)

Integrity Flags

0 Integrity Flags for Review

Our system's algorithms look deeply at a document for any inconsistencies that would set it apart from a normal submission. If we notice something strange, we flag it for you to review.

A Flag is not necessarily an indicator of a problem. However, we'd recommend you focus your attention there for further review.

Match Groups

- **170** Not Cited or Quoted 5%
  Matches with neither in-text citation nor quotation marks
- **40** Missing Quotations 2%
  Matches that are still very similar to source material
- **1** Missing Citation 0%
  Matches that have quotation marks, but no in-text citation
- **0** Cited and Quoted 0%
  Matches with in-text citation present, but no quotation marks

Top Sources

2% Internet sources
5% Publications
4% Submitted works (Student Papers)

Top Sources

The sources with the highest number of matches within the submission. Overlapping sources will not be displayed.

1	Publication	
G.K. Jaiswal, U. Nangia, N.K. Jain. "A novel hybrid optimization approach for stoch...		2%
2	Student papers	
Universidad de Jaén on 2023-03-06		<1%
3	Internet	
www.researchgate.net		<1%
4	Student papers	
Uttar Pradesh Technical University on 2026-01-30		<1%
5	Internet	
umpir.ump.edu.my		<1%
6	Student papers	
National University of Singapore on 2012-05-24		<1%
7	Internet	
livrepository.liverpool.ac.uk		<1%
8	Student papers	
Universiti Putra Malaysia on 2017-08-05		<1%
9	Internet	
cyberleninka.org		<1%
10	Publication	
Preethi Vela Anandam, Shunmugalatha Alagarsamy, Babulal Chittu Kuppusamy. ...		<1%

11 Student papers
Asian Institute of Technology on 2015-06-07 <1%

12 Student papers
Jawaharlal Nehru Technological University on 2013-07-22 <1%

13 Publication
Agbugba, Emmanuel Emenike. "Hybridization of Particle Swarm Optimization wit... <1%

14 Internet
vdoc.pub <1%

15 Student papers
Dayalbag Educational Institute on 2014-10-27 <1%

16 Student papers
Victoria University on 2019-02-19 <1%

17 Student papers
Institute of Research & Postgraduate Studies, Universiti Kuala Lumpur on 2025-0... <1%

18 Internet
ir.library.nitw.ac.in:8080 <1%

19 Publication
"Swarm, Evolutionary, and Memetic Computing", Springer Nature, 2013 <1%

20 Student papers
Institute of Research & Postgraduate Studies, Universiti Kuala Lumpur on 2025-0... <1%

21 Student papers
Anna University on 2025-03-06 <1%

22 Student papers
Edith Cowan University on 2015-05-25 <1%

23 Publication
Hana Merah, Mohammed Jameel, Abdelmalek Gacem, Djilani Ben Attous, Moham... <1%

24 Publication
Quintas, José Miguel Rodrigues. "Evolutionary Multi-Objective Optimization for M... <1%

25 Publication
Ahmed M. Abd-El Wahab, Salah Kamel, Hamdy M. Sultan, Mohamed H. Hassan, Fr... <1%

26 Publication
Mohammed Hamouda Ali, Ahmed Mohammed Attiya Soliman, Mohamed Abdeen,... <1%

27 Publication
Susanta Dutta, Provas Kumar Roy, Debashis Nandi. "Optimal location of STATCO... <1%

28 Publication
Ahmed H.A. Adam, Salah Kamel, Mohamed H. Hassan. "An Enhanced Adaptive Cr... <1%

29 Publication
Souhil Mouassa, Tarek Bouktir. "Multi-objective ant lion optimization algorithm t... <1%

30 Student papers
National Institute of Technology, Hamirpur on 2020-06-09 <1%

31 Publication
Salah K. Elsayed, Salah Kamel, Ali Selim, Mahrous Ahmed. "An Improved Heap-ba... <1%

32 Student papers
National Institute of Technology Jamshedpur on 2023-07-17 <1%

33 Publication
Shehadeh, Hisham Ahmad Theeb. "Single-Objective and Multi-Objective Optimiza... <1%

34 Internet
thesis.univ-biskra.dz <1%

35 Publication
Hamdi Tolga Kahraman, Mustafa Akbel, Serhat Duman. "Optimization of Optimal ... <1%

36 Publication
Hamdy M. Sultan, Ahmed A. Zaki Diab, Ahmed S. Menesy, Mahmoud Kassas, Moh... <1%

37 Student papers
Jawaharlal Nehru Technological University on 2010-03-25 <1%

38 Publication
Lecture Notes in Computer Science, 2015. <1%

39 Student papers

National Institute of Technology, Hamirpur on 2017-09-13 <1%

40 Publication

Tanmay Das, Ranjit Roy, Kamal Krishna Mandal. "Solving the ORPD problem for a... <1%

41 Student papers

University of Louisiana, Lafayette on 2019-04-11 <1%

42 Internet

assets.researchsquare.com <1%

43 Publication

Abhishek Bajirao Katkar, Himmat Tukaram Jadhav. "A Novel Hybrid Metaheuristic... <1%

44 Student papers

Asia Pacific University College of Technology and Innovation (UCTI) on 2025-05-07 <1%

45 Publication

Joby Boxall, Čedo Maksimović. "Integrating Water Systems", CRC Press, 2009 <1%

46 Publication

Partha P. Biswas, P.N. Suganthan, R. Mallipeddi, Gehan A.J. Amaratunga. "Optima... <1%

47 Publication

Phenikaa University <1%

48 Internet

dr.ntu.edu.sg <1%

49 Student papers

National Institute of Technology, Hamirpur on 2017-07-18 <1%

50 Publication

Abhishek Bajirao Katkar, Himmat Tukaram Jadhav. "A Distributionally Robust Cha... <1%

51 Student papers

Sardar Vallabhbhai National Inst. of Tech.Surat on 2022-03-14 <1%

52 Publication

Kasem Nuaekaew, Pramin Artrit, Nantiwat Pholdee, Sujin Bureerat. "Optimal rea... <1%

53 Publication
Tanmay Das, Ranjit Roy, Kamal Krishna Mandal. "Modelling and optimization of a ... <1%

54 Publication
Tanmay Das, Ranjit Roy, Kamal Krishna Mandal. "Solving Hybrid High Voltage AC-... <1%

55 Student papers
Universidad de Jaén on 2024-06-06 <1%

56 Student papers
Universidad de Jaén on 2024-08-30 <1%

57 Internet
dspace.univ-eloued.dz <1%

58 Student papers
Amrita Vishwa Vidyapeetham on 2020-11-24 <1%

59 Publication
Joshi, Aditya Santosh. "Collaborative Hierarchical Agent Reorganization and Man... <1%

60 Publication
Amal Amin Mohamed, Salah Kamel, Mohamed H. Hassan. "Hybrid AEO–MFO for o... <1%

61 Publication
C. Guedes Soares, T.A. Santos. "Developments in Maritime Technology and Engin... <1%

62 Publication
Power Grid Complexity, 2011. <1%

63 Publication
Prisma Megantoro, Syahirah Abd Halim, Nor Azwan Mohamed Kamari, Lilik Jamil... <1%

64 Internet
journal.buitms.edu.pk <1%

65 Publication
G. K. Jaiswal, U. Nangia, N. K. Jain. "An Advanced Machine Learning Framework fo... <1%

66 Student papers
Indian Institute of Technology Patna on 2019-11-17 <1%

67 Student papers
Victoria University on 2017-06-07 <1%

68 Internet
dspace.univ-setif.dz:8888 <1%

69 Internet
icee-4.eb2a.com <1%

70 Publication
"Applications of Modern Heuristic Optimization Methods in Power and Energy Sys... <1%

71 Publication
Aamir Ali, Ghulam Abbas, Muhammad U. Keerio, Ezzeddine Touti, Zahoor Ahmed, ... <1%

72 Publication
Abhishek Bajirao Katkar, Himmat Tukaram Jadhav. "A dual-state epsilon driven h... <1%

73 Student papers
Brunel University on 2016-12-01 <1%

74 Student papers
Higher Education Commission Pakistan on 2024-07-24 <1%

75 Publication
Mahmoudian Esfahani, Mohammad. "Optimal and Secure Electricity Market Fram... <1%

76 Publication
Ton Duc Thang University <1%

77 Student papers
University of Louisiana, Lafayette on 2018-04-05 <1%

78 Student papers
University of Sydney on 2016-10-11 <1%

79 Publication
V K Mathew, Archana Chandak, Man Mohan, Bhumeshwar K. Patle. "Metaheuristi... <1%

80 Student papers
VIT University on 2015-02-17 <1%

81 Student papers

VIT University on 2019-10-04 <1%

82 Publication

Yasir Muhammad, Rahimdad Khan, Muhammad Asif Zahoor Raja, Farman Ullah, ... <1%

83 Publication

Zelan Li, Yijia Cao, Le Van Dai, Xiaoliang Yang, Thang Trung Nguyen. "Finding Sol... <1%

84 Internet

ir.mksu.ac.ke <1%

85 Publication

"[Front matter]", 2017 Smart Grid Conference (SGC), 2017 <1%

86 Publication

A. B. Katkar, H. T. Jadhav. "A hybrid gbestABC–NSGA-II metaheuristic framework ... <1%

87 Publication

Abdulsalam, Sheikh Mohmadishak. "Robust State Estimation for Power System B... <1%

88 Publication

Edgar E. Tibaduiza-Rincón, Walter M. Villa-Acevedo, Jesús M. López-Lezama. "Adva... <1%

89 Student papers

Jawaharlal Nehru Technological University on 2011-04-01 <1%

90 Publication

Mostafa NasouriGilvaei, Hossein Jafari, Mojtaba JabbariGhadi, Li Li. "A novel hybri... <1%

91 Publication

Rahman, Mir Toufikur. "Optimal Charging Coordination of Plug-In Electric Vehicle... <1%

92 Student papers

Rangsit University on 2021-09-20 <1%

93 Publication

S. A. Sisson, Y. Fan, M. A. Beaumont. "Handbook of Approximate Bayesian Compu... <1%

94 Student papers

Sardar Vallabhbhai National Inst. of Tech.Surat on 2015-07-20 <1%

95 Publication
Sinjlawi, Abdullah Saeed. "The Assessment of Using High Nitrogen Austenitic Stai... <1%

96 Publication
Sumika Chauhan. "Diversity-Driven Evolutionary Algorithms For Solving Engineer... <1%

97 Publication
Truong Hoang Bao Huy, Tri Phuoc Nguyen, Nursyarizal Mohd Nor, Irraivan Elamv... <1%

98 Student papers
University of Mauritius on 2015-03-31 <1%

99 Student papers
University of Technology, Sydney on 2017-07-14 <1%

100 Student papers
Victoria University on 2016-11-25 <1%

101 Student papers
Victoria University on 2017-12-07 <1%

102 Internet
ijeecs.iaescore.com <1%

103 Internet
jad.shahroodut.ac.ir <1%

104 Internet
ruja.ujaen.es <1%

105 Internet
www.engineeringletters.com <1%

106 Internet
www.iaeng.org <1%

107 Internet
www.jemat.org <1%

MULTI-OBJECTIVE OPTIMAL REACTIVE POWER DISPATCH FOR HYBRID ENERGY SYSTEMS

18

A Thesis Submitted
In Partial Fulfillment of the Requirements
for the Degree of

DOCTOR OF PHILOSOPHY

by

GANESH KUMAR JAISWAL

(Roll No. 2K19/PHDEE/16)

Under the Supervision of

Prof. Uma Nangia and Prof. N. K. Jain



Department of Electrical Engineering

DELHI TECHNOLOGICAL UNIVERSITY

(Formerly Delhi College of Engineering)

Shahbad Daulatpur, Main Bawana Road, Delhi - 110042. INDIA

2026

©DELHI TECHNOLOGICAL UNIVERISITY, DELHI-2026
ALL RIGHTS RESERVED

Acknowledgements

I would like to begin by expressing my heartfelt gratitude to my advisors, **Professor Uma Nangia** and **Professor N. K. Jain**, Department of Electrical Engineering, Delhi Technological University, for their constant guidance, invaluable suggestions, and continuous encouragement throughout my Ph.D. journey. Their mentorship, support, and confidence in my abilities greatly motivated me during every stage of this research work. I feel truly fortunate and honored to have completed my doctoral studies under their supervision.

I would like to express my sincere gratitude to **Professor M. Rizwan** for providing excellent research facilities and a highly motivating and pleasant working environment in the UEE Laboratory, which greatly supported the successful completion of my research work. I also owe my heartfelt thanks to **Professor J. N. Rai** and **Professor Suman Bhowmick** for their valuable guidance, encouragement, and continuous support throughout my Ph.D. journey.

I would like to extend my sincere thanks to **Professor Rachana Garg**, Head of the Department of Electrical Engineering, Delhi Technological University, along with all the faculty members and staff, for fostering a supportive and encouraging research environment throughout my Ph.D. journey. Their guidance, cooperation, and assistance at various stages of my research are deeply appreciated. I am also grateful for the administrative support provided during this period, which greatly facilitated the smooth progress of my doctoral work.

I owe my deepest appreciation to my family for their endless love, patience, understanding, and unwavering belief in me. Their sacrifices, encouragement, and blessings have been the foundation of my strength and determination throughout this journey. Whatever I have accomplished today is a reflection of their support and faith in me.

I would also like to acknowledge my friends, both within and outside Delhi Technological University, for their companionship, motivation, and constant support. Their encouragement, discussions, and memorable moments made this long academic journey more enjoyable and meaningful.

I am also thankful to the Editors-in-Chief, Editors, and the reviewers of Elsevier, Springer, and IEEE for their constructive comments, which helped me gain deeper insights into the subject.

Above all, I express my sincere gratitude to the Almighty for granting me the strength, perseverance, and courage to face every challenge and successfully complete my doctoral research.

Date: Ganesh Kumar Jaiswal

Dedicated to my family for their boundless love, sacrifices, and unwavering support throughout my academic journey and life.

DELHI TECHNOLOGICAL UNIVERSITY

(Formerly Delhi College of Engineering)
Shahbad Daulatpur, Main Bawana Road, Delhi-42

CANDIDATE'S DECLARATION

I hereby certify that the work which is being presented in the thesis entitled MULTI-OBJECTIVE OPTIMAL REACTIVE POWER DISPATCH FOR HYBRID ENERGY SYSTEMS in partial fulfillment of the requirements for the award of the degree of Doctor of Philosophy and submitted to the Department of Electrical Engineering, Delhi Technological University, is an authentic record of my own work carried out during the period from August, 2019 to May, 2026 under the supervision of Dr. Uma Nangia, Professor, Department of Electrical Engineering and Dr. N. K. Jain, Professor, Department of Electrical Engineering.

The content of this thesis has not been submitted by me for the award of any other degree of this or any other Institute.

(Ganesh Kumar Jaiswal)

DELHI TECHNOLOGICAL UNIVERSITY

(Formerly Delhi College of Engineering)
Shahbad Daulatpur, Main Bawana Road, Delhi-42

CERTIFICATE BY THE SUPERVISORS

Certified that **Ganesh Kumar Jaiswal** (2K19/PHDEE/16) has carried out his work presented in this thesis entitled "**MULTI-OBJECTIVE OPTIMAL REACTIVE POWER DISPATCH FOR HYBRID ENERGY SYSTEMS**" for the award of **Doctor of Philosophy** from Department of Electrical Engineering, Delhi Technological University, Delhi, under our supervision. The thesis embodies results of original work, and studies are carried out by the student himself and the content of the thesis do not form the basis for the award of any other degree to the candidate or to anybody else from this or any other University/Institute.

(Prof. Uma Nangia)
Supervisor

(Prof. N. K. Jain)
Co-Supervisor

Date:

turnitin Page 19 of 208 - Integrity Submission Submission ID trn:oid:::27535:142293373

Abstract

Optimal Reactive Power Dispatch (ORPD) is an important aspect of modern power system operation that deals with the effective management and control of reactive power while satisfying nonlinear equality and inequality constraints. The increasing integration of renewable energy sources (RESs), coupled with the stochastic nature of load demand and generation, has significantly increased the complexity and uncertainty associated with ORPD, rendering conventional optimization approaches inadequate. Consequently, the development of robust, efficient, and scalable optimization frameworks has become imperative for addressing both deterministic and stochastic variants of the ORPD problem.

This thesis presents a systematic and comprehensive investigation into advanced optimization methodologies for solving deterministic, stochastic, and multi-objective ORPD problems. Initially, a novel hybrid optimization algorithm is proposed by integrating Opposition-Based Learning (OBL), Differential Evolution (DE), and the Giza Pyramids Construction (GPC) algorithm. The proposed hybridization strategically enhances the exploration–exploitation trade-off by incorporating population diversity mechanisms and adaptive search strategies. The effectiveness of the proposed method is rigorously validated using standard unimodal and multimodal benchmark functions, followed by its application to deterministic ORPD problems on IEEE 30-bus and IEEE 57-bus systems. The obtained results demonstrate significant improvements in system performance, including reduced real power losses, improved voltage profiles, and enhanced voltage stability, compared to existing state-of-the-art metaheuristic algorithms. Furthermore, the framework is extended to stochastic ORPD by incorporating probabilistic representations of uncertainties associated with load demand, wind speed, solar irradiance, and small-hydro inflows, thereby capturing the inherent variability and intermittency of renewable resources.

Subsequently, the proposed hybrid algorithm is extended within a multi-objective optimization paradigm through its integration with the Non-dominated Sorting Genetic Algorithm II (NSGA-II). This formulation facilitates the simultaneous optimization of multiple conflicting objectives, resulting in the

turnitin Page 19 of 208 - Integrity Submission Submission ID trn:oid:::27535:142293373

generation of a well-defined Pareto-optimal solution set. The performance of the proposed multi-objective framework is evaluated using established benchmark test suites, including ZDT and DTLZ, and is quantitatively assessed through widely recognized performance indicators such as Inverted Generational Distance (IGD), Hypervolume (HV), Generational Distance (GD), Maximum Spread (MS), and Spacing (S). The results indicate superior convergence characteristics and diversity preservation capabilities, outperforming several contemporary multi-objective optimization techniques. The developed framework is further employed to solve both deterministic and stochastic multi-objective ORPD problems.

In addition, a machine learning-assisted optimization framework, termed Improved Evolutionary Algorithm–Self Organized Maps (IEASOM), has been developed to further enhance the solution search process. The incorporation of Self-Organized Maps (SOM) enables adaptive learning and efficient mapping of the high-dimensional search space, thereby improving convergence behavior and solution robustness. The proposed IEASOM method is applied to deterministic and stochastic ORPD models using the IEEE 30-bus system. Its performance is further evaluated on large-scale power networks, including the IEEE 118-bus test system. The results confirm the scalability and computational efficiency of the proposed approach.

Overall, the proposed methodologies provide a unified and robust framework for solving complex ORPD problems under both deterministic and uncertain environments. This research work contributes to the advancement of power systems optimization techniques. The proposed approaches support efficient power system operation and improve voltage security. They also assist in the effective integration of RESs into modern power networks.

turnitin Page 21 of 208 - Integrity Submission Submission ID trn:oid:::27535:142293373

Contents

Acknowledgements iii
Abstract viii
Table of Contents xi
List of Tables xv
List of Figures xvii
List of Acronyms xxi
List of Symbols xxiii

1 Introduction 1
1.1 Background 1
1.2 Importance of Reactive Power in Power Systems 2
1.2.1 Voltage Regulation and Voltage Stability 3
1.2.2 Reduction of Transmission Losses 3
1.2.3 Enhancement of Power Transfer Capability 4
1.2.4 Support for Inductive Loads 4
1.2.5 Improvement of Power Factor 4
1.2.6 Prevention of Voltage Collapse 5
1.2.7 Overall Significance of Reactive Power 6
1.3 Motivation and Challenges 6
1.3.1 Need for Advanced Optimization Techniques 6
1.3.2 Integration of Renewable Energy Sources 6
1.3.3 Uncertainty in Load Demand 7
1.3.4 Increasing Power System Complexity 7
1.3.5 Deregulation and Market Complexity 7
1.3.6 Role of Multi-Objective Optimization 7
1.4 Problem Statement 8
1.5 Research Objectives 9
1.6 Structure of the Thesis 9

turnitin Page 21 of 208 - Integrity Submission Submission ID trn:oid:::27535:142293373

2 Literature Review **11**
2.1 Introduction 11
2.2 Conventional Optimization Methods for ORPD 11
2.3 Single-Objective Metaheuristic ORPD Methods 12
2.4 Hybrid Optimization Methods for ORPD 16
2.5 Multi-Objective ORPD Methods 18
2.6 Stochastic and Uncertainty-Based ORPD Methods 21
2.7 Research Gaps 25

3 Optimal Reactive Power Dispatch **27**
3.1 Introduction 27
3.2 Problem Formulation 28
3.2.1 Independent (control) variables 28
3.2.2 Dependent variables 28
3.3 Objective functions for deterministic ORPD 29
3.4 Constraints 30
3.4.1 Equality constraints: 31
3.4.2 Inequality constraints: 31
3.4.3 Constraints Handling 32
3.5 Multi-Objective ORPD 32
3.6 Standard Test Systems for ORPD Analysis 34
3.6.1 IEEE 30-bus System 34
3.6.2 IEEE 57-bus System 34
3.6.3 IEEE 118-bus System 35

4 Proposed Opposition-Based Hybrid Differential Evolution-Giza Pyramids Construction Optimization Algorithm **37**
4.1 Introduction 37
4.2 Opposition–Based Hybrid Differential Evolution – Giza Pyramids Construction Optimization Algorithm 38
4.3 Modeling the Load and RESs Uncertainties 43
4.3.1 Scenario Generation 43
4.3.2 Scenario Reduction 48
4.3.3 Objective function for stochastic ORPD 49

turnitin Page 23 of 208 - Integrity Submission Submission ID trn:oid:::27535:142293373

4.4 Results and Discussion 51
4.4.1 Benchmark Functions 51
4.4.2 Deterministic ORPD 55
4.4.2.1 IEEE 30-bus system 55
4.4.2.2 IEEE 57-bus system 61
4.4.3 Stochastic ORPD 68
4.5 Conclusion 72

5 Proposed Machine Learning Framework 75
5.1 Introduction 75
5.2 Improved Evolutionary Algorithm–Self Organized Maps Algorithm 76
5.2.1 Evolutionary Algorithm- Self Organized Maps (EASOM) 76
5.2.2 Improvement in EASOM algorithm 79
5.3 Mathematical Modeling of Solar PV System 82
5.3.1 Background 82
5.3.2 Expected average of objective function values for stochastic ORPD problem 84
5.4 Results and Discussion 85
5.4.1 SOM Parameter Setup and Grid Size Sensitivity Analysis 85
5.4.2 IEEE 30-bus system 86
5.4.3 Modified IEEE-30 bus system 93
5.4.4 IEEE 118-bus system 99
5.5 Conclusions 106

6 Proposed Hybrid Multi-Objective Optimization Algorithm 107
6.1 Introduction 107
6.2 Overview of the Hybrid Multi-Objective Optimization Algorithm 108
6.3 Uncertainty modeling and scenario generation 113
6.4 Objective function for stochastic ORPD 113
6.5 Results and Discussions 114
6.5.1 Benchmark Functions 114
6.5.2 Deterministic MOORPD 121
6.5.2.1 IEEE-30 Bus System 121
6.5.2.2 IEEE-57 Bus System 121

turnitin Page 23 of 208 - Integrity Submission Submission ID trn:oid:::27535:142293373

turnitin Page 24 of 208 - Integrity Submission Submission ID trn:oid:::27535:142293373

6.5.2.3 Modified IEEE-30 Bus System 121
6.5.3 Decision Making in MOORPD problem 122
6.5.4 IEEE 30-bus system 123
6.5.5 IEEE 57-bus system 128
6.5.6 Stochastic MOORPD 134
6.6 Conclusions 141

7 Conclusions, Future Scope and Societal Impact 143
7.1 Conclusions 143
7.2 Future Work 144
7.3 Societal Impact 145

List of Publications 149

References 151

A Supplementary Data 167

turnitin Page 24 of 208 - Integrity Submission Submission ID trn:oid:::27535:142293373

turnitin Page 25 of 208 - Integrity Submission Submission ID trn:oid:::27535:142293373

List of Tables

2.1 Summary of algorithms for renewable technologies and variable load demand. 23

4.1 Chosen scenarios with appropriate scenario aspects. 49
4.2 Parameter settings of different methods. 50
4.3 Comparison of optimization algorithms on unimodal and multi-modal benchmark functions. 53
4.4 Results of single-objective ORPD problem for the IEEE 30-bus system. 56
4.5 Comparison of results over 20 independent runs with different algorithms for the IEEE 30-bus system. 60
4.6 Results of single-objective ORPD problem for the IEEE 57-bus system. 62
4.7 Comparison of results over 20 independent runs with different algorithms for the IEEE-57 bus system. 67
4.8 Results for stochastic ORPD problem of the modified IEEE 30-bus. 69

5.1 Various constants for estimation of solar PV power. 83
5.2 Sensitivity analysis of SOM dimension on objective functions. 86
5.3 Single-objective ORPD results for IEEE 30-bus system. 87
5.4 Comparison of results for 20 Independent runs with different algorithms of the IEEE-30 bus system. 92
5.5 Single objective ORPD results for the modified IEEE 30-Bus System. 94
5.6 Single objective ORPD results for the IEEE 118-bus system. 100

6.1 Parameter settings of the multi-objective algorithms used for comparison. 116
6.2 Statistical performance comparison of different algorithms over ten independent runs on benchmark test functions. 117
6.3 Comparison of BCS for various cases of the IEEE 30-bus system. 126

22

turnitin Page 25 of 208 - Integrity Submission Submission ID trn:oid:::27535:142293373

6.4 Results of the BCS for the IEEE 30-bus system using the proposed method. 127
6.5 Comparison of BCS for various cases of the IEEE 57-bus system. 132
6.6 Results of the BCS for the IEEE 57-bus system using the proposed method. 133
6.7 Representative reduced scenarios and corresponding system parameters used for stochastic ORPD analysis. 136
6.8 Results of the BCS for the modified IEEE 30-bus system using the proposed method. 138

A.1 Benchmark functions considered for performance evaluation. 167
A.2 IEEE 30 bus system generator data for various cases (Including solar, wind & hybrid). 168
A.3 IEEE 57 bus system generator data for various cases. 169
A.4 IEEE 30 bus system generator data for various cases (Including solar). 169
A.5 IEEE 118 bus system generator data. 169
A.6 Mathematical formulation of multi-objective benchmark test functions. 171

turnitin Page 27 of 208 - Integrity Submission Submission ID trn:oid:::27535:142293373

List of Figures

4.1 Flowchart of the proposed hybrid method. 42
4.2 Wind speed scenarios created using Weibull PDF (bus 5). 43
4.3 Solar irradiance scenarios created using Lognormal PDF (bus 8). 44
4.4 Solar irradiance scenarios created using Lognormal PDF (bus 13). 45
4.5 Water flow rate scenarios created using Gumbel PDF (bus 13). 46
4.6 Load demand scenarios created using Normal PDF. 47
4.7 Comparative convergence profiles of algorithms employed on benchmark functions. 54
4.8 P_{Loss} minimization (CASE 1). 57
4.9 VD minimization (CASE 2). 58
4.10 VSI minimization (CASE 3). 59
4.11 Percentage saving achieved in P_{Loss}, VD, and VSI by each method for the IEEE 30-bus system. 61
4.12 P_{Loss} minimization (CASE 4). 64
4.13 VD minimization (CASE 5). 65
4.14 VSI minimization (CASE 6). 66
4.15 Percentage saving achieved in P_{Loss}, VD, and VSI by each method for the IEEE 57-bus system. 67
4.16 Modified IEEE 30-bus system. 68
4.17 Load bus voltage profiles for the ten stochastic scenarios. 70
4.18 Reactive power generation for the ten stochastic scenarios. 71

5.1 Flowchart of the proposed ML-based method. 81
5.2 Solar PV power estimation. 83
5.3 P_{Loss} minimization (CASE 1). 88
5.4 VD minimization (CASE 2). 89
5.5 VSI minimization (CASE 3). 90

turnitin Page 27 of 208 - Integrity Submission Submission ID trn:oid:::27535:142293373

turnitin Page 28 of 208 - Integrity Submission Submission ID trn:oid:::27535:142293373

5.6 Percentage saving achieved in P_{Loss}, VD, and VSI by each method for the IEEE 30-bus system. 92
5.7 Modified IEEE 30-bus system. 93
5.8 Performance comparison of the proposed algorithm with the EASOM, DTBO, and COOT. 95
5.9 Hourly profiles of the objective functions obtained using the proposed algorithm. 96
5.10 Hourly load-bus voltage profiles obtained using the proposed algorithm. 97
5.11 Generator reactive power distribution over a 24-hour interval. 98
5.12 Percentage saving achieved in P_{Loss}, VD and VSI by each method for IEEE 118-bus. 102
5.13 P_{Loss} minimization (CASE 7). 103
5.14 VD minimization (CASE 8). 104
5.15 VSI minimization (CASE 9). 105

6.1 Flowchart of the proposed multi-objective method. 112
6.2 Comparison of true and obtained Pareto front for ZDT1–ZDT6 using different multi-objective optimization algorithms. 119
6.3 Comparison of true and obtained Pareto front for DTLZ2 and DTLZ4 using different multi-objective optimization algorithms. 120
6.4 Pareto solutions for the IEEE 30-bus system. 124
6.5 Comparison of saving percentages achieved by different algorithms for the IEEE 30-bus ORPD problem under the multi-objective cases. 125
6.6 IEEE 30-bus load bus voltage profile corresponding to the BCS obtained for the three cases. 126
6.7 Pareto solutions for the IEEE 57-bus system. 130
6.8 Comparison of saving percentages achieved by different algorithms for the IEEE 57-bus ORPD problem under the multi-objective cases. 131
6.9 IEEE 57-bus system load bus voltage profiles corresponding to the BCS obtained for the three cases. 134
6.10 Modified IEEE 30-bus system. 135
6.11 Pareto solutions for the modified IEEE 30-bus system under stochastic operating conditions. 137

turnitin Page 28 of 208 - Integrity Submission Submission ID trn:oid:::27535:142293373

turnitin Page 29 of 208 - Integrity Submission Submission ID trn:oid:::27535:142293373

6.12 Saving percentages achieved by the proposed method for different cases of the modified IEEE 30 bus. 139
6.13 Modified IEEE 30-bus system load bus voltage profiles corresponding to the BCS for ten scenarios (Case 7). 140
6.14 Modified IEEE 30-bus system load bus voltage profiles corresponding to the BCS for ten scenarios (Case 8). 140
6.15 Modified IEEE 30-bus system load bus voltage profiles corresponding to the BCS for ten scenarios (Case 9). 140

turnitin Page 29 of 208 - Integrity Submission Submission ID trn:oid:::27535:142293373

turnitin Page 31 of 208 - Integrity Submission Submission ID trn:oid:::27535:142293373

List of Acronyms

OPF	Optimal Power Flow
ORPD	Optimal Reactive Power Dispatch
MOORPD	Multi-objective Optimal Reactive Power Dispatch
RESs	Renewable Energy Sources
PV	Photovoltaic
WT	Wind Technology
HT	Hydro Technology
LM	Load Modelling
DE	Differential Evolution
GPC	Giza Pyramids Construction Algorithm
OBL	Opposition-Based Learning
NSGA-II	Non-dominated Sorting Genetic Algorithm II
IEASOM	Improved Evolutionary Algorithm–Self Organized Map
SOM	Self Organized Map
COOT	COOT Optimization Algorithm
HBA	Honey Badger Algorithm
DTBO	Driving Training-Based Optimization
EASOM	Evolutionary Algorithm–Self Organized Map

turnitin Page 31 of 208 - Integrity Submission Submission ID trn:oid:::27535:142293373

MOPSO	Multi-objective Particle Swarm Optimization
MOGOA	Multi-objective Grasshopper Optimization Algorithm
MOMA	Multi-objective Mayfly Algorithm
MOSFO	Multi-objective Sunflower Optimization
ZDT	Zitzler–Deb–Thiele Test Functions
DTLZ	Deb–Thiele–Laumanns–Zitzler Test Functions
IGD	Inverted Generational Distance
GD	Generational Distance
HV	Hypervolume
MS	Maximum Spread
S	Spacing
PDF	Probability Density Function
CDF	Cumulative Distribution Function
MCS	Monte Carlo Simulation
Std.	Standard Deviation
BCS	Best Compromise Solution
GCM	Global Criterion Method
FACTS	Flexible AC Transmission Systems
SVC	Static VAR Compensator
TCSC	Thyristor Controlled Series Capacitor
UPFC	Unified Power Flow Controller
TC	Transmission Cost

turnitin Page 33 of 208 - Integrity Submission Submission ID trn:oid:::27535:142293373

List of Symbols

ORPD Objective Functions		
P_{Loss}	Real power loss	MW
VD	Voltage deviation	p.u.
VSI	Voltage stability index	p.u.
L_k	Voltage stability index at bus k	p.u.
Control Variables		
V_{Gk}	Generator voltage magnitude of bus k	p.u.
Q_{Ck}	Shunt compensator reactive power of bus k	MVAr
T_k	Tap ratio of kth transformer	p.u.
N_G	Number of generators	–
N_C	Number of compensators	–
N_T	Number of transformers	–
State Variables		
V_{Lk}	Load bus voltage magnitude of kth bus	p.u.
Q_{Gk}	Reactive power generation of bus k	MVAr
S_{Lk}	Apparent power flow in kth line	MVA
N_{TL}	Number of transmission lines	–
Power System Parameters		
Y	Bus admittance matrix	p.u.
Y_{kj}	Element of admittance matrix	p.u.
G_{kj}	Conductance between bus k and j (real part of Y_{kj})	p.u.
B_{kj}	Susceptance between bus k and j (imaginary part of Y_{kj})	p.u.
V_k, V_j	Voltage magnitudes of kth and jth bus respectively	p.u.
δ_{kj}	Voltage angle difference between kth and jth bus	rad

turnitin Page 33 of 208 - Integrity Submission Submission ID trn:oid:::27535:142293373

θ_{ij}	Phase angle difference between *ith* and *jth* bus	rad
F_{ji}	Element used in voltage stability index formulation	–
Power Balance		
P_G	Active power generation	MW
Q_G	Reactive power generation	MVAr
P_D	Active power demand	MW
Q_D	Reactive power demand	MVAr
Q_{Loss}	Reactive power loss	MVAr
Operational Limits		
V_G^{min}, V_G^{max}	Generator voltage limits	p.u.
Q_G^{min}, Q_G^{max}	Generator eactive power limits	MVAr
T_k^{min}, T_k^{max}	Transformer tap limits	p.u.
Q_C^{min}, Q_C^{max}	Shunt compensator limits	MVAr
V_L^{min}, V_L^{max}	Load voltage limits	p.u.
S_L^{max}	Line flow limit	MVA
Stochastic Modeling		
EP_{Loss}	Expected power loss	MW
$EA_{P_{Loss}}$	Expected average of power loss	MW
EVD	Expected voltage deviation	p.u.
EA_{VD}	Expected average of voltage deviation	p.u.
$EVSI$	Expected voltage stability index	p.u.
EA_{VSI}	Expected average of voltage stability index	p.u.
N_{sc}	Number of scenarios	–
Δ_{sc}	Probability of scenario	–
Renewable Energy Modeling		
G	Solar irradiance	W/m^2
T_m	Module temperature	°C
T_{amb}	Ambient temperature	°C
W_{in}	Wind speed	m/s
v_w	Wind velocity	m/s
P_w	Wind power output	MW
P_s	Solar PV power output	MW
P_H	Hydro power output	MW

turnitin Page 35 of 208 - Integrity Submission Submission ID trn:oid:::27535:142293373

η	Efficiency	–
ρ	Water density	$\mathrm{kg/m^3}$
g	Gravitational acceleration	$\mathrm{m/s^2}$
$K_1, \ldots, K_6$	PV model constants	–
D_m, D_a	Height parameters	m
Time and Statistics		
t	Time index	s
P_t	Power at time t	MW
Δt	Time interval	s
RR_t	Ramp rate	MW/s
μ	Mean value	–
σ	Standard deviation	–
$\mathcal{U}$	Uniform distribution	–
$\mathcal{N}$	Normal distribution	–
Differential Evolution		
F	Scaling factor	–
C_r	Crossover rate	–
$\vec{q}_a, \vec{q}_b, \vec{q}_c$	Random solution vectors	–
GPC Algorithm		
d	Displacement	m
x	Movement component	m
v_0	Initial velocity	m/s
θ	Ramp angle	rad
μ_k	Friction coefficient	–
EA-SOM Algorithm		
x	Decision vector	–
$P(k)$	Population	–
Q_t	Offspring population	–
R_t	Combined population	–
$H(k)$	Historical memory	–
$T(k)$	Training set	–
w_j	SOM weight vector	–
r_j	Neuron position	–
r_g	Winning neuron position	–

turnitin Page 35 of 208 - Integrity Submission Submission ID trn:oid:::27535:142293373

g	Winning neuron index	–
$\eta(t)$	Learning rate	–
$h_{g,j}(t)$	Neighborhood function	–
$\sigma(t)$	Neighborhood radius	–
α	Influence radius	–
D_w, D_A, D_B	Distance measures	–
p_{best}	Best solution	–
$p_{perturb}$	Perturbed solution	–
Δp	Step size	–
$MaxGen$	Maximum generations	–
Multi-objective Metrics		
IGD	Inverted Generational Distance	–
GD	Generational Distance	–
HV	Hypervolume	–
MS	Maximum spread	–
S	Spacing metric	–

Chapter 1

Introduction

1.1 Background

Modern electrical power systems are becoming increasingly complex due to continuous growth in electricity demand, rapid expansion of transmission networks, integration of Renewable Energy Sources (RESs), and advancements in power system technologies. As power systems operate under heavily loaded and dynamic conditions, efficient management of both active and reactive power has become essential for ensuring secure, stable, and economical operation. While active power performs useful work, reactive power is primarily responsible for maintaining voltage levels and supporting efficient transmission of real power. Since most power system components, such as transmission lines and transformers, exhibit inductive characteristics, effective reactive power management is necessary for minimizing transmission losses, improving voltage stability, and enhancing overall system reliability [1].

The concept of Optimal Power Flow (OPF) was introduced by Carpentier in 1962. OPF is an advanced form of the economic dispatch problem that considers both power flow equations and operating constraints. OPF determines the optimal operating condition of a power system while satisfying system constraints such as generator limits, voltage limits, transformer tap settings, and transmission line capacities. Besides minimizing generation cost, practical OPF problems also focus on reducing transmission losses while improving voltage conditions and enhancing system stability. However, the OPF problem is naturally nonlinear, non-convex, multimodal, and constrained, involving both continuous and discrete decision variables, which makes it computationally challenging [2–4].

turnitin Page 38 of 208 - Integrity Submission Submission ID trn:oid:::27535:142293373

Optimal Reactive Power Dispatch (ORPD) is a significant part of the OPF problem that deals with the effective management of reactive power in power systems. ORPD aims to obtain suitable values for control variables such as generator voltages, transformer tap settings, and reactive power compensators to achieve efficient system operation under specified operating limits. The problem is highly challenging because it involves nonlinear power flow relationships, multiple operational constraints, and both continuous and discrete decision variables [5, 6].

The increasing integration of RESs such as wind and solar power provides significant environmental and economic benefits by reducing greenhouse gas emissions and dependence on fossil fuels. However, the intermittent and stochastic nature of RESs introduces additional uncertainty into power system operation. Variations in solar irradiance, wind speed and load demand may significantly affect voltage stability, reactive power balance, and system security. Consequently, modern power systems require efficient uncertainty-aware optimization frameworks capable of maintaining reliable and economical operation under varying operating conditions [7, 8].

1.2 Importance of Reactive Power in Power Systems

Reactive power is an essential component of alternating current (AC) power systems and plays a significant role in maintaining stable, secure, and efficient operation of electrical networks. Although reactive power does not directly perform useful mechanical work like active power, it is necessary for establishing the electric and magnetic fields required for the operation of generators, transformers, transmission lines, induction motors, and other inductive loads. Proper management of reactive power is therefore crucial for voltage regulation, transmission efficiency, power quality improvement, and reliable operation of modern power systems [9].

In practical power systems, reactive power continuously flows between generating units, transmission lines, and connected loads to support electromagnetic energy conversion processes. Inadequate reactive power support may lead to voltage instability, excessive transmission losses, reduced transmission capability, poor power factor, and in severe cases, system collapse. Consequently, reactive

turnitin Page 38 of 208 - Integrity Submission Submission ID trn:oid:::27535:142293373

turnitin Page 39 of 208 - Integrity Submission Submission ID trn:oid:::27535:142293373

power optimization has become one of the major concerns in power system planning and operation [10].

1.2.1 Voltage Regulation and Voltage Stability

One of the primary functions of reactive power is maintaining acceptable voltage levels throughout the power system network. The voltage magnitude at different buses strongly depends on the availability and distribution of reactive power. When reactive power demand exceeds the available supply, voltage levels begin to decrease, which may eventually result in voltage instability or voltage collapse [11, 12].

Maintaining proper voltage profiles is essential for secure and reliable system operation. Reactive power compensation devices such as capacitor banks, synchronous condensers, and Flexible AC Transmission System (FACTS) devices are commonly employed to regulate voltage levels and improve system stability [13, 14]. Efficient reactive power management is essential in enhancing voltage stability and preventing voltage-related disturbances.

1.2.2 Reduction of Transmission Losses

Reactive power flow through transmission lines increases the current flowing in the network. Excessive current flow causes higher transmission losses and reduces overall system efficiency. Proper reactive power dispatch minimizes unnecessary reactive power circulation and helps reduce active power losses in transmission lines [15, 16].

Reduction of transmission losses offers several advantages, including:

- Improved system efficiency
- Reduced operating costs
- Better utilization of transmission infrastructure
- Lower thermal stress on system components

Hence, minimization of transmission losses is considered one of the primary objectives of ORPD.

turnitin Page 39 of 208 - Integrity Submission Submission ID trn:oid:::27535:142293373

turnitin Page 40 of 208 - Integrity Submission Submission ID trn:oid:::27535:142293373

1.2.3 Enhancement of Power Transfer Capability

Reactive power significantly affects the power transfer capability of transmission systems. Excessive reactive power flow occupies a portion of transmission line capacity, thereby reducing the amount of active power that can be transferred [17, 18].

Efficient reactive power management improves voltage regulation and enhances the loadability of transmission lines. Modern power systems utilize FACTS devices such as Static Var Compensator (SVC), Static Synchronous Compensator (STATCOM), Thyristor Controlled Series Capacitor (TCSC) and Unified Power Flow Controller (UPFC) to provide dynamic reactive power support, improve voltage stability, and enhance transmission capability [19]

1.2.4 Support for Inductive Loads

Most practical electrical loads are inductive in nature and require reactive power for their operation. Common inductive loads include induction motors, transformers, industrial machinery, pumps, compressors, and air-conditioning systems. Reactive power is necessary for establishing the magnetic fields required for proper operation of these devices [20, 21].

Insufficient reactive power support may result in:

- Poor equipment performance
- Voltage fluctuations
- Reduced efficiency
- Overheating of electrical equipment

Therefore, adequate reactive power support is essential for ensuring efficient and reliable operation of inductive loads.

1.2.5 Improvement of Power Factor

Reactive power has a direct influence on the power factor of electrical systems. Poor reactive power management leads to low power factor conditions, which

turnitin Page 40 of 208 - Integrity Submission Submission ID trn:oid:::27535:142293373

turnitin Page 41 of 208 - Integrity Submission Submission ID trn:oid:::27535:142293373

result in increased current flow, higher transmission losses, larger voltage drops, and reduced system efficiency [22, 23].

Reactive power compensation improves the power factor of the system and provides several operational benefits such as:

- Reduction in line current
- Improved voltage profile
- Enhanced transmission efficiency
- Better utilization of electrical equipment

Improved power factor also reduces operational costs and utility penalties associated with inefficient power usage.

1.2.6 Prevention of Voltage Collapse

Voltage collapse is a serious problem in heavily loaded systems and generally occurs due to inadequate reactive power support. When reactive power demand continuously increases beyond system capability, bus voltages progressively decline and may eventually lead to large-scale system failure [24].

Maintaining sufficient reactive power reserves and implementing efficient ORPD strategies are therefore essential for:

- Voltage security enhancement
- Prevention of cascading failures
- Reliable operation under stressed conditions
- Improvement of system stability margins

Thus, reactive power management is considered a critical aspect of power system security assessment and operation.

turnitin Page 41 of 208 - Integrity Submission Submission ID trn:oid:::27535:142293373

turnitin Page 42 of 208 - Integrity Submission Submission ID trn:oid:::27535:142293373

1.2.7 Overall Significance of Reactive Power

Reactive power is essential in maintaining stable, secure, and economical operation of electrical power systems. It supports voltage regulation, improves transmission efficiency, enhances power transfer capability, and ensures proper operation of inductive equipment [25, 26].

With the increasing complexity of modern interconnected power systems, efficient reactive power management has become more important than ever. Consequently, ORPD has emerged as an important research area aimed at developing advanced optimization techniques for minimizing transmission losses, improving voltage stability, and enhancing overall system performance.

1.3 Motivation and Challenges

1.3.1 Need for Advanced Optimization Techniques

Over the years, considerable attention has been given to the optimal operation of power systems with the aim of improving system efficiency, lowering operating cost, reducing losses, and maintaining better voltage performance and stability. However, these optimization problems are extremely nonlinear, nonconvex, and multimodal, and hence, achieving an accurate global optimum remains difficult. This necessitates the development of new optimization approaches capable of finding near-global optimum solutions [27, 28].

1.3.2 Integration of Renewable Energy Sources

From the economic, environmental and technological perspectives, the transition from fossil fuel-based power to RESs is imperative. This integration minimizes greenhouse gas emissions, lowers fuel consumption and improves system functioning. Among the various RESs, wind and solar energy systems are the most widely adopted. Nevertheless, the fluctuating behavior of wind speed and solar radiation introduces uncertainty and variability into modern power systems [29–31].

turnitin Page 42 of 208 - Integrity Submission Submission ID trn:oid:::27535:142293373

turnitin Page 43 of 208 - Integrity Submission Submission ID trn:oid:::27535:142293373

1.3.3 Uncertainty in Load Demand

The load demand of electric power systems varies hourly and daily due to consumer activity and seasonal changes. These variations create uncertainty in the power system. It is thus important to incorporate load demand uncertainty in the system planning and operational decision-making [32].

1.3.4 Increasing Power System Complexity

Modern power systems have become more complex with the growing incorporation of distributed generation, RESs, FACTS devices and advanced control technologies [33]. This increased complexity leads to strong interdependencies among system variables, making system analysis, control, and optimization more challenging [34].

1.3.5 Deregulation and Market Complexity

The deregulation of electricity markets has transformed traditional power systems into competitive environments with multiple stakeholders. This introduces conflicting objectives and increases the complexity of decision-making processes, thereby requiring advanced multi-objective optimization techniques [35].

1.3.6 Role of Multi-Objective Optimization

Multi-objective optimization is a key aspect of power systems since multiple conflicting objectives should be solved simultaneously, and a set of trade-off solutions is required instead of a single optimal solution. However, the nonlinear, nonconvex, high-dimensional nature of the problem makes it difficult to generate a well-converged, uniformly distributed set of solutions. Moreover, it is difficult to select the best solution from several equally good trade-offs, depending on the system requirements and preferences. Therefore, there is a strong need for effective approaches that provide high-quality solutions and support reliable, balanced decision-making [36–38].

turnitin Page 43 of 208 - Integrity Submission Submission ID trn:oid:::27535:142293373

turnitin Page 44 of 208 - Integrity Submission Submission ID trn:oid:::27535:142293373

1.4 Problem Statement

The increasing demand for electrical energy, rapid expansion of transmission networks, and integration of renewable energy resources have made modern power systems highly complex and challenging to operate. Maintaining voltage stability, minimizing transmission real power losses, and ensuring secure and economical operation are among the major concerns in power system management [39]. Reactive power is essential in maintaining acceptable voltage profiles and improving the overall efficiency and reliability of the system. Poor reactive power management can result in excessive transmission losses, voltage instability, reduced power quality, and increased operating costs [40].

ORPD is an important optimization problem that determines the optimal settings of control variables such as generator voltages, transformer tap settings, and reactive power compensation devices while satisfying system operational constraints. In practical applications, real-world power system problems are inherently multi-objective in nature, where several conflicting objectives must be optimized simultaneously. Objectives such as minimization of active power losses, reduction of voltage deviation, improvement of voltage stability, and enhancement of system security often conflict with each other, and improving one objective may adversely affect another. Therefore, a balanced and effective multi-objective optimization approach is required to obtain practical operating solutions.

However, the ORPD problem is highly nonlinear, non-convex, multimodal, and constrained, making it difficult to solve using conventional optimization techniques. Conventional optimization methods often experience slow convergence and may become trapped in local optima, particularly when applied to large-scale power systems. Hence, there is a need for efficient, robust optimization techniques capable of effectively solving the multi-objective ORPD problem and ensuring the reliable, secure, and economical operation of modern power systems under varying operating conditions.

turnitin Page 44 of 208 - Integrity Submission Submission ID trn:oid:::27535:142293373

turnitin Page 45 of 208 - Integrity Submission Submission ID trn:oid:::27535:142293373

1.5 Research Objectives

The specific objectives of this thesis work are formulated to address the identified research gaps in ORPD and are presented as follows:

- To develop a new intelligent technique or modifications/improvements in the existing techniques for solving multi-objective ORPD problems.
- To evaluate the proposed ORPD technique's effectiveness and feasibility on various standard test systems.
- To formulate ORPD problems considering multiple scenarios in load demand and renewable energy sources.
- To investigate the various possibilities of obtaining the compromise solutions and to identify the best compromise solution for multi-objective ORPD problems.

1.6 Structure of the Thesis

This thesis is organized into seven chapters to systematically present the research work carried out on ORPD problems in modern power systems.

Chapter 1 introduces the concept and significance of ORPD in modern electrical power systems. It discusses the growing challenges associated with reactive power management, voltage stability, transmission power loss minimization, and the impact of renewable energy integration. The chapter also presents the research motivation, objectives, problem statement, and scope of the proposed work.

Chapter 2 provides a comprehensive review of existing literature related to ORPD. Various conventional, evolutionary, metaheuristic, and hybrid optimization techniques reported in the literature are critically analyzed. The strengths, limitations, and research gaps associated with existing methods are also discussed to establish the need for improved optimization approaches.

Chapter 3 presents the mathematical formulation of the ORPD problem, including objective functions, equality constraints, and inequality constraints. The chapter explains the modeling of different control variables and system parameters

turnitin Page 45 of 208 - Integrity Submission Submission ID trn:oid:::27535:142293373

turnitin Page 46 of 208 - Integrity Submission Submission ID trn:oid:::27535:142293373

involved in ORPD. In addition, the IEEE standard test systems used for simulation and performance evaluation are described in detail.

Chapter 4 introduces a hybrid optimization algorithm that combines Opposition-Based Learning (OBL), Differential Evolution (DE), and the Giza Pyramids Construction (GPC) algorithm for solving single-objective deterministic and stochastic ORPD problems. The methodology, implementation procedure, and performance analysis of the proposed hybrid approach are discussed and validated using standard test systems.

Chapter 5 presents a machine learning-based optimization framework using the Improved Evolutionary Algorithm–Self Organized Maps (IEASOM) for solving single-objective deterministic and stochastic ORPD problems. The proposed approach is applied to both small-scale and large-scale power systems to improve optimization performance, convergence characteristics, and solution quality under varying operating conditions.

Chapter 6 develops a multi-objective hybrid optimization framework incorporating the Non-dominated Sorting Genetic Algorithm II (NSGA-II) selection scheme for solving deterministic and stochastic ORPD problems. The proposed framework simultaneously addresses multiple conflicting objectives such as power loss minimization, voltage profile improvement, and voltage stability enhancement while considering uncertain operating conditions.

Finally, Chapter 7 summarizes the major findings and contributions of the thesis. The chapter discusses the effectiveness of the proposed optimization techniques, highlights the practical significance and societal impact of the research work, and provides recommendations for future research directions in ORPD and modern power system optimization.

turnitin Page 46 of 208 - Integrity Submission Submission ID trn:oid:::27535:142293373

Chapter 2

Literature Review

2.1 Introduction

ORPD is widely acknowledged as an essential optimization problem in the planning and operation of power systems. The basic goal of ORPD is to optimize control variables, including generator voltages, transformer tap locations, and reactive power compensation devices, to minimize P_{Loss}, reduce VD, and improve VSI. The use of RESs, including solar and wind power, has grown in popularity in recent years, introducing significant uncertainty and volatility into power systems and broadening the scope of ORPD. Thus, the ORPD problem has shifted from a deterministic optimization problem to a stochastic, nonconvex, and highly nonlinear optimization problem that requires advanced solution techniques.

This chapter presents a comprehensive review of ORPD optimization techniques reported in the literature. The literature review is systematically categorized into conventional optimization techniques, single-objective metaheuristic methods, hybrid optimization frameworks, multi-objective ORPD approaches and stochastic uncertainty-aware optimization techniques. In addition, a critical analysis of existing literature is presented to identify major research challenges and potential future research directions in ORPD optimization.

2.2 Conventional Optimization Methods for ORPD

Early research in ORPD relied heavily on conventional mathematical optimization techniques, including the Newton method [41] and Interior Point (IP) [42], Mixed Integer Non-Linear Programming (MINLP) [43], Revised Linear Programming

turnitin Page 48 of 208 - Integrity Submission Submission ID trn:oid:::27535:142293373

[44], Conic Programming and Lagrangian Method (LM) [45]. These methods are mathematically rigorous and provide exact solutions under simplified conditions. However, their application to real-world ORPD problems is limited due to several inherent drawbacks. The ORPD problem involves nonlinear power flow equations, discrete and continuous control variables, and multiple operational constraints, which make it difficult for classical methods to converge to global optima. Additionally, these methods are highly sensitive to initial conditions and often require simplifications that compromise solution accuracy. Furthermore, their computational burden increases significantly with system size, making them unsuitable for large-scale modern power systems.

Due to these limitations, researchers have increasingly shifted their attention toward metaheuristic optimization techniques capable of effectively solving nonlinear, multimodal, and large-scale ORPD problems without requiring gradient information. These intelligent optimization approaches demonstrated superior global search capabilities and greater flexibility in handling practical ORPD optimization problems.

2.3 Single-Objective Metaheuristic ORPD Methods

Metaheuristic algorithms are generally population-based optimization approaches inspired by natural evolution, biological behavior, swarm intelligence, social interactions, and physical phenomena. Over the past decade, a wide range of metaheuristic algorithms have been developed to solve the ORPD problem. Among them, Mahdad et al. [46] suggested an intelligent strategy-based novel algorithm known as the Salp Swarm Algorithm (SSA) to enhance ORPD solutions by optimizing P_{Loss} and VD separately, while also taking static VAR compensators (SVCs) into account. The proposed intelligent planning strategy has been evaluated using the IEEE 30 and the large-scale Algerian 114-bus system. SSA performed exceptionally in global exploration but was susceptible to stagnation as population variety reduced. Dai et al. [47] applied the Seeker Optimization Algorithm (SOA) for ORPD in which VD and VSI are considered as objective functions, and the results demonstrated better performance compared to several GA, DE, and PSO variants on IEEE 57 and 118-bus systems. Abdelmoumene et al. [48] proposed a Differential Evolution (DE) based method for solving the ORPD

turnitin Page 48 of 208 - Integrity Submission Submission ID trn:oid:::27535:142293373

turnitin Page 49 of 208 - Integrity Submission Submission ID trn:oid:::27535:142293373

problem with voltage profile control. The proposed method minimized P_{Loss} while improving VD performance in the IEEE 30-bus system. The results demonstrated the robustness of the DE algorithm for nonlinear ORPD optimization problems. Abou El-Ela et al. [49] applied Ant Colony Optimization (ACO) to solve the ORPD problem in IEEE 14 and 30-bus systems. The proposed method effectively minimized P_{Loss} and demonstrated strong optimization capability through the cooperative search behavior of artificial ants. Ghasemi et al. [50] utilized a Teaching–Learning-Based Optimization (TLBO) algorithm for ORPD applications to minimize transmission P_{Loss}. The algorithm improved convergence performance without requiring algorithm-specific control parameters, thereby simplifying the optimization process. Gupta et al. [51] proposed a simplified Sine Cosine Algorithm (SCA) to address the ORPD problems by estimating the control variables. This method generates random solutions using sine and cosine functions to obtain the ideal solution by oscillating inward or outward. The algorithm was utilized in ORPD to discover the best control variables for lowering power loss and boosting net savings in three test system case studies: IEEE-30, 57, and 118-bus systems. Although it improved exploration, its oscillations sometimes produced instability during solution refining. Roy et al. [52] proposed the JAYA Algorithm to minimize P_{Loss} in IEEE 14, 30, 57, and 118-bus systems. JAYA's algorithm is characterized by its simplicity and robustness due to its parameter-free nature. It lacks mechanisms to balance exploration and exploitation, which might cause premature convergence. Mouassa et al. [53] applied the Ant Lion Optimizer (ALO) algorithm to solve the ORPD problem. The proposed method optimized control variables to minimize real P_{Loss} while satisfying operational constraints. Simulation results on standard IEEE 30, 118 and 300-bus test systems demonstrated that the ALO algorithm provided high-quality solutions with better convergence characteristics and computational efficiency compared with several existing optimization techniques. Mei et al. [54] applied the Moth-Flame Optimization (MFO) algorithm to solve the ORPD problem with the objectives of minimizing total P_{Loss} and VD. Inspired by the navigation behavior of moths, the MFO technique optimized generator voltages, transformer tap settings, and reactive compensation devices. Simulation studies on IEEE 30, 57, and 118-bus systems demonstrated that the proposed approach achieved lower P_{Loss} and improved voltage profiles compared with several existing optimization algorithms. Lai et al. [55] utilized the Membrane Search Algorithm

turnitin Page 49 of 208 - Integrity Submission Submission ID trn:oid:::27535:142293373

turnitin Page 50 of 208 - Integrity Submission Submission ID trn:oid:::27535:142293373

(MSA) for the ORPD problem, showing faster convergence and reduced P_{Loss} in IEEE 57, 118, and 300-bus systems. Nonetheless, the algorithm's dependability on complex membrane processes increases the computational challenges.

Several researchers have also proposed improved or modified variants of existing metaheuristic algorithms to overcome issues such as premature convergence, local optima entrapment, and insufficient exploration-exploitation balance. Biswas et al. [56] proposed a modified Differential Evolution (DE) technique incorporating random localization to solve the ORPD problem with the objective of minimizing P_{Loss} while maintaining acceptable bus voltage profiles. The proposed approach addressed the slow convergence of conventional DE and demonstrated improved optimization performance on the IEEE 14 and 30-bus systems compared with basic DE and other soft-computing techniques. Shaw et al. [57] introduced an Opposition-Based Gravitational Search Algorithm (OGSA) for ORPD optimization. The integration of opposition-based learning with gravitational search mechanisms improved convergence speed and enhanced optimization accuracy. Yapici [58] proposed a modified version of the Pathfinder Algorithm (mPFA) that draws inspiration from the coordinated movement of a swarm led by a single member. The algorithm's performance and feasibility were showcased through simulation cases on IEEE 57 and 118-bus systems, with the aim of minimizing P_{Loss}. However, its reliance on its leader and followers increased the likelihood of being trapped in local optima. Shaheen et al. [59] proposed an Enhanced Transient Search Optimization Algorithm (ETSOA) for optimizing the ORPD problem by integrating electric vehicles, minimizing P_{Loss} and VD at load buses, and testing it on IEEE 30, 57 and 118-bus systems. Nonetheless, it required enhanced computational capabilities and precise parameter adjustments. Sarhan et al. [60] proposed an Augmented Social Network Search Algorithm (ASNSA) that enhances the performance of the social network search (SNS) algorithm by boosting search capability around the optimal solution. The ASNSA algorithm was evaluated on IEEE 30, 57, and 118-bus systems, including comparisons and statistical analysis to confirm its performance. It enhanced the exploitation of potential solutions but still needed more iterations for convergence. Wahab et al. [61] proposed the Chaotic Turbulent Flow of Water-Based Optimization Algorithm (CTFWO) method to solve the ORPD problem using chaotic maps. The CTFWO algorithm was employed to minimize P_{Loss} and VD for IEEE 30 and

turnitin Page 50 of 208 - Integrity Submission Submission ID trn:oid:::27535:142293373

turnitin Page 51 of 208 - Integrity Submission Submission ID trn:oid:::27535:142293373

57-bus power systems. Although chaotic maps increased diversity, the method exhibited significant sensitivity to initial conditions. Kanagasabai [62] employed the Improved Meadow Fritillary Butterfly Optimization Algorithm (IMFBOA) to effectively reduce the P_{Loss} for IEEE 30 and 57-bus systems. The exploration method in the Meadow Fritillary Butterfly optimization (MFBO) algorithm is influenced by the behavior of meadow fritillary butterflies. To overcome this problem, firefly's algorithm exploration strategy has been included in the standard MFBO algorithm. However, adding search mechanisms increased computing complexity, making the approach more difficult than the MFBO algorithm. Li et al. [63] proposed an Improved Ant Lion Optimization (IALO) algorithm for solving the ORPD problem in IEEE 30, 57, and 118-bus systems. The method enhanced the standard ALO algorithm through a modified solution generation mechanism, improving convergence speed, solution stability, and global search capability while satisfying all operational constraints. Comparative results showed that the proposed IALO outperformed conventional ALO and several existing optimization techniques. Dora et al. [64] presented an Enhanced Butterfly Optimization Algorithm (EBOA) that incorporates Exchange Market Algorithm (EMA) crossover and non-uniform mutation to optimize the equilibrium between exploration and exploitation. The algorithm was verified on the IEEE 30, 118, and Indian 62-bus systems, achieving significant reductions in P_{Loss}, VD, and VSI, thereby proving enhanced efficiency and robustness compared to the conventional BOA. Despite its robust outcomes, the approach escalates computing complexity and parameter sensitivity, potentially limiting its scalability in extensive applications.

Single-objective metaheuristic optimization techniques significantly improved ORPD optimization performance compared with conventional mathematical optimization methods. These algorithms demonstrated strong global exploration capability, improved convergence characteristics, and flexibility in handling nonlinear and constrained optimization problems.

Evolutionary algorithms such as DE and TLBO demonstrated good convergence behavior and strong optimization capability for transmission loss minimization. Swarm intelligence algorithms such as PSO, ACO, SSA, ALO, and MFBO provided improved global search performance and computational efficiency. Physics-based and bio-inspired optimization techniques further improved exploration mechanisms and solution diversity.

turnitin Page 51 of 208 - Integrity Submission Submission ID trn:oid:::27535:142293373

turnitin Page 52 of 208 - Integrity Submission Submission ID trn:oid:::27535:142293373

Despite significant progress, several challenges still remain unresolved. Many optimization algorithms suffer from premature convergence, limited exploitation, parameter sensitivity, and increased computational complexity. Furthermore, most existing single-objective optimization techniques focus primarily on transmission loss minimization while neglecting practical multi-objective operational requirements.

Consequently, researchers increasingly focused on developing hybrid optimization frameworks and multi-objective optimization approaches that achieve a better balance between exploration and exploitation while simultaneously satisfying multiple practical operating objectives.

2.4 Hybrid Optimization Methods for ORPD

Although single-objective metaheuristic optimization methods demonstrated significant improvement over conventional mathematical optimization methods, many standalone algorithms still suffer from several limitations, such as premature convergence, weak local exploitation capability, slow convergence speed, and poor balance between exploration and exploitation. In practical ORPD problems, optimization algorithms are required to efficiently explore the search space while simultaneously exploiting promising regions to obtain high-quality global optimal solutions. To further improve performance, hybrid techniques are also employed to tackle the ORPD problem, integrating several metaheuristic optimization methodologies to reap each strategy's benefits simultaneously.

Li et al. [65] proposed a hybrid artificial bee colony that collaborated with the differential evolution algorithm (DE-ABC) to improve global search and alleviate DE's large population. This method minimizes P_{Loss} in the IEEE 14, 30 and 57-bus systems. Shareef and Rao [66] proposed a hybrid swarm intelligence approach combining Artificial Bee Colony (ABC) and Firefly (FF) algorithms for solving the ORPD problem under unbalanced operating conditions. The proposed ABC-FF algorithm minimized VD and P_{Loss} by optimally adjusting control variables. Simulation results on IEEE 14 and 39-bus systems demonstrated superior ORPD performance compared with other evolutionary optimization methods. Padaiyatchi and Daniel [67] investigated reactive power planning under single-line outage contingency conditions using Differential Evolution (DE) and

turnitin Page 52 of 208 - Integrity Submission Submission ID trn:oid:::27535:142293373

turnitin Page 53 of 208 - Integrity Submission Submission ID trn:oid:::27535:142293373

Evolutionary Programming (EP) algorithms in the IEEE 30-bus system. The proposed approach optimized generator voltages, transformer tap settings, and TCSC parameters to improve voltage stability and reactive power reserves under contingency conditions. Huang and Huang [68] applied a hybrid optimization method combining Differential Evolution (DE) and Ant System for solving the ORPD problem. The method integrated variable scaling, mutation and probabilistic state transition mechanisms to minimize active power transmission losses, and simulation results on the IEEE 30-bus system demonstrated improved convergence characteristics and better optimization performance compared with Evolutionary Programming (EP) and Particle Swarm Optimization (PSO) methods. Chen et al. [69] introduced a fuzzy adaptive hybrid Particle Swarm Optimization (HPSO) method for reactive power and voltage control in distribution systems that contain distributed generators. The proposed technique minimized a comprehensive operational cost function, including P_{Loss} and operating costs of transformers and capacitors, while satisfying reactive power and voltage constraints. Results on a modified IEEE 33-node distribution system showed improved convergence speed and solution quality compared with other intelligent optimization approaches. Ghasemi et al. [70] proposed a hybrid optimization framework combining Modified Teaching Learning Algorithm (MTLA) and Double Differential Evolution (DDE) for ORPD optimization. The proposed hybrid approach achieved improved convergence characteristics and better-quality solutions compared with conventional standalone optimization methods. Naderi et al. [71] introduced a Fuzzy Adaptive Heterogeneous Comprehensive Learning PSO (FAHC-LPSO) method with improved exploration and exploitation for the ORPD problem. The method was analyzed on three standard systems to minimize P_{Loss} and VD. Rajan [72] implemented the hybrid Nelder-Mead Simplex (NMS)-Firefly Algorithm (FA) to solve the ORPD problem. The FA algorithm's local optima stagnation problem is solved by adding the NMS subroutine. The hybrid strategy uses the FA algorithm exploration and exploitation by NMS to avoid premature convergence. Wahab et al. [73] developed a hybrid Artificial Rabbits Optimization (ARO)-Gradient Based Optimization (GBO) method to address the ORPD problem in the IEEE 30, 57 and 118-bus systems for minimizing P_{Loss} and VD.

Hybrid optimization techniques improve ORPD performance by combining the strengths of multiple optimization algorithms, resulting in better exploration

turnitin Page 53 of 208 - Integrity Submission Submission ID trn:oid:::27535:142293373

turnitin Page 54 of 208 - Integrity Submission Submission ID trn:oid:::27535:142293373

and exploitation balance. They provide faster convergence, higher optimization accuracy, and reduce the risk of getting trapped in local optima. Additionally, hybrid methods offer greater robustness and are more suitable for large-scale and uncertain power system environments.

However, despite significant progress, challenges such as computational complexity, parameter dependency, scalability, and uncertainty handling still remain unresolved. Consequently, researchers increasingly focused on multi-objective optimization frameworks and stochastic ORPD techniques capable of simultaneously addressing multiple practical operational objectives under uncertain operating conditions.

2.5 Multi-Objective ORPD Methods

In addition to single-objective optimization, multi-objective ORPD (MOORPD) has gained considerable attention due to the need to simultaneously optimize multiple conflicting objectives. These objectives typically include minimizing power loss, reducing VD, improving voltage stability, and minimizing operational costs. Multi-objective optimization techniques are generally classified into weighted sum and Pareto-based approaches. While the weighted sum method is simple and easy to implement, it is sensitive to the selection of weighting factors and may fail to capture non-convex Pareto fronts. On the other hand, Pareto-based methods generate a set of non-dominated solutions, providing a comprehensive representation of trade-offs among objectives.

Jeyadevi et al. [74] developed a modified NSGA-II with enhanced elitism to solve the MOORPD on IEEE 30 and 118-bus systems and its performance was compared with MOPSO. The TOPSIS method was applied to determine the Best Compromise Solution (BCS) from the non-dominated solutions, although it resulted in relatively higher computational time. Niknam et al. [75] present an opposition-based self-adaptive modified Gravitational Search Algorithm (GSA) to tackle the MOORPD problem, where Pareto optimality was used to generate the non-dominated solutions, while a fuzzy decision-making technique was adopted to derive the BCS for minimizing the P_{Loss}, VD and improving the VSI. Li et al. [76] formulated a MORPO optimization model for an AC-DC hybrid system using a piecewise-normalized normal constraint technique to generate well-spread Pareto

turnitin Page 54 of 208 - Integrity Submission Submission ID trn:oid:::27535:142293373

turnitin Page 55 of 208 - Integrity Submission Submission ID trn:oid:::27535:142293373

solutions over a 24-hour period. The proposed approach achieved significant reductions in P_{Loss} and improvement in voltage profile performance. Srivastava and Singh [77] proposed a fuzzy adaptive hybrid Particle Swarm Optimization (HPSO) technique for MOORPD and voltage control in distribution systems with distributed generators. The proposed approach minimized comprehensive operating costs, including P_{Loss} and device operating costs, while satisfying reactive power and voltage constraints, and demonstrated superior convergence and computational efficiency on a modified IEEE 33-bus distribution system compared with other artificial intelligence methods. Nuaekaew et al. [78] applied a Two Archive Multi-Objective Grey Wolf Optimizer (MOGWO) to the MOORPD problem, incorporating a dual-archive mechanism and an improved reproduction strategy to enhance convergence and solution diversity. The proposed algorithm was evaluated alongside other multi-objective methods on the IEEE 30, 57, and 118-bus systems. Panthagani et al. [79] proposed the Pareto-based Kinetic Gas Molecule Optimization (KGMO) method using FACTS devices such as SVC, TCSC, and UPFC. The proposed algorithm was implemented on the IEEE 30-bus system and demonstrated improved performance in achieving multiple operational objectives. Aljohani et al. [80] introduced a hybrid Artificial Physics-Particle Swarm Optimization (AP-PSO) algorithm to address both single-objective and MOORPD problems. The algorithm was evaluated on IEEE 30, 57, and 118 bus systems for P_{Loss} minimization, VD minimization, and VSI improvement. It shows better convergence and robustness than the PSO algorithm. Sani et al.[81] proposed a MOORPD framework integrating a wind farm's reactive power capability with conventional control devices to minimize P_{Loss} and VD. The MOORPD problem was first scalarized using the Global Criterion Method (GCM) and subsequently reformulated as a mixed-integer linear programming model to boost computational efficiency. Zhang et al. [82] proposed a two-stage framework for the MOORPD problem, where Classification and Pareto domination-based Multi-Objective Evolutionary Algorithm (CPSMOEA) was utilized to generate solutions and Fuzzy C-means clustering combined with grey relation projection was applied to identify the BCS. The method demonstrated improved performance over MOPSO on the IEEE 30 and 118-bus systems. Karimi et al. [83] proposed a stochastic MOORPD model that accounts for uncertainty in load demand and renewable penetration, where a modified GWO was employed to minimize P_{Loss} and improve

turnitin Page 55 of 208 - Integrity Submission Submission ID trn:oid:::27535:142293373

turnitin Page 56 of 208 - Integrity Submission Submission ID trn:oid:::27535:142293373

the VD under various uncertainty scenarios. Bhurt et al. [84] formulated a comprehensive MOORPD framework that simultaneously minimized P_{Loss}, VD, operational cost and emission of thermal generators integrated with renewable sources. A bidirectional co-evolutionary NSGA-II algorithm was employed to generate uniformly distributed Pareto solutions. The study emphasized the importance of including emission objectives in the ORPD for sustainable power system operation. Dutta et al. [85] have incorporated FACTS components like SVC and TCSC within an MOORPD model by employing the Quasi-Oppositional Chemical Reaction Optimization (QOCRO) approach, aiming at achieving the minimization of both P_{Loss} and VD. The use of FACTS equipment greatly helped in increasing voltage stability and efficiency. The Fuzzy Tuned Mayfly Algorithm (FTMA) was proposed by Gangil et al. [86] to solve MOORPD problems through minimizing the P_{Loss} and VD. The Pareto optimization approach was applied to generate a set of non-dominated solutions, following which the fuzzy logic approach was employed to obtain the BCS. Ebeed et al. [87] addressed a FACTS embedded MOORPD problem involving RESs through the implementation of the Adaptive Beluga Whale Optimization (ABWO) algorithm. FACTS integrated MOORPD problem using RESs by using the two objectives considered in this research were P_{Loss} minimization and VD minimization. This method showed better results regarding voltage profile and minimized system losses for different loading scenarios. Panthagani and Rao [88] came up with the KGMO algorithm for the FACTS-integrated MOORPD problem. They managed to achieve the minimization of both P_{Loss} and VD with their method, having superior converging properties as well as solution diversity.

Multi-objective optimization techniques significantly improved the practical applicability of ORPD optimization by simultaneously considering multiple conflicting objectives. Weighted sum approaches, Pareto-based optimization methods, NSGA-II frameworks, swarm intelligence techniques, FACTS integrated optimization approaches, and RESs integrated MOORPD frameworks demonstrated improved optimization flexibility and operational performance. However, despite substantial achievements in research related to multi-objective optimization, there remain important issues that are yet unresolved within MOORPD. These are mainly associated with the intensive computational requirements of solving multi-objective problems of a large scale in real time or near real time.

turnitin Page 56 of 208 - Integrity Submission Submission ID trn:oid:::27535:142293373

turnitin Page 57 of 208 - Integrity Submission Submission ID trn:oid:::27535:142293373

Furthermore, obtaining global optimality in solutions obtained via meta-heuristic algorithms is a daunting task. The other challenge is that there is no standard procedure for selecting one representative solution from the Pareto set for actual application. Most of the present techniques find it hard to achieve a balance between diversification and approaching the Pareto set. However, most of the time, they exhibit poor scalability characteristics when applied to problems in very high dimensionality, stringent constraints, or multiple objective functions. Another issue with these approaches is their high computational costs and their heavy dependence on algorithm-specific parameters. The improvements achieved through such algorithms are minimal and rely heavily on classical techniques. Improvements suggested in this regard are mostly small and traditional, as they do not address any other problem or involve real-world applications.

2.6 Stochastic and Uncertainty-Based ORPD Methods

Recent research articles have explored the influence of various uncertainties on the ORPD problem. These include uncertainty about RESs and load demand. The system has become vulnerable because of the fluctuation of load demand and RES, and voltage-related problems are probable. However, shifting from fossil fuel to renewable production is vital for environmental, economic, and technological reasons. This integration minimizes greenhouse gas emissions, lowers production fuel costs, and increases system efficiency. Table 2.1 presents the findings of the recent research on the ORPD problem, considering uncertainty about RESs and loads. This table provides an overview of the algorithm's objectives, the test systems utilized, the main highlights, and the limitations of different approaches based on previous research findings.

Kamel et al. [89] suggested an Enhanced Grey Wolf Optimizer (EGWO) for solving ORPD with load uncertainty. The EGWO improves the original GWO's exploration capabilities by utilizing Levy flight distribution with adjustable operators. Das et. al. [90] used the parameter-free JAYA algorithm to solve the stochastic ORPD problem with load uncertainties and Weibull distribution-modeled probabilistic wind power. They tested this method on IEEE 30 and 57-bus systems under various loads. JAYA consistently had the lowest P_{Loss} and VD and converged more quickly than other optimization approaches. Biswas et

turnitin Page 57 of 208 - Integrity Submission Submission ID trn:oid:::27535:142293373

turnitin Page 58 of 208 - Integrity Submission Submission ID trn:oid:::27535:142293373

al. [91] solved the stochastic ORPD problem utilizing the Success History Based Adaptive Differential Evolution (SHADE) approach. Considering the inherent unpredictability of the nature of wind speed, solar irradiation and load demand, the authors utilized various PDFs. Following the generation of scenarios, a Monte Carlo simulation (MCS) was employed and a reduction-based approach was used to pick the desired scenarios from the created scenarios. The suggested approach was utilized to reduce P_{Loss} and VD in the IEEE 30 and 57-bus systems. Khan et al. [92] developed a Fractional Calculus with PSO and Gravitation Search Algorithm (FPSOGSA) to improve PSOGSA's global search capabilities by adding a fractional derivative of the velocity component. The study focused on utilizing FPSOGSA to reduce P_{Loss} and VD in the ORPD problems of IEEE 30 and 57-bus systems, taking into account wind and solar power variability at different loads. Ebeed et al. [93] applied the Marine Predators algorithm (MPA), which addresses the ORPD issue while accounting for solar, wind, and load demand uncertainties. The algorithm was examined on the IEEE 30-bus system to reduce system P_{Loss} and VD. Ebeed et al. [94] used an improved Lightning Attachment Procedure Optimization (LAPO) to address uncertainty in RESs while solving the ORPD problem. To increase the searching capabilities and minimize stagnation of the conventional LAPO, Levy flight and spiral motion of particles have been used. The suggested technique was implemented using the IEEE 30-bus system for reducing P_{Loss} and VD under deterministic and probabilistic ORPD problems. Hassan et al. [95] used the Rao-3 technique, a simple optimization technique for the constrained nonlinear ORPD problem in power systems with solar, wind, and load demand uncertainties. The algorithm was tested and validated using the IEEE 30, 57 and 118-bus systems to minimize P_{Loss} and VD. Khan et al. [96] suggested an improved Marine Predators Algorithm (IMPA) that updates particle positions in orientation movement around sorted particles and adaptive steps near the best particle. The algorithm was implemented on the IEEE 30 and 57-bus systems to minimize P_{Loss} and VD while considering solar and wind power uncertainties under various loading situations. Naidji et al. [97] proposed a Quantum-behaved Particle Swarm Optimization Differential Mutation (QPSODM) algorithm to solve the ORPD problem with uncertainties of RES and load demand. The algorithm was tested on Adrar's isolated system and IEEE 14-bus systems for minimizing P_{Loss} and VD, and its performance was compared with recent algorithms.

turnitin Page 58 of 208 - Integrity Submission Submission ID trn:oid:::27535:142293373

turnitin Page 59 of 208 - Integrity Submission Submission ID trn:oid:::27535:142293373

Table 2.1: Summary of algorithms for renewable technologies and variable load demand.

Ref	Algorithm	LM	PV	WT	HT	Highlights	Objectives	System	Limitations
[89]	EGWO	✓	✗	✗	✗	Improved exploration using Lévy flight; mitigates premature convergence	$\mathbf{P}_{\text{Loss}}$, VD	IEEE 30-bus	Dependent on scaling factor; high computational complexity
[90]	JAYA	✓	✗	✓	✗	Parameter-free approach; simple and robust performance	$\mathbf{P}_{\text{Loss}}$, VD	IEEE 30/57-bus	Scalability issues; sensitive to problem characteristics
[91]	SHADE	✓	✓	✓	✗	Efficient search; strong constraint handling using epsilon method	$\mathbf{P}_{\text{Loss}}$, VD	IEEE 30/57-bus	Slow convergence; complex constraint handling
[92]	FPSOGSA	✓	✓	✓	✗	Combines PSO and GSA; enhanced exploration via fractional calculus	$\mathbf{P}_{\text{Loss}}$, VD, VSI	IEEE 30-bus	High computational complexity; sensitive to parameters
[93]	MPA	✓	✓	✓	✗	Lévy flight and Brownian motion improve global search ability	$\mathbf{P}_{\text{Loss}}$, VD	IEEE 30-bus	Risk of premature convergence; problem dependent
[93]	ILAPO	✓	✓	✓	✗	Enhanced LAPO with Lévy flight; avoids local optima	$\mathbf{P}_{\text{Loss}}$, VD	IEEE 30/57-bus	Slower convergence; limited generalization
[95]	Rao-3	✓	✓	✓	✗	Simple structure; fewer parameters; balanced search capability	$\mathbf{P}_{\text{Loss}}$, VD	IEEE 30/57/118-bus	Initialization dependent; limited scalability

turnitin Page 59 of 208 - Integrity Submission Submission ID trn:oid:::27535:142293373

turnitin Page 60 of 208 - Integrity Submission Submission ID trn:oid:::27535:142293373

Ref	Algorithm	LM	PV	WT	HT	Highlights	Objectives	System	Limitations
[96]	IMPA	✓	✓	✓	✗	Spiral predator motion; adaptive mechanism improves exploitation	P_{Loss}, VD, VSI	IEEE 30-bus	Limited exploration; high computational cost
[97]	QPSODM	✓	✓	✓	✗	Quantum-based behavior enables adaptive search capability	P_{Loss}, VD	IEEE 14 bus, Adrar isolated system	Many parameters; increased complexity
[98]	ESOA	✓	✓	✓	✗	Strong balance between exploration and exploitation	P_{Loss}	IEEE 118-bus	High computational burden
[99]	EAOA	✓	✓	✓	✗	Simple and robust mathematical framework; balanced exploration and exploitation	P_{Loss}, VD	IEEE 57-bus	May suffer from slow convergence in high-dimensional search spaces
[100]	MAHA	✓	✓	✓	✓	Robust against local optima; adapts to different problem scales	P_{Loss}, VD, VSI	IEEE 30-bus	High computational load; difficult parameter tuning

Note: LM: Load Modelling, PV: Photovoltaic, WT: Wind Technology, HT: Hydro Technology

Khan et al. [98] proposed an Enhanced Skilled Optimization Algorithm (ESOA) for stochastic ORPD that reduced expected P_{Loss} by 24% by optimally placing wind and PV units in the IEEE 118-bus system, demonstrating resilience to uncertainty. Megantoro et al. [99] proposed an Enhanced Archimedes Optimization Algorithm (EAOA) to solve the multi-objective ORPD (MOORPD) problem in a hybrid wind–solar integrated power system. Wind speed and solar irradiance uncertainties were modeled using Weibull and lognormal probability distributions, respectively. The proposed method was validated on the IEEE 57-bus test system and demonstrated effective ORPD performance under RESs uncertainty conditions. Jamal et al. [100] implemented a novel approach called the Modified Artificial

turnitin Page 60 of 208 - Integrity Submission Submission ID trn:oid:::27535:142293373

turnitin Page 61 of 208 - Integrity Submission Submission ID trn:oid:::27535:142293373

Hummingbird Algorithm (MAHA) to tackle the difficulties of optimizing ORPD considering variability in RES and load demand. The research provides an efficient version of the AHA for solving stochastic and deterministic ORPD problems using Levy flight and distance bandwidth motion. This method was validated and executed on the IEEE 30-bus system to minimize P_{Loss}, VD and VSI.

2.7 Research Gaps

Over the past few decades, extensive research has been conducted to improve the performance of metaheuristic optimization techniques, motivated by the No Free Lunch Theorem [101], which states that no single optimization algorithm can effectively solve all optimization problems. Consequently, numerous enhanced and hybrid algorithms have been developed to overcome the limitations of existing methods. However, despite these advancements, several research challenges remain unresolved in the field of ORPD.

Traditional single-objective optimization techniques are unable to adequately address the conflicting nature of ORPD objectives, as they focus on obtaining only one optimal solution. Although scalarization methods such as the weighted sum approach are widely used, they often fail to accurately approximate non-convex and discontinuous Pareto fronts. Therefore, more efficient and scalable multi-objective optimization approaches are required to achieve better convergence, solution diversity, and practical applicability in MOORPD problems.

Furthermore, the increasing penetration of RESs and the dynamic nature of modern power systems have significantly increased the complexity of ORPD problems. Although considerable progress has been made using conventional, metaheuristic, and hybrid optimization methods, several important gaps still exist in both single-objective and multi-objective ORPD formulations.

The major research gaps identified from the literature are summarized as follows:

- **Difficulty in obtaining feasible solutions under complex constraints:** Existing optimization methods often struggle to consistently generate feasible solutions while satisfying all operational constraints. This challenge becomes

turnitin Page 61 of 208 - Integrity Submission Submission ID trn:oid:::27535:142293373

turnitin Page 62 of 208 - Integrity Submission Submission ID trn:oid:::27535:142293373

more critical in multi-objective ORPD problems due to the simultaneous consideration of multiple conflicting objectives.

- **Limited consideration of time-varying load conditions:** Most ORPD studies are conducted under static loading assumptions, which do not accurately represent practical power system operation. The integration of time-varying load profiles in both single-objective and multi-objective ORPD remains insufficiently investigated.

- **Insufficient uncertainty modeling in ORPD:** Although RESs uncertainties associated with wind and solar generation have been addressed in some studies, comprehensive frameworks that simultaneously incorporate uncertainties in renewable generation and load demand are still lacking.

- **Limited analysis of objective interrelationships:** The interactions and trade-offs among important ORPD objectives, such as P_{Loss} minimization, VD reduction, and VSI, are not thoroughly explored. This limitation reduces the effectiveness of multi-objective decision-making strategies.

- **Lack of robust decision-making mechanisms for MOORPD:** Multi-objective optimization algorithms generally produce a set of Pareto-optimal solutions; however, identifying the most suitable compromise solution remains a major challenge. Existing decision-making approaches are often inadequate for reflecting practical operational priorities.

- **Exploration–exploitation imbalance in optimization algorithms:** Many optimization techniques fail to maintain an effective balance between global exploration and local exploitation, which may result in premature convergence, reduced solution diversity, and poor optimization performance.

- **Scalability limitations in large-scale power systems:** Several optimization methods demonstrate satisfactory performance on standard benchmark systems but experience reduced efficiency and increased computational complexity when applied to large-scale and practical power networks.

turnitin Page 62 of 208 - Integrity Submission Submission ID trn:oid:::27535:142293373

turnitin Page 63 of 208 - Integrity Submission Submission ID trn:oid:::27535:142293373

Chapter 3

Optimal Reactive Power Dispatch

3.1 Introduction

The ORPD problem is a subset of the OPF problem that focuses on the optimal allocation and control of reactive power resources in a power system. The primary objective of ORPD is to improve voltage profiles, minimize real P_{Loss}, and enhance voltage stability while satisfying system constraints. Effective reactive power management contributes significantly to the secure, reliable, and economical operation of modern power systems. Moreover, proper dispatch of reactive power resources improves transmission efficiency and increases the loadability margin of the network.

Similar to OPF, the ORPD problem involves a combination of objective functions and constraints. The solution aims to determine the optimal settings of control variables such as generator voltages, transformer tap ratios, and reactive power compensation devices. The resulting system operating condition is represented through a set of state variables, including bus voltages and phase angles.

The ORPD problem is governed by equality and inequality constraints. The equality constraints are represented by power flow equations that maintain the balance between generated and demanded power at each bus. The inequality constraints define the operating limits of system components, including generator reactive power outputs, bus voltage magnitudes, transformer tap settings, and reactive power compensation limits. Satisfying these constraints is essential for obtaining a feasible and secure operating solution.

turnitin Page 63 of 208 - Integrity Submission Submission ID trn:oid:::27535:142293373

turnitin Page 64 of 208 - Integrity Submission Submission ID trn:oid:::27535:142293373

3.2 Problem Formulation

The ORPD problem may be stated as follows [102]:

Minimize:

$$\min_{u,v} \quad f(u,v) \tag{3.1}$$

$$\text{subject to} \quad g(u,v) \leq 0 \tag{3.2}$$

$$\text{and} \quad h(u,v) = 0 \tag{3.3}$$

where the function $f(u,v)$ denotes the objective function for the ORPD problem. u is a vector denoting the independent variables. The vector, v represents the state variables. $g(u,v)$ & $h(u,v)$ reflect the constraints applied in the form of both inequality and equality, respectively.

3.2.1 Independent (control) variables

The independent variables are represented by the following vector:

$$u = [V_{G_1}, \ldots, V_{G_{N_G}}, \; Q_{C_1}, \ldots, Q_{C_{N_C}}, \; T_1, \ldots, T_{N_T}] \tag{3.4}$$

where $V_{G_1}, \ldots\ldots, V_{G_{N_G}}$ are the magnitudes of voltage at PV buses. $Q_{C_1}, \ldots, Q_{C_{N_C}}$ are shunt VAR compensators. $T_1, \ldots, T_{N_T}$ are tap ratios of transformers. N_G, N_C, and N_T are the number of generators, VAR compensators, and transformer taps, respectively.

3.2.2 Dependent variables

The following is a vector representation of the dependent variables:

$$v = [V_{L_1}, \ldots, V_{L_{N_{PQ}}}, \; Q_{G_1}, \ldots, Q_{G_{N_G}}, \; S_{L_1}, \ldots, S_{L_{N_{TL}}}] \tag{3.5}$$

where $V_{L_1}\ldots\ldots, V_{L_{N_{PQ}}}$ are load bus voltage magnitudes. $Q_{G_1}, \ldots\ldots, Q_{G_{N_G}}$ are reactive power generations. $S_{L_1}, \ldots\ldots, S_{L_{N_{TL}}}$ are transmission line apparent power flows.

turnitin Page 64 of 208 - Integrity Submission Submission ID trn:oid:::27535:142293373

turnitin Page 65 of 208 - Integrity Submission Submission ID trn:oid:::27535:142293373

3.3 Objective functions for deterministic ORPD

The proposed work in this thesis addresses the deterministic and stochastic ORPD problem, considering P_{Loss}, VD, and VSI as objective functions, which are defined as follows.

- **Minimizing Power Loss (P_{Loss})**

The minimization of P_{Loss} is a primary objective in the OPF and ORPD problems. The P_{Loss} arises due to the resistive components of transmission lines and depend on network parameters, bus voltage magnitudes, and phase angle differences. High power losses reduce system efficiency and increase operational costs.

Since P_{Loss} is strongly influenced by line conductance and voltage differences between buses, it can be effectively minimized by proper control of reactive power sources, generator voltages, and transformer tap settings. This leads to improved system efficiency and enhanced overall network performance.

$$f_L = \min P_{\text{Loss}} = \sum_{k=1}^{N_{TL}} \left[G_{kj} \left(V_k^2 + V_j^2 - 2V_k V_j \cos \delta_{kj} \right) \right] \tag{3.6}$$

where V_k and V_j correspond to the voltage magnitudes at the k-th and j-th buses, respectively. G_{kj} is the conductance across the lines k and j and δ_{kj} is the phase difference of the k-th and j-th bus. N_{TL} refers to the total number of transmission lines [103, 104].

- **Minimizing Voltage Deviation (VD)**

Voltage deviation (VD) is an important performance index used to assess the quality of voltage profiles in power systems. It represents the total deviation of load bus voltages from a specified reference value. Large voltage deviations may lead to poor power quality, reduced system efficiency, and potential voltage instability.

The voltage deviation is defined as:

$$f_{\text{VD}} = \min(VD) = \sum_{k=1}^{N_L} \left| V_k - V_i^{\text{ref}} \right| \tag{3.7}$$

where V_k is the voltage magnitude at the k-th load bus, V_i^{ref} is the reference voltage (typically taken as 1 p.u.), and N_L denotes the number of load buses [103, 104].

turnitin Page 65 of 208 - Integrity Submission Submission ID trn:oid:::27535:142293373

turnitin Page 66 of 208 - Integrity Submission Submission ID trn:oid:::27535:142293373

The objective of minimizing VD is to maintain bus voltages as close as possible to their desired reference values, thereby improving system security and operational reliability. This can be achieved by proper control of reactive power sources, generator voltages, and transformer tap settings.

- **Minimizing Voltage Stability Index (VSI)**

The Voltage Stability Index (VSI) minimization based on the L-index is formulated to enhance the overall voltage stability of a system by reducing the maximum instability level among all the load buses. The objective function is expressed as minimizing the maximum L-index value across all the load buses is given by

$$f_{\text{VSI}} = \min(L_{\max}) = \min\left[\max(L_K)\right] \tag{3.8}$$

Where $K = 1, 2, 3, \ldots, N_{PQ}$

$$L_K = \left|1 - \sum_{i=1}^{N_G} \frac{F_{ji} V_i}{V_j} \angle(\theta_{ij} + \delta_{ij})\right| \tag{3.9}$$

$$F_{ji} = -[Y_{jj}]^{-1}[Y_{ji}] \tag{3.10}$$

where Y is the admittance, θ is its phase angle, and δ is the voltage angle.

Since the L-index varies between 0 (stable condition) and 1 (voltage collapse), minimizing $\max(L_k)$ ensures that the system operates far from instability. This approach effectively identifies and strengthens the weakest buses, improves voltage profiles, and enhances the overall stability of the power system, making it widely applicable in OPF and ORPD problems [104, 105].

3.4 Constraints

The ORPD problem involves the following equality and inequality constraints [106, 107].

turnitin Page 66 of 208 - Integrity Submission Submission ID trn:oid:::27535:142293373

turnitin Page 67 of 208 - Integrity Submission Submission ID trn:oid:::27535:142293373

3.4.1 Equality constraints:

$$\sum_{k=1}^{N_G} P_{G_k} - \sum_{k=1}^{N_{PQ}} P_{D_k} - P_{\text{Loss}} = 0 \tag{3.11}$$

$$\sum_{k=1}^{N_G} Q_{G_k} - \sum_{k=1}^{N_{PQ}} Q_{D_k} - Q_{\text{Loss}} = 0 \tag{3.12}$$

where P_{G_k} and Q_{G_k} represent the active and reactive power generation at the k-th bus, P_{D_k} and Q_{D_k} denote the active and reactive power demand (load), and P_{Loss} and Q_{Loss} are the total active and reactive power losses in the system.

3.4.2 Inequality constraints:

- **Constraint on Generators:**

$$V_{G_k}^{\min} \leq V_{G_k} \leq V_{G_k}^{\max}, \quad \forall k \in N_G \tag{3.13}$$

$$P_{G_k}^{\min} \leq P_{G_k} \leq P_{G_k}^{\max}, \quad \forall k \in N_G \tag{3.14}$$

$$Q_{G_k}^{\min} \leq Q_{G_k} \leq Q_{G_k}^{\max}, \quad \forall k \in N_G \tag{3.15}$$

where V_{G_k} is the voltage at the kth bus.

- **Constraint on Transformers:**

$$T_k^{\min} \leq T_k \leq T_k^{\max}, \quad \forall k \in N_T \tag{3.16}$$

where, T_k is the tap ratio of the k-th transformer.

- **Constraint on shunt VAR compensators:**

$$Q_{C_k}^{\min} \leq Q_{C_k} \leq Q_{C_k}^{\max}, \quad \forall k \in N_C \tag{3.17}$$

where Q_{C_k} denotes the reactive power of the k-th shunt VAR compensator.

- **Security Limitations:**

$$V_{L_k}^{\min} \leq V_{L_k} \leq V_{L_k}^{\max}, \quad \forall k \in N_{PQ} \tag{3.18}$$

$$S_{L_k} \leq S_{L_k}^{\max}, \quad \forall k \in N_{TL} \tag{3.19}$$

where V_{L_k} is the voltage at the k-th load bus and S_{L_k} denotes the k-th transmission line loading.

turnitin Page 67 of 208 - Integrity Submission Submission ID trn:oid:::27535:142293373

turnitin Page 68 of 208 - Integrity Submission Submission ID trn:oid:::27535:142293373

3.4.3 Constraints Handling

The ORPD problem involves several equality and inequality constraints that must be satisfied during the optimization process. In this work, inequality constraints are handled using a penalty function approach. The method transforms the constrained optimization problem into an unconstrained one by adding penalty terms to the objective function whenever any dependent variable violates its permissible operating limit. Consequently, infeasible solutions are assigned larger objective values, which guides the optimization process toward feasible operating conditions [108].

The augmented objective function is expressed as

$$f_{\text{aug}} = f_{\text{obj}} + \text{Penalty} \tag{3.20}$$

where f_{obj} represents the selected objective function and the penalty term is given by

$$\text{Penalty} = \lambda_1 \sum_{i=1}^{N_{PQ}} (V_{L_i} - V_{L_i}^{\lim})^2 + \lambda_2 \sum_{i=1}^{N_G} (Q_{G_i} - Q_{G_i}^{\lim})^2 + \lambda_3 \sum_{i=1}^{N_{TL}} (S_{L_i} - S_{L_i}^{\max})^2 \tag{3.21}$$

where λ_1, λ_2, and λ_3 denote the penalty coefficients. In this research work, all penalty coefficients are assigned a value of 10^6.

The violated limit value of a dependent variable y is determined as

$$y^{\lim} = \begin{cases} y^{\max}, & y > y^{\max} \\ y^{\min}, & y < y^{\min} \end{cases} \tag{3.22}$$

This constraint-handling mechanism helps maintain generator reactive power outputs, load bus voltages and transmission line loadings within their specified operating limits throughout the optimization process.

3.5 Multi-Objective ORPD

The multi-objective ORPD problem aims to optimize several conflicting objectives simultaneously while satisfying all equality and inequality constraints. In general,

turnitin Page 68 of 208 - Integrity Submission Submission ID trn:oid:::27535:142293373

turnitin Page 69 of 208 - Integrity Submission Submission ID trn:oid:::27535:142293373

a multi-objective optimization problem can be expressed as [109]

$$\begin{aligned} \min \quad & f_i(u,v), \qquad i = 1,2,\ldots,M && (3.23)\\ \text{subject to} \quad & g_j(u,v) \leq 0, \qquad j = 1,2,\ldots,N_g && (3.24)\\ & h_k(u,v) = 0, \qquad k = 1,2,\ldots,N_h && (3.25) \end{aligned}$$

where M denotes the total number of objective functions, while N_g and N_h represent the number of inequality and equality constraints, respectively.

For the ORPD problem, the objective vector is represented as

$$F_{\text{obj}}(u,v) = [f_1(u,v), f_2(u,v), \ldots, f_M(u,v)] \tag{3.26}$$

In this thesis, both bi-objective and tri-objective ORPD problems are investigated. The bi-objective formulation considers the simultaneous optimization of any two objectives among P_{Loss}, VD and VSI.

Accordingly, the bi-objective cases considered are

$$F_{\text{obj}}(u,v) = [P_{\text{Loss}}, VD] \tag{3.27}$$

$$F_{\text{obj}}(u,v) = [P_{\text{Loss}}, VSI] \tag{3.28}$$

The tri-objective formulation simultaneously minimizes all three objectives and is expressed as

$$F_{\text{obj}}(u,v) = [P_{\text{Loss}}, VD, VSI] \tag{3.29}$$

The solution of the MO-ORPD problem is obtained as a set of Pareto-optimal solutions that represent the trade-offs among the conflicting objectives. Constraint violations are handled using the same penalty function approach described previously. During fitness evaluation, the penalty value is incorporated into each objective function to discourage infeasible solutions.

turnitin Page 69 of 208 - Integrity Submission Submission ID trn:oid:::27535:142293373

turnitin Page 70 of 208 - Integrity Submission Submission ID trn:oid:::27535:142293373

3.6 Standard Test Systems for ORPD Analysis

Standardized test systems are commonly used in ORPD studies to validate and benchmark various optimization algorithms and solution methodologies. These benchmark systems provide realistic operating environments for evaluating the effectiveness, robustness, convergence performance, and scalability of optimization techniques under different network configurations and operating constraints. The IEEE 30-bus, IEEE 57-bus, and IEEE 118-bus systems considered in this research are widely used in the literature for minimizing P_{Loss}, reducing VD, and enhancing VSI in ORPD problems. The Newton-Raphson method [110] is employed for power flow analysis, while MATPOWER [111] serves as the computational tool for system analysis and performance evaluation.

3.6.1 IEEE 30-bus System

This system is one of the most widely used benchmark systems for ORPD analysis due to its moderate complexity and computational efficiency. The system consists of 6 generators, 4 tap-changing transformers, 9 shunt reactive compensation devices, and 41 transmission branches with 19 control variables. The total connected load of the system is 283.4 MW and 126.2 MVAr. The base case real P_{Loss}, VD, and VSI of the system are 6.212 MW, 1.1758 p.u., and 0.1672 p.u., respectively. Owing to its balanced complexity and realistic operational characteristics, the IEEE 30-bus system is widely utilized for validating ORPD optimization algorithms [112].

3.6.2 IEEE 57-bus System

This system provides a larger and more complex network configuration suitable for comprehensive ORPD analysis. The system consists of 7 generators, 17 tap-changing transformers, 3 shunt reactive compensation devices, and 89 transmission branches with 27 control variables. The total connected load of the system is 1250.8 MW and 336.4 MVAr. The corresponding base case real (P_{Loss}), VD, and VSI are 28.462 MW, 1.5543 p.u., and 0.3218 p.u., respectively. Due to its larger search space and increased operational complexity, the IEEE 57-bus system is extensively

turnitin Page 70 of 208 - Integrity Submission Submission ID trn:oid:::27535:142293373

turnitin Page 71 of 208 - Integrity Submission Submission ID trn:oid:::27535:142293373

used for evaluating the robustness, convergence characteristics, and computational efficiency of advanced ORPD optimization techniques [111].

3.6.3 IEEE 118-bus System

This system is a highly interconnected, large-scale benchmark network extensively employed for advanced ORPD and power system optimization studies. The system comprises 186 transmission lines, 54 generators, 9 tap-changing transformers and 14 shunt reactive compensation devices with 77 control variables. The total connected load of the system is approximately 4242 MW and 1438 MVAr. The base case real power loss (P_{Loss}), voltage deviation (VD), and voltage stability index (VSI) of the system are 132.863 MW, 1.4393 p.u., and 0.0694 p.u., respectively. Owing to its large-scale structure, multiple operational constraints, and highly interconnected network configuration, the IEEE 118-bus system closely resembles practical modern power systems and is highly suitable for evaluating the scalability and applicability of advanced optimization and machine learning-assisted ORPD algorithms [113].

turnitin Page 71 of 208 - Integrity Submission Submission ID trn:oid:::27535:142293373

turnitin Page 73 of 208 - Integrity Submission Submission ID trn:oid:::27535:142293373

Chapter 4

Proposed Opposition-Based Hybrid Differential Evolution-Giza Pyramids Construction Optimization Algorithm

4.1 Introduction

This chapter presents a novel opposition-based hybrid Differential Evolution–Giza Pyramids Construction (DE-GPC) algorithm for solving deterministic and stochastic ORPD problems in electrical power systems. The proposed method combines Opposition-Based Learning (OBL) [114], Differential Evolution (DE) [115], and the Giza Pyramids Construction (GPC) [116] algorithm to improve convergence performance, exploration capability, and solution quality for complex nonlinear optimization problems.

The performance of the hybrid algorithm is initially validated using thirteen benchmark functions consisting of both unimodal and multimodal test functions. Further, the algorithm is applied to solve single-objective deterministic ORPD problems on the IEEE 30-bus and IEEE 57-bus systems. The hybrid algorithm is also extended to solve stochastic ORPD problems on a modified IEEE 30-bus system by incorporating uncertainties in load demand, wind speed, solar irradiation, and small-hydro inflows. These uncertainties represent the intermittent and fluctuating nature of RESs and load variations in practical power systems.

The robustness and effectiveness of the hybrid algorithm are evaluated through a comparative analysis carried out with recently developed optimization algorithms, including the GPC algorithm, Honey Badger Algorithm (HBA), and

turnitin Page 73 of 208 - Integrity Submission Submission ID trn:oid:::27535:142293373

turnitin Page 74 of 208 - Integrity Submission Submission ID trn:oid:::27535:142293373

COOT Algorithm. The detailed formulation of the deterministic and stochastic ORPD problems, benchmark function analysis, uncertainty modeling, proposed hybrid algorithm, implementation procedure, and comparative simulation results are explained in the subsequent sections and subsections of this chapter.

4.2 Opposition–Based Hybrid Differential Evolution – Giza Pyramids Construction Optimization Algorithm

This section discusses the steps included in the proposed Opposition-based hybrid DE-GPC algorithm. This hybrid algorithm employs contemporary computational strategies and historical construction techniques to provide a unique and efficient approach to identifying optimal solutions in complex search spaces. The various steps involved in this novel hybrid algorithm are summarized below.

Step 1: Initialization using GPC

The GPC [116] is a meta-heuristic algorithm motivated by ancient ideologies, focusing on the Giza Necropolis, including the Khufu, Khafre, and Menkaure pyramids. Each pyramid has unique construction methods, highlighting the evolution of pyramid-building skills over time. The ancient Egyptian civilization implemented strategies to optimize construction, resulting in cost reductions and improved workforce management.

Assume that stone blocks are scattered over a construction site, and workers transport them using ramps. The starting position and cost of each block are known. The displacement depends on ramp inclination and friction. Workers continuously reposition themselves for optimal control. To seize control of the stone block, the labor force is in a constant flux; those who perform their duties most effectively are referred to as Pharaoh's special emissaries.

turnitin Page 74 of 208 - Integrity Submission Submission ID trn:oid:::27535:142293373

turnitin Page 75 of 208 - Integrity Submission Submission ID trn:oid:::27535:142293373

- **Specify the parameters**

Define population size (N), search space limits ($\vec{p_{max}}$ and $\vec{p_{min}}$), maximum iterations (it_{max}), angle (θ), crossover rate (C_r) and scaling factor (F).

- **Population initialization**

Generate an initial population of N candidate solutions (stone block or workers), where each solution $\vec{p}_i$ is sampled uniformly from the search space limits.

$$\vec{p}_i = \text{unifrnd}(\vec{p}_{\min}, \vec{p}_{\max}), \quad i = 1, 2, \ldots, N \tag{4.1}$$

- **Calculate the initial fitness**

Calculate the fitness (F_i) of each solution.

$$\mathrm{F}_i = f(\vec{p}_i), \quad i = 1, 2, \ldots, N \tag{4.2}$$

- **Selection of best initial solution (Pharaoh's special agent)**

Select the best initial solution (Pharaoh's special agent) by identifying the individual with the lowest fitness value.

$$\vec{p_{\text{best}}} = \arg\min_{\vec{p}_i}(\mathrm{F}_i) \tag{4.3}$$

Step 2: Position update using GPC

The quantity of stone block displacement on the incline relative to its prior location is given as.

$$d = \frac{v_0^2}{2g\,(\sin\theta + \mu_k \cos\theta)} \tag{4.4}$$

where v_0 represents the initial velocity of the stone blocks, g represents gravity, θ denotes the inclination angle formed by the ramp with the horizontal plane and μ_k represents the coefficient of kinetic friction. The friction effect is ignored for the worker. The worker's new position is given by.

$$x = \frac{v_0^2}{2g \sin\theta} \tag{4.5}$$

turnitin Page 75 of 208 - Integrity Submission Submission ID trn:oid:::27535:142293373

turnitin Page 76 of 208 - Integrity Submission Submission ID trn:oid:::27535:142293373

Equations (4.4) and (4.5), yield a new position (solution) $\vec{p}_i^{\text{new}}$, which is represented by Equation (4.6).

$$\vec{p}_i^{\text{new}} = (\vec{p}_i + d) \times x \times \vec{\varepsilon}_i \tag{4.6}$$

where $\vec{p}_i$ represents the current position, d is the stone block displacement, x is the worker movement along the ramp, and $\vec{\varepsilon}_i$ is a stochastic vector sampled from a Uniform distribution centered at zero, with values within ± half of the range of each decision variable.

Step 3: Opposition-Based Learning (OBL)

In 2005, Tizhoosh developed OBL [114], an efficient optimization algorithm that efficiently explores search spaces by examining solutions and their opposites, enhancing convergence rates and obtaining superior solutions. The opposite position of $\vec{p}_i^{\text{new}}$ is calculated as follows.

$$\vec{p}_i^{\text{opp}} = \vec{p}_{\max} + \vec{p}_{\min} - \vec{p}_i^{\text{new}} \tag{4.7}$$

where, $\vec{p}_i^{\text{opp}}$ represents the opposite of the current position. Where $\vec{p}_{\max}$ is the maximum and $\vec{p}_{\min}$ is the minimum allowable limit of the search space. This strategy in the proposed hybrid algorithm improves exploration in the initial phases by enhancing population diversity, while in the later phases, it improves exploitation by guiding the search toward the most promising areas of the solution space. Although the enhancement mechanism differs across domains, similar strategies have been justified in related optimization research, where energy-driven approaches explicitly motivate their design choices in terms of exploration–exploitation trade-offs [117].

Step 4: DE Mutation and Crossover

DE, created by Storn et. al. [115], is a well-recognized and most extensively utilized optimization technique that solves complex optimization problems. DE is a member of the Evolutionary Algorithm (EA) family and is a popular approach to tackling a broad range of optimization issues. DE's search strategy is fundamental

turnitin Page 76 of 208 - Integrity Submission Submission ID trn:oid:::27535:142293373

turnitin Page 77 of 208 - Integrity Submission Submission ID trn:oid:::27535:142293373

and robust, featuring only a handful of specific parameters like crossover rate and scaling factor. Like other EAs, DE uses three techniques to generate new solutions: mutation, crossover, and selection.

Select three unique individual $(\vec{q}_a, \vec{q}_b, \vec{q}_c)$ randomly from the population. Construct the donor vector employing the mutation strategy:

$$\vec{u} = \vec{q}_a + F \cdot (\vec{q}_b - \vec{q}_c) \tag{4.8}$$

For each element i of the vector, perform crossover to create the trial vector:

$$\vec{w}_i = \begin{cases} u_i, & \text{if } r_i \leq C_r \text{ or } i = k \\ p_i, & \text{otherwise} \end{cases} \tag{4.9}$$

where $r_i \sim U(0,1)$, and k is an arbitrarily selected dimension index to ensure that the trial vector $\vec{w}_i$ inherits one or more dimensional components from the donor vector $\vec{u}_i$.

Step 6: Selection

To ensure a constant population size throughout subsequent generations, the algorithm's successive phase entails selection to decide which of the trial, target or opposite vector will persist until the subsequent generation. For each worker, the new solution $f(\vec{p}_i^{\text{new}})$, opposite $f(\vec{p}_i^{\text{opp}})$, and trial $f(\vec{w}_i)$ is compared. The description of the selection operation is as follows:

$$\vec{p}_i = \arg\min \left\{ f\left(\vec{p}_i^{\text{new}}\right), f\left(\vec{p}_i^{\text{opp}}\right), f\left(\vec{w}_i\right) \right\} \tag{4.10}$$

This ensures the solution contains the best population. Repeat the above steps until the termination criterion is satisfied. Figure 4.1 illustrates the proposed hybrid algorithm flowchart.

turnitin Page 77 of 208 - Integrity Submission Submission ID trn:oid:::27535:142293373

turnitin Page 78 of 208 - Integrity Submission Submission ID trn:oid:::27535:142293373

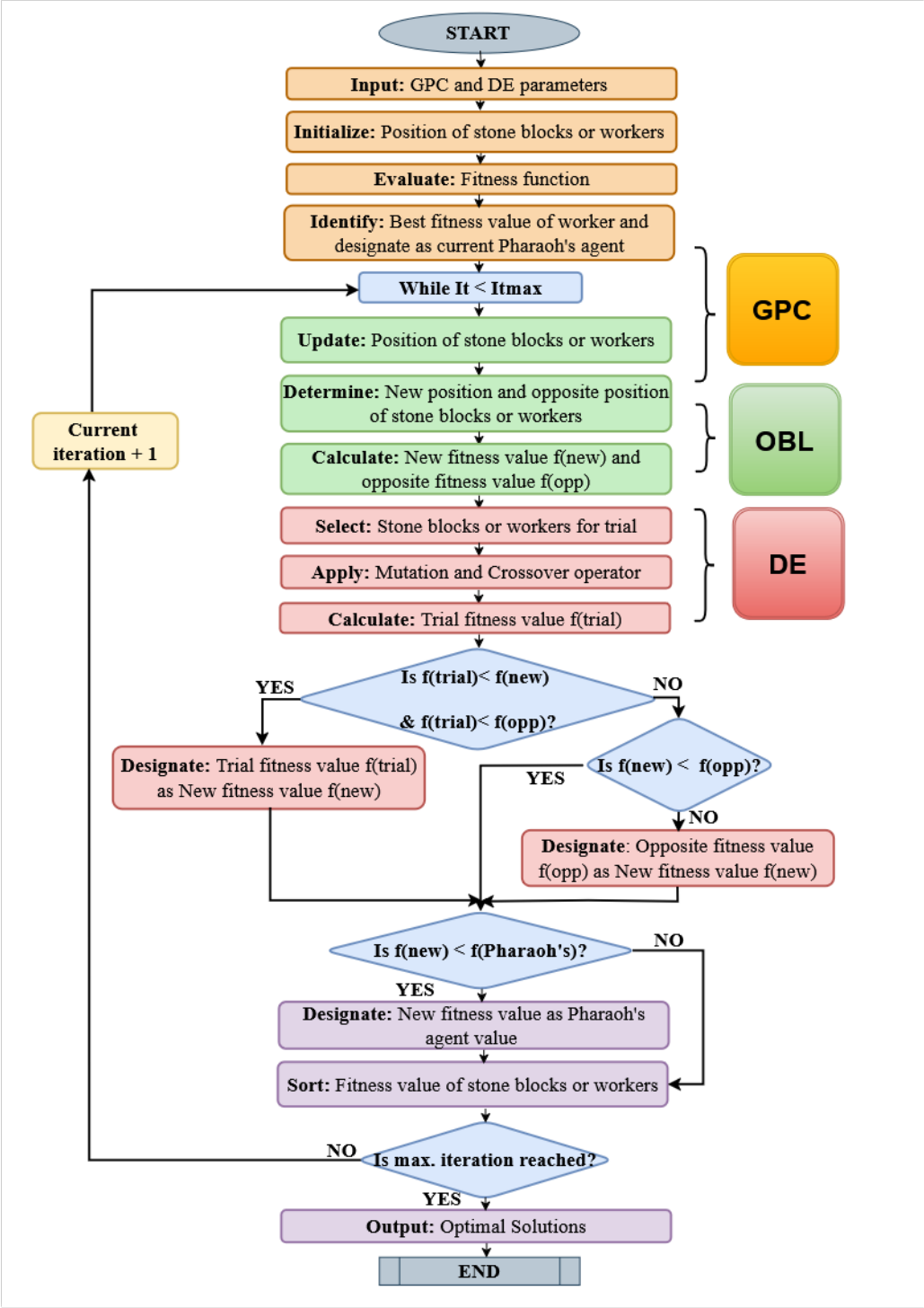


Fig. 4.1: Flowchart of the proposed hybrid method.

turnitin Page 78 of 208 - Integrity Submission Submission ID trn:oid:::27535:142293373

turnitin Page 79 of 208 - Integrity Submission Submission ID trn:oid:::27535:142293373

4.3 Modeling the Load and RESs Uncertainties

4.3.1 Scenario Generation

This research work uses continuous PDFs to model uncertainties in load demand and the power generation from wind, solar and hydro power plants.

- **Wind Power**

Wind speed uncertainty is estimated using the following Weibull PDF function [118].

$$f_v(v_w) = \frac{\beta}{\alpha}\left(\frac{v_w}{\alpha}\right)^{\beta-1} \exp\left[-\left(\frac{v_w}{\alpha}\right)^{\beta}\right], \quad 0 < v_w < \infty \tag{4.11}$$

Here, the Weibull PDF has a scale parameter (α) of 9, while the shape parameter (β) is 2.

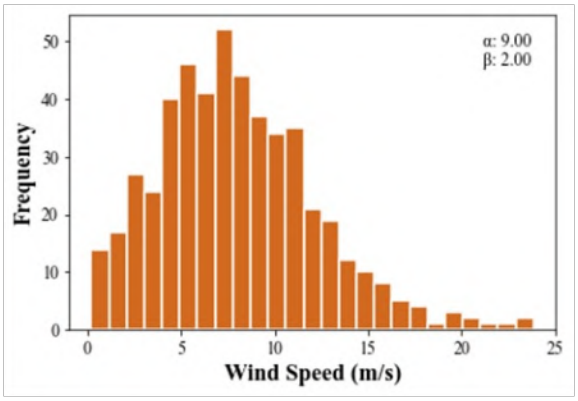


Fig. 4.2: Wind speed scenarios created using Weibull PDF (bus 5).

The mathematical expression that describes the correlation of the output power in a wind farm (P_w) and wind speed is expressed as follows:

$$P_w(v_w) = \begin{cases} 0, & v_w < v_{w,i} \text{ or } v_w > v_{w,\text{out}} \\ P_{\text{wr}}\left(\frac{v_w - v_{w,i}}{v_{\text{wr}} - v_{w,i}}\right), & v_{w,i} \le v_w \le v_{\text{wr}} \\ P_{\text{wr}}, & v_{\text{wr}} \le v_w \le v_{w,\text{out}} \end{cases} \tag{4.12}$$

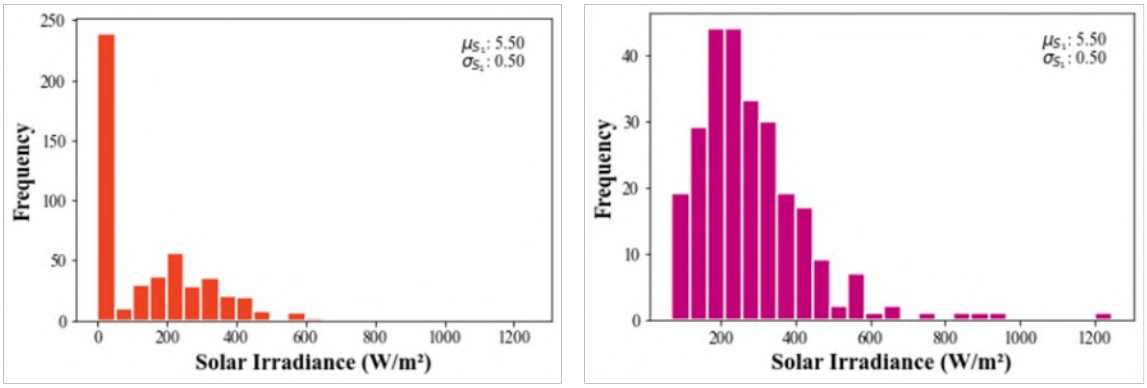
where P_{wr} denotes the nominal power of a single wind turbine. The cut-in ($v_{w,i}$), cut-out ($v_{w,out}$) and rated (v_{wr}) wind speeds of the wind turbine are 3 m/s, 25 m/s and 16 m/s, respectively, identical to the statistical data of the 3-MW

77

turnitin Page 79 of 208 - Integrity Submission Submission ID trn:oid:::27535:142293373

turnitin Page 80 of 208 - Integrity Submission Submission ID trn:oid:::27535:142293373

Enercon E82-E4 turbine. Figure 4.2 shows 500 MCS of the Weibull PDF-based wind speed distribution. In this research work, a thermal generator located at bus 5 of the IEEE-30 bus has been substituted by a wind farm having 25 turbines, each rated at 3 MW.



(a) Scenarios for solar irradiance of the generator bus.

(b) Scenarios for solar irradiance (without zero irradiance) of the generator bus

Fig. 4.3: Solar irradiance scenarios created using Lognormal PDF (bus 8).

- **PV Power**

The output of solar PV units changes depending on the daily and seasonal fluctuations in solar irradiation. The lognormal PDF employed for assessing solar irradiation is defined as follows [31]:

$$f_s(g_{s_1}) = \frac{1}{g_{s_1}\,\sigma_{s_1}\,\sqrt{2\pi}} \exp\left(-\frac{(\ln g_{s_1} - \mu_{s_1})^2}{2\sigma_{s_1}^2}\right), \quad \text{for } g_{s_1} \geq 0 \tag{4.13}$$

where μ_{s_1} signifies the mean and σ_{s_1} denotes the standard deviation (Std.) of the natural logarithm of solar irradiance, i.e., $\ln(g_{s_1})$. The values selected for μ_{s1} and σ_{s_1} are 5.5 & 0.5, respectively. Figure 4.3 (a) illustrates the solar irradiance possibilities generated by the MCS. It's essential to acknowledge that the lognormal distribution of solar irradiance incorporates the period of sunlight availability, especially during daytime. Due to the absence of sunlight for half the day, a zero-irradiance initialization is applied with a probability of 50%, representing the day/night split assumption. During the nighttime, solar irradiation and therefore

turnitin Page 80 of 208 - Integrity Submission Submission ID trn:oid:::27535:142293373

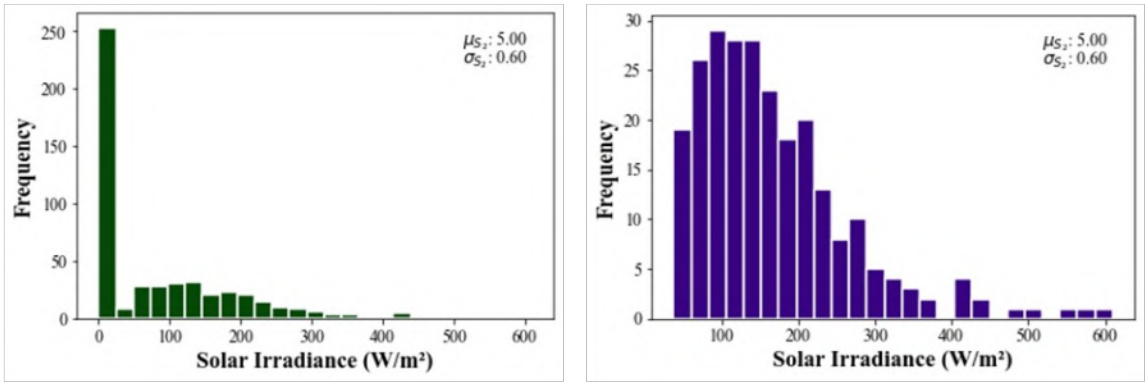
turnitin Page 81 of 208 - Integrity Submission Submission ID trn:oid:::27535:142293373

the generation of photovoltaic (PV) energy are typically negligible due to the absence of sunlight, which accounts for almost half of the 24-hour day. The remaining 50% chance encompasses the potential outcomes of solar irradiation generated using a lognormal distribution. Figure 4.3 (b) reproduces the pattern of solar irradiance after removing the zero-irradiance seen in Figure 4.3 (a).

The equation presented below illustrates the correlation between solar radiation (g_{s_1}) and power output (P_{s_1}).

$$P_{s_1}(g_{s_1}) = \begin{cases} P_{sr_1}\left(\dfrac{g_{s_1}^2}{g_{std}\, r_c}\right), & \text{for } 0 < g_{s_1} < r_c \\ P_{sr_1}\left(\dfrac{g_{s_1}}{g_{std}}\right), & \text{for } g_{s_1} \geq r_c \end{cases} \tag{4.14}$$

The PV plant's rated power (P_{sr_1}) is set at 50 MW. The standard environment's solar irradiation (g_{std}) is 1000 W/m^2. The irradiation point r_c has been set at 120 W/m^2. In this research, we employed a solar PV system on bus 8 of the IEEE-30 bus as a substitute for the traditional generator.



(a) Scenarios for Solar irradiance of the generator bus

(b) Scenarios for Solar irradiance (without zero irradiance) of the generator bus

Fig. 4.4: Solar irradiance scenarios created using Lognormal PDF (bus 13).

- **Hybrid (Solar and Small-Hydro) System**

In the modified IEEE 30-bus system, a solar PV plant (45 MW) and a small hydro plant (5 MW) have been incorporated at bus number 13, replacing the thermal generator. The small hydro and solar PV units jointly generate power at this bus.

turnitin Page 81 of 208 - Integrity Submission Submission ID trn:oid:::27535:142293373

turnitin Page 82 of 208 - Integrity Submission Submission ID trn:oid:::27535:142293373

- **PV Power**

The lognormal PDF, which is described in Equation 4.13, is also used to generate scenarios for a solar PV unit connected at bus no. 13. Here, the values of mean (μ_{s_2}) and Std. (σ_{s_2}) are taken as 5 and 0.6, respectively. Figure 4.4 (a) displays the solar irradiance (g_{s_2}) scenarios generated using the MCS. After eliminating zero irradiance, the remaining scenarios are replicated in Figure 4.4 (b). Equation 4.14 determines the power output of the chosen scenarios using the solar PV unit's rated power of 45 MW.

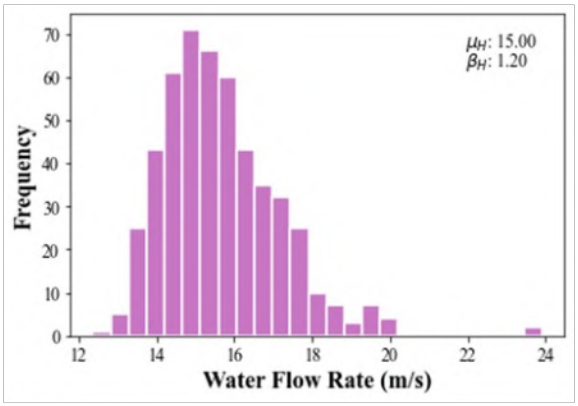


Fig. 4.5: Water flow rate scenarios created using Gumbel PDF (bus 13).

- **Hydro Power**

The Gumbel, an extreme value distribution, is widely accepted as the model for river flow rates. The Gumbel distribution is characterized by its PDF, which may be expressed as:

$$f_Q(Q_w) = \frac{1}{\gamma_H} \exp\left(\frac{Q_w - \lambda_H}{\gamma_H}\right) \exp\left[-\exp\left(\frac{Q_w - \lambda_H}{\gamma_H}\right)\right] \tag{4.15}$$

where γ_H denotes the shape parameter, λ_H represents a location parameter and Q_w denotes the water flow rate. The values of λ_H and γ_H are 15 and 1.2, respectively. Figure 4.5 demonstrates the 500 MCS produced for the Q_w using the Gumbel PDF. The power generated by a small hydro plant is determined by the rate

turnitin Page 82 of 208 - Integrity Submission Submission ID trn:oid:::27535:142293373

turnitin Page 83 of 208 - Integrity Submission Submission ID trn:oid:::27535:142293373

at which water flows (Q_w) and the effective pressure head (H_w). Mathematically, the small hydro unit's power output can be shown by the equation below.

$$P_H(Q_w) = \eta * g * \rho * H_w * Q_w \tag{4.16}$$

where η represents the turbine-generator assembly's efficiency, ρ denotes the density of water and g represents gravitational acceleration. The variables used to compute a small hydropower plant's output are η=0.85, $g = 9.81 m/s^2$, $\rho = 1000 Kg/m^3$ and $H_w = 25m$.

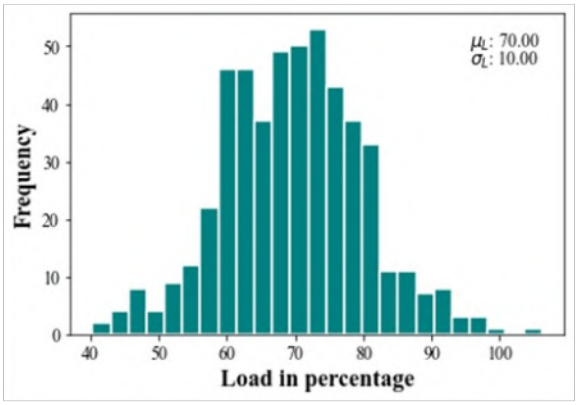


Fig. 4.6: Load demand scenarios created using Normal PDF.

- **Load Demand**

The equation for load uncertainty based on a Normal PDF is given below [119]:

$$f_l(p_L) = \frac{1}{\sigma_L \sqrt{2\pi}} \exp\left(-\frac{(P_L - \mu_L)^2}{2\sigma_L^2}\right) \tag{4.17}$$

where p_L denotes the load's normal distribution probability density. μ_L and σ_L denote the load demand's mean and Std., respectively. The selected value for μ_L and σ_L is 70 and 10, respectively. Figure 4.6 demonstrates the 500 MCS produced for load demand using the normal PDF.

Initially, each of the 500 scenarios generated using MCS for solar irradiance, wind speed, water flow rate and load demand is integrated into a comprehensive multidimensional scenario vector, as illustrated in the equation below, which

turnitin Page 83 of 208 - Integrity Submission Submission ID trn:oid:::27535:142293373

turnitin Page 84 of 208 - Integrity Submission Submission ID trn:oid:::27535:142293373

encapsulates all pertinent system variables concurrently. The i-th element of the scenario vector, denoted by S_i, is defined as:

$$S_i = \begin{bmatrix} v_{w,i} & g_{s_1,i} & g_{s_2,i} & Q_{w,i} & p_{L,i} \end{bmatrix}, where \quad i = 1, 2, \ldots, N_s \tag{4.18}$$

Algorithm 1 : Backward Reduction Algorithm

Initialization:

- Load $S_1, S_2, \ldots, S_{N_s}$ scenarios. (where N_s =500)
- Allocate the same probability $p_i = 1/N_s$ to each scenario.
- Calculate pair-wise distances $X_{S_i S_j} = \|S_i - S_j\|$ for all scenarios. Where $i = 1, 2, \ldots, N_s$ and $j = 1, 2, \ldots, N_s$.
- Create the distance matrix with elements $X_{ii} = 0$ and $X_{ij} = X_{ji}$.
- Set the current number of scenarios $N_{\text{current}} = N_s$ and define the stopping number N_{target}. (where N_{target} =10)

Steps:

1. Determine the two nearest situations based on the distance matrix.
2. Eliminate the scenario with a lower probability and allocate its probability to the remaining scenario.
3. Update $N_{\text{current}} \leftarrow N_{\text{current}} - 1$.
4. Conduct distance calculations for the remaining scenarios.
5. Repeat until $N_{\text{current}} = N_{\text{target}}$.

4.3.2 Scenario Reduction

Considering the computational complexity and time constraints, utilizing all generated scenarios directly in stochastic optimization problems is often not feasible. Therefore, scenario reduction is essential to reduce computational

turnitin Page 84 of 208 - Integrity Submission Submission ID trn:oid:::27535:142293373

turnitin Page 85 of 208 - Integrity Submission Submission ID trn:oid:::27535:142293373

complexity while preserving the important characteristics of uncertainty. For scenario reduction, the Backward Reduction Algorithm [120] is used. The steps involved in this algorithm are explained in detail in Algorithm 1. Using this algorithm, 10 scenarios were selected from the 500 scenarios. Table 4.1 provides a list of the selected illustrative scenarios and associated probabilities.

Table 4.1: Chosen scenarios with appropriate scenario aspects.

Selected Scenarios	Wind Speed V_w (m/s)	Wind Power (MW) Bus 5	Irrad. G_s (W/m^2)	PV Power (MW) Bus 8	River Flow Rate (m^3/s)	Hydro Power (MW) Bus 13	Irrad. G_s (W/m^2)	PV Power (MW) Bus 13	Load Demand (%)	Scenario Prob. Δ_{sc}
1	4.78	10.25	0.00	0.00	15.24	3.18	0.00	0.00	71.22	0.796
2	6.17	18.31	336.18	16.81	14.18	2.96	0.00	0.00	62.54	0.094
3	9.37	36.72	786.63	39.33	16.98	3.54	248.83	11.20	68.44	0.002
4	8.76	33.24	498.58	24.93	14.93	3.11	733.23	33.00	64.45	0.002
5	11.64	49.82	382.04	19.10	17.13	3.57	229.16	10.31	66.01	0.068
6	3.37	2.12	668.86	33.44	15.30	3.19	485.87	21.86	74.15	0.004
7	8.62	32.43	601.03	30.05	16.15	3.37	0.00	0.00	67.76	0.018
8	9.22	35.90	816.81	40.84	14.58	3.04	0.00	0.00	56.47	0.006
9	14.32	65.32	1000.00	50.00	14.46	3.01	60.36	1.37	86.25	0.002
10	8.02	28.94	0.00	0.00	18.76	3.91	539.42	24.27	89.39	0.008

4.3.3 Objective function for stochastic ORPD

In the event of uncertainty in the power system, numerous scenarios may be considered. A scenario-based strategy has been explored for solving the stochastic ORPD that accounts for fluctuating load demand, wind, solar and hydro power generation. All control variables are optimized under all scenarios with the appropriate levels of renewable power and load demand. Therefore, the expected P_{Loss}, VD and VSI under these scenarios must be calculated. The following formula

turnitin Page 85 of 208 - Integrity Submission Submission ID trn:oid:::27535:142293373

turnitin Page 86 of 208 - Integrity Submission Submission ID trn:oid:::27535:142293373

can determine the expected power loss for all scenarios:

$$EP_{\text{Loss,sc}} = \sum_{sc=1}^{N_{sc}} P_{\text{Loss,sc}} \times \Delta_{sc} \tag{4.19}$$

Similarly, Equation 4.20 is used to calculate the expected sum of the voltage deviation.

$$\text{EVD}_{\text{sc}} = \sum_{sc=1}^{N_{sc}} \text{VD}_{\text{sc}} \times \Delta_{sc} \tag{4.20}$$

Similar to that, Equation 4.21 is used to calculate the expected sum of the voltage stability index.

$$\text{EVSI}_{\text{sc}} = \sum_{sc=1}^{N_{sc}} \text{VSI}_{\text{sc}} \times \Delta_{sc} \tag{4.21}$$

where N_{sc} is the total scenarios that were created, Δ_{sc} is the probability of the scenarios provided.

Table 4.2: Parameter settings of different methods.

Method	Parameter	Values
COOT	Leaders (N_{Leader})	$0.1 \times N$
	Coots (N_{Coot})	$N - N_{Leader}$
HBA	Density factor (β)	6
	Control coefficient (C)	2
	Random numbers (r)	Uniform in $[0, 1]$
GPC	Ramp Angle (θ)	10
	Gravity (g)	9.8
	Friction (μ, min–max)	(1,10)
	Substitution Probability (ζ)	0.5
Proposed	Ramp Angle (θ)	10
	Gravity (g)	9.8
	Friction (μ, min–max)	(1,10)
	Crossover Rate (Cr)	0.9
	Scaling Factor (F)	0.5

turnitin Page 86 of 208 - Integrity Submission Submission ID trn:oid:::27535:142293373

turnitin Page 87 of 208 - Integrity Submission Submission ID trn:oid:::27535:142293373

4.4 Results and Discussion

4.4.1 Benchmark Functions

The proposed algorithm's performance on thirteen benchmark functions is shown in this section. The mathematical formulations for these benchmark functions [121] are presented in Table A.1 of Appendix A. Among the 13 benchmark functions shown in this table, seven are unimodal ($F1$–$F7$) and six are multimodal ($F8$–$F13$). Benchmark studies were performed using MATLAB (R2018a) on a personal computer equipped with an Intel(R) Core i5-1155G7 processor running at 2.50 GHz and 16 GB RAM. We conducted a comparative statistical analysis to evaluate the efficacy of the proposed algorithm on thirteen established benchmark functions, demonstrating its effectiveness relative to recently developed optimizers, including the GPC [116], Honey Badger Algorithm (HBA) [122], and COOT [121] algorithms. To ensure an equitable assessment in this study, each algorithm is allowed up to 500 iterations with a fixed population size of 30, a search dimension of 30 and is subjected to 30 trial runs. Table 4.2 presents the values of all the parameters for each algorithm used in this research work. Evaluation of solution quality relies on best, worst, mean, and Std. The statistical outcomes (best, worst, mean, and Std.) obtained utilizing the implementation of the proposed algorithm alongside three established methods to address thirteen functions are shown in Table 4.3.

For unimodal functions ($F1$–$F7$), which primarily test exploitation, the proposed method consistently achieved the global optimal solutions for functions $F1$ to $F4$ and near-optimal solutions for the remaining functions. Table 4.3 clearly shows that the proposed algorithm attained the lowest values in the context of best, mean, worst and Std. across all unimodal functions. Except for the function $F5$, where it achieved the highest worst (380.65), mean (87.245) and the Std. (73.399) values in comparison with other methods. This signifies that the proposed algorithm effectively utilized search.

For multimodal functions ($F8$–$F13$), which emphasize exploration, the proposed algorithm consistently showed superior performance. For functions $F9$ and $F11$, the proposed method consistently achieved the global optimal value (zero) across all statistical measures (best, worst, mean, and Std.). Even in extremely deceptive functions like $F8$ and $F10$, where other algorithms exhibit high variation (for

turnitin Page 87 of 208 - Integrity Submission Submission ID trn:oid:::27535:142293373

turnitin Page 88 of 208 - Integrity Submission Submission ID trn:oid:::27535:142293373

example, HBA obtained a worst value of 19.926 for function ($F10$), the proposed method obtains the global optimal value (8.88×10^{-16}) with minimum possible Std. (zero). For functions such as $F13$, which exhibit both multimodal and noisy features, the proposed algorithm achieved the optimal balance with a mean (2.88×10^{-8}) and a minimum Std. (1.72×10^{-8}), signifying resilience against local optima entrapments.

Furthermore, Table 4.3 presents the Friedman rank analysis, in which rankings are assigned based on the best objective values obtained by each algorithm across the 13 benchmark functions. The table reports the Summation Rank (SR), the Friedman Mean Rank (FMR), and the Overall Rank (OR) of the compared algorithms. The results demonstrate the superiority of the proposed algorithm. According to the Friedman rank analysis, the proposed algorithm achieved the best Friedman Mean Rank (FMR) of 1.0, followed by HBA (1.8462), COOT (2.6923), and GPC (3.1538). This exceptional performance of the proposed algorithm on benchmark functions demonstrates high precision, stability, and computational reliability in tackling complicated optimization problems. The convergence behavior of the proposed algorithm and the other algorithms for the thirteen benchmark functions is shown in Figure 4.7. For the unimodal functions (F1–F7), the proposed algorithm converges rapidly and attains near-optimal solutions within approximately 20–100 iterations, demonstrating its strong exploitation capability. For the multimodal functions (F8–F13), it effectively avoids local optima and attains better final fitness values than COOT, HBA, and GPC. In particular, for F8, the proposed method quickly converges to approximately (-1.2×10^4), while the competing algorithms stagnate at higher objective values. The convergence profiles show that the proposed method strikes a better balance between exploration and exploitation, leading to quicker convergence and more accurate solutions for a variety of optimization problems.

turnitin Page 88 of 208 - Integrity Submission Submission ID trn:oid:::27535:142293373

turnitin Page 89 of 208 - Integrity Submission Submission ID trn:oid:::27535:142293373

Table 4.3: Comparison of optimization algorithms on unimodal and multimodal benchmark functions.

Unimodal Functions					Multimodal Functions				
Metric	**COOT**	**HBA**	**GPC**	**Proposed**	**Metric**	**COOT**	**HBA**	**GPC**	**Proposed**
	F1					**F8**			
Best	3.72×10^{-48}	7.79×10^{-143}	2.01×10^{-23}	**0**	Best	-9443.7	-10328	-5694.5	**-12096**
Worst	1.10×10^{-25}	1.49×10^{-133}	1.29×10^{-19}	0	Worst	-6092.4	-5279.2	-4822.4	-9901.4
Mean	7.82×10^{-27}	7.55×10^{-135}	1.61×10^{-20}	0	Mean	-7422.8	-8740.7	-5236.7	-10725
Std.	2.76×10^{-26}	2.82×10^{-134}	2.67×10^{-20}	0	Std.	760.7	1069.8	206.02	513.48
Rank	3	2	4	**1**	Rank	3	2	4	**1**
	F2					**F9**			
Best	5.83×10^{-24}	2.26×10^{-75}	2.43×10^{-13}	**0**	Best	0	0	0	**0**
Worst	1.10×10^{-9}	1.71×10^{-71}	8.18×10^{-11}	0	Worst	1.13×10^{-9}	0	0	0
Mean	3.68×10^{-11}	1.19×10^{-72}	1.74×10^{-11}	0	Mean	3.78×10^{-11}	0	0	0
Std.	2.01×10^{-10}	3.44×10^{-72}	2.03×10^{-11}	0	Std.	2.06×10^{-10}	0	0	0
Rank	3	2	4	**1**	Rank	1	1	1	**1**
	F3					**F10**			
Best	1.45×10^{-47}	1.51×10^{-106}	2.40×10^{-23}	**0**	Best	8.88×10^{-16}	8.88×10^{-16}	1.61×10^{-12}	8.88×10^{-16}
Worst	9.10×10^{-23}	2.44×10^{-92}	6.94×10^{-18}	0	Worst	3.20×10^{-11}	19.926	2.70×10^{-10}	8.88×10^{-16}
Mean	3.23×10^{-24}	8.14×10^{-94}	6.60×10^{-19}	0	Mean	1.27×10^{-12}	0.6642	3.95×10^{-11}	8.88×10^{-16}
Std.	1.66×10^{-23}	4.45×10^{-93}	1.34×10^{-18}	0	Std.	5.84×10^{-12}	3.638	5.51×10^{-11}	0
Rank	3	2	4	**1**	Rank	1	1	2	**1**
	F4					**F11**			
Best	1.50×10^{-24}	6.18×10^{-60}	3.31×10^{-12}	**0**	Best	0	0	0	**0**
Worst	8.93×10^{-11}	4.94×10^{-55}	6.03×10^{-10}	0	Worst	1.80×10^{-14}	0	0	0
Mean	4.20×10^{-12}	1.99×10^{-56}	1.71×10^{-10}	0	Mean	7.11×10^{-16}	0	0	0
Std.	1.68×10^{-11}	9.04×10^{-56}	1.77×10^{-10}	0	Std.	3.30×10^{-15}	0	0	0
Rank	3	2	4	**1**	Rank	1	1	1	**1**
	F5					**F12**			
Best	28.367	21.941	27.200	**1.4695**	Best	1.96×10^{-3}	5.80×10^{-7}	0.4018	2.02×10^{-13}
Worst	208.94	26.955	28.043	380.65	Worst	1.5042	6.574×10^{-3}	0.5601	7.93×10^{-12}
Mean	47.137	23.968	27.697	87.245	Mean	0.1815	2.26×10^{-4}	0.4843	2.46×10^{-12}
Std.	45.283	0.9707	18.996	73.399	Std.	0.3582	1.20×10^{-3}	0.0399	1.93×10^{-12}
Rank	4	2	3	**1**	Rank	3	2	4	**1**
	F6					**F13**			
Best	0.0737	6.09×10^{-6}	3.9915	5.25×10^{-11}	Best	0.10699	6.85×10^{-5}	2.5246	4.56×10^{-9}
Worst	0.8491	0.2532	5.0449	7.15×10^{-10}	Worst	3.1245	1.4408	2.9860	6.88×10^{-8}
Mean	0.2229	0.0246	4.6636	2.89×10^{-10}	Mean	0.5395	0.2848	2.6767	2.88×10^{-8}
Std.	0.1504	0.0747	0.2587	1.87×10^{-10}	Std.	0.6258	0.3057	0.1059	1.72×10^{-8}
Rank	3	2	4	**1**	Rank	3	2	4	**1**
	F7					**Summary**			
Best	5.36×10^{-4}	1.02×10^{-5}	2.26×10^{-6}	8.07×10^{-8}	SR	**35**	**24**	**41**	**13**
Worst	2.33×10^{-2}	1.09×10^{-3}	2.57×10^{-4}	8.32×10^{-5}					
Mean	6.06×10^{-3}	3.46×10^{-4}	8.17×10^{-5}	2.61×10^{-5}	FMR	**2.6923**	**1.8462**	**3.1538**	**1**
Std.	5.17×10^{-3}	2.66×10^{-4}	7.61×10^{-5}	2.41×10^{-5}					
Rank	4	3	2	**1**	OR	**3**	**2**	**4**	**1**

turnitin Page 89 of 208 - Integrity Submission Submission ID trn:oid:::27535:142293373

turnitin Page 90 of 208 - Integrity Submission Submission ID trn:oid:::27535:142293373

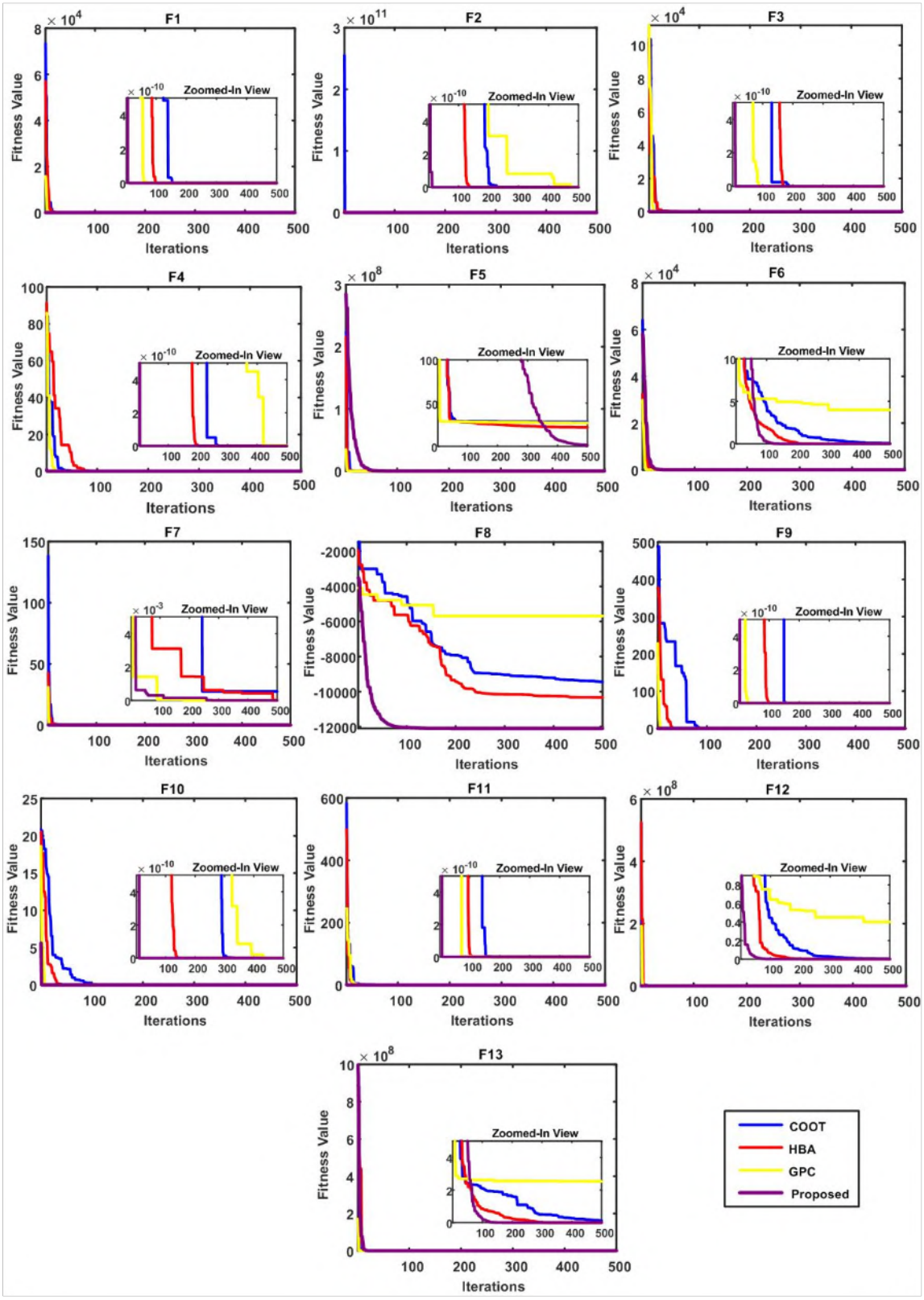


Fig. 4.7: Comparative convergence profiles of algorithms employed on benchmark functions.

turnitin Page 90 of 208 - Integrity Submission Submission ID trn:oid:::27535:142293373

turnitin Page 91 of 208 - Integrity Submission Submission ID trn:oid:::27535:142293373

4.4.2 Deterministic ORPD

4.4.2.1 IEEE 30-bus system

This section addresses the ORPD problem in the IEEE 30-bus system. The generator data of this system are provided in Table A.2 of Appendix A. The system comprises nine shunt VAR compensators, six generators, and four off-nominal tap ratio regulating transformers. The total connected load to this system is 283.4 MW and 126.2 MVAr. All variables are considered continuous, and this study maintains a constant generation (excluding swing). Shunt VAR compensators vary from 0-5 MVAr, and tap settings from 0.9-1.1 p.u. The permissible load voltage range for this system is considered to be 0.95–1.05 p.u. Therefore, the maximum allowable aggregate voltage deviation from the nominal value (1.0 p.u.) across all 24 load buses should not exceed 1.2 p.u. ($24 \times 0.05 = 1.2$). The objective of this research is to examine the versatility and efficacy of the proposed algorithm by comparing its performance with recent optimization approaches, including HBA, GPC, and COOT algorithms. For this system, each algorithm is allowed up to 300 iterations with a fixed population size of 50, and is subjected to 20 trial runs. This study focused on three objectives related to the ORPD problem: P_{Loss}, VD, and VSI.

Table 4.4 shows the optimum values for all calculated state and control variables and the permissible ranges for case studies using the IEEE 30-bus to minimize their respective objective functions. It also compares the optimal values attained for the three objectives using the proposed algorithms and other alternatives. Furthermore, the table provides the values of the remaining two objectives while minimizing the selected objective. When compared to other approaches, Table 4.4 indicates that the proposed strategy achieves the optimal values in terms of P_{Loss} (4.8612 MW), VD (0.0877 p.u.), and VSI (0.1121 p.u.). This table also displays the control variable values and reactive power produced in each case while addressing the ORPD issue using the other three algorithms. The table clearly illustrates that all values provided in every case are within the acceptable ranges. Figure 4.8 (a), Figure 4.9 (a), and Figure 4.10 (a) demonstrate the convergence characteristics achieved for optimal values across all four methods in minimizing P_{Loss} (Case 1), VD (Case 2), and VSI (Case 3) for the IEEE 30-bus system.

turnitin Page 91 of 208 - Integrity Submission Submission ID trn:oid:::27535:142293373

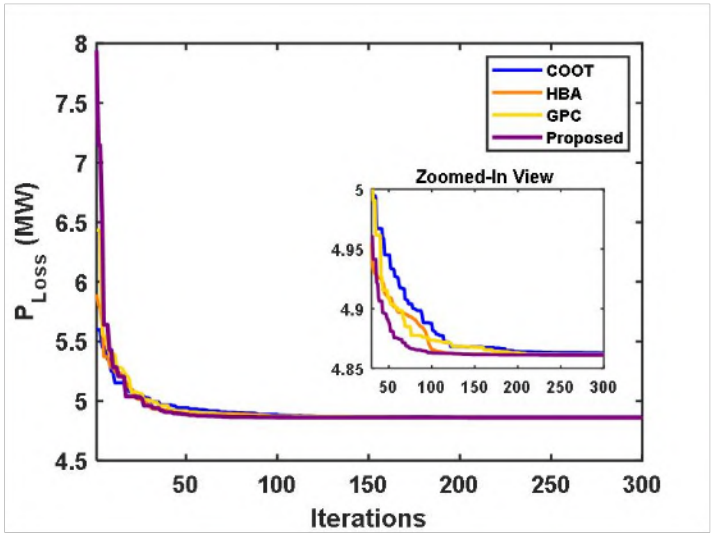
turnitin Page 92 of 208 - Integrity Submission Submission ID trn:oid:::27535:142293373

Table 4.4: Results of single-objective ORPD problem for the IEEE 30-bus system.

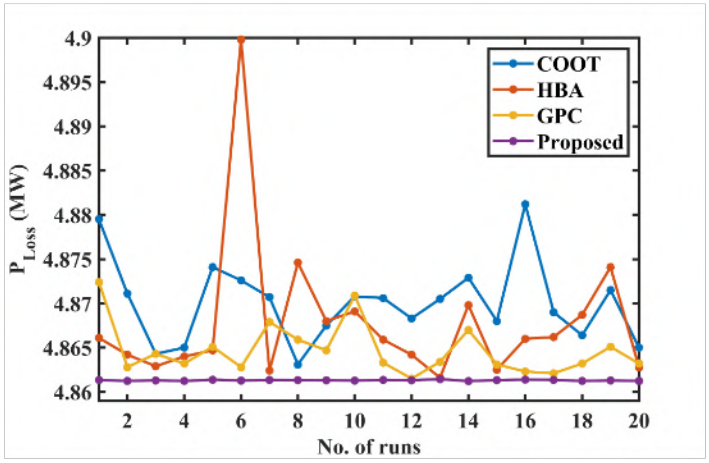
Variables	Min	Max	CASE 1 (Min P_{Loss})				CASE 2 (Min VD)				CASE 3 (Min VSI)			
			COOT	HBA	GPC	Prop.	COOT	HBA	GPC	Prop.	COOT	HBA	GPC	Prop.
Generator Voltage (p.u.)														
V1	0.95	1.10	1.0713	1.0721	1.0720	1.0718	1.0121	1.0060	1.0169	1.0032	1.0803	1.1000	1.0504	1.0533
V2	0.95	1.10	1.0622	1.0629	1.0627	1.0626	1.0097	1.0022	1.0159	0.9987	1.0566	1.0669	1.0351	1.0483
V5	0.95	1.10	1.0399	1.0404	1.0409	1.0403	1.0209	1.0200	1.0177	1.0164	1.0143	0.9914	1.0355	1.0353
V8	0.95	1.10	1.0397	1.0404	1.0403	1.0404	1.0052	1.0057	1.0072	1.0076	1.0027	1.0029	1.0064	1.0106
V11	0.95	1.10	1.0849	1.0807	1.0898	1.0896	1.0199	1.0346	1.0420	1.0741	1.0305	1.0289	1.0440	1.0290
V13	0.95	1.10	1.0553	1.0483	1.0502	1.0514	1.0204	1.0241	1.0021	1.0214	1.0316	1.0292	1.0294	1.0292
Tap Position (p.u.)														
T11	0.90	1.10	1.0269	1.0909	1.0555	1.0713	1.0351	1.0507	1.0601	1.0995	0.9338	0.9261	0.9491	0.9378
T12	0.90	1.10	0.9534	0.9004	0.9228	0.9058	0.9047	0.9000	0.9003	0.9001	0.9001	0.9000	0.9000	0.9000
T15	0.90	1.10	0.9952	0.9856	0.9885	0.9891	0.9980	1.0148	0.9641	0.9996	0.9121	0.9000	0.9001	0.9002
T36	0.90	1.10	0.9743	0.9751	0.9753	0.9747	0.9584	0.9666	0.9702	0.9694	0.9237	0.9173	0.9207	0.9234
Capacitor Bank (MVAr)														
QC10	0	5	2.0235	4.8289	0.1552	0.3436	4.7598	5.0000	4.2110	4.9386	3.7655	4.9932	5.0000	4.8045
QC12	0	5	4.9554	5.0000	4.9878	4.3832	1.1735	4.9995	0.0020	1.1693	2.0008	0.0000	0.0000	0.1943
QC15	0	5	3.8793	3.9906	4.1389	4.0096	4.6788	4.9993	5.0000	4.9874	0.0001	2.1998	1.7024	0.0000
QC17	0	5	4.9214	5.0000	4.9928	4.9980	2.3686	0.0000	0.4812	0.0196	3.3802	0.0000	4.9989	4.9957
QC20	0	5	3.2929	4.2206	3.8937	3.9408	4.9975	4.9998	4.9925	4.9981	0.8206	0.0000	3.5155	4.1689
QC21	0	5	4.9994	5.0000	5.0000	4.9997	4.9588	4.9995	5.0000	4.9994	4.9499	4.9697	3.9808	5.0000
QC23	0	5	2.5729	2.9448	3.0983	2.9627	4.9926	4.9987	5.0000	4.9992	2.7934	0.0000	2.2816	0.0077
QC24	0	5	4.9996	5.0000	5.0000	4.9997	4.4932	5.0000	5.0000	4.9994	3.4436	0.0000	0.0008	0.0959
QC29	0	5	2.3552	2.3991	2.5086	2.4596	1.6960	2.5801	3.1371	2.6395	0.0036	0.0002	0.0000	0.0013
Objective Functions														
P_{Loss} (MW)	6.212		4.8631	4.8616	4.8615	**4.8612**	5.7571	5.9361	5.6208	6.0001	5.8753	6.936	5.6997	5.7052
VD (p.u.)	1.1758		0.9085	0.9137	0.9178	0.9193	0.09433	0.08799	0.09164	**0.0877**	0.7404	0.7023	0.7293	0.7381
VSI (p.u.)	0.1672		0.122	0.1214	0.1219	0.1217	0.128	0.1301	0.1296	0.1316	0.11289	0.11256	0.11274	**0.1121**
Generator Reactive Power (MVAr)														
QG1	-20	150	-0.336	0.1039	0.2665	0.022	5.7571	-20	5.6208	-19.73	5.8753	74.5583	5.6997	0.7914
QG2	-20	60	16.0921	16.454	15.991	16.1691	0.09433	-13.41	0.09164	-19.11	0.7404	47.8731	0.7293	45.9895
QG5	-15	62.5	24.5825	24.177	25.023	24.4297	-19.72	57.0684	-19.25	53.7081	46.6401	-6.463	20.0419	45.7499
QG8	-15	48.7	29.5038	28.429	29.233	29.5615	0.9086	48.581	13.5802	46.9479	35.6777	36.9954	9.3892	47.5483
QG11	-10	40	20.0709	25.921	25.586	27.313	54.1673	17.6137	46.0623	38.6612	20.9004	-10	54.7819	-9.948
QG13	-15	44.7	4.2327	-1.033	0.4193	1.2919	48.5969	11.4384	47.6333	9.4735	32.6695	-15	45.1655	-15

turnitin Page 92 of 208 - Integrity Submission Submission ID trn:oid:::27535:142293373

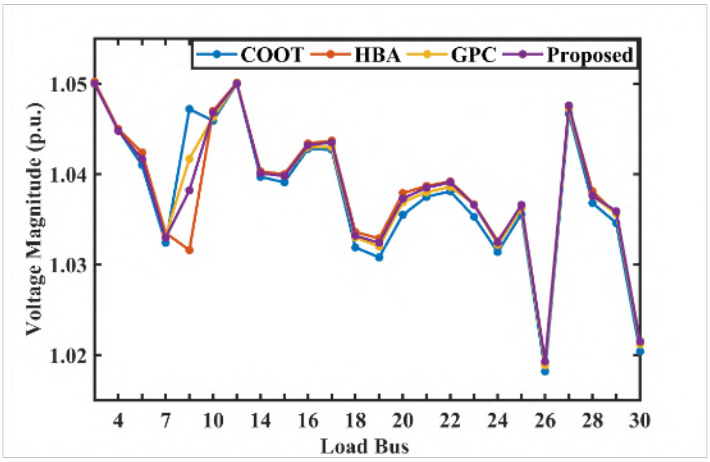
turnitin Page 93 of 208 - Integrity Submission Submission ID trn:oid:::27535:142293373



(a) Convergence curve.



(b) P_{Loss} obtained in 20 independent runs.

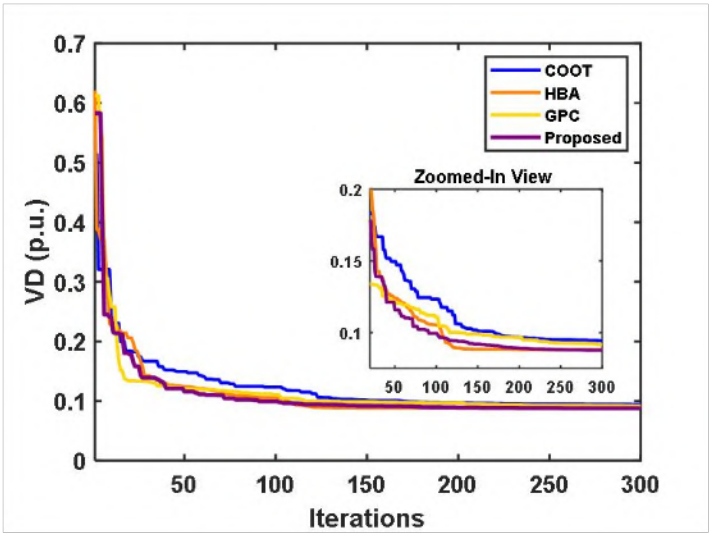


(c) Voltage magnitudes of load buses.

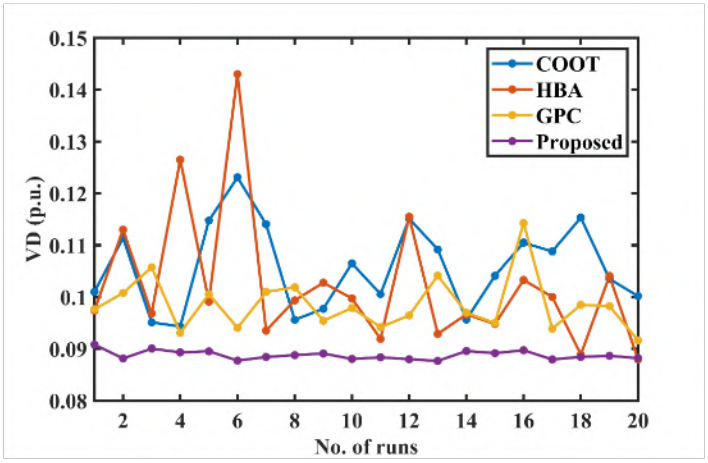
Fig. 4.8: P_{Loss} minimization (CASE 1).

turnitin Page 93 of 208 - Integrity Submission Submission ID trn:oid:::27535:142293373

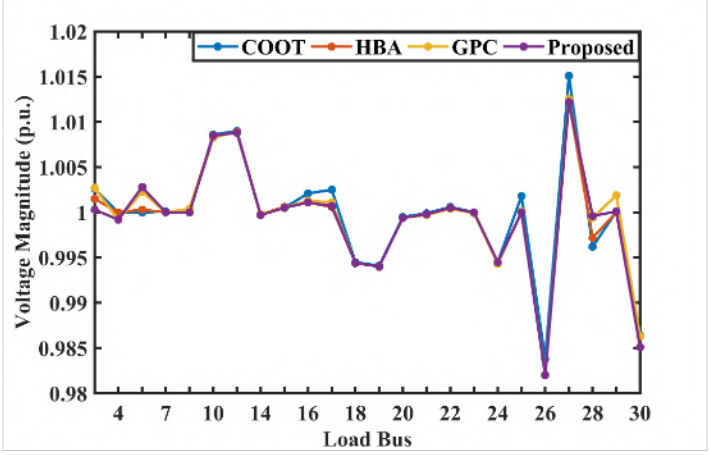
turnitin Page 94 of 208 - Integrity Submission Submission ID trn:oid:::27535:142293373



(a) Convergence curve.



(b) VD obtained in 20 independent runs.

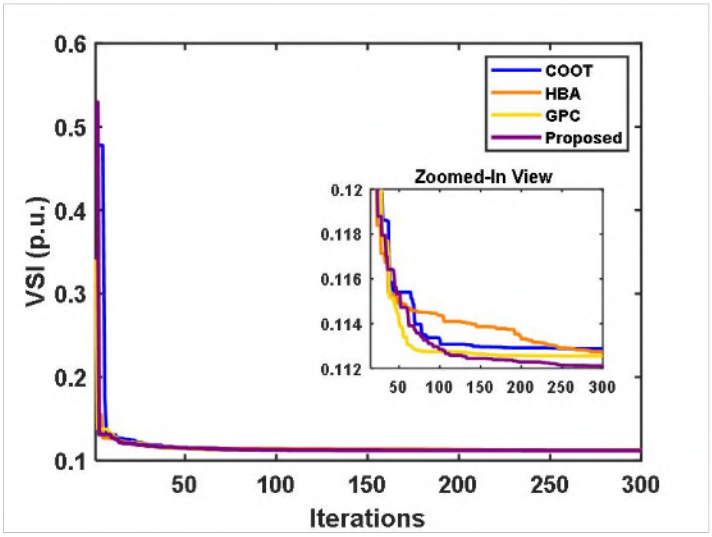


(c) Voltage magnitudes of load buses.

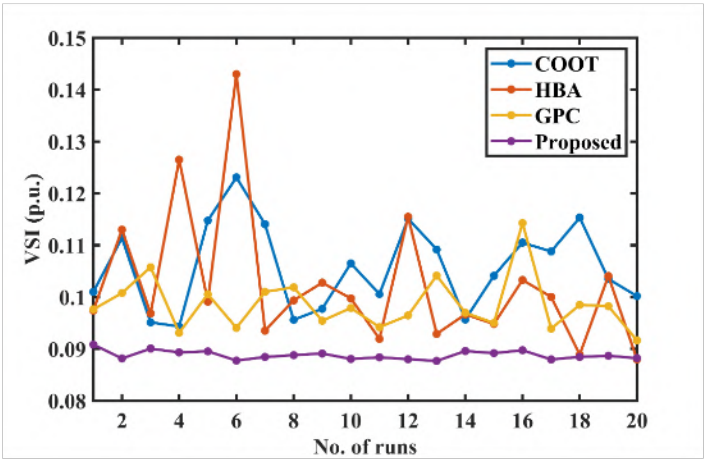
Fig. 4.9: VD minimization (CASE 2).

turnitin Page 94 of 208 - Integrity Submission Submission ID trn:oid:::27535:142293373

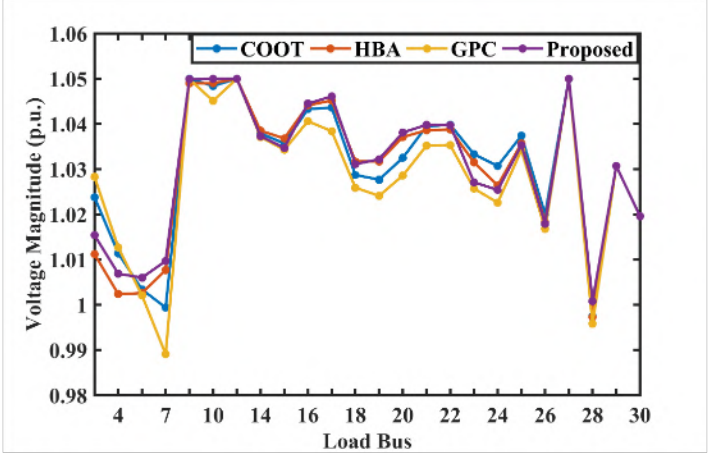
turnitin Page 95 of 208 - Integrity Submission Submission ID trn:oid:::27535:142293373



(a) Convergence curve.



(b) *VSI* obtained in 20 independent runs.



(c) Voltage magnitudes of load buses.

Fig. 4.10: *VSI* minimization (CASE 3).

turnitin Page 95 of 208 - Integrity Submission Submission ID trn:oid:::27535:142293373

turnitin Page 96 of 208 - Integrity Submission Submission ID trn:oid:::27535:142293373

Figure 4.8 (b), Figure 4.9 (b), and Figure 4.10 (b) depict the values of P_{Loss}, VD, and VSI, respectively, obtained from all four methods across 20 runs. Figure 4.8 (c), Figure 4.9 (c), and Figure 4.10 (c) provide the voltage magnitudes at the load buses achieved for each case of the IEEE 30-bus. While minimizing P_{Loss} (Case 1), the voltages of a few load buses increased to their maximum levels, as shown in Figure 4.8 (c), however, this was not the case with minimizing VD (CASE 2) and VSI (CASE 3), as shown in Figure 4.9 (c) and Figure 4.10 (c), respectively. However, minimizing voltage deviation may have a major influence on generators, forcing them to exceed reactive power production limits. A change in demand for reactive power may encourage nearby generators to deliver or absorb more VAR. Table 4.5 displays each objective's best, worst, and mean and the Std. calculated through the proposed algorithm and other algorithms over 20 runs. The statistical outcomes demonstrate that the proposed algorithm attains the minimal values for the best, worst, mean, and Std. metrics. Figure 4.11 depicts the percentage savings for each objective relative to the base scenario, utilizing all four methods. The proposed method yields the highest savings among all four methods for P_{Loss}, VD, and VSI, which are 21.75%, 92.54%, and 32.95%, respectively.

Table 4.5: Comparison of results over 20 independent runs with different algorithms for the IEEE 30-bus system.

CASE	Objective Function	Algorithm	Best	Worst	Mean	Std.
CASE 1	Power Loss minimization (MW)	COOT	4.8631	4.8812	4.8701	4.527E-03
		HBA	4.8616	4.8998	4.8679	8.134E-03
		GPC	4.8615	4.8724	4.8647	2.812E-03
		Proposed	**4.8612**	4.8614	4.8613	5.740E-05
CASE 2	Voltage Deviation minimization (p.u.)	COOT	0.09433	0.12309	0.10583	8.082E-03
		HBA	0.08799	0.1155	0.10237	1.297E-02
		GPC	0.09164	0.1143	0.09858	5.129E-03
		Proposed	**0.0877**	0.09084	0.08879	5.17E-04
CASE 3	Voltage Stability Index minimization (p.u.)	COOT	0.11289	0.1145	0.11371	1.225E-03
		HBA	0.11274	0.1178	0.11414	5.08E-04
		GPC	0.11256	0.11435	0.11347	5.17E-04
		Proposed	**0.1121**	0.11235	0.11222	7.28E-05

turnitin Page 96 of 208 - Integrity Submission Submission ID trn:oid:::27535:142293373

turnitin Page 97 of 208 - Integrity Submission Submission ID trn:oid:::27535:142293373

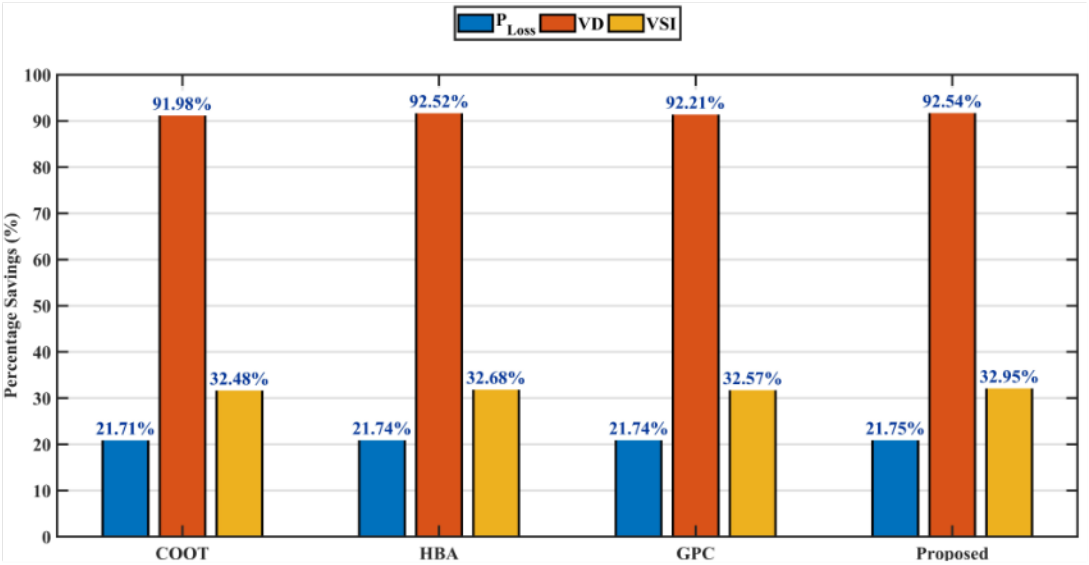


Fig. 4.11: Percentage saving achieved in P_{Loss}, VD, and VSI by each method for the IEEE 30-bus system.

4.4.2.2 IEEE 57-bus system

This section addresses the ORPD problem in the IEEE 57-bus system. The generator data of this system are provided in Table A.3 of Appendix A. This test system comprises seven generation units, three shunt VAR compensators, and seventeen off-nominal tap-changing transformers. All variables are regarded as continuous in this case, and the generation (excluding swing) remains consistent. Shunt VAR compensators vary from 0-20 MVAr, and tap settings from 0.9-1.1 p.u. The permissible load voltage range of this system is taken within the range of 0.94 to 1.06 p.u. Table 4.6 displays the optimum values for all calculated state and control variables and the acceptable ranges to optimize the corresponding objectives of the case studies using this system. The simulation results are compared to recently introduced optimization approaches such as the HBA, GPC, and COOT algorithms to illustrate the efficacy of the proposed algorithm. Each optimization algorithm runs the same number of trials for each situation to validate findings statistically. Each algorithm takes a maximum iteration of 600 for this system, a fixed population size of 50, and a trial run of 20 times. This study focused on three objectives related to the ORPD problem: P_{Loss}, VD, and VSI. Table 4.6 compares the best values attained for each of the three objectives by utilizing all four applied

turnitin Page 97 of 208 - Integrity Submission Submission ID trn:oid:::27535:142293373

turnitin Page 98 of 208 - Integrity Submission Submission ID trn:oid:::27535:142293373

methods. Furthermore, this table presents the values of the other two objectives while minimizing the specified objective.

Table 4.6: Results of single-objective ORPD problem for the IEEE 57-bus system.

Variables	Min	Max	CASE 4 (Min P_{Loss})				CASE 5 (Min VD)				CASE 6 (Min VSI)			
			COOT	HBA	GPC	Prop.	COOT	HBA	GPC	Prop.	COOT	HBA	GPC	Prop.
Generator Voltage (p.u.)														
V1	0.95	1.10	1.0873	1.0866	1.0872	1.0877	1.0242	1.0303	1.0149	1.0211	1.0323	0.9853	1.0200	1.0189
V2	0.95	1.10	1.0757	1.0761	1.0756	1.0769	1.0003	1.0206	0.9936	1.0123	1.0093	0.9560	0.9959	1.0062
V3	0.95	1.10	1.0614	1.0651	1.0613	1.0650	1.0025	1.0155	1.0003	1.0106	0.9856	0.9536	1.0005	1.0061
V6	0.95	1.10	1.0521	1.0560	1.0549	1.0565	1.0053	0.9996	1.0045	1.0028	0.9565	0.9500	1.0075	1.0320
V8	0.95	1.10	1.0693	1.0753	1.0712	1.0742	1.0398	1.0093	1.0208	1.0274	0.9556	0.9800	1.0350	1.0851
V9	0.95	1.10	1.0398	1.0439	1.0404	1.0425	1.0125	0.9903	0.9951	1.0057	0.9503	0.9560	0.9858	1.0318
V12	0.95	1.10	1.0459	1.0470	1.0455	1.0451	1.0346	1.0192	1.0215	1.0358	1.0017	0.9903	0.9715	1.0220
Transformer Tap Position (p.u.)														
T19	0.90	1.10	1.0258	0.9668	0.9565	0.9608	0.9904	1.0298	1.0716	0.9317	0.9777	0.9165	1.0921	0.9783
T20	0.90	1.10	1.0184	1.0057	0.9941	1.0207	0.9806	1.0193	0.9955	1.0247	0.9000	0.9000	0.9707	0.9450
T31	0.90	1.10	0.9989	1.0179	0.9957	1.0076	0.9737	0.9752	0.9724	0.9715	1.0998	1.1000	1.0023	1.0102
T35	0.90	1.10	1.0115	0.9954	0.9888	0.9586	1.0093	0.9943	1.0383	1.0476	0.9292	0.9000	0.9000	0.9000
T36	0.90	1.10	0.9681	1.0293	1.0343	1.0725	0.9743	1.1000	1.0533	1.0997	0.9009	0.9260	1.0746	0.9841
T37	0.90	1.10	0.9879	1.0130	1.0008	1.0037	1.0147	1.0074	1.0061	1.0087	1.0300	1.0525	1.0938	1.0856
T41	0.90	1.10	0.9921	0.9956	0.9954	0.9971	0.9962	0.9820	0.9933	0.9978	0.9000	0.9000	0.9310	0.9716
T46	0.90	1.10	0.9470	0.9648	0.9445	0.9530	0.9280	0.9173	0.9315	0.9178	0.9000	0.9000	0.9000	0.9000
T54	0.90	1.10	0.9920	0.9022	0.9575	0.9087	0.9000	0.9000	0.9000	0.9000	0.9000	0.9000	0.9000	0.9232
T58	0.90	1.10	0.9846	0.9897	0.9858	0.9896	0.9290	0.9401	0.9324	0.9303	0.9200	0.9000	0.9263	0.9418
T59	0.90	1.10	0.9677	0.9677	0.9713	0.9693	0.9583	0.9565	0.9648	0.9859	0.9000	0.9000	0.9000	0.9268
T65	0.90	1.10	0.9781	0.9826	0.9728	0.9742	0.9877	0.9977	0.9872	1.0114	0.9011	0.9000	0.9000	0.9506
T66	0.90	1.10	0.9437	0.9472	0.9484	0.9397	0.9298	0.9000	0.9000	0.9000	0.9002	0.9000	0.9000	0.9001
T71	0.90	1.10	0.9578	0.9811	0.9625	0.9707	0.9723	0.9389	0.9226	0.9576	0.9003	0.9000	0.9031	0.9821
T73	0.90	1.10	0.9940	0.9917	1.0043	0.9866	0.9895	1.0011	1.0523	1.0077	0.9688	0.9000	1.1000	0.9423
T76	0.90	1.10	0.9887	0.9440	0.9734	0.9604	0.9117	0.9025	0.9000	0.9001	1.1000	1.0987	1.0267	0.9790
T80	0.90	1.10	0.9891	0.9855	0.9789	0.9841	0.9975	0.9720	0.9754	0.9868	0.9000	0.9000	0.9795	0.9631
Capacitor Bank (MVAr)														
QC18	0	20	13.7926	6.9602	1.2632	8.6231	4.3041	16.9434	19.9404	0.5001	20.0000	20.0000	20.0000	11.8678
QC25	0	20	13.0556	14.6233	14.6891	14.6505	12.0698	16.5281	19.4971	19.9921	0.0137	0.0000	4.5609	0.0002
QC53	0	20	12.7986	12.3945	13.0130	13.5788	19.9195	19.5346	20.0000	20.0000	19.5390	20.0000	3.0355	0.0110
Objective Functions														
P_{Loss}	28.462		23.4159	23.3335	23.3804	**23.3039**	27.5497	26.7082	27.9832	27.6947	28.6570	30.7399	28.5457	28.5879
VD	1.5543		1.5678	1.6929	1.6259	1.7413	0.64230	0.61739	0.62781	**0.59821**	1.5397	1.6443	1.3767	1.3627
VSI	0.3218		0.2252	0.2693	0.2640	0.2651	0.2321	0.2666	0.2623	0.2753	0.20176	0.20141	0.21235	**0.19815**
Generator Reactive Power (MVAr)														
QG1	-140	200	58.3604	48.6811	57.8829	53.4971	52.1880	19.9629	42.9632	-11.23	105.564	80.7324	103.48	407.8445
QG2	-17	50	50.0091	49.9996	49.9910	50.0059	-8.868	49.4406	-3.802	48.9588	23.4851	-16.99	-11.55	33.5168

Continued on next page

turnitin Page 98 of 208 - Integrity Submission Submission ID trn:oid:::27535:142293373

turnitin Page 99 of 208 - Integrity Submission Submission ID trn:oid:::27535:142293373

Variables	Min	Max	CASE 4 (Min P_{Loss})				CASE 5 (Min VD)				CASE 6 (Min VSI)			
			COOT	HBA	GPC	Prop.	COOT	HBA	GPC	Prop.	COOT	HBA	GPC	Prop.
QG3	-10	60	38.5869	49.8809	44.6244	47.0367	41.1422	59.7877	44.3377	59.5817	30.7212	29.3673	52.9689	17.2529
QG6	-8	25	-1.762	-0.917	5.7369	0.0467	-7.97	0.7882	7.9272	-5.697	8.7596	-2.997	12.7858	-2.656
QG8	-140	200	60.8396	68.6244	62.1808	65.9130	74.2731	25.4249	45.8413	47.3831	-7.034	65.8288	128.621	171.339
QG9	-3	9	8.9160	9.0000	8.5055	8.9874	8.7410	8.9986	6.7003	8.9084	8.6153	5.0830	6.5121	8.0231
QG12	-150	155	53.8809	48.8658	51.2124	46.1331	142.524	120.823	140.871	154.449	135.596	154.999	26.312	92.1797

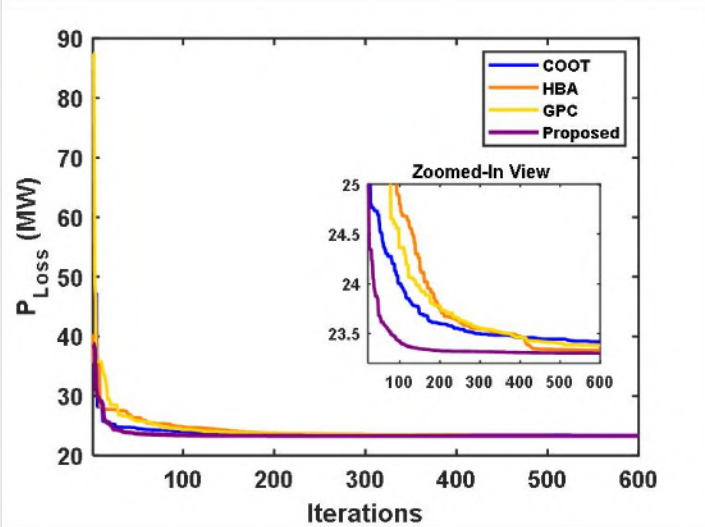
Table 4.6 shows that the proposed algorithm achieves the best results in the context of P_{Loss} (23.3039 MW), VD (0.59821 p.u.), and VSI (0.19815 p.u.). This table also displays the control variable values and reactive power produced in each case while addressing the ORPD issue using the other three algorithms. The table clearly illustrates that all values provided in every case are within the acceptable ranges. Figure 4.12 (a), Figure 4.13 (a), and Figure 4.14 (a) illustrate the convergence characteristics achieved for optimal values across all four methods in minimizing P_{Loss} (Case 4), VD (Case 5), and VSI (Case 6), respectively, for the IEEE 57-bus system. Figure 4.12 (b), Figure 4.13 (b), and Figure 4.14 (b) depict the values of P_{Loss}, VD, and VSI obtained from all four methods across 20 runs, respectively. Figure 4.12 (c), Figure 4.13 (c), and Figure 4.14 (c) demonstrate the voltage levels at the load buses achieved across all cases of the system.

Table 4.7 provides each objective's best, worst, and mean and their corresponding Std. obtained through the proposed algorithm and other methods over 20 runs. The results show that the proposed algorithm attains the lowest values for the best, worst, mean, and Std. metrics. Figure 4.15 depicts the percentage savings for each objective relative to the base scenario, utilizing all four methods. The proposed method yields the highest savings among all four methods for P_{Loss}, VD, and VSI, which are 18.12%, 61.51%, and 38.42%, respectively.

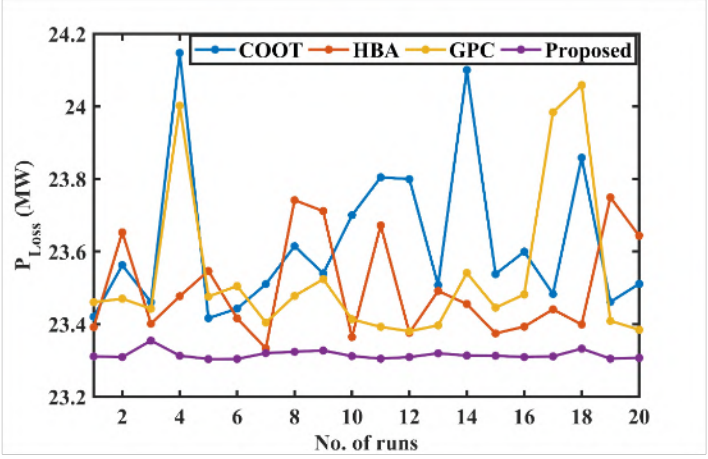
Even though the variation in percentage savings across the four methods is relatively small, the proposed algorithm consistently achieves better results for all three key objectives for the IEEE 30 and 57-bus systems. The low variation in results can be observed over twenty independent runs for all three objectives (P_{Loss}, VD, and VSI) in both IEEE 30 and 57-bus systems, highlighting the algorithm's strong convergence behavior, stability, and robustness for solving complex power system optimization problems.

turnitin Page 99 of 208 - Integrity Submission Submission ID trn:oid:::27535:142293373

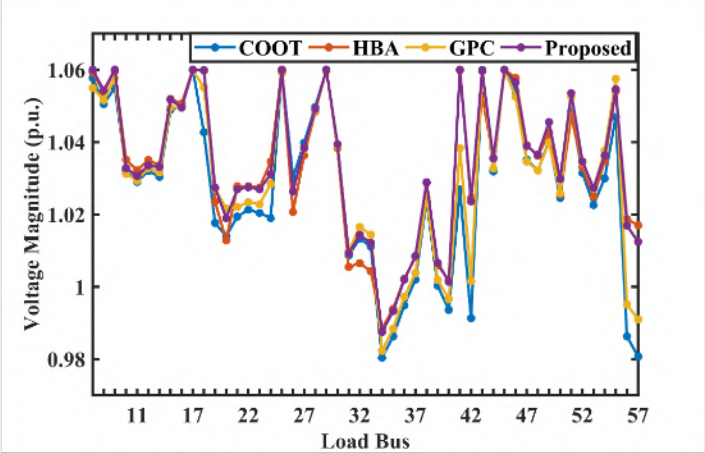
turnitin Page 100 of 208 - Integrity Submission Submission ID trn:oid:::27535:142293373



(a) Convergence curve.



(b) P_{Loss} obtained in 20 independent runs.

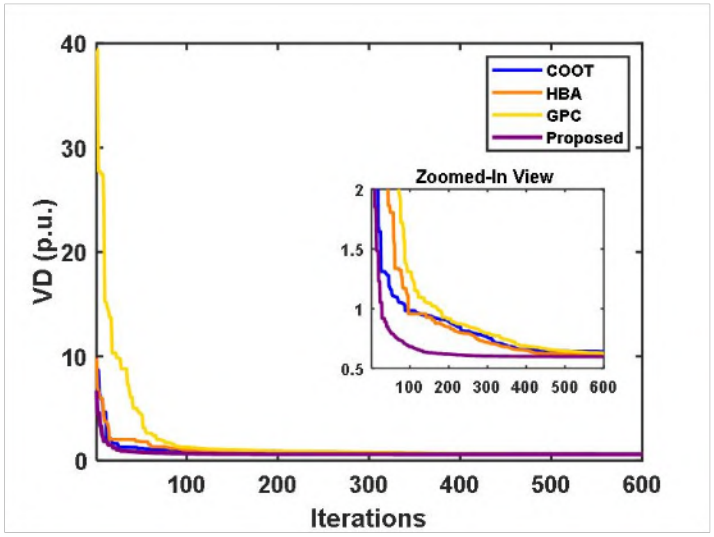


(c) Voltage magnitudes of load buses.

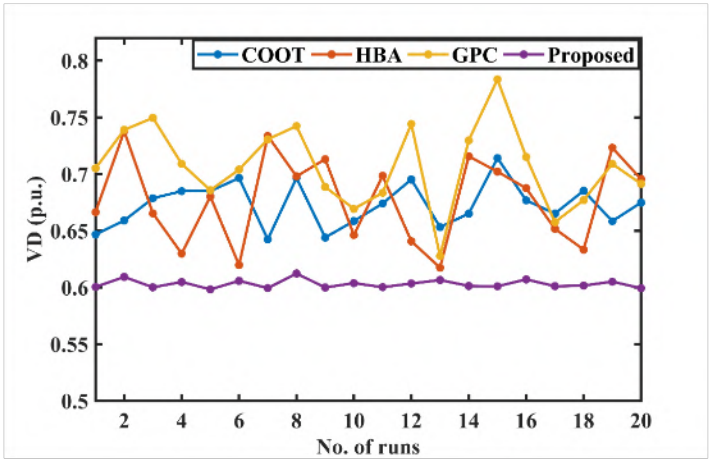
Fig. 4.12: P_{Loss} minimization (CASE 4).

turnitin Page 100 of 208 - Integrity Submission Submission ID trn:oid:::27535:142293373

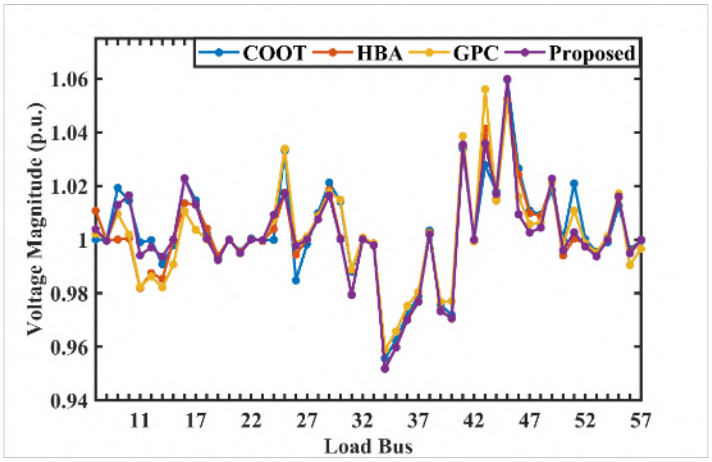
turnitin Page 101 of 208 - Integrity Submission Submission ID trn:oid:::27535:142293373



(a) Convergence curve.



(b) *VD* obtained in 20 independent runs.

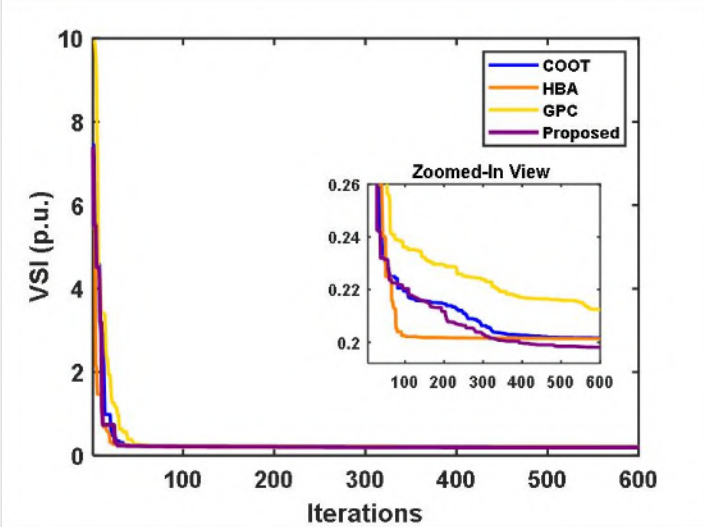


(c) Voltage magnitudes of load buses.

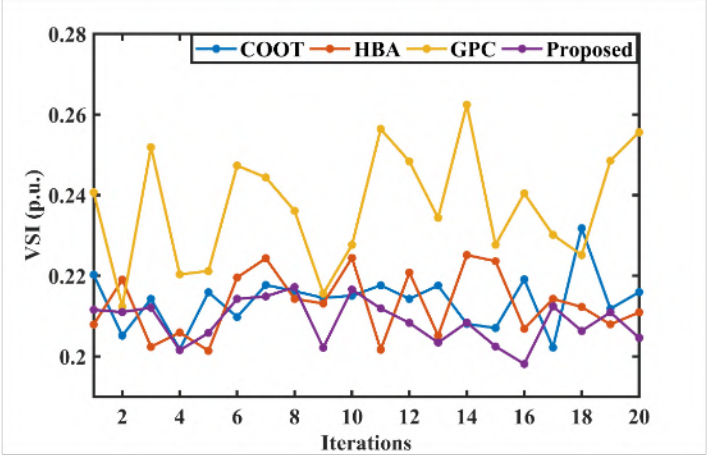
Fig. 4.13: *VD* minimization (CASE 5).

turnitin Page 101 of 208 - Integrity Submission Submission ID trn:oid:::27535:142293373

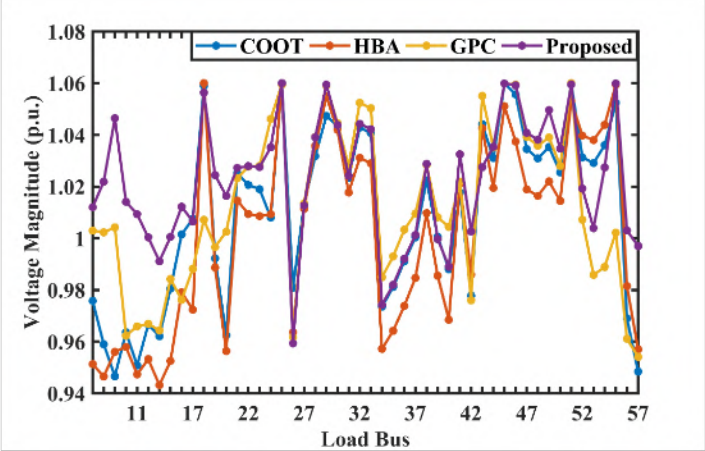
turnitin Page 102 of 208 - Integrity Submission Submission ID trn:oid:::27535:142293373



(a) Convergence curve.



(b) *VSI* obtained in 20 independent runs.



(c) Voltage magnitudes of load buses.

Fig. 4.14: *VSI* minimization (CASE 6).

turnitin Page 102 of 208 - Integrity Submission Submission ID trn:oid:::27535:142293373

turnitin Page 103 of 208 - Integrity Submission Submission ID trn:oid:::27535:142293373

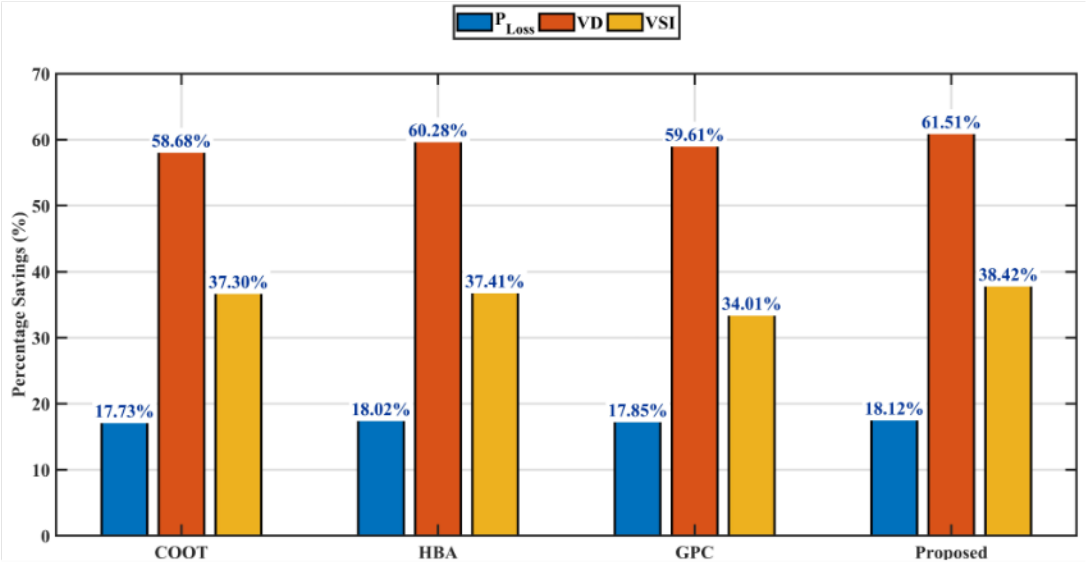


Fig. 4.15: Percentage saving achieved in P_{Loss}, VD, and VSI by each method for the IEEE 57-bus system.

Table 4.7: Comparison of results over 20 independent runs with different algorithms for the IEEE-57 bus system.

CASE	Objective Function	Algorithm	Best	Worst	Mean	Std.
CASE 4	Power Loss minimization (MW)	COOT	23.4159	24.1478	23.6241	0.21452
		HBA	23.3335	23.7495	23.5017	0.14044
		GPC	23.3804	24.0591	23.5326	0.21334
		Proposed	**23.3039**	23.3548	23.3153	0.012195
CASE 5	Voltage Deviation minimization (p.u.)	COOT	0.64230	0.71401	0.67265	0.019695
		HBA	0.61739	0.73771	0.67773	0.038329
		GPC	0.62781	0.78340	0.70703	0.036334
		Proposed	**0.59821**	0.61220	0.60298	0.003727
CASE 6	Voltage Stability Index minimization (p.u.)	COOT	0.20176	0.23180	0.21381	0.006915
		HBA	0.20141	0.22515	0.21305	0.008092
		GPC	0.21235	0.26242	0.23733	0.014512
		Proposed	**0.19815**	0.21720	0.20870	0.005432

The improvements achieved in the IEEE 30-bus and IEEE 57-bus systems provide tangible benefits for efficient operation in the grid. The noted decrease in P_{Loss} immediately results in reduced generation needs, which yields savings in fuel

turnitin Page 103 of 208 - Integrity Submission Submission ID trn:oid:::27535:142293373

turnitin Page 104 of 208 - Integrity Submission Submission ID trn:oid:::27535:142293373

cost and a decrease in greenhouse gas emissions. The substantial reduction in VD across both testing methods enhances power quality, allowing grid operators to maintain bus voltages within acceptable limits and diminish the risk of equipment stress or voltage-related issues for customers. Continuous improvement in VSI indicates increased system resilience to voltage collapse, which is crucial in modern grids marked by substantial renewable integration and demand fluctuations. The percentage savings reported, are statistically significant and practically beneficial, illustrating the potential of the proposed hybrid algorithm to provide economic and reliability improvements in diverse system configurations.

4.4.3 Stochastic ORPD

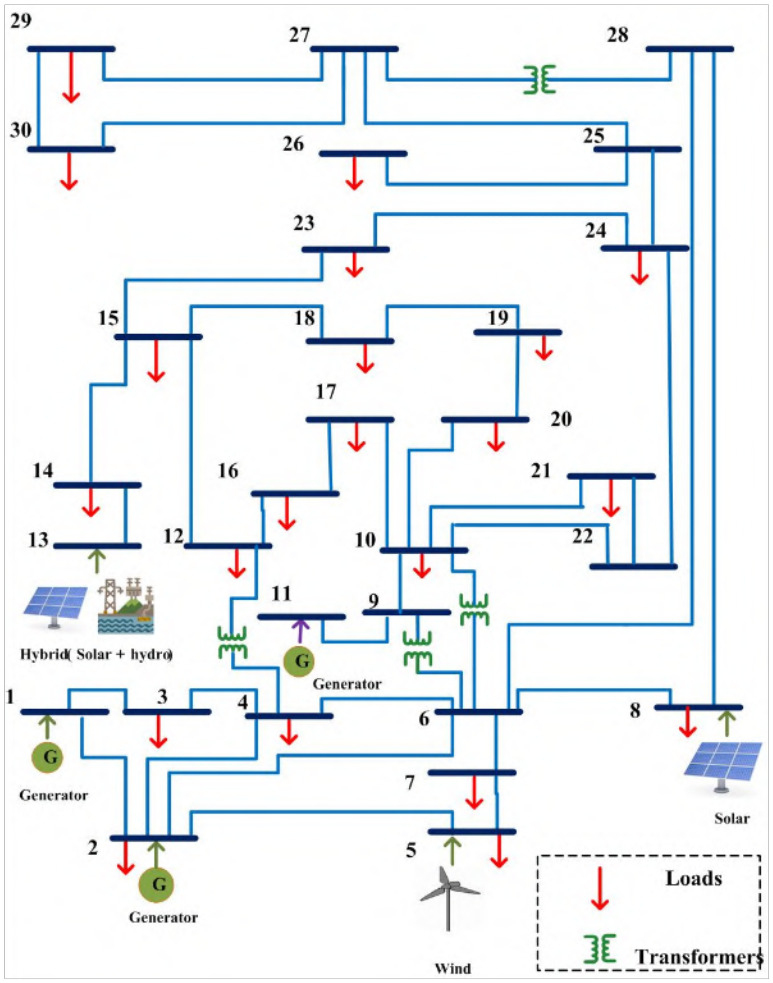


Fig. 4.16: Modified IEEE 30-bus system.

turnitin Page 104 of 208 - Integrity Submission Submission ID trn:oid:::27535:142293373

turnitin Page 105 of 208 - Integrity Submission Submission ID trn:oid:::27535:142293373

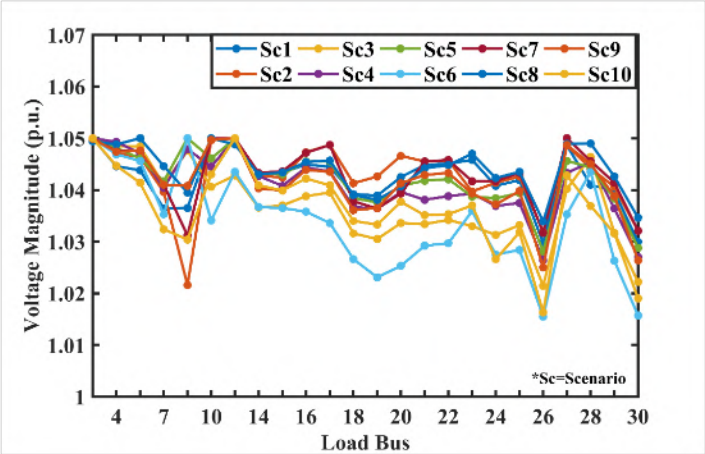
Table 4.8: Results for stochastic ORPD problem of the modified IEEE 30-bus.

Scenario	Wind Power (MW)	PV Power (MW)	Hybrid Power (MW)	Load (%)	Scenario Probability	Case 7 P_{Loss} (MW)	Case 8 VD (p.u.)	Case 9 VSI (p.u.)
1	10.25	0.00	3.18	71.22	0.796	4.3729	0.0611	0.0784
2	18.31	16.81	2.96	62.54	0.094	2.0062	0.0495	0.0683
3	36.72	39.33	14.74	68.44	0.002	1.2035	0.0532	0.0752
4	33.24	24.93	36.11	64.45	0.002	1.1497	0.0494	0.0710
5	49.82	19.10	13.88	66.01	0.068	1.1251	0.0513	0.0724
6	2.12	33.44	25.05	74.15	0.004	3.1391	0.0628	0.0820
7	32.43	30.05	3.37	67.76	0.018	1.6125	0.0538	0.0743
8	35.90	40.84	3.04	56.47	0.006	0.8112	0.0417	0.0611
9	65.32	50.00	4.38	86.25	0.002	1.7720	0.0423	0.0956
10	28.94	0.00	28.18	89.39	0.008	5.2327	0.0832	0.1000
Expected Sum						**3.8425**	**0.0592**	**0.0771**

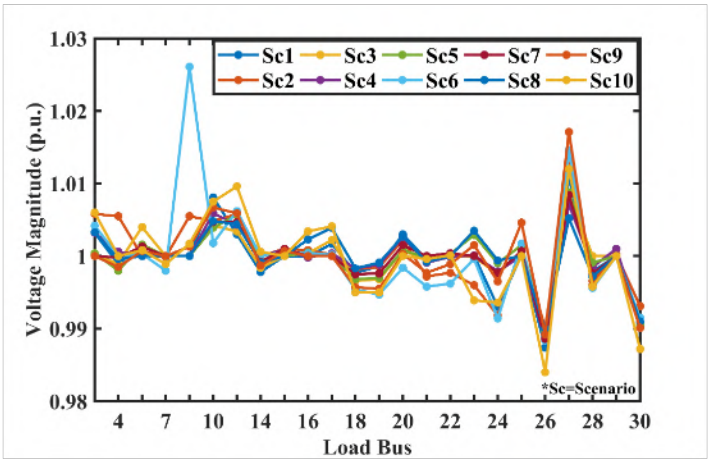
In the modified IEEE 30-bus system, thermal generators at buses 5, 8, and 13 have been swapped out for a wind generator, a photovoltaic unit, and a hybrid energy system (solar and small hydro), respectively, as illustrated in Figure 4.16. According to various scenarios, as previously described, the load demand, power produced by wind turbines, PV power and hybrid power are all variable. In the event of a deficit in real power from RES, the swing generator must adjust to balance the real power. Transformer taps and shunt VAR compensators are regarded as continuous, much like in Cases 1, 2, and 3. In this analysis, the swing generator's maximum real power production (200 MW) has been considered significant enough to allow the generator to supply power to the load even if RES does not produce active power. The expected P_{Loss}, VD, and VSI for the selected 10 scenarios are calculated using Equation 4.19, Equation 4.20, and Equation 4.21, respectively.

turnitin Page 105 of 208 - Integrity Submission Submission ID trn:oid:::27535:142293373

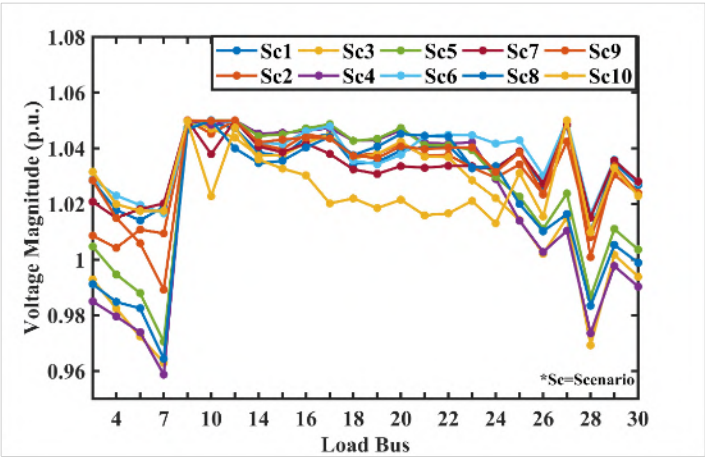
turnitin Page 106 of 208 - Integrity Submission Submission ID trn:oid:::27535:142293373



(a) P_{Loss} minimization (Case 7).



(b) VD minimization (Case 8).

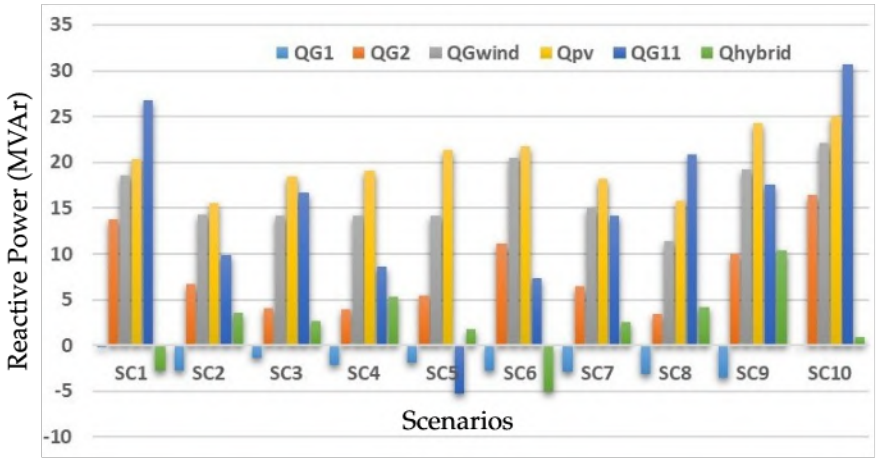


(c) VSI minimization (Case 9).

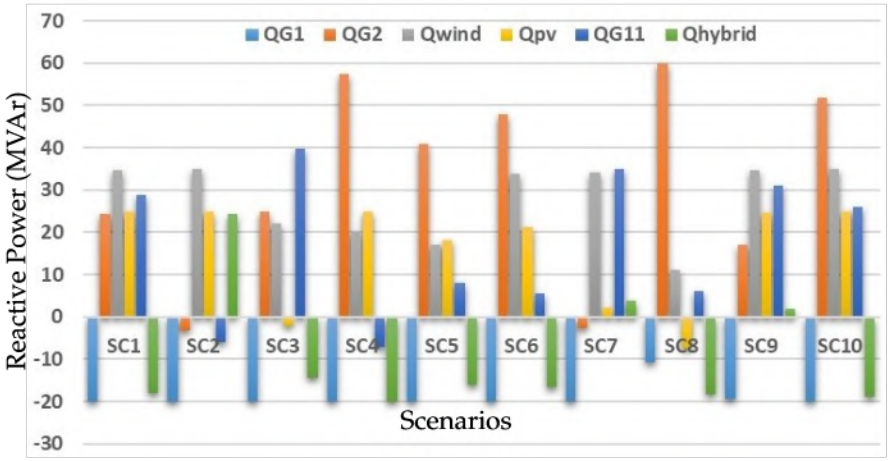
Fig. 4.17: Load bus voltage profiles for the ten stochastic scenarios.

turnitin Page 106 of 208 - Integrity Submission Submission ID trn:oid:::27535:142293373

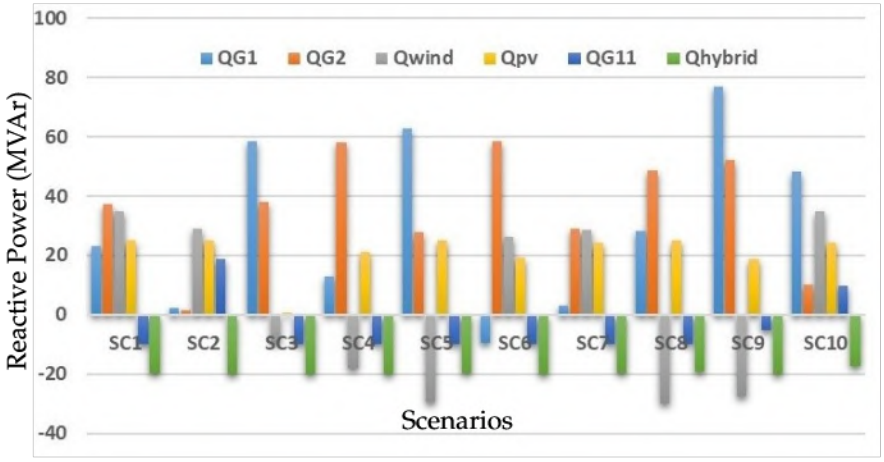
turnitin Page 107 of 208 - Integrity Submission Submission ID trn:oid:::27535:142293373



(a) P_{Loss} minimization (Case 7).



(b) VD minimization (Case 8).



(c) VSI minimization (Case 9).

Fig. 4.18: Reactive power generation for the ten stochastic scenarios.

turnitin Page 107 of 208 - Integrity Submission Submission ID trn:oid:::27535:142293373

turnitin Page 108 of 208 - Integrity Submission Submission ID trn:oid:::27535:142293373

For Cases 7, 8, and 9, the obtained values of the expected sum of P_{Loss}, VD and VSI are 3.8425 MW, 0.0592 p.u., and 0.0771 p.u., respectively. Table 4.8 indicates that in scenario 8, when the system's percentage loading was at its lowest (56.47%), the expected P_{Loss}, VD, and VSI are minimal, exhibiting enhanced system performance under light loading. On the other hand, in scenario 10, when network demand is at its peak (89.39%) and PV power is unavailable, the system's expected VD and VSI are at their highest (0.0832 p.u. and 0.1000 p.u., respectively). Figure 4.17 (a), (b) and (c) show the load voltage profiles created during optimization for each of the 10 scenarios for minimizing the P_{Loss}, VD and VSI, respectively. Figure 4.18 (a), Figure 4.18 (b) and Figure 4.18 (c) show the actual reactive power values produced at the generator bus during optimization across each of the 10 scenarios with the objective of minimizing P_{Loss}, VD, and VSI, respectively.

4.5 Conclusion

This research work introduced a novel hybrid optimization algorithm that integrates opposition-based strategies with the DE and GPC algorithms. This novel algorithm is initially evaluated on thirteen benchmarks (7 unimodal and 6 multimodal) functions, where it consistently demonstrates superior performance in terms of solution accuracy, convergence behavior, and robustness. This algorithm further solves the non-linear single-objective deterministic ORPD problem for the IEEE 30-bus and 57-bus systems. Additionally, the hybrid algorithm solves the stochastic ORPD problem of the modified IEEE-30 bus system, considering time-varying demand and uncertainty of solar, wind, and small-hydro energy sources. The ORPD problem considers three objectives, which are P_{Loss}, VD, and VSI. The performance of the hybrid algorithm is evaluated through a statistical analysis, comparing it with the recently developed GPC, HBA, and COOT algorithms. For the deterministic ORPD problem, the hybrid algorithm achieves the highest savings among all four methods for P_{Loss}, VD, and VSI that are 21.75%, 92.54%, and 32.95% for the IEEE 30-bus system, and 18.12%, 61.51% and 38.42% for the IEEE 57-bus system, respectively. In the stochastic ORPD problem, the hybrid algorithm obtained the expected sum of P_{Loss}, VD and VSI as 3.8425 MW, 0.0592 p.u., and 0.0771 p.u., respectively. The results indicate that the hybrid algorithm is both reliable and superior in solving the complex optimization

turnitin Page 108 of 208 - Integrity Submission Submission ID trn:oid:::27535:142293373

turnitin Page 109 of 208 - Integrity Submission Submission ID trn:oid:::27535:142293373

problem, demonstrating its capability to effectively explore the search space. In future works, the proposed algorithm could address multi-objective problems, seeking to achieve a balance among conflicting objectives.

turnitin Page 109 of 208 - Integrity Submission Submission ID trn:oid:::27535:142293373

turnitin Page 111 of 208 - Integrity Submission Submission ID trn:oid:::27535:142293373

Chapter 5

Proposed Machine Learning Framework

5.1 Introduction

This chapter presents an improved machine learning-based optimization framework, termed the Improved Evolutionary Algorithm–Self Organized Maps (IEASOM), for solving the ORPD problem in electrical power systems. The proposed method is developed by introducing improvements in the existing Evolutionary Algorithm–Self Organized Maps (EASOM) to enhance convergence performance, search capability, and solution quality.

The proposed IEASOM algorithm is applied to solve deterministic and stochastic single-objective ORPD problems on the IEEE 30-bus test system. In addition, the algorithm is applied on the IEEE 118-bus system to examine its effectiveness for large-scale power systems. In the stochastic ORPD problem, a mathematical model for solar PV power is utilized, which involves various meteorological parameters such as real-time solar irradiance, wind velocity, and photovoltaic panel temperature.

To demonstrate the effectiveness of the proposed algorithm, a comprehensive comparative statistical analysis is carried out with recently developed optimization algorithms such as the existing EASOM [123], Driving Training-Based Optimization (DTBO) [124], and the COOT [121] algorithm. The comparative evaluation is performed based on convergence characteristics, robustness, solution quality, and computational efficiency for both deterministic and stochastic ORPD problems. The simulation results indicate that the proposed IEASOM

turnitin Page 111 of 208 - Integrity Submission Submission ID trn:oid:::27535:142293373

turnitin Page 112 of 208 - Integrity Submission Submission ID trn:oid:::27535:142293373

algorithm significantly outperforms the existing approaches and provides superior optimization performance.

The detailed formulation of the proposed ML framework, uncertainty modeling, implementation procedure, and simulation results are discussed in the subsequent sections and subsections of this chapter.

5.2 Improved Evolutionary Algorithm–Self Organized Maps Algorithm

This section discusses the steps included in the Improved Evolutionary Algorithm-Self Organized Maps (IEASOM). This proposed algorithm employs contemporary computational strategies with historical information to provide a unique and efficient approach to identifying optimal solutions in complex search spaces.

5.2.1 Evolutionary Algorithm- Self Organized Maps (EASOM)

EASOM [123] is a machine learning-based optimization approach that utilizes extracted knowledge to guide the search process effectively. By incorporating self-organizing maps with evolutionary computation, the algorithm enhances exploration and exploitation capabilities, thereby improving convergence performance and solution quality. The methodology employs a Self-Organizing Map (SOM) as an exploratory knowledge technique to pinpoint potential regions through the minimization of the search space. A SOM is an unsupervised neural network extensively used in information extraction and machine learning. In every generation, the suggested approach trains a selection of produced solutions to identify the best possible solution. The neural unit within the SOM lattice is recognized, and by leveraging local information, a comprehensive array of candidate solutions is generated. The approach attains an optimal equilibrium between precision and computational expense when juxtaposed with alternative optimization approaches. This section provides an in-depth explanation of the methodology of the EASOM algorithm. The EASOM algorithm is developed to identify the optimal solution of a nonlinear optimization problem subject to upper and lower variable limits according to the following formulation. The steps

turnitin Page 112 of 208 - Integrity Submission Submission ID trn:oid:::27535:142293373

turnitin Page 113 of 208 - Integrity Submission Submission ID trn:oid:::27535:142293373

involved in this method are outlined below.

Step 1: Problem formulation

EASOM solves a nonlinear optimization problem formulated as:

$$\text{Minimize } f(\mathbf{x}), \quad \mathbf{x} \in \mathbb{R}^n \quad \text{subject to} \quad \mathbf{x} \in \Omega \tag{5.1}$$

Where, $\Omega = \{\mathbf{x} \mid l_i \leq x_i \leq u_i, i = 1, 2, \ldots, n\}$, function $f(\mathbf{x})$ represents the objective function to be minimized, n represents the number of decision variables, and Ω defines the feasible search space with bounds l_i and u_i.

Step 2: Initialization

Generate an initial population P(k) of 2N candidate solutions, where

$$P(k) = \{\vec{x}_i(k) \mid i = 1, \ldots, 2N\} \tag{5.2}$$

and each solution is sampled uniformly from the feasible bounds:

$$\vec{\mathbf{x}}_i(k) \sim \mathcal{U}(\vec{\mathbf{l}}, \vec{\mathbf{u}}), \quad i = 1, 2, \ldots, 2N \tag{5.3}$$

Evaluate the fitness $f(\vec{\mathbf{x}}_i(k))$ for each solution and store the population in a historical memory:

$$H(k) = P(k) \tag{5.4}$$

Set the maximum number of generations (MaxGen) and initialize the iteration counter k=0.

Step 3: Training SOM

Define a SOM with n input neurons and an h*h lattice of neurons. Each neuron has a weight vector

$$\vec{w}_j \in \mathbb{R}^n, \quad \text{such that} \quad S = \left\{ \vec{w}_j \,\middle|\, j = 1, 2, \ldots, h^2 \right\} \tag{5.5}$$

turnitin Page 113 of 208 - Integrity Submission Submission ID trn:oid:::27535:142293373

turnitin Page 114 of 208 - Integrity Submission Submission ID trn:oid:::27535:142293373

Train the SOM using a training set T(k) composed of the current population and randomly selected historical solutions:

$$T(k) = P(k) \cup \text{random samples from } H(k) \tag{5.6}$$

For each training vector $\vec{x} \in T(k)$, identify the winning neuron g in the SOM lattice:

$$g = \arg\min_j \left\| \vec{x} - \vec{w}_j \right\| \tag{5.7}$$

Update the weights of the winning neuron and its neighbors using:

$$\vec{w}_j \leftarrow \vec{w}_j + \eta(t) \cdot h_{g,j}(t) \cdot \left(\vec{x} - \vec{w}_j \right), \quad j \in N_g \tag{5.8}$$

Where, $\eta(t)$ is the learning rate decaying with iterations. $h_{g,j}(t)$ is the neighbourhood function, defined as:

$$h_{g,j}(t) = \exp\left(-\frac{\left\| \vec{r}_g - \vec{r}_j \right\|^2}{2\sigma^2(t)} \right) \tag{5.9}$$

Where $\vec{r}_g$ and $\vec{r}_j$ are the positions of neurons g and j in the lattice, and $\sigma(t)$ is the neighborhood radius that decreases over time.

Step 4: Knowledge extraction

After training the SOM, identify the winner neuron g corresponding to the best-performing solution $\vec{x}_{\text{best}} \in T(k)$:

$$g = \arg\min_j \left\| \vec{x}_{\text{best}} - \vec{w}_j \right\| \tag{5.10}$$

Let $\vec{w} = \vec{w}_g$ be the weight vector of the winning neuron. Find the neighboring neurons A and B, closest to neuron g in the lattice. Compute the influence radius α based on the distances:

$$\alpha = \frac{D_w + D_A + D_B}{3} \tag{5.11}$$

turnitin Page 114 of 208 - Integrity Submission Submission ID trn:oid:::27535:142293373

turnitin Page 115 of 208 - Integrity Submission Submission ID trn:oid:::27535:142293373

where,

$$D_w = \|\vec{x}_{\text{best}} - \vec{w}\|, \quad D_A = \|\vec{x}_{\text{best}} - \vec{w}_A\|, \quad D_B = \|\vec{x}_{\text{best}} - \vec{w}_B\|$$

are the distances of neurons g, A, and B to the best solution, respectively.

Step 5: New solutions generation

Generate N new solutions around the region defined by the winner neuron $\vec{w}$:

$$\vec{x}_j(k+1) = \vec{w} + \alpha \cdot R \cdot r, \quad r \sim \mathcal{U}[-1,1] \tag{5.12}$$

where

$$R = 1 - \frac{\|\vec{w} - \vec{m}\|}{n} \tag{5.13}$$

and $\vec{m}$ is the center of the SOM lattice.
Clip each generated solution to ensure it lies within the feasible bounds:

$$\vec{x}_j(k+1) \leftarrow \text{clip}(\vec{x}_j(k+1), \vec{l}, \vec{u}) \tag{5.14}$$

5.2.2 Improvement in EASOM algorithm

The optimization method based on EASOM presents certain limitations, including significant computational overheads due to the training of the self-organizing map, a sensitivity to the chosen parameter configurations, and a propensity to get stuck in local minima. Furthermore, it may encounter difficulties when addressing high-dimensional issues because of its fixed grid configuration. To address these challenges, a small adaptive step size is incorporated, facilitating efficient solution refinement, enhancing convergence, and achieving an equilibrium between exploration and exploitation, all while preserving diversity through historical memory. The algorithm's adaptive step size reduces as it progresses, allowing for more refined perturbations in both forward and backward directions. This approach ensures convergence by introducing small, controlled changes to the current best solution. A random factor guides these perturbations, allowing the algorithm to evade local optima and move towards a more optimal solution.

turnitin Page 115 of 208 - Integrity Submission Submission ID trn:oid:::27535:142293373

turnitin Page 116 of 208 - Integrity Submission Submission ID trn:oid:::27535:142293373

Step 6: Specify a decreasing step size

$$\Delta\vec{x} = 0.01 \cdot (\vec{u} - \vec{l}) \cdot \left(1 - \frac{k}{\text{MaxGen}}\right) \tag{5.15}$$

Step 7: Perform perturbations in both forward and backward directions

$$\vec{x}_{\text{perturb}} = \vec{x}_{\text{best}} \pm \Delta\vec{x} \cdot \vec{e}_i \cdot \mathcal{N}(0, 10^{-5}) \tag{5.16}$$

where e_i is the unit basis vector in the ith dimension.

Step 8: Update best solution if perturbed solution is better

$$\vec{x}_{\text{best}} = \arg\min f(\vec{x}_{\text{perturb}}) \tag{5.17}$$

Step 9: Update Historical Memory

Add the newly generated solutions to the historical memory:

$$H(k+1) = H(k) \cup P(k+1) \tag{5.18}$$

Construct the next training set T(k+1) by combining new solutions with randomly sampled elements from H(k):

$$T(k+1) = P(k+1) \cup \text{random samples from } H(k) \tag{5.19}$$

Step 10: Iterative Process

Increment the iteration counter:

$$k \leftarrow k + 1 \tag{5.20}$$

Repeat the above steps until the termination criterion k=MaxGen is satisfied. Figure 5.1 below displays the flowchart of the proposed algorithm.

turnitin Page 116 of 208 - Integrity Submission Submission ID trn:oid:::27535:142293373

turnitin Page 117 of 208 - Integrity Submission Submission ID trn:oid:::27535:142293373

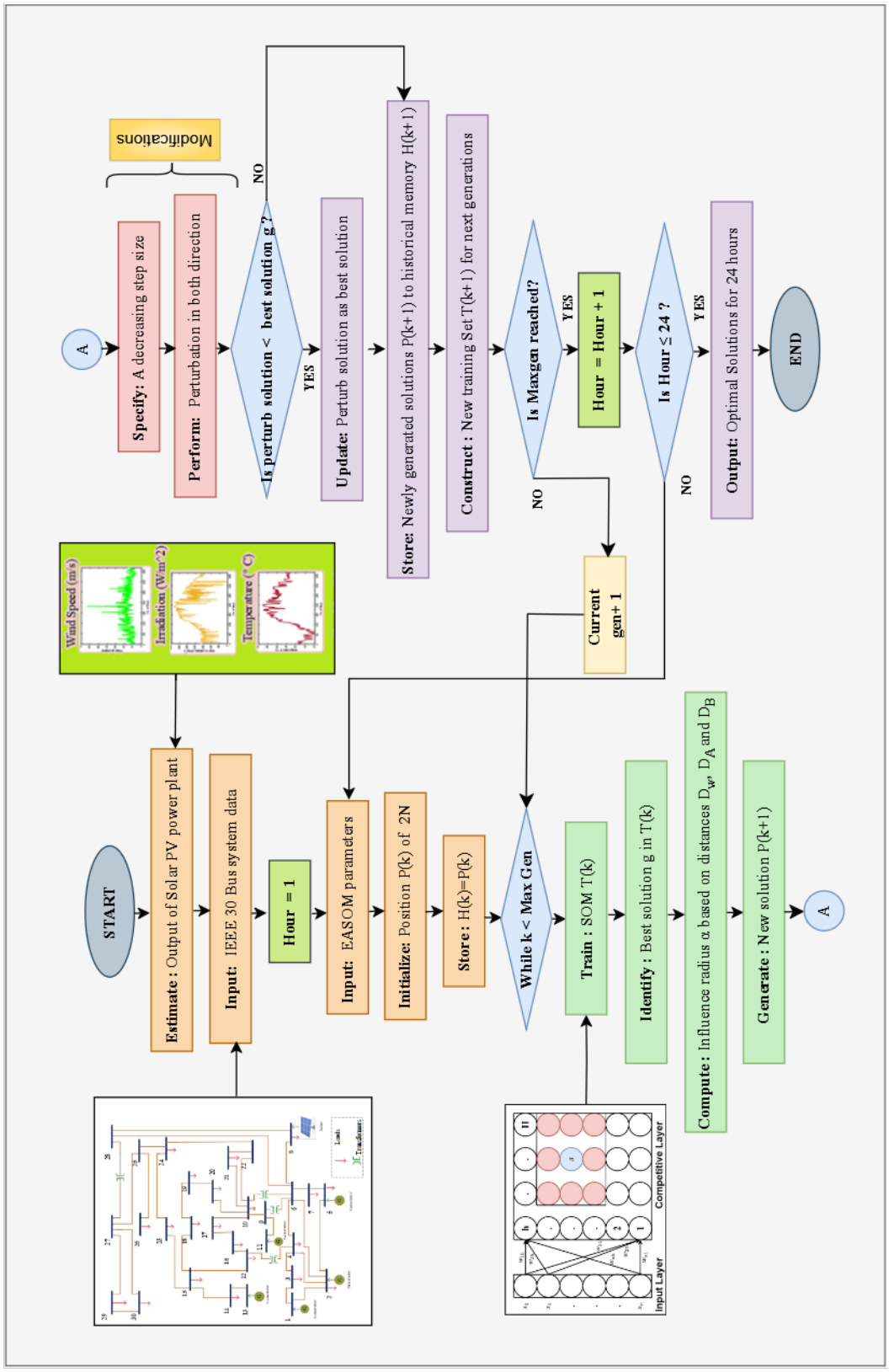


Fig. 5.1: Flowchart of the proposed ML-based method.

turnitin Page 117 of 208 - Integrity Submission Submission ID trn:oid:::27535:142293373

turnitin Page 118 of 208 - Integrity Submission Submission ID trn:oid:::27535:142293373

5.3 Mathematical Modeling of Solar PV System

5.3.1 Background

An accurate assessment of solar photovoltaic (PV) power production necessitates taking into account a number of meteorological parameters that affect PV module performance. The essential parameters are real-time solar irradiance, wind velocity, and photovoltaic panel temperature. These parameters denote the surrounding environmental conditions of the installation location. Meteorological data for New Delhi, India, were obtained from the Solcast site [125]. This PV power modelling method comprises a sequence of equations that simulate the thermal and electrical characteristics of the PV module under diverse environmental circumstances. A comprehensive explanation of each equation is shown below. The estimated power for a 50 MW solar power plant is calculated using the following equations.

$$T_m = T_{\text{amb}} + \frac{G}{26.9 + 6.2 \times w_{\text{in}}} \tag{5.21}$$

$$T_a = T_m - 25^{\circ}\text{C} \tag{5.22}$$

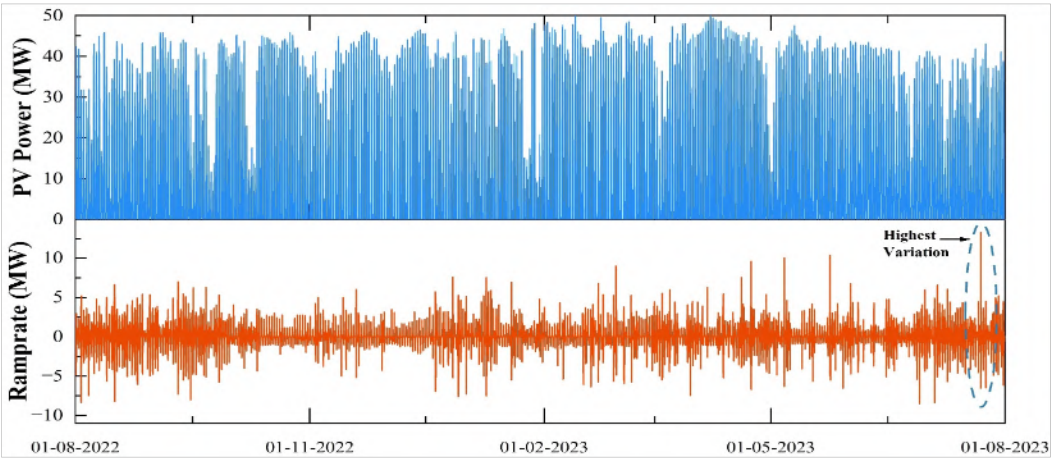
$$W_{\text{in}} = \left(\frac{D_m}{D_a}\right)^{0.2} \times w_s \tag{5.23}$$

$$P_c = P_r \times G \left(1 + K_1 \log(G) + K_2 \log^2(G) + K_3 T_a + K_4 T_a \log(G) + K_5 T_a \log^2(G) + K_6 T_a^2\right) \tag{5.24}$$

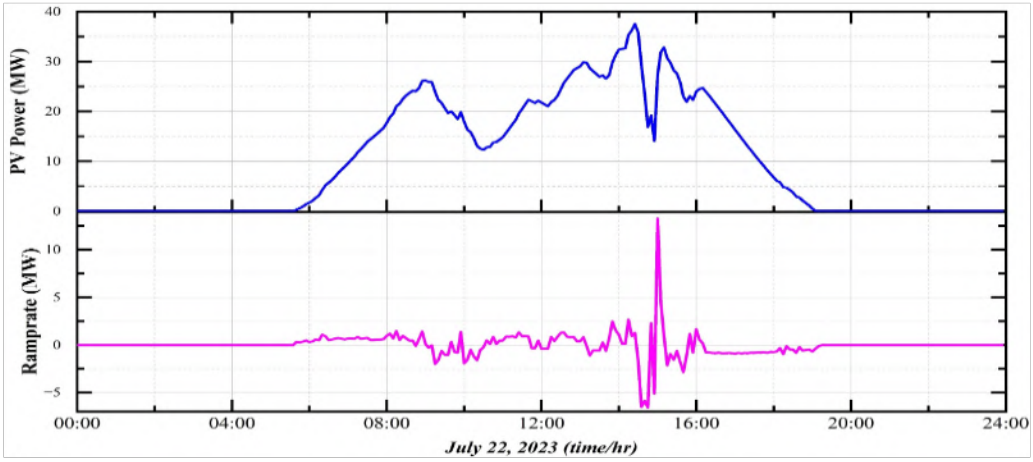
Where, P_c is the estimated power of a real-time module, W_{in} indicates the wind speed measured at the module height and w_s denotes the wind speed at anemometer's measurement height, G is the irradiation, T_a is the wind-induced temperature change, T_m is the module temperature, T_{amb} is the ambient temperature calculated from solcast and $K_1 - K_6$ are constants of the PV module. D_a and D_m represent the vertical distances from the PV module and the anemometer to the ground surface, respectively. Table 5.1 below displays the constant values required to estimate solar PV power[126]. Here, P_r is set at 50 MW.

turnitin Page 118 of 208 - Integrity Submission Submission ID trn:oid:::27535:142293373

turnitin Page 119 of 208 - Integrity Submission Submission ID trn:oid:::27535:142293373



(a) Estimated annual solar PV power and the corresponding ramp rate.



(b) Estimated hourly solar PV power and the corresponding ramp rate for a day.

Fig. 5.2: Solar PV power estimation.

Table 5.1: Various constants for estimation of solar PV power.

K_1	K_2	K_3	K_4	K_5	K_6	D_m	D_a
-0.046689	-0.072844	-0.002262	0.000276	0.000159	-0.000006	10 m	7.2 m

The photovoltaic power generation is inherently associated with meteorological parameters such as solar irradiance and atmospheric temperature, exhibiting significant stochastic behavior in the output. To mathematically represent the variability in power production, the ramp rate statistic is calculated:

$$RR_t = \frac{P_t - P_{t-1}}{\Delta t} \tag{5.25}$$

turnitin Page 119 of 208 - Integrity Submission Submission ID trn:oid:::27535:142293373

turnitin Page 120 of 208 - Integrity Submission Submission ID trn:oid:::27535:142293373

where, P_t represents the power output at time t, and Δt denotes the time interval. The projected annual solar PV power and the corresponding ramp rate for that duration are shown in Figure 5.2 (a).

To validate the practicality of the proposed algorithm, a day characterized by the highest ramp rate values, as shown in Figure 5.2 (a), was chosen for the analysis. The selection illustrates days characterized by significant uncertainties within the system, attributed to the rapid fluctuations in power output, highlighting the critical challenges associated with maintaining grid stability. The selection process highlights the strength and adaptability of the proposed algorithm, thereby ensuring optimal dispatch under dynamic conditions. Figure 5.2 (b) illustrates the estimated hourly solar PV power for the chosen day corresponding to the maximum ramp rate acquired for the ORPD problem.

5.3.2 Expected average of objective function values for stochastic ORPD problem

In stochastic ORPD, the system operating conditions vary due to the uncertainty in solar power generation over time. Therefore, unlike deterministic ORPD, the objective functions are evaluated using their expected average values over a 24-hour period to achieve a more realistic and reliable optimization solution under varying solar generation conditions.

The expected average of power loss ($EA_{P_{\text{Loss}}}$) for a day can be determined by the following formula:

$$\text{EA}_{P_{\text{Loss}}} = \sum_{t=1}^{T} \sum_{k=1}^{N_{TL}} \frac{G_{kj}\left(V_k^2 + V_j^2 - 2V_kV_j\cos(\delta_{kj})\right)}{24} \tag{5.26}$$

where 't' signifies the duration in hours, while T denotes the complete time span for a day. In a similar manner, Equation 5.27 is used to determine the expected average of voltage deviation (EA_{VD}).

$$\text{EA}_{VD} = \sum_{t=1}^{T} \sum_{k=1}^{N_L} \frac{|V_k - V_{i_{\text{ref}}}|}{24} \tag{5.27}$$

turnitin Page 120 of 208 - Integrity Submission Submission ID trn:oid:::27535:142293373

turnitin Page 121 of 208 - Integrity Submission Submission ID trn:oid:::27535:142293373

Similar to that, Equation 5.28 is used to calculate the expected average of the voltage stability index (EA_{VSI}).

$$\mathrm{EA}_{VSI} = \sum_{t=1}^{T} \frac{\min\left[\max(L_K)\right]}{24} \tag{5.28}$$

5.4 Results and Discussion

This section presents the findings, an in-depth evaluation, and comparisons for two distinct IEEE 30-bus test systems: one standard and one modified. Additionally, the proposed algorithm is tested on the IEEE 118 bus system to assess its usefulness in a large and complex network. The generator data of the IEEE 30-bus system for all studied cases are listed in Table A.4 of Appendix A. The system comprises 6 generators, 9 shunt VAR compensators, and 4 transformers with off-nominal tap ratios. The total load connected to this system is 283.4 MW and 126.2 MVAr, with all variables as continuous, and the generation (excluding swing) is kept constant. Shunt VAR compensators vary from 0-5 MVAr, and tap settings from 0.9-1.1 p.u. The load voltage range of this system is set within 0.95 to 1.05 p.u. Therefore, the aggregate voltage drop across all load buses must not exceed 1.2 p.u. The research begins with deterministic ORPD cases involving only thermal generators, subsequently transitioning to the stochastic ORPD issue considering solar PV power using the modified IEEE 30 bus system. Cases 1-3 were analyzed using the IEEE 30-bus system to minimize P_{Loss}, VD, and VSI, respectively. To address the stochastic ORPD problem, the modified IEEE 30-bus system has been analyzed in cases 4-6 with the aim of reducing P_{Loss}, VD, and VSI, respectively.

5.4.1 SOM Parameter Setup and Grid Size Sensitivity Analysis

To study the influence of SOM grid dimensionality on the performance of the proposed algorithm, we performed a parameter sensitivity analysis. This analysis is carried out using the IEEE 30-bus system. Five different combinations of the SOM dimension have been used (5x5, 10x10, 15x15, 20x20 and 25x25). A training sample size of 100, which is twice the population size, along with an initial learning rate of $\eta_0 = 1$ and an initial neighborhood distance of $\sigma_0 = 10$, are utilized in this study, as these parameters represent the optimal values identified in the original

turnitin Page 121 of 208 - Integrity Submission Submission ID trn:oid:::27535:142293373

turnitin Page 122 of 208 - Integrity Submission Submission ID trn:oid:::27535:142293373

EASOM research [123]. Twenty separate runs were conducted to evaluate each configuration. The mean and Std. for each of the three objectives (P_{Loss}, VD and VSI) obtained are shown in Table 5.2.

Table 5.2: Sensitivity analysis of SOM dimension on objective functions.

SOM Dimension	P_{Loss} (MW)	VD (p.u.)	VSI (p.u.)
	Mean ± Std.	**Mean ± Std.**	**Mean ± Std.**
5×5	4.8723 ± 0.00737	0.0999 ± 0.00587	0.1143 ± 0.000955
10×10	**4.8634 ± 0.00177**	**0.0906 ± 0.00178**	**0.1134 ± 0.000783**
15×15	4.8729 ± 0.00491	0.1040 ± 0.00889	0.1153 ± 0.00142
20×20	4.8734 ± 0.00588	0.1046 ± 0.0104	0.1159 ± 0.00167
25×25	4.8764 ± 0.00767	0.1104 ± 0.0151	0.1162 ± 0.00134

Table 5.2 illustrates the effect of different SOM grid dimensions on the goal functions for the IEEE 30-bus system. The 10×10 SOM grid size demonstrated excellent performance, characterized by the lowest mean P_{Loss} (4.8634 MW), mean VD (0.0906 p.u.), mean VSI (0.1134), and the highest consistency, shown by minimum Std. across all metrics. Consequently, the 10×10 grid size is identified as the most suitable size for the SOM in subsequent experimental assessments for the EASOM method and proposed algorithm in this research work.

5.4.2 IEEE 30-bus system

The research aims to validate the versatility and efficacy of the proposed algorithm, demonstrating its effectiveness through comparison with recent optimization approaches like COOT, DTBO and EASOM algorithms. For this system, each algorithm is allowed up to 300 iterations with a fixed population size of 50, and is subjected to 20 trial runs. This comparative analysis utilizes the optimum values of parameters for DTBO, COOT, and EASOM from their original research work to provide a fair and consistent performance evaluation. This research considered three objectives for the ORPD problem: P_{Loss}, VD, and VSI.

turnitin Page 122 of 208 - Integrity Submission Submission ID trn:oid:::27535:142293373

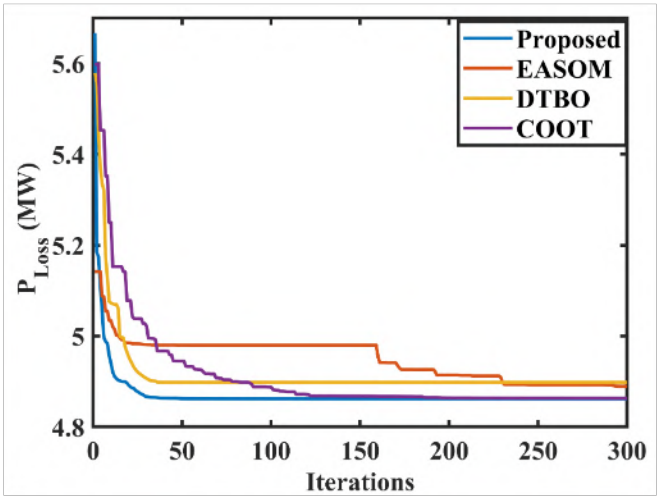
turnitin Page 123 of 208 - Integrity Submission Submission ID trn:oid:::27535:142293373

Table 5.3: Single-objective ORPD results for IEEE 30-bus system.

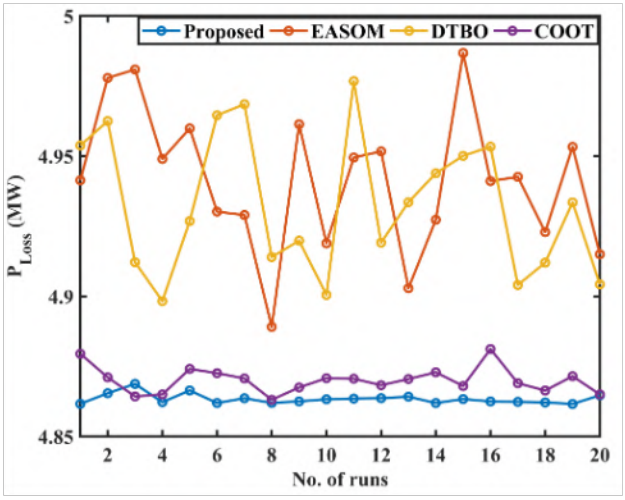
Variables	Min	Max	CASE 1 (Min P_{Loss})				CASE 2 (Min VD)				CASE 3 (Min VSI)			
			COOT	DTBO	EASOM	Prop.	COOT	DTBO	EASOM	Prop.	COOT	DTBO	EASOM	Prop.
Generator Voltage (p.u.)														
V1	0.95	1.1	1.0713	1.0731	1.0715	1.0724	1.0121	1.0236	1.0157	1.0053	1.0803	1.0772	1.0943	1.0611
V2	0.95	1.1	1.0622	1.0638	1.0624	1.0631	1.0097	1.0243	1.0131	1.0014	1.0566	1.0548	1.0624	1.0446
V5	0.95	1.1	1.0399	1.0415	1.0399	1.0406	1.0209	1.0211	1.0216	1.0206	1.0143	1.0358	0.9959	1.0366
V8	0.95	1.1	1.0397	1.0419	1.0407	1.0408	1.0052	1.0026	1.0046	1.0054	1.0027	1.0133	1.0097	1.0120
V11	0.95	1.1	1.0849	1.0998	1.0788	1.0894	1.0199	1.0142	1.0213	1.0329	1.0305	1.0262	1.0337	1.0290
V13	0.95	1.1	1.0553	1.0508	1.0629	1.0528	1.0204	1.0044	1.0205	1.0303	1.0316	1.0329	1.0292	1.0292
Tap Position (p.u.)														
T11	0.90	1.1	1.0269	1.0568	1.0354	1.0235	1.0351	1.0272	1.0178	1.0482	0.9338	0.9478	0.9259	0.9380
T12	0.90	1.1	0.9534	0.9020	0.9042	0.9682	0.9047	0.9000	0.9000	0.9000	0.9001	0.9006	0.9135	0.9000
T15	0.90	1.1	0.9952	0.9834	1.0003	0.9851	0.9980	0.9666	0.9919	1.0172	0.9121	0.9272	0.9006	0.9072
T36	0.90	1.1	0.9743	0.9731	0.9743	0.9752	0.9584	0.9642	0.9619	0.9667	0.9237	0.9284	0.9225	0.9257
Capacitor Bank (MVAr)														
QC10	0	5	2.0235	1.6737	1.6632	2.8223	4.7598	4.5438	3.8230	4.7756	3.7655	4.0446	1.7713	4.9979
QC12	0	5	4.9554	4.6527	2.4421	1.9580	1.1735	0.2644	2.8693	1.8851	2.0008	4.4400	0.9752	1.3405
QC15	0	5	3.8793	4.2156	2.7769	3.7622	4.6788	4.9988	4.0230	5.0000	0.0001	2.4063	1.4110	1.7459
QC17	0	5	4.9214	2.0853	1.9122	4.9995	2.3686	0.0001	3.5468	0.0000	3.3802	4.0719	0.4372	4.9196
QC20	0	5	3.2929	2.1006	3.0117	4.1522	4.9975	4.9999	2.1968	5.0000	0.8206	4.0804	0.6730	2.7373
QC21	0	5	4.9994	2.1117	4.4650	4.9986	4.9588	4.9993	3.7284	4.9997	4.9499	4.5747	1.6919	3.7482
QC23	0	5	2.5729	1.4361	3.5258	3.0550	4.9926	4.9989	3.7272	5.0000	2.7934	0.0452	1.5805	0.5225
QC24	0	5	4.9996	3.5862	3.1458	5.0000	4.4932	4.9996	2.7106	5.0000	3.4436	0.3334	0.9803	1.3354
QC29	0	5	2.3552	2.8114	2.1070	2.4333	1.6960	2.4636	3.2652	2.6906	0.0036	0.0000	0.5231	0.0000
Objective Functions														
P_{Loss}	6.212		4.8631	4.8983	4.8891	**4.8612**	5.7571	5.5862	5.7061	5.9675	5.8753	5.6174	6.5127	5.6412
VD	1.1758		0.9085	0.8979	0.8949	0.9315	0.09433	0.0927	0.1238	**0.0877**	0.7404	0.7700	0.6722	0.7500
VSI	0.1672		0.1220	0.1219	0.1223	0.1219	0.1280	0.1281	0.1285	0.1305	0.11289	0.1129	0.11354	**0.1121**
Generator Reactive Power (MVAr)														
QG1	-20	150	-0.336	0.9261	-0.35	0.45	-19.72	-19.99	-17.73	-19.99	46.64	39.605	68.837	24.7246
QG2	-20	60	16.0921	17.5139	17.1072	16.7159	0.9086	30.5787	5.9901	-14.82	35.6777	14.08	37.3794	15.9221
QG5	-15	62	24.5825	25.0142	25.0743	24.3518	54.1673	46.8604	53.4659	58.1854	20.9004	39.5579	-1.403	48.4976
QG8	-10	40	29.5038	33.8012	35.4333	29.8821	48.5969	41.9327	48.519	48.6983	32.6695	37.7465	46.5923	48.3398
QG11	-6	24	20.0709	29.804	18.3348	21.0745	10.1619	7.3549	8.5353	16.7547	-9.272	-9.932	-7.677	-9.992
QG13	-6	24	4.2327	0.8578	10.0728	2.3218	8.5209	-3.08	7.426	15.9232	-13.32	-12.35	-14.93	-14.99

turnitin Page 123 of 208 - Integrity Submission Submission ID trn:oid:::27535:142293373

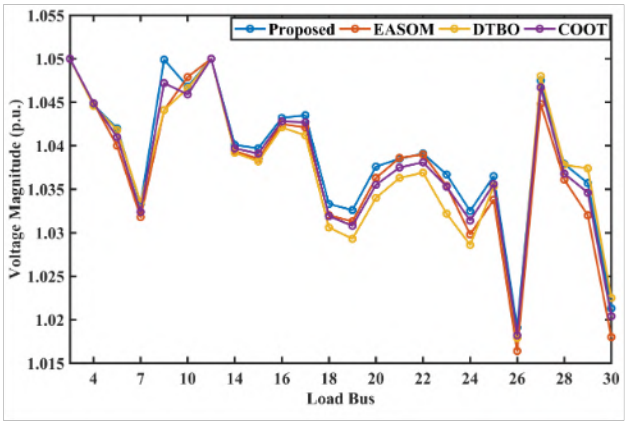
turnitin Page 124 of 208 - Integrity Submission Submission ID trn:oid:::27535:142293373



(a) Convergence curve.



(b) P_{Loss} obtained in 20 independent runs.

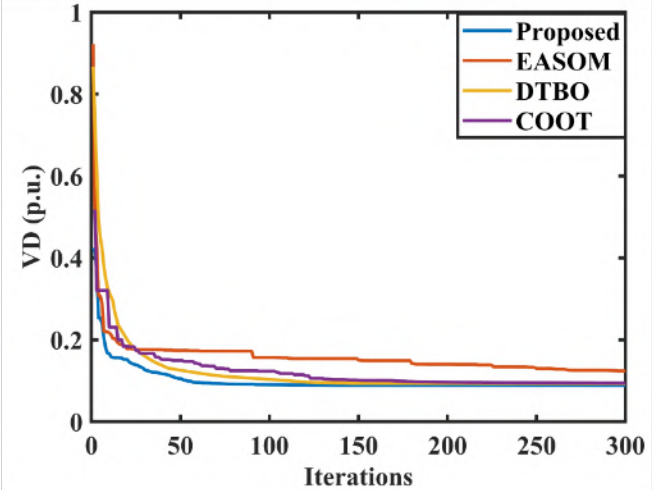


(c) Voltage magnitudes of load buses.

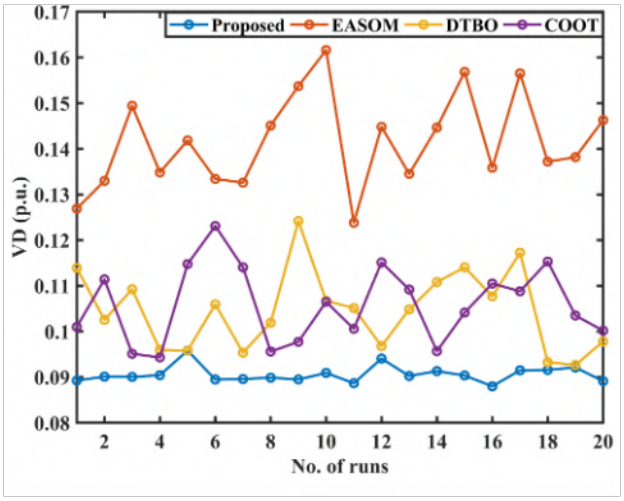
Fig. 5.3: P_{Loss} minimization (CASE 1).

turnitin Page 124 of 208 - Integrity Submission Submission ID trn:oid:::27535:142293373

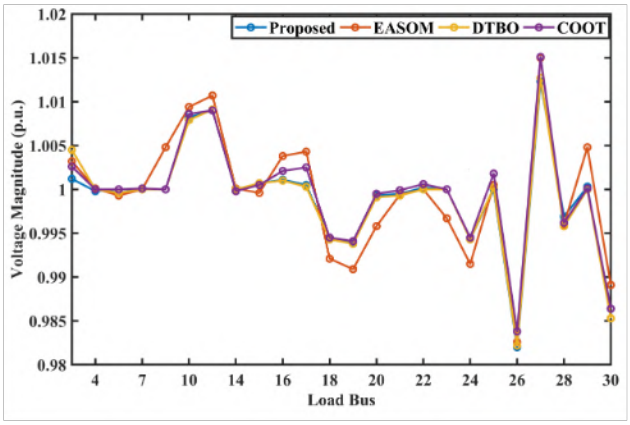
turnitin Page 125 of 208 - Integrity Submission Submission ID trn:oid:::27535:142293373



(a) Convergence curve.



(b) VD obtained in 20 independent runs.

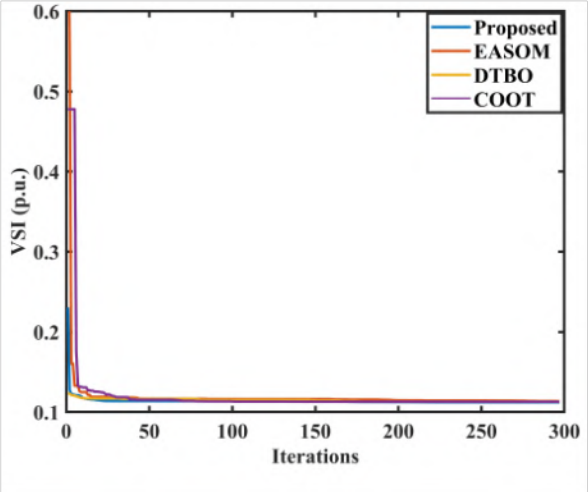


(c) Voltage magnitudes of load buses.

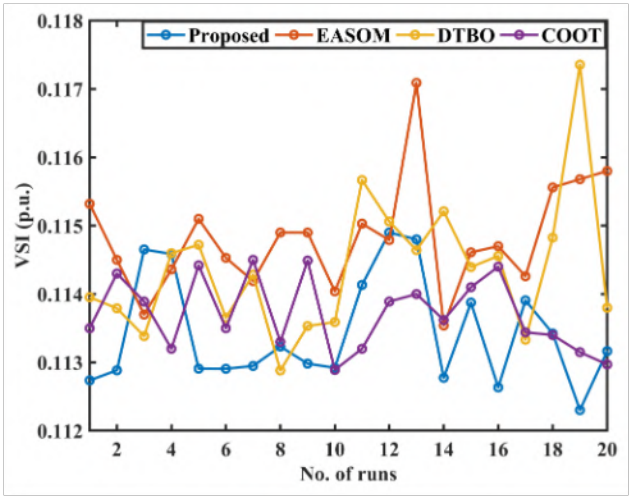
Fig. 5.4: VD minimization (CASE 2).

turnitin Page 125 of 208 - Integrity Submission Submission ID trn:oid:::27535:142293373

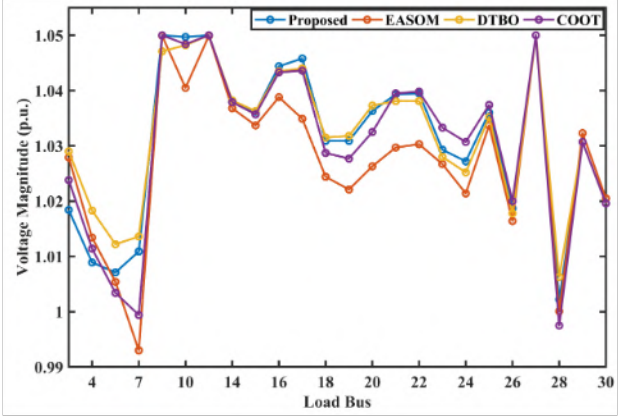
turnitin Page 126 of 208 - Integrity Submission Submission ID trn:oid:::27535:142293373



(a) Convergence curve.



(b) *VSI* obtained in 20 independent runs.



(c) Voltage magnitudes of load buses.

Fig. 5.5: *VSI* minimization (CASE 3).

turnitin Page 126 of 208 - Integrity Submission Submission ID trn:oid:::27535:142293373

turnitin Page 127 of 208 - Integrity Submission Submission ID trn:oid:::27535:142293373

The optimum values for all calculated state and control variables, together with permissible ranges, are presented in Table 5.3 for case studies utilizing the IEEE 30-bus to achieve minimization of their respective objective functions. The analysis further evaluates the best values achieved for each of the three objectives through the implementation of the suggested algorithms in comparison to other available options. Additionally, the table presents the values of the other two objectives while focusing on minimizing the chosen objective. The proposed method delivers the best trade-off between optimization performance and computational time. It achieves the lowest P_{Loss} (4.8612 MW), VD (0.0877 p.u.), and VSI (0.1121 p.u.). It also presents the values of control variables and the reactive power generated in each case while tackling the ORPD problem through three additional algorithms. The table distinctly demonstrates that all values presented in each instance fall within the permissible limits.

Figures 5.3 (a), 5.4 (a), and 5.5 (a) illustrate the convergence characteristics attained for optimal values across all four methods in reducing P_{Loss} (Case 1), VD (Case 2), and VSI (Case 3) for the IEEE 30-bus system. Figures 5.3 (b), 5.4 (b), and 5.5 (b) illustrate the values of P_{Loss}, VD, and VSI obtained by all four methods, respectively, over 20 runs. Figures 5.3 (c), 5.4 (c), and 5.5 (c) depict the load bus voltage magnitudes for each case of this system. In the case of reducing P_{Loss} (Case 1), the voltages at several load buses reached their peak levels, as illustrated in Figure 5.3 (c). Conversely, this phenomenon did not occur when focusing on minimizing VD (CASE 2) and VSI (CASE 3), as depicted in Figures 5.4 (c) and 5.5 (c), respectively. Nonetheless, reducing voltage deviation can significantly impact generators, compelling them to surpass their reactive power production limits. An alteration in the demand for reactive power could prompt adjacent generators to either supply or take in additional VAR.

The best, worst, and mean values for each objective are shown in Table 5.4, along with the standard deviation (Std.) that was acquired using the proposed algorithm and alternative approaches over the course of twenty runs. The statistical outcomes show that the proposed algorithm attains the least values for the best and mean values for the P_{Loss}, VD, and VSI. Figure 5.6 depicts the percentage savings for each objective relative to the base scenario, utilizing all four methods. The proposed method yields the highest savings among all four methods for P_{Loss}, VD, and VSI, which are 21.75%, 92.54%, and 32.95%, respectively.

turnitin Page 127 of 208 - Integrity Submission Submission ID trn:oid:::27535:142293373

turnitin Page 128 of 208 - Integrity Submission Submission ID trn:oid:::27535:142293373

Table 5.4: Comparison of results for 20 Independent runs with different algorithms of the IEEE-30 bus system.

CASE	Objective Function	Algorithm	Best	Worst	Mean	Std.
CASE 1	Min P_{Loss} (MW)	COOT	4.8631	4.8812	4.8701	4.527E-03
		DTBO	4.8983	4.9768	4.9326	2.44E-02
		EASOM	4.8891	4.9868	4.9415	2.48E-02
		Proposed	**4.8612**	4.8688	4.8634	1.77E-03
CASE 2	Min VD (p.u.)	COOT	0.09433	0.12309	0.10583	8.082E-03
		DTBO	0.0927	0.1242	0.1046	8.43E-03
		EASOM	0.1238	0.1616	0.1415	1.01E-02
		Proposed	**0.0877**	0.0958	0.0906	1.78E-03
CASE 3	Min VSI (p.u.)	COOT	0.11289	0.1145	0.11371	1.225E-03
		DTBO	0.1129	0.1174	0.1144	9.80E-04
		EASOM	0.1135	0.1171	0.1148	7.89E-04
		Proposed	**0.1121**	0.1149	0.1134	7.83E-04

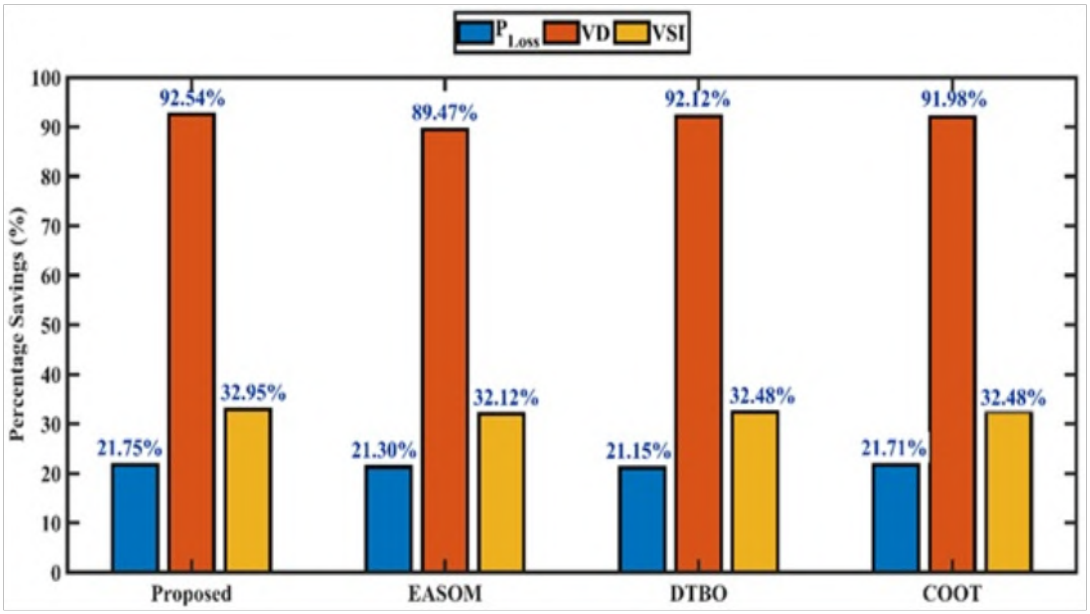


Fig. 5.6: Percentage saving achieved in P_{Loss}, VD, and VSI by each method for the IEEE 30-bus system.

turnitin Page 128 of 208 - Integrity Submission Submission ID trn:oid:::27535:142293373

turnitin Page 129 of 208 - Integrity Submission Submission ID trn:oid:::27535:142293373

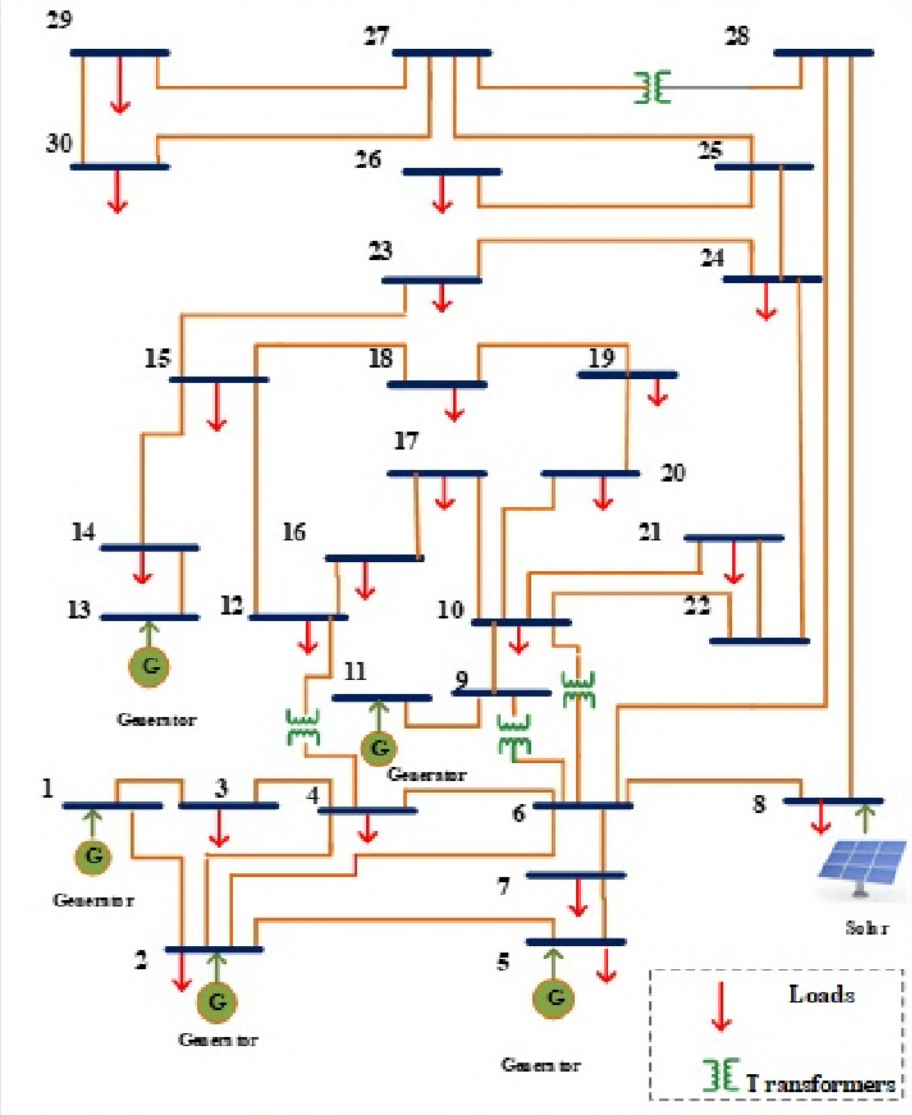


Fig. 5.7: Modified IEEE 30-bus system.

5.4.3 Modified IEEE-30 bus system

In the system, the thermal generator at bus 8 has been substituted with a photovoltaic unit, as shown in Figure 5.7. The hourly estimated solar PV power for a day shown in Figure 5.2 (b) has been utilized to carry out this study. If there is insufficient power generation from the solar PV unit, the swing generator is required to adjust and provide the necessary balance of real power. Table A.4 of Appendix A contains the generating data for this system. The permissible limits

turnitin Page 129 of 208 - Integrity Submission Submission ID trn:oid:::27535:142293373

turnitin Page 130 of 208 - Integrity Submission Submission ID trn:oid:::27535:142293373

on the state and control variables are taken similarly to the scenarios presented in Cases 1, 2, and 3. This analysis assumes the swing generator's maximum real power output of 200 MW is sufficient to supply the load, even when solar generation is unavailable. The expected average P_{Loss}, VD, and VSI for a day are determined using Equations 5.26, 5.27, and 5.28, respectively.

Table 5.5: Single objective ORPD results for the modified IEEE 30-Bus System.

CASE	Objective Function	Algorithm	$\mathbf{EA}_{P_{\text{Loss}}}$	EA_{VD}	EA_{VSI}
CASE 4	Min $\text{EA}_{P_{\text{Loss}}}$ (MW)	COOT	5.5493	0.8622	0.1242
		DTBO	5.6990	0.4267	0.1486
		EASOM	5.6335	0.4543	0.1391
		Proposed	**5.5267**	0.8958	0.1391
CASE 6	Min EA_{VD} (p.u.)	COOT	6.4483	0.1160	0.1280
		DTBO	6.4395	0.1521	0.1288
		EASOM	6.5558	0.1391	0.1284
		Proposed	6.3907	**0.0966**	0.1292
CASE 6	Min EA_{VSI} (p.u.)	COOT	6.8143	0.7199	0.1135
		DTBO	6.5278	0.7699	0.1162
		EASOM	6.1303	0.5658	0.1233
		Proposed	6.8476	0.7562	**0.1128**

Table 5.5 presents the optimized values for the expected average of P_{Loss} ($\text{EA}_{P_{\text{Loss}}}$), VD (EA_{VD}), and VSI (EA_{VSI}) obtained using all four methods. The table also displays the values of the other two objectives while concentrating on reducing the selected objective. For Cases 4, 5, and 6, the expected average of P_{Loss}, VD and VSI obtained by the proposed algorithm are 5.5267 MW, 0.0966 p.u., and 0.1128 p.u., respectively, representing the lowest values across all the methods applied.

As shown in Figure 5.8, the proposed algorithm achieves the lowest $\text{EA}_{P_{\text{Loss}}}$, yielding a saving of 1.93% compared to EASOM, 3.12% relative to DTBO and 0.41% against the COOT algorithm. Additionally, it improves EA_{VD} by approximately 44% in comparison to EASOM and achieves a 57.45% reduction in EA_{VD} relative to

turnitin Page 130 of 208 - Integrity Submission Submission ID trn:oid:::27535:142293373

turnitin Page 131 of 208 - Integrity Submission Submission ID trn:oid:::27535:142293373

DTBO and 20.1% compared to COOT. Comparatively, it improves EA_{VSI} by 9.31% in relation to EASOM and achieves a 3.02% decrease in EA_{VSI} relative to DTBO and 0.62% relative to COOT. Figure 5.9 (a), 5.9 (b) and 5.9 (c) show the hourly profile of three objectives obtained during optimization for each of the cases for minimizing the P_{Loss}, VD and VSI, respectively, using all four methods. Figure 5.9 (a) illustrates that increased solar power penetration in the system correlates with reduced P_{Loss}. Likewise, when the solar PV power production is nil, the power loss in the system is highest.

Figure 5.10 (a), 5.10 (b) and 5.10 (c) show the load voltage profiles obtained during optimization for each of the cases for minimizing the P_{Loss}, VD and VSI, respectively, using all four methods. Figure 5.11 (a), 5.11 (b), and 5.11 (c) illustrate the distribution of the reactive power produced at the generator bus across a 24-hour interval during optimization aimed at minimizing P_{Loss}, VD, and VSI, respectively, using all four methods.

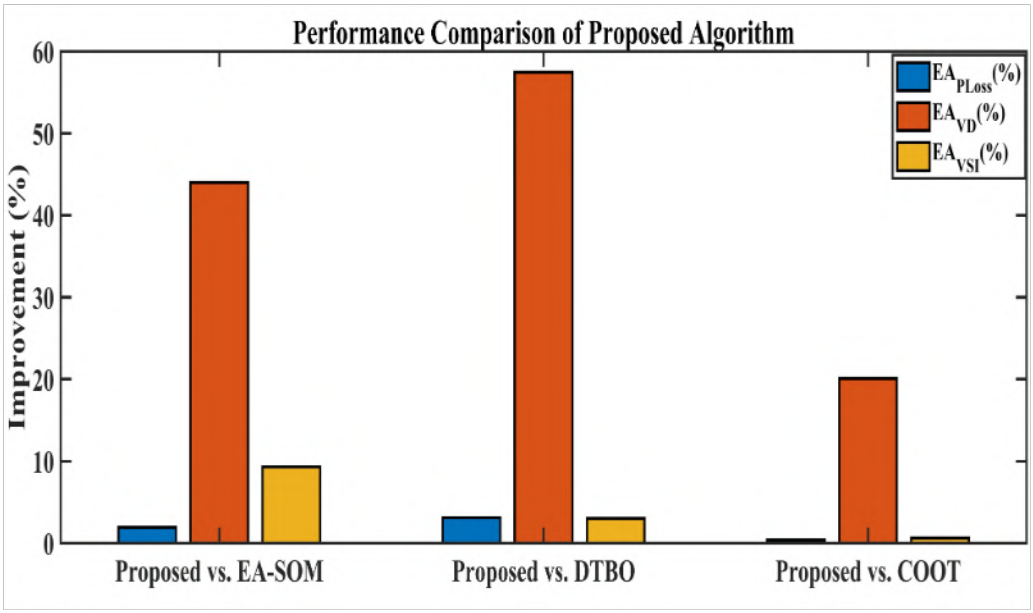
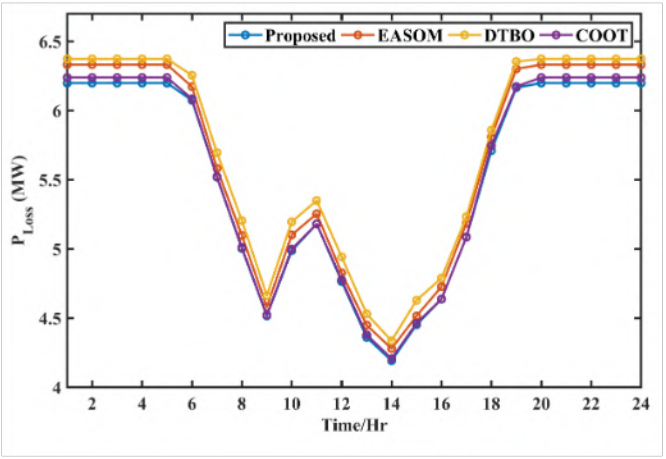


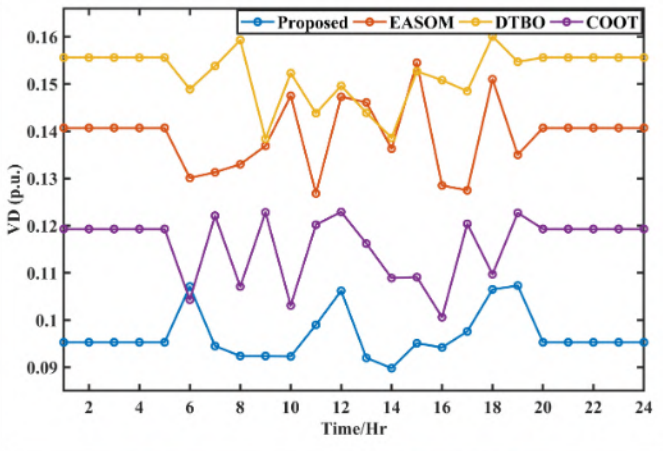
Fig. 5.8: Performance comparison of the proposed algorithm with the EASOM, DTBO, and COOT.

turnitin Page 131 of 208 - Integrity Submission Submission ID trn:oid:::27535:142293373

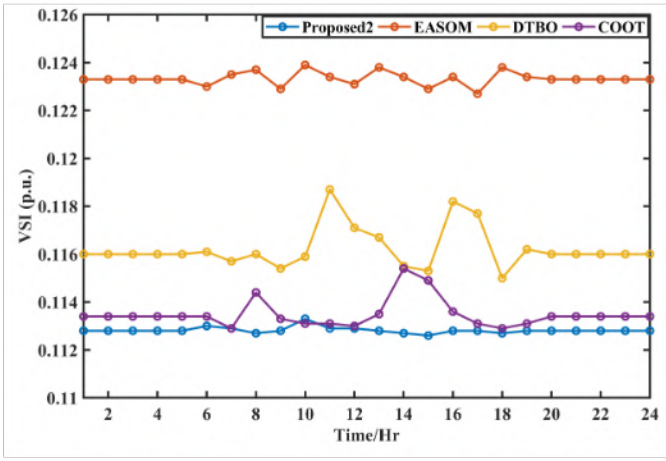
turnitin Page 132 of 208 - Integrity Submission Submission ID trn:oid:::27535:142293373



(a) P_{Loss} minimization (CASE 4).



(b) VD minimization (CASE 5).

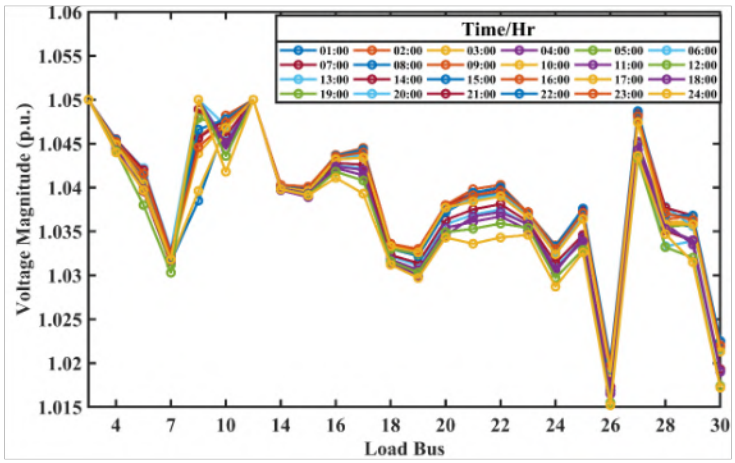


(c) VSI minimization (CASE 6).

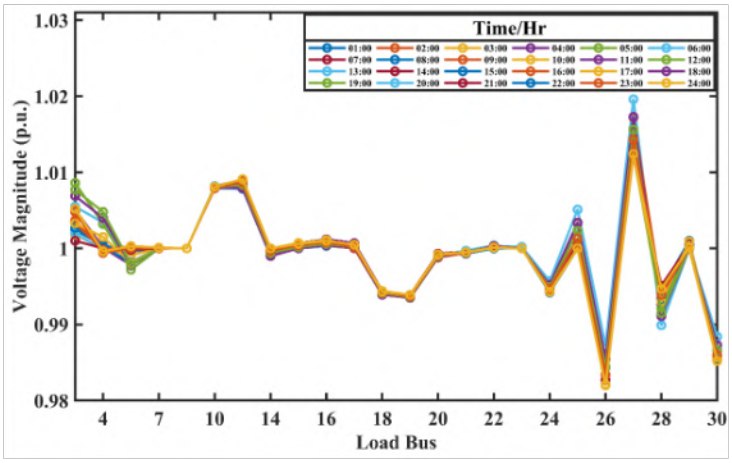
Fig. 5.9: Hourly profiles of the objective functions obtained using the proposed algorithm.

turnitin Page 132 of 208 - Integrity Submission Submission ID trn:oid:::27535:142293373

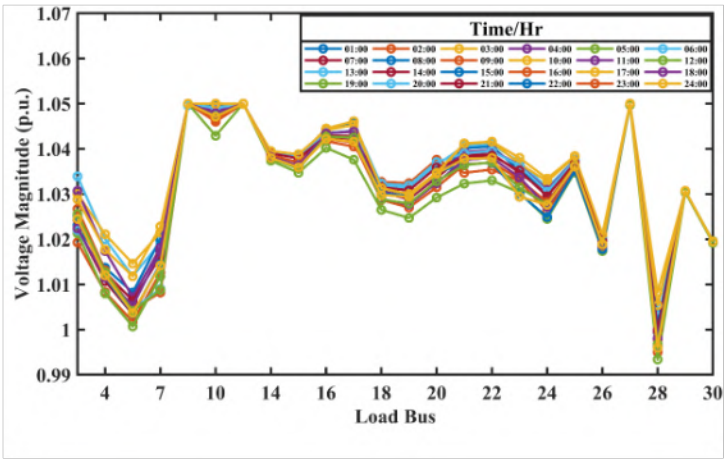
turnitin Page 133 of 208 - Integrity Submission Submission ID trn:oid:::27535:142293373



(a) P_{Loss} minimization (CASE 4).



(b) VD minimization (CASE 5).

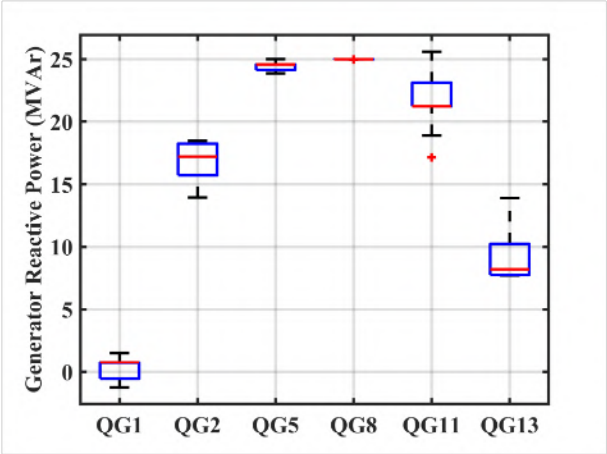


(c) VSI minimization (CASE 6).

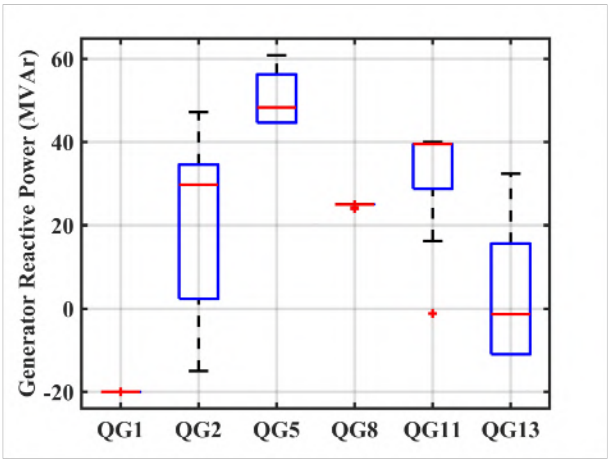
Fig. 5.10: Hourly load-bus voltage profiles obtained using the proposed algorithm.

turnitin Page 133 of 208 - Integrity Submission Submission ID trn:oid:::27535:142293373

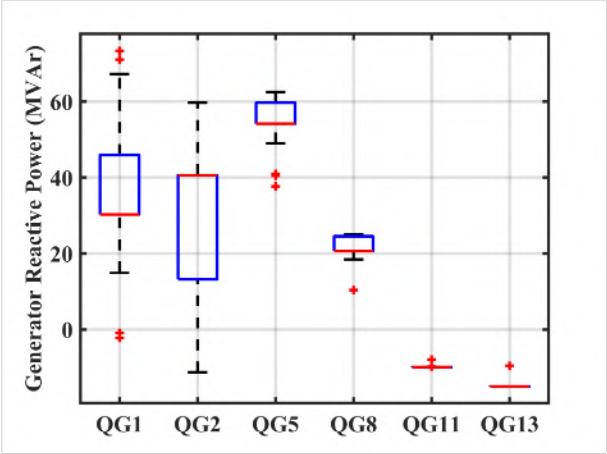
turnitin Page 134 of 208 - Integrity Submission Submission ID trn:oid:::27535:142293373



(a) P_{Loss} minimization (CASE 4).



(b) VD minimization (CASE 5).



(c) VSI minimization (CASE 6).

Fig. 5.11: Generator reactive power distribution over a 24-hour interval.

turnitin Page 134 of 208 - Integrity Submission Submission ID trn:oid:::27535:142293373

turnitin Page 135 of 208 - Integrity Submission Submission ID trn:oid:::27535:142293373

5.4.4 IEEE 118-bus system

To evaluate the suitability of the proposed algorithm for large-scale systems, it is applied to the ORPD problem of the IEEE 118-bus system. This system comprises 54 generators, 14 shunt VAR compensators, and 9 transformers with off-nominal tap ratios. The total load connected to this system is 4242 MW and 1438 MVAr. All variables are treated as continuous and the generation (excluding swing) is kept constant in this study. Table A.5 of Appendix A contains the generating data for this system. The control variable limits for all cases in this study are shown in Table 5.6. The load bus voltage range of this system is taken between 0.94 and 1.06 p.u. For this system, each algorithm is allowed up to 600 iterations with a fixed population size of 50. The effectiveness and reliability of the proposed algorithm are evaluated for this system using DTBO, COOT, and EASOM methods. Three case studies (Case 7, 8 and 9) are used to compare the proposed algorithm with other methods, focusing on minimizing P_{Loss}, VD, and VSI, respectively.

Table 5.6 shows the best values and allowable ranges for all estimated state and control variables for case studies using the IEEE 118-bus to minimize objective functions. The study compares the best values for each of the three objectives attained by the applied algorithms to alternative possibilities. The table also shows the other two objectives while reducing the selected one. Table 5.6 shows that the proposed algorithm achieves the best results for P_{Loss} (117.9167 MW), VD (0.3383 p.u.), and VSI (0.0652 p.u.) compared to other techniques. Figure 5.12 depicts the percentage savings for each objective relative to the base scenario, utilizing all four methods. The proposed method yields the highest savings among all four methods for P_{Loss}, VD, and VSI, which are 11.25%, 76.50%, and 6.05%, respectively.

Figures 5.13 (a), 5.14 (a), and 5.15 (a) illustrate convergence curves for four methods to reduce P_{Loss} (Case 7), VD (Case 8), and VSI (Case 9) in the IEEE 118-bus system. Figures 5.13 (b), 5.14 (b), and 5.15 (b) illustrate the magnitudes of load bus voltages in each case. For each system condition, Figures 5.13 (c), 5.14 (c), and 5.15 (c) demonstrate reactive power generated by each generator during minimization of the aforesaid objectives.

turnitin Page 135 of 208 - Integrity Submission Submission ID trn:oid:::27535:142293373

turnitin Page 136 of 208 - Integrity Submission Submission ID trn:oid:::27535:142293373

Table 5.6: Single objective ORPD results for the IEEE 118-bus system.

Var.	Min	Max	CASE 7 (Min P_{Loss})				CASE 8 (Min VD)				CASE 9 (Min VSI)			
			Prop	EASOM	DTBO	COOT	Prop	EASOM	DTBO	COOT	Prop	EASOM	DTBO	COOT
Generator Voltage (p.u.)														
V1	0.94	1.06	0.9984	0.9893	0.9952	1.0094	0.9845	0.9817	0.9861	0.9898	0.9889	1.0033	0.9837	0.9873
V4	0.94	1.06	1.0357	1.0247	1.0343	1.0451	1.0205	1.0190	1.0098	1.0140	1.0430	1.0296	1.0499	1.0197
V6	0.94	1.06	1.0210	1.0153	1.0213	1.0356	1.0060	0.9957	1.0010	1.0072	1.0127	1.0334	1.0194	1.0076
V8	0.94	1.06	1.0381	1.0357	1.0470	1.0396	0.9938	0.9938	0.9806	1.0023	0.9888	1.0261	1.0227	1.0131
V10	0.94	1.06	1.0591	1.0600	1.0501	1.0578	0.9889	0.9892	1.0019	1.0157	1.0243	1.0296	1.0072	0.9876
V12	0.94	1.06	1.0196	1.0100	1.0150	1.0284	1.0119	1.0099	1.0118	1.0141	1.0135	1.0262	1.0082	1.0097
V15	0.94	1.06	1.0147	1.0097	1.0129	1.0100	0.9916	1.0035	1.0002	0.9971	1.0007	1.0061	1.0019	1.0043
V18	0.94	1.06	1.0157	1.0113	1.0186	1.0146	0.9919	1.0098	1.0053	1.0016	1.0071	1.0083	1.0052	1.0105
V19	0.94	1.06	1.0121	1.0085	1.0128	1.0092	0.9899	1.0032	0.9993	0.9967	0.9969	1.0027	1.0006	1.0039
V24	0.94	1.06	1.0283	1.0276	1.0269	1.0286	1.0376	1.0411	1.0061	1.0131	1.0154	1.0244	1.0251	1.0539
V25	0.94	1.06	1.0598	1.0581	1.0587	1.0591	1.0166	1.0200	1.0437	1.0502	1.0292	1.0169	1.0183	1.0546
V26	0.94	1.06	1.0600	1.0597	1.0593	1.0572	0.9566	0.9777	0.9915	0.9757	0.9991	1.0189	1.0074	0.9889
V27	0.94	1.06	1.0263	1.0153	1.0130	1.0152	1.0086	1.0069	1.0111	1.0039	1.0045	1.0136	0.9962	1.0127
V31	0.94	1.06	1.0139	1.0104	1.0131	1.0117	1.0021	1.0036	1.0132	1.0059	0.9933	1.0026	1.0063	0.9940
V32	0.94	1.06	1.0193	1.0127	1.0154	1.0125	1.0016	1.0034	1.0128	1.0057	0.9971	1.0010	0.9962	1.0077
V34	0.94	1.06	1.0249	1.0257	1.0346	1.0179	1.0068	1.0053	1.0039	1.0054	1.0130	1.0270	1.0186	1.0174
V36	0.94	1.06	1.0204	1.0215	1.0306	1.0128	1.0004	0.9999	0.9971	0.9997	1.0066	1.0225	1.0146	1.0110
V40	0.94	1.06	0.9998	1.0059	1.0143	0.9997	1.0058	1.0069	1.0078	1.0074	1.0167	0.9862	1.0130	1.0222
V42	0.94	1.06	1.0049	1.0112	1.0137	1.0053	1.0107	1.0074	1.0001	1.0052	1.0153	1.0442	1.0402	1.0208
V46	0.94	1.06	1.0255	1.0216	1.0229	1.0159	1.0493	0.9994	1.0436	1.0413	1.0491	1.0597	1.0406	1.0600
V49	0.94	1.06	1.0429	1.0354	1.0414	1.0381	1.0049	1.0153	1.0032	1.0047	1.0348	1.0311	1.0508	1.0368
V54	0.94	1.06	1.0093	1.0043	1.0114	1.0149	1.0211	1.0083	1.0241	1.0241	1.0017	1.0240	1.0106	1.0163
V55	0.94	1.06	1.0073	1.0008	1.0081	1.0127	1.0099	0.9988	1.0125	1.0112	0.9935	1.0142	1.0025	1.0069
V56	0.94	1.06	1.0079	1.0020	1.0089	1.0131	1.0129	1.0017	1.0153	1.0138	0.9965	1.0168	1.0052	1.0095
V59	0.94	1.06	1.0296	1.0226	1.0302	1.0376	1.0046	1.0065	0.9989	0.9853	0.9997	1.0041	0.9808	1.0037
V61	0.94	1.06	1.0305	1.0164	1.0288	1.0388	1.0021	1.0027	1.0025	1.0080	0.9910	1.0169	1.0065	1.0009
V62	0.94	1.06	1.0283	1.0157	1.0249	1.0368	0.9994	0.9959	0.9965	1.0035	0.9882	1.0055	0.9989	0.9905
V65	0.94	1.06	1.0534	1.0391	1.0595	1.0583	1.0070	1.0027	1.0218	1.0005	1.0159	1.0031	1.0360	1.0268
V66	0.94	1.06	1.0554	1.0491	1.0500	1.0559	1.0119	1.0158	1.0151	1.0078	1.0124	1.0093	1.0209	1.0032
V69	0.94	1.06	1.0589	1.0496	1.0521	1.0539	1.0463	1.0250	1.0541	1.0550	1.0568	1.0467	1.0600	1.0342
V70	0.94	1.06	1.0191	1.0134	1.0115	1.0157	0.9987	1.0043	1.0056	1.0026	1.0085	0.9991	1.0251	1.0100
V72	0.94	1.06	1.0182	1.0169	1.0134	1.0153	0.9414	1.0221	0.9767	0.9480	1.0452	0.9404	1.0048	1.0491
V73	0.94	1.06	1.0129	1.0089	1.0156	1.0164	1.0261	1.0019	1.0264	1.0098	1.0255	1.0350	1.0581	1.0269
V74	0.94	1.06	0.9972	0.9915	0.9887	0.9941	0.9751	0.9816	0.9826	0.9801	0.9775	0.9651	0.9943	0.9771
V76	0.94	1.06	0.9872	0.9768	0.9753	0.9808	0.9620	0.9740	0.9681	0.9662	0.9593	0.9415	0.9696	0.9563
V77	0.94	1.06	1.0308	1.0209	1.0170	1.0236	1.0060	1.0246	1.0094	1.0075	1.0058	0.9943	1.0091	0.9996
V80	0.94	1.06	1.0470	1.0353	1.0315	1.0383	1.0220	1.0543	1.0272	1.0232	1.0371	1.0178	1.0233	1.0268

turnitin Page 136 of 208 - Integrity Submission Submission ID trn:oid:::27535:142293373

turnitin Page 137 of 208 - Integrity Submission Submission ID trn:oid:::27535:142293373

Var.	Min	Max	CASE 7 (Min P_{Loss})				CASE 8 (Min VD)				CASE 9 (Min VSI)			
			Prop	EASOM	DTBO	COOT	Prop	EASOM	DTBO	COOT	Prop	EASOM	DTBO	COOT
V85	0.94	1.06	1.0405	1.0309	1.0325	1.0290	1.0037	1.0054	1.0041	1.0050	0.9813	0.9911	1.0032	0.9848
V87	0.94	1.06	1.0474	1.0398	1.0326	1.0043	1.0219	1.0172	1.0201	1.0161	1.0180	1.0197	1.0126	1.0115
V89	0.94	1.06	1.0597	1.0504	1.0538	1.0546	1.0144	1.0203	1.0130	1.0181	0.9993	1.0164	1.0337	0.9981
V90	0.94	1.06	1.0305	1.0180	1.0200	1.0279	1.0421	1.0144	1.0128	0.9843	1.0151	0.9995	0.9979	0.9967
V91	0.94	1.06	1.0278	1.0176	1.0113	1.0290	1.0273	1.0146	1.0064	0.9964	0.9919	1.0088	1.0153	1.0057
V92	0.94	1.06	1.0390	1.0308	1.0301	1.0344	1.0075	1.0092	1.0058	1.0017	0.9935	1.0030	1.0146	0.9918
V99	0.94	1.06	1.0364	1.0318	1.0218	1.0283	1.0584	0.9994	0.9948	1.0097	0.9981	0.9899	0.9932	1.0054
V100	0.94	1.06	1.0445	1.0350	1.0325	1.0344	1.0238	1.0168	1.0302	1.0096	1.0188	1.0166	1.0202	1.0124
V103	0.94	1.06	1.0311	1.0240	1.0227	1.0228	1.0122	1.0136	1.0227	0.9949	1.0049	1.0090	1.0064	1.0060
V104	0.94	1.06	1.0184	1.0100	1.0095	1.0077	0.9999	0.9961	1.0138	0.9879	0.9951	0.9998	0.9943	0.9999
V105	0.94	1.06	1.0142	1.0059	1.0079	1.0051	1.0012	0.9967	1.0125	0.9965	0.9998	1.0042	0.9992	1.0025
V107	0.94	1.06	1.0015	0.9954	1.0004	0.9981	1.0224	1.0132	1.0212	1.0536	1.0221	1.0512	1.0274	1.0403
V110	0.94	1.06	1.0082	1.0090	1.0121	1.0075	1.0060	1.0101	0.9901	1.0076	1.0057	1.0015	1.0054	1.0018
V111	0.94	1.06	1.0183	1.0260	1.0307	1.0232	1.0203	1.0286	0.9855	1.0185	1.0292	1.0143	1.0258	1.0193
V112	0.94	1.06	0.9966	0.9963	1.0008	0.9981	1.0136	1.0133	0.9823	1.0258	1.0024	0.9980	1.0083	1.0017
V113	0.94	1.06	1.0274	1.0210	1.0251	1.0230	1.0041	1.0204	1.0129	0.9993	1.0330	1.0246	1.0287	1.0255
V116	0.94	1.06	1.0431	1.0307	1.0448	1.0529	0.9937	0.9942	0.9946	0.9967	1.0058	0.9992	1.0195	0.9902
Transformer Tap Position (p.u.)														
T8	0.90	1.10	0.9953	0.9910	0.9917	0.9791	1.0143	1.0297	0.9463	0.9515	0.9800	0.9094	0.9758	0.9686
T32	0.90	1.10	0.9879	1.0210	1.0230	0.9984	0.9983	0.9812	0.9897	0.9372	1.0070	1.0112	0.9898	0.9741
T36	0.90	1.10	1.0048	1.0001	1.0121	1.0206	1.0101	0.9860	0.9938	0.9845	0.9847	1.0111	0.9981	0.9646
T51	0.90	1.10	0.9932	0.9839	0.9857	0.9984	0.9799	0.9824	0.9750	0.9839	0.9823	0.9412	0.9884	0.9700
T93	0.90	1.10	1.0022	0.9814	1.0036	0.9960	1.0005	0.9968	1.0038	1.0181	0.9638	0.9375	0.9996	0.9598
T95	0.90	1.10	1.0016	1.0351	1.0326	1.0214	0.9851	0.9905	0.9745	0.9882	0.9871	0.9192	0.9773	0.9735
T102	0.90	1.10	0.9791	0.9804	1.0077	0.9994	1.0000	0.9772	0.9927	0.9773	1.0138	1.0037	1.0277	1.0530
T107	0.90	1.10	0.9331	0.9484	0.9677	0.9425	0.9595	0.9922	0.9295	0.9322	1.0062	1.0046	0.9103	0.9079
T127	0.90	1.10	0.9893	0.9853	1.0013	1.0112	0.9616	0.9342	0.9552	0.9646	0.9580	0.9048	0.9845	0.9915
Shunt Compensators (MVAr)														
QL5	-40	0	-10.27	-28.65	-22.67	-12.19	-34.10	-39.29	-23.49	-28.5	-6.45	-6.072	-10.13	-2.12
QC34	0	14	7.2561	6.3280	12.9323	7.5607	8.9657	8.4017	4.5102	8.5033	12.0087	8.2430	4.5352	6.6465
QL37	-20	0	-0.124	-2.163	-11.9	-20.00	-2.593	-19.44	-7.466	-7.203	-13.53	-0.377	-7.264	-13.20
QC44	0	10	9.0676	8.7386	4.0213	9.2087	7.8206	8.1439	7.4349	9.7074	9.9605	6.6333	8.4287	8.2166
QC45	0	10	8.3120	8.7615	8.8378	7.4791	6.9363	9.9311	9.9431	9.8101	9.8223	9.9814	8.9348	9.9359
QC46	0	10	4.9577	2.9709	9.2822	6.9616	0.5001	1.9994	5.7036	1.5826	0.5907	0.1054	7.5064	9.6304
QC48	0	15	9.4439	9.5941	4.0599	7.9681	5.8494	4.0976	0.0584	4.4652	6.5481	12.0884	2.4980	7.1288
QC74	0	12	6.7158	11.1524	7.4711	9.9265	4.4725	10.3647	10.5296	5.8760	4.5272	8.5528	9.9287	11.2725
QC79	0	20	12.4139	19.4387	10.6620	18.9657	11.0202	0.5709	0.0070	9.7400	17.1062	10.2302	12.7434	18.6294
QC82	0	20	10.5863	19.7056	13.5142	9.1923	19.9028	7.9379	19.9678	19.4327	14.8483	6.2148	17.1790	2.8481
QC83	0	10	7.2785	8.4303	6.9547	3.2027	7.5812	9.4836	4.4413	5.5920	6.0255	9.9033	3.2592	5.9327
QC105	0	20	10.0033	9.8791	16.4796	9.2636	19.2246	10.7667	19.2896	16.5713	17.0894	14.9837	14.9280	11.9395

turnitin Page 137 of 208 - Integrity Submission Submission ID trn:oid:::27535:142293373

turnitin Page 138 of 208 - Integrity Submission Submission ID trn:oid:::27535:142293373

Var.	Min	Max	CASE 7 (Min P_{Loss})				CASE 8 (Min VD)				CASE 9 (Min VSI)			
			Prop	EASOM	DTBO	COOT	Prop	EASOM	DTBO	COOT	Prop	EASOM	DTBO	COOT
QC107	0	6	0.0000	0.6028	1.5792	3.7738	2.1923	3.4270	1.2061	3.2036	2.5328	0.6941	3.5502	3.1649
QC110	0	6	1.5425	5.8167	3.1355	1.1174	4.4152	4.4903	4.0975	5.1462	0.9551	5.0509	2.9793	2.5629
Objective Functions														
P_{Loss} (MW)	132.863		**117.9167**	119.5425	118.9962	118.4339	136.6235	130.9738	132.2536	135.0365	132.6672	135.9679	129.9780	132.7068
VD (p.u.)	1.4393		1.3551	1.0023	1.1878	1.2298	**0.3383**	0.4086	0.3617	0.3665	0.7586	0.9667	0.7496	0.7859
VSI (p.u.)	0.0694		0.0668	0.0674	0.0702	0.0681	0.0692	0.0706	0.0689	0.0674	**0.0652**	0.0664	0.0661	0.0654

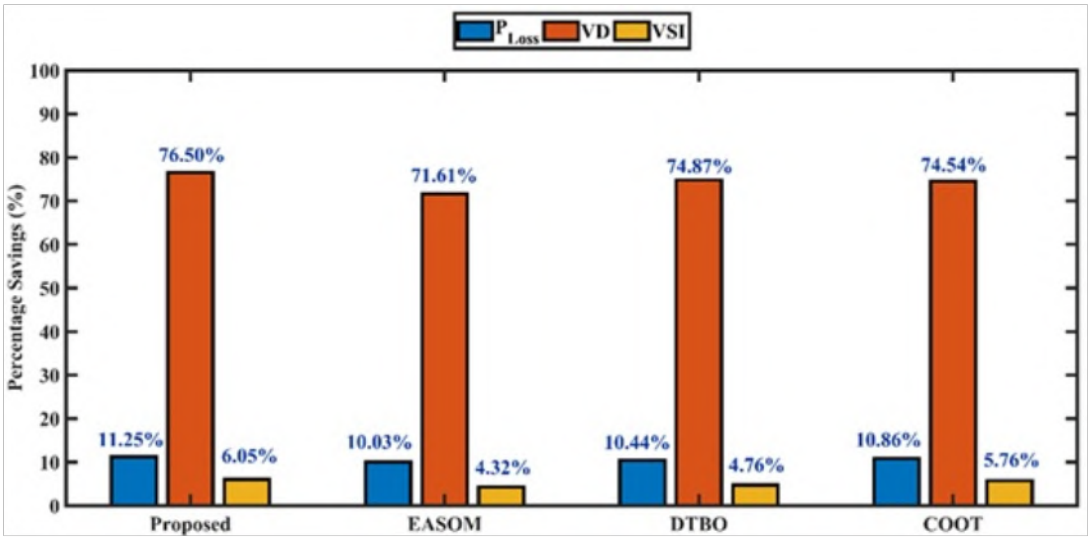
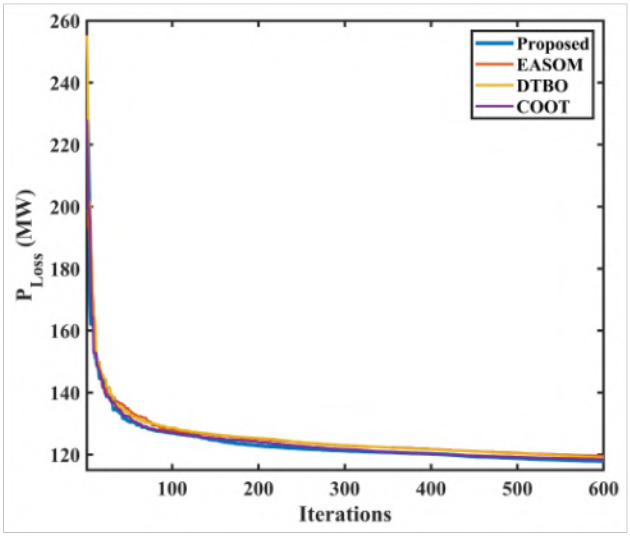


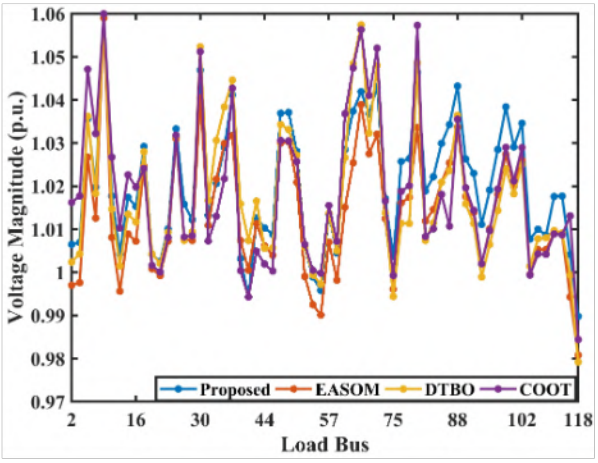
Fig. 5.12: Percentage saving achieved in P_{Loss}, VD and VSI by each method for IEEE 118-bus.

turnitin Page 138 of 208 - Integrity Submission Submission ID trn:oid:::27535:142293373

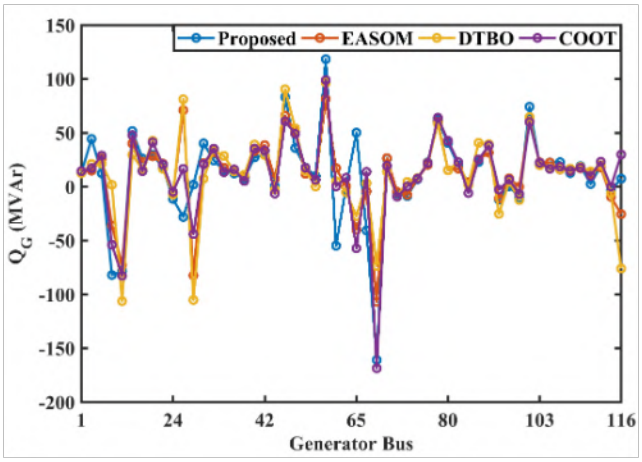
turnitin Page 139 of 208 - Integrity Submission Submission ID trn:oid:::27535:142293373



(a) Convergence curve.



(b) Voltage magnitudes of load buses.

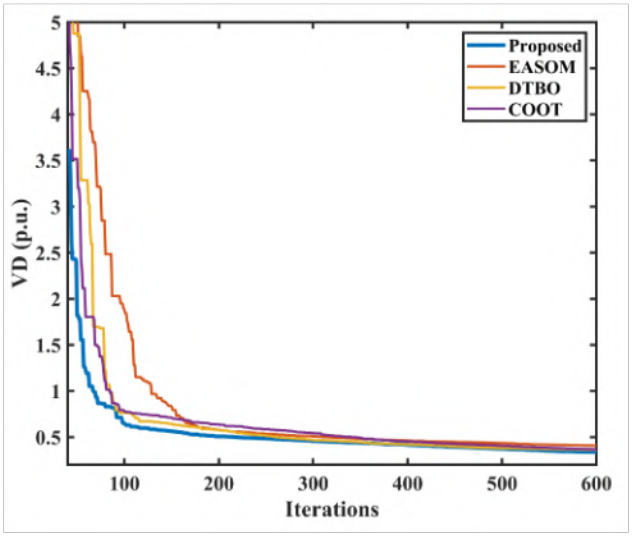


(c) Generator reactive power.

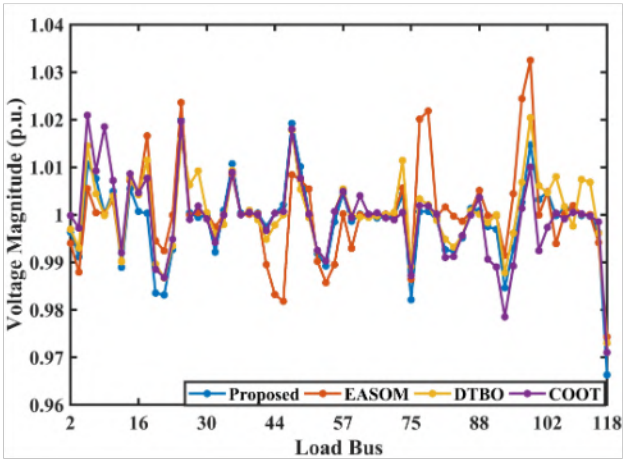
Fig. 5.13: P_{Loss} minimization (CASE 7).

turnitin Page 139 of 208 - Integrity Submission Submission ID trn:oid:::27535:142293373

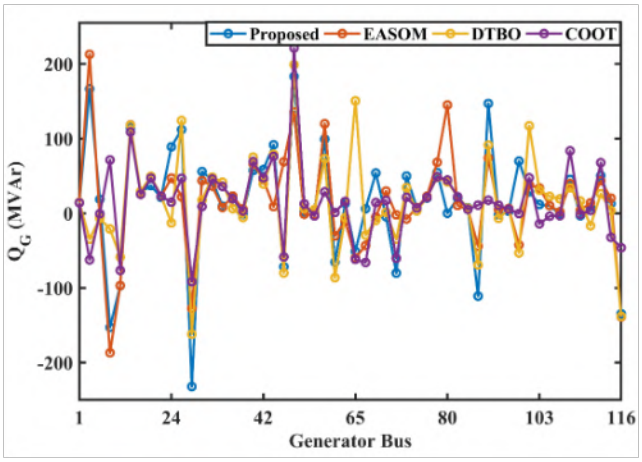
turnitin Page 140 of 208 - Integrity Submission Submission ID trn:oid:::27535:142293373



(a) Convergence curve.



(b) Voltage magnitudes of load buses.

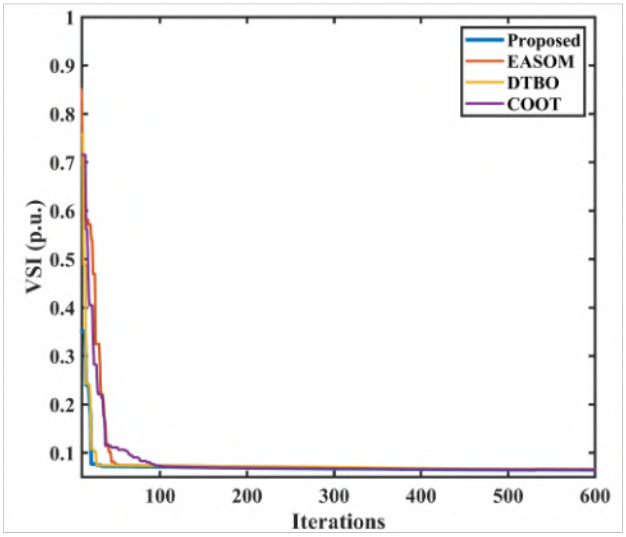


(c) Generator reactive power.

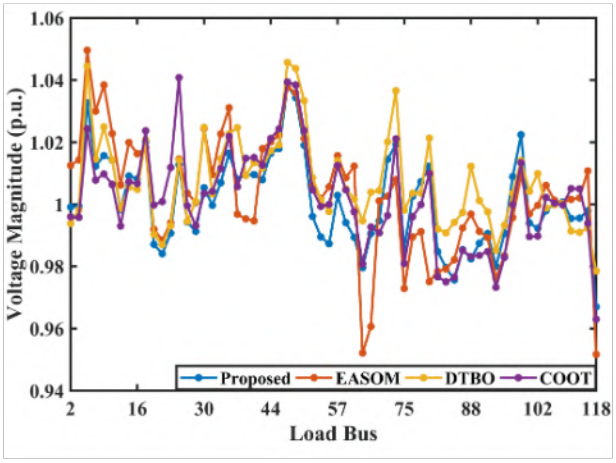
Fig. 5.14: *VD* minimization (CASE 8).

turnitin Page 140 of 208 - Integrity Submission Submission ID trn:oid:::27535:142293373

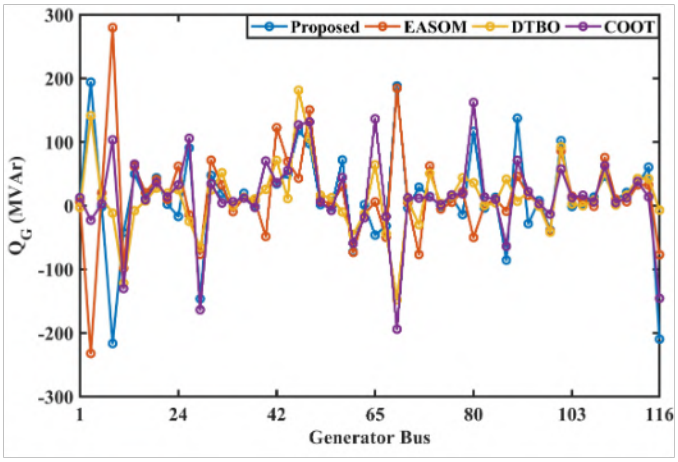
turnitin Page 141 of 208 - Integrity Submission Submission ID trn:oid:::27535:142293373



(a) Convergence curve.



(b) Voltage magnitudes of load buses.



(c) Generator reactive power.

Fig. 5.15: *VSI* minimization (CASE 9).

turnitin Page 141 of 208 - Integrity Submission Submission ID trn:oid:::27535:142293373

turnitin Page 142 of 208 - Integrity Submission Submission ID trn:oid:::27535:142293373

5.5 Conclusions

This research work introduced a novel machine learning-based improved EASOM method for the deterministic and stochastic ORPD problem in the IEEE 30-bus test system. A detailed statistical analysis is carried out to compare the performance of the proposed algorithm with recently developed algorithms such as EASOM, DTBO, and COOT, which showcases the proficiency and strength of the proposed algorithm, which was used to tackle the same issue. For the deterministic ORPD problem, the proposed algorithm yields the best results regarding P_{Loss} (4.8612 MW), VD (0.0877 p.u.), and VSI (0.1121 p.u.) compared to all other methods applied. The stochastic ORPD problem is analyzed using the modified IEEE 30-bus system, considering a solar PV power plant at bus 8. For the stochastic ORPD problem, the proposed algorithm achieves the lowest EA_{PL}, yielding a saving of 1.93% compared to EASOM, 3.12% relative to DTBO and 0.41% against the COOT algorithm. Additionally, it improves EA_{VD} by approximately 44% in comparison to EASOM and achieves a 57.45% reduction in EA_{VD} relative to DTBO and 20.1% compared to COOT. Comparatively, it improves EA_{VSI} by 9.31% in relation to EASOM and achieves a 3.02% decrease in EA_{VSI} relative to DTBO and 0.62% relative to COOT. To assess its applicability for larger-scale systems, it is also used to tackle the deterministic ORPD problem in the IEEE 118-bus system. Among all the considered methods, the proposed algorithm achieves the best performance for this system with respect to P_{Loss} (117.9167 MW), VD (0.3383 p.u.), and VSI (0.0652 p.u.). The proposed approach may be implemented in further studies to solve multi-objective problems with the goal of achieving equilibrium among conflicting objectives. These multi-objective problems may include P_{Loss}, VD, and VSI, and other objectives.

turnitin Page 142 of 208 - Integrity Submission Submission ID trn:oid:::27535:142293373

turnitin Page 143 of 208 - Integrity Submission Submission ID trn:oid:::27535:142293373

Chapter 6

Proposed Hybrid Multi-Objective Optimization Algorithm

6.1 Introduction

This chapter presents an extension of the single-objective optimization method discussed in Chapter 4 to a multi-objective optimization framework for solving complex power system optimization problems. While the method presented in the previous chapter was designed to optimize a single objective effectively, practical power system operation generally involves multiple conflicting objectives that must be satisfied simultaneously. Therefore, the proposed approach is further enhanced to address multi-objective optimization requirements with improved convergence and diversity characteristics.

The developed multi-objective hybrid evolutionary algorithm integrates Opposition-Based Learning (OBL), Differential Evolution (DE), and the Giza Pyramids Construction (GPC) algorithm with an NSGA-II-based selection mechanism. The incorporation of these strategies improves the exploration and exploitation capabilities of the algorithm and enables efficient generation of well-distributed Pareto-optimal solutions. Opposition-Based Learning enhances population initialization and accelerates convergence, Differential Evolution strengthens local search capability, while the GPC algorithm contributes toward maintaining population diversity and avoiding premature convergence. The NSGA-II-based selection mechanism ensures proper non-dominated sorting and elitism during the optimization process.

To evaluate the effectiveness of the proposed multi-objective extension, the

turnitin Page 143 of 208 - Integrity Submission Submission ID trn:oid:::27535:142293373

turnitin Page 144 of 208 - Integrity Submission Submission ID trn:oid:::27535:142293373

algorithm is first tested on standard benchmark problems, including the ZDT and DTLZ test suites. These benchmark functions are widely used for analyzing convergence behavior, solution diversity, and Pareto front approximation quality of multi-objective optimization algorithms. The performance of the proposed method is assessed using several established performance indicators such as Inverted Generational Distance (IGD), Hypervolume (HV), Generational Distance (GD), Maximum Spread (MS), and Spacing (S). Comparative analysis is carried out against recently developed algorithms such as Multi-objective Particle Swarm Optimization (MOPSO) [127], Multi-objective Grasshopper Optimization Algorithm (MOGOA) [128], Multi-objective Mayfly Algorithm (MOMA) [129], and Multi-objective Sunflower Optimization (MOSFO) [130].

Furthermore, the proposed algorithm is applied to solve the MOORPD problem on the IEEE 30-bus and IEEE 57-bus test systems. The optimization process simultaneously minimizes active P_{Loss}, VD, and VSI under various operating conditions while satisfying all system constraints. In addition, the proposed method is extended to solve stochastic ORPD problems considering uncertainties associated with RESs and load demand variations.

The detailed mathematical formulation of the proposed multi-objective hybrid algorithm, benchmark problem descriptions, performance evaluation criteria, simulation setup, and comparative analyses are presented in the subsequent sections and subsections of this chapter. The application of the proposed methodology to deterministic as well as stochastic MOORPD problems is also discussed comprehensively in the following sections.

6.2 Overview of the Hybrid Multi-Objective Optimization Algorithm

The various steps involved in this novel multi-objective hybrid algorithm are summarized below.

Step 1: Multi-Objective Problem Formulation

The multi-objective optimization problem can be generally expressed as follows:

$$\min_{\vec{p}_i \in \Omega} F(\vec{p}_i) = [f_1(\vec{p}_i), f_2(\vec{p}_i), \ldots, f_M(\vec{p}_i)] \tag{6.1}$$

turnitin Page 144 of 208 - Integrity Submission Submission ID trn:oid:::27535:142293373

turnitin Page 145 of 208 - Integrity Submission Submission ID trn:oid:::27535:142293373

subject to

$$\vec{p}_i \in [\vec{p}_{\min}, \vec{p}_{\max}], \quad i = 1, 2, \ldots, N \tag{6.2}$$

where M specifies the total number of objectives and N represents the population size.

Step 2: Initialization

The initial population is initialized as follows

$$\vec{p}_i = \text{unifrnd}(\vec{p}_{\min}, \vec{p}_{\max}), \quad i = 1, 2, \ldots, N \tag{6.3}$$

Each solution is evaluated using

$$F_i = [f_1(\vec{p}_i), \ldots, f_M(\vec{p}_i)] \tag{6.4}$$

Step 3: Pareto Dominance

A solution $\vec{p}_a$ dominates $\vec{p}_b$ if

$$f_m(\vec{p}_a) \leq f_m(\vec{p}_b), \quad \forall m = 1, \ldots, M \tag{6.5}$$

and

$$f_m(\vec{p}_a) < f_m(\vec{p}_b) \quad \text{for at least one objective } m. \tag{6.6}$$

By using this dominance relation, successive non-dominated fronts are ranked. At iteration t, the parent population is defined as

$$P_t = \{\vec{p}_1^t, \vec{p}_2^t, \ldots, \vec{p}_N^t\} \tag{6.7}$$

Step 4: GPC Position Update

The displacement component is computed as

$$d = \frac{v_0^2}{2g(\sin\theta + \mu_k \cos\theta)} \tag{6.8}$$

The worker movement component is

turnitin Page 145 of 208 - Integrity Submission Submission ID trn:oid:::27535:142293373

turnitin Page 146 of 208 - Integrity Submission Submission ID trn:oid:::27535:142293373

$$x = \frac{v_0^2}{2g \sin\theta} \tag{6.9}$$

The updated solution is

$$\vec{p}_i^{new} = \vec{p}_i + d + x \cdot \vec{\varepsilon}_i \tag{6.10}$$

Boundary control:

$$\vec{p}_i^{new} = \min(\vec{p}_{\max}, \max(\vec{p}_{\min}, \vec{p}_i^{new})) \tag{6.11}$$

Step 5: Opposition-Based Learning

The opposite solution is computed from the current position as

$$\vec{p}_i^{opp} = \vec{p}_{\max} + \vec{p}_{\min} - \vec{p}_i \tag{6.12}$$

Boundary control:

$$\vec{p}_i^{opp} = \min(\vec{p}_{\max}, \max(\vec{p}_{\min}, \vec{p}_i^{opp})) \tag{6.13}$$

Step 6: DE Mutation and Crossover

Three distinct individuals $\vec{q}_a, \vec{q}_b, \vec{q}_c$ are selected randomly.

Mutation:

$$\vec{u}_i = \vec{q}_a + F(\vec{q}_b - \vec{q}_c) \tag{6.14}$$

Crossover:

$$w_{ij} = \begin{cases} u_{ij}, & r_j \le C_r \text{ or } j = k \\ p_{ij}, & \text{otherwise} \end{cases} \tag{6.15}$$

Boundary control:

$$\vec{w}_i = \min(\vec{p}_{\max}, \max(\vec{p}_{\min}, \vec{w}_i)) \tag{6.16}$$

Step 7: Local Dominance-Based Selection

First comparison:

turnitin Page 146 of 208 - Integrity Submission Submission ID trn:oid:::27535:142293373

turnitin Page 147 of 208 - Integrity Submission Submission ID trn:oid:::27535:142293373

$$\vec{p}_i^{(1)} = \begin{cases} \vec{w}_i, & \text{if } \vec{w}_i \text{ dominates } \vec{p}_i^{new} \\ \vec{p}_i^{new}, & \text{if } \vec{p}_i^{new} \text{ dominates } \vec{w}_i \\ \vec{w}_i, & \text{otherwise} \end{cases} \tag{6.17}$$

Second comparison:

$$\vec{p}_i^{t+1} = \begin{cases} \vec{p}_i^{opp}, & \text{if } \vec{p}_i^{opp} \text{ dominates } \vec{p}_i^{(1)} \\ \vec{p}_i^{(1)}, & \text{otherwise} \end{cases} \tag{6.18}$$

Step 8: Offspring Population Generation

Once the above selection has been performed on all of the individuals, the population of the offspring is generated as

$$Q_t = \{\vec{p}_1^{t+1}, \vec{p}_2^{t+1}, \ldots, \vec{p}_N^{t+1}\} \tag{6.19}$$

Step 9: Population Merging

$$R_t = P_t \cup Q_t \tag{6.20}$$

Step 10: Non-Dominated Sorting and Crowding Distance

Using non-dominated sorting, the merged population is ranked into fronts $F_1, F_2, \ldots F_n$.

Crowding distance is computed as

$$CD_i = \sum_{m=1}^{M} \frac{f_m^{i+1} - f_m^{i-1}}{f_m^{\max} - f_m^{\min}} \tag{6.21}$$

Step 11: Elitist Selection

The next generation is constructed as

$$P_{t+1} = \bigcup_{k=1}^{l-1} F_k \cup \text{Top}_{CD}(F_l) \tag{6.22}$$

Step 12: Termination

The procedure is repeated until $t = it_{\max}$.

The final Pareto-optimal solution set corresponds to the first front F_1.

turnitin Page 147 of 208 - Integrity Submission Submission ID trn:oid:::27535:142293373

turnitin Page 148 of 208 - Integrity Submission Submission ID trn:oid:::27535:142293373

101 The overall steps of the proposed method are illustrated through the flowchart shown in Figure 6.1.

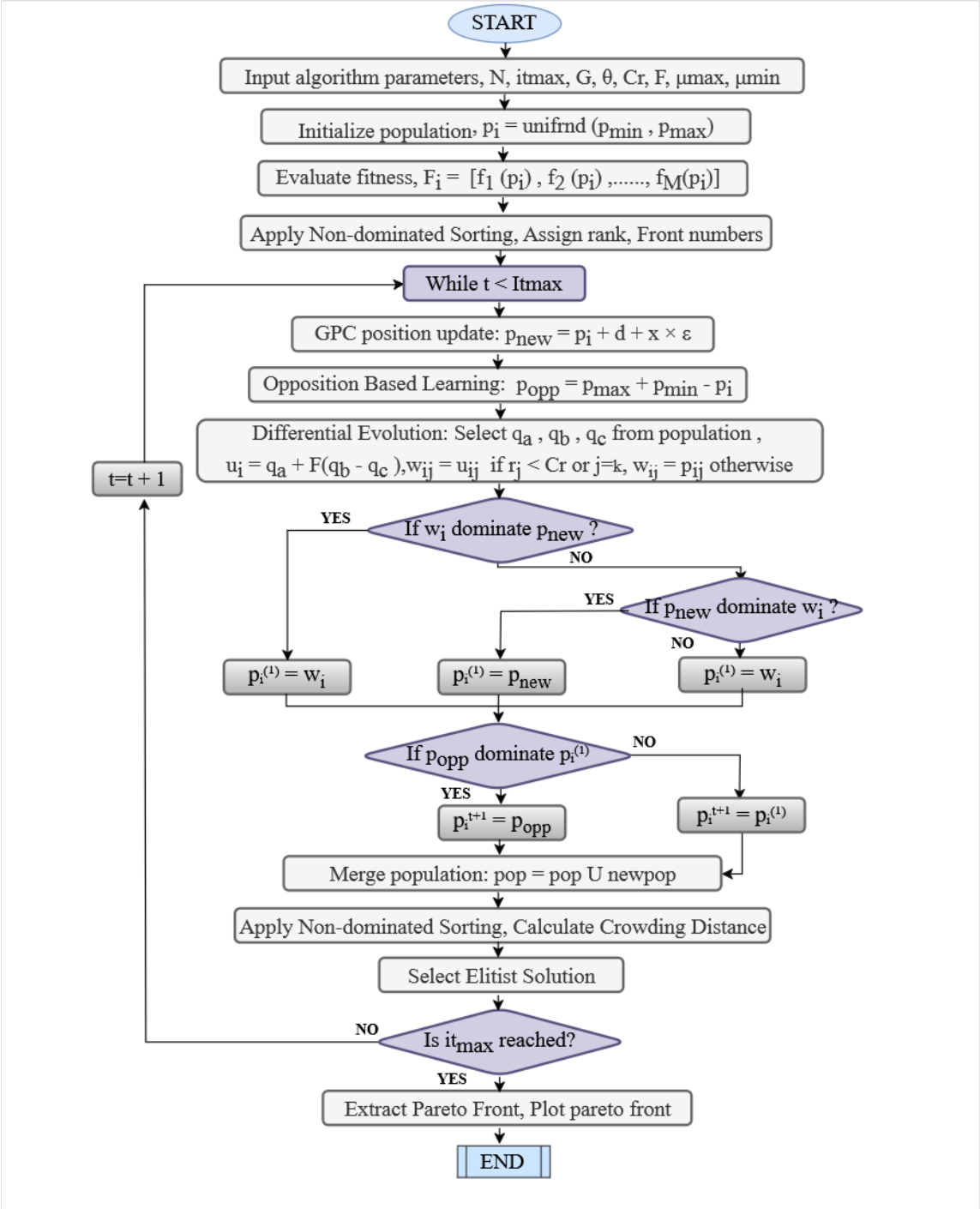


Fig. 6.1: Flowchart of the proposed multi-objective method.

turnitin Page 148 of 208 - Integrity Submission Submission ID trn:oid:::27535:142293373

turnitin Page 149 of 208 - Integrity Submission Submission ID trn:oid:::27535:142293373

6.3 Uncertainty modeling and scenario generation

The uncertainties related to wind, solar, hydro generation and load demand are modeled using probabilistic distributions as detailed in Chapter 4. Based on this modeling framework, 500 scenarios are generated using Monte Carlo simulation (MCS), where each scenario represents a possible realization of system operating conditions. For the purpose of lessening the computational load, the scenario reduction method is employed in reverse to derive 10 representative scenarios along with their respective probabilities. These simplified scenarios are part of the suggested multi-objective optimization model. The objective function is assessed according to the probability of each scenario. Such an analysis will ensure that there is a thorough evaluation of the system's performance under conditions of uncertainty. In addition, such a method will help identify Pareto optimal solutions.

6.4 Objective function for stochastic ORPD

Under conditions of uncertainty, a number of scenarios are considered in order to consider variations in load demand and generation from renewable sources like wind, solar, and hydropower. A single set of control variables is optimized across all scenarios, using a scenario-based approach.

The objective functions are assessed based on their expected values, considering the probability of each scenario. As a result, the expected P_{Loss}, VD and VSI are expressed as follows:

The expected P_{Loss} is given by:

$$EP_{\text{Loss,sc}} = \sum_{sc=1}^{N_{sc}} P_{\text{Loss,sc}} \times \Delta_{sc} \tag{6.23}$$

The expected VD is expressed as:

$$EVD_{sc} = \sum_{sc=1}^{N_{sc}} VD_{sc}\, \Delta_{sc} \tag{6.24}$$

turnitin Page 149 of 208 - Integrity Submission Submission ID trn:oid:::27535:142293373

turnitin Page 150 of 208 - Integrity Submission Submission ID trn:oid:::27535:142293373

The expected VSI is given by:

$$EVSI_{sc} = \sum_{sc=1}^{N_{sc}} VSI_{sc}\,\Delta_{sc} \tag{6.25}$$

where, N_{sc} is the total scenarios that were created, Δ_{sc} is the probability of the scenarios provided.

6.5 Results and Discussions

6.5.1 Benchmark Functions

Benchmark multi-objective test functions consisting of two objectives (ZDT1-ZDT6) [131] and three objectives (DTLZ2 and DTLZ4) [132] are utilized in the testing of the proposed method. It is because of their Pareto front characteristics that have made them an appropriate choice for the test problem sets, having properties like convexity, concavity, continuity, and multimodality. Hence, they make a good set of problems for analyzing convergence and diversity. Their respective mathematical formulations are given in Table A.6 of Appendix A. Performance of the developed technique will be evaluated through well-known metrics such as Inverted Generational Distance (IGD), Generational Distance (GD), Hypervolume (HV), Maximum Spread (MS) and Spacing (S). The above-mentioned metrics will help to measure the convergence, spread and evenness of Pareto solutions. IGD and GD metrics are widely used to quantify how closely the obtained solutions approximate the true Pareto front, while HV measures both convergence and diversity simultaneously. MS reflects the extent of spread in the objective space and Spacing (S) quantifies the uniformity of the obtained solutions. Lower IGD and GD values indicate improved convergence toward the true Pareto front. Additionally, Higher MS values reflect better diversity, while lower Spacing values correspond to better uniformity of solutions and larger HV values signify enhanced convergence and diversity [133]. The mathematical formulation of these metrics is defined below:

- **Inverted Generational Distance (IGD)**

turnitin Page 150 of 208 - Integrity Submission Submission ID trn:oid:::27535:142293373

turnitin Page 151 of 208 - Integrity Submission Submission ID trn:oid:::27535:142293373

$$IGD(P^*, \Omega) = \frac{1}{|P^*|} \sum_{x \in P^*} \min_{y \in \Omega} \|x - y\| \tag{6.26}$$

where P^* denotes the true Pareto front, Ω represents the obtained Pareto set, $x \in P^*$ and y represent points on the true and obtained Pareto front, respectively.

- **Generational Distance (GD)**

$$GD = \sqrt{\frac{1}{n} \sum_{i=1}^{n} d_i^2} \tag{6.27}$$

where

$$d_i = \min_{x \in P^*} \|y_i - x\| \tag{6.28}$$

where, n denotes the number of solutions in Ω, $y_i \in \Omega$ is the i-th solution obtained.

- **Maximum Spread (MS)**

$$MS = \sqrt{\sum_{k=1}^{m} \left(f_k^{\max} - f_k^{\min}\right)^2} \tag{6.29}$$

61

where, $f_k^{\max}$ and $f_k^{\min}$ denote the maximum and minimum values of the k-th objective in Ω and m denotes the number of objectives.

- **Spacing (S)**

$$S = \sqrt{\frac{1}{n-1} \sum_{i=1}^{n} (\bar{d} - d_i)^2} \tag{6.30}$$

where

$$\bar{d} = \frac{1}{n} \sum_{i=1}^{n} d_i \tag{6.31}$$

where, d_i denotes the minimum distance between the i-th solution and its nearest neighbor in Ω and n denotes the number of solutions.

- **Hypervolume (HV)**

$$HV(A, r) = \text{Leb}\left(\bigcup_{a \in \Omega} \left(\prod_{k=1}^{m} [a_k, r_k]\right)\right) \tag{6.32}$$

turnitin Page 151 of 208 - Integrity Submission Submission ID trn:oid:::27535:142293373

turnitin Page 152 of 208 - Integrity Submission Submission ID trn:oid:::27535:142293373

where r represents the reference point (usually formed using the nadir point of each objective) and Leb$(\cdot)$ represents the Lebesgue measure.

To assess the performance of the proposed algorithm, we compare the proposed method with MOPSO, MOGOA, MOSFO and MOMA on standard benchmark functions, including five ZDT functions (ZDT1-ZDT6) and two DTLZ functions (DTLZ2 and DTLZ4). The parameter values of all algorithms are shown in Table 6.1. For consistency, the population size (N) and the maximum number of iterations (it_{max}) are fixed at 100 and 1000, respectively, for all methods. In addition, each algorithm is executed 10 times independently to reduce the influence of random factors. The mean and standard deviation (Std.) values of IGD, GD, HV, S and MS metrics are computed to evaluate the performance of the proposed method.

Table 6.1: Parameter settings of the multi-objective algorithms used for comparison.

MOPSO	MOGOA	MOSFO	MOMA	Proposed
N = 100	N = 100	N = 100	N = 100	N = 100
$it_{\max} = 1000$	$it_{\max} = 1000$	$it_{\max} = 1000$	$it_{\max} = 1000$	$it_{\max} = 1000$
Archive Size = 100	Archive Size = 100	Archive Size = 100	Repository Size = 100	Gravity $(G) = 9.8$
Inertia Weight $(W) = 0.4$	$c_{max} = 1$	Probability $(p) = 0.1$	Inertia Weight $(g) = 0.8$	Ramp Angle $(\theta) = 12°$
$C_1 = 2, C_2 = 2$	$c_{min} = 4 \times 10^{-5}$	Mutation Rate $(m) = 0.1$	Personal Learning $(a_1) = 1$	Friction $(\mu) \in [1, 10]$
Grid Size = 20	Grid Size = 20	Grid Size = 20	Global Learning $(a_2, a_3) = 1.5$	Crossover Rate $(C_r) = 0.7$
Mutation Probability = 0.5			Mutation Rate $(\mu) = 0.02$	Scaling Factor $(F) = 0.5$

The values of IGD, GD, HV, MS, and Spacing (S) computed by all five methods are listed in Table 6.2. Among these metrics, IGD, GD, and HV provide a more reliable assessment of performance because they directly measure closeness to the true Pareto front and the quality of objective space coverage. However, MS and Spacing simply measure the uniformity of solution distribution and hence do not adequately represent the approximation to the optimal front. Thus, an algorithm can have good diversity (high MS, or well-distributed spacing) and still be far from the true Pareto front. Hence, the comparative analysis focuses mainly on IGD, GD and HV.

turnitin Page 152 of 208 - Integrity Submission Submission ID trn:oid:::27535:142293373

turnitin Page 153 of 208 - Integrity Submission Submission ID trn:oid:::27535:142293373

Table 6.2: Statistical performance comparison of different algorithms over ten independent runs on benchmark test functions.

Metric	MOPSO	MOSFO	MOOGOA	MOMA	Proposed
	Mean ± Std	Mean ± Std	Mean ± Std	Mean ± Std	Mean ± Std
			ZDT1		
IGD	7.35E-03 ± 4.77E-04	5.63E-01 ± 2.62E-01	1.98E-01 ± 1.07E-01	5.44E-03 ± 3.75E-04	**4.62E-03** ± 2.25E-04
Rank	3	5	4	2	**1**
GD	**6.64E-04** ± 7.56E-05	6.13E-01 ± 3.00E-01	1.89E-02 ± 1.22E-02	2.15E-03 ± 5.72E-04	1.40E-03 ± 3.52E-04
Rank	**1**	5	4	3	2
HV	**1.10E-01** ± 1.46E-17	6.93E-03 ± 7.35E-03	3.85E-02 ± 2.40E-02	**1.10E-01** ± 1.67E-04	**1.10E-01** ± 1.45E-05
Rank	**1**	5	4	**1**	**1**
Spacing	3.66E-03 ± 5.68E-04	5.91E-03 ± 4.84E-04	**3.43E-03** ± 2.12E-03	6.01E-03 ± 8.32E-04	4.68E-03 ± 3.59E-04
Rank	2	4	**1**	5	3
MS	1.41E+00 ± 3.18E-05	**1.74E+00** ± 1.34E-01	1.39E+00 ± 1.54E-01	1.41E+00 ± 1.78E-02	1.41E+00 ± 6.18E-06
Rank	2	**1**	5	2	2
			ZDT2		
IGD	7.54E-03 ± 3.54E-04	1.55E+00 ± 5.96E-01	4.69E-01 ± 2.27E-01	5.17E-03 ± 3.47E-04	**4.70E-03** ± 1.27E-04
Rank	3	5	4	2	**1**
GD	6.97E-04 ± 5.45E-05	1.20E-01 ± 5.25E-02	4.36E-02 ± 6.68E-02	9.15E-04 ± 6.28E-04	**4.90E-04** ± 3.37E-05
Rank	2	5	4	3	**1**
HV	**1.10E-01** ± 1.46E-17	9.83E-05 ± 3.11E-04	7.94E-02 ± 3.19E-02	**1.10E-01** ± 1.46E-17	**1.10E-01** ± 2.83E-05
Rank	**1**	5	4	**1**	**1**
Spacing	4.08E-03 ± 6.46E-04	**6.74E-04** ± 1.43E-03	1.53E-03 ± 1.21E-03	6.13E-03 ± 7.75E-04	5.06E-03 ± 4.62E-04
Rank	3	**1**	2	5	4
MS	**1.41E+00** ± 2.34E-16	2.30E-01 ± 4.85E-01	1.03E+00 ± 2.56E-02	**1.41E+00** ± 3.80E-04	**1.41E+00** ± 2.02E-05
Rank	**1**	5	4	**1**	**1**
			ZDT3		
IGD	6.40E-03 ± 3.31E-04	3.90E-01 ± 1.63E-01	1.96E-01 ± 9.41E-02	1.97E-02 ± 1.71E-02	**5.04E-03** ± 1.57E-04
Rank	3	5	4	2	**1**
GD	3.90E-03 ± 4.88E-04	5.50E-01 ± 2.66E-01	1.94E-01 ± 1.06E-01	1.85E-03 ± 3.04E-04	**1.75E-03** ± 9.14E-05
Rank	3	5	4	2	**1**
HV	9.52E-02 ± 1.58E-03	8.30E-03 ± 5.51E-03	6.36E-02 ± 4.74E-02	9.49E-02 ± 5.44E-04	**9.52E-02** ± 9.81E-07
Rank	2	5	4	3	**1**
Spacing	5.85E-03 ± 8.37E-04	6.79E-03 ± 6.88E-04	7.17E-03 ± 2.88E-03	7.24E-03 ± 8.19E-04	**6.75E-03** ± 8.98E-04
Rank	**1**	3	4	5	2
MS	1.96E+00 ± 4.46E-03	**2.35E+00** ± 1.33E-01	1.86E+00 ± 1.80E-01	1.80E+00 ± 2.12E-01	1.97E+00 ± 3.74E-05
Rank	3	**1**	4	5	2
			ZDT4		
IGD	8.85E+00 ± 7.29E+00	3.47E+01 ± 9.87E+00	1.46E+01 ± 6.21E+00	6.53E-03 ± 1.13E-03	**4.87E-03** ± 2.41E-04
Rank	3	5	4	2	**1**
GD	1.00E+01 ± 9.09E+00	3.98E+00 ± 8.99E-01	1.55E+01 ± 6.71E+00	4.01E-03 ± 1.56E-03	**1.63E-03** ± 2.13E-04
Rank	4	3	5	2	**1**

turnitin Page 153 of 208 - Integrity Submission Submission ID trn:oid:::27535:142293373

turnitin Page 154 of 208 - Integrity Submission Submission ID trn:oid:::27535:142293373

Metric	MOPSO	MOSFO	MOOGOA	MOMA	Proposed
	Mean ± Std	Mean ± Std	Mean ± Std	Mean ± Std	Mean ± Std
HV	0.00E+00 ± 0.00E+00	0.00E+00 ± 0.00E+00	0.00E+00 ± 0.00E+00	1.02E-01 ± 4.11E-03	**1.10E-01** ± 2.19E-05
Rank	4	4	4	2	**1**
Spacing	1.66E-01 ± 3.47E-01	6.42E-02 ± 6.36E-02	N/A	5.64E-03 ± 7.00E-04	**5.07E-03** ± 3.86E-04
Rank	4	3	5	2	**1**
MS	**3.80E+00** ± 3.33E+00	1.17E+00 ± 8.43E+00	N/A	1.42E+00 ± 1.45E-03	1.41E+00 ± 7.05E-06
Rank	**1**	4	5	2	3
			ZDT6		
IGD	5.75E-03 ± 4.30E-04	1.62E+00 ± 2.61E+00	2.41E-01 ± 2.69E-01	**3.84E-03** ± 6.77E-04	4.45E-03 ± 2.00E-04
Rank	3	5	4	**1**	2
GD	4.55E-01 ± 6.49E-02	1.91E+00 ± 2.27E+00	5.86E-01 ± 2.83E-01	2.83E-02 ± 8.08E-02	**3.49E-04** ± 2.30E-05
Rank	3	5	4	2	**1**
HV	6.29E-02 ± 2.40E-02	5.59E-02 ± 3.87E-02	7.03E-02 ± 5.59E-02	7.77E-02 ± 1.35E-02	**8.19E-02** ± 1.83E-10
Rank	4	5	3	2	**1**
Spacing	1.20E-01 ± 5.30E-02	6.47E-02 ± 1.56E-01	4.60E-02 ± 7.39E-02	2.13E-02 ± 5.43E-02	**5.84E-03** ± 3.78E-04
Rank	5	4	3	2	**1**
MS	**4.34E+00** ± 7.69E-01	3.02E+00 ± 2.56E+00	2.32E+00 ± 1.48E+00	1.40E+00 ± 7.06E-01	1.17E+00 ± 5.39E-10
Rank	**1**	2	3	4	5
			DTLZ2		
IGD	9.53E-02 ± 4.93E-03	1.20E-01 ± 1.25E-02	1.79E-01 ± 3.18E-02	3.77E-01 ± 5.62E-02	**8.00E-02** ± 2.75E-03
Rank	2	3	4	5	**1**
GD	1.18E-01 ± 3.44E-02	9.72E-02 ± 1.46E-02	**2.26E-03** ± 1.01E-03	1.23E-02 ± 5.71E-04	3.94E-02 ± 1.06E-03
Rank	4	3	**1**	5	2
HV	6.15E-01 ± 9.25E-03	5.95E-01 ± 9.44E-03	5.74E-01 ± 3.92E-02	2.97E-01 ± 2.89E-02	**6.78E-01** ± 1.56E-03
Rank	2	3	4	5	**1**
Spacing	6.09E-02 ± 2.30E-02	5.93E-02 ± 8.54E-03	2.77E-02 ± 1.98E-02	**2.08E-02** ± 7.34E-03	3.79E-02 ± 1.25E-03
Rank	5	4	2	**1**	3
MS	2.20E+00 ± 2.65E-01	**2.38E+00** ± 1.59E-01	1.70E+00 ± 1.47E-01	6.73E-01 ± 1.40E-01	1.78E+00 ± 7.65E-03
Rank	2	**1**	4	5	3
			DTLZ4		
IGD	9.67E-02 ± 6.50E-03	1.25E-01 ± 4.37E-03	3.35E-01 ± 1.75E-01	6.91E-01 ± 2.25E-01	**7.27E-02** ± 1.08E-03
Rank	2	3	4	5	**1**
GD	8.81E-03 ± 1.89E-03	4.49E-01 ± 4.55E-02	**2.31E-03** ± 1.75E-03	8.51E-03 ± 4.94E-03	3.37E-02 ± 2.29E-03
Rank	3	5	**1**	2	4
HV	6.25E-01 ± 6.83E-03	5.73E-01 ± 2.55E-03	5.74E-01 ± 8.79E-02	3.31E-01 ± 1.14E-01	**6.82E-01** ± 5.39E-04
Rank	2	4	3	5	**1**
Spacing	4.65E-02 ± 9.80E-03	5.77E-02 ± 1.44E-03	1.68E-02 ± 8.41E-03	**1.32E-02** ± 1.16E-02	3.53E-02 ± 2.98E-03
Rank	4	5	2	**1**	3
MS	1.98E+00 ± 1.65E-01	**3.44E+00** ± 8.09E-02	1.70E+00 ± 1.92E-01	8.88E-01 ± 4.99E-01	1.77E+00 ± 5.41E-03
Rank	2	**1**	4	5	3
Average					

turnitin Page 154 of 208 - Integrity Submission Submission ID trn:oid:::27535:142293373

turnitin Page 155 of 208 - Integrity Submission Submission ID trn:oid:::27535:142293373

Metric	MOPSO	MOSFO	MOOGOA	MOMA	Proposed
	Mean ± Std	Mean ± Std	Mean ± Std	Mean ± Std	Mean ± Std
Rank	2.60	3.77	3.57	2.91	**1.8**

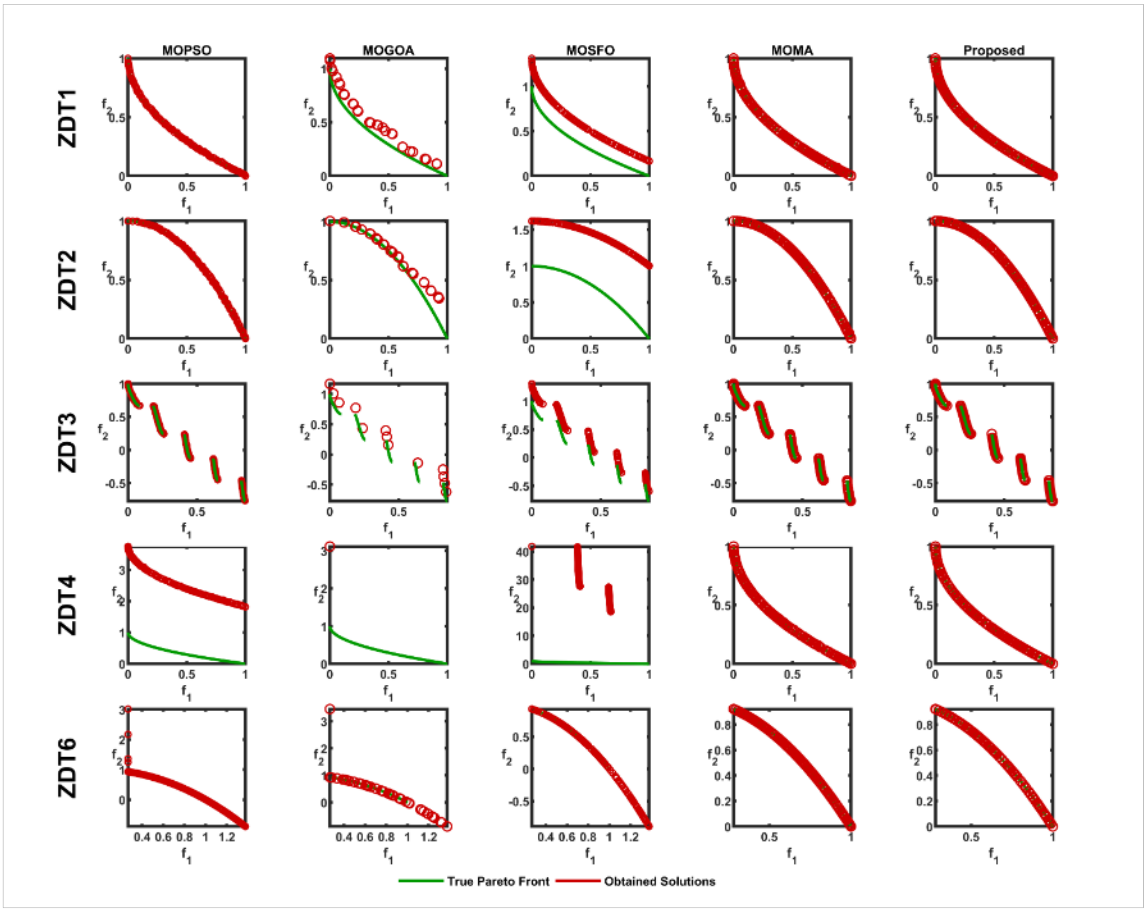


Fig. 6.2: Comparison of true and obtained Pareto front for ZDT1–ZDT6 using different multi-objective optimization algorithms.

As shown in Table 6.2, the quantitative results based on these three primary metrics (IGD, GD and HV) show that the proposed algorithm performs better than the other algorithms in most cases. For ZDT1, the proposed algorithm has the lowest IGD of 4.62E-03 and a comparable GD of 1.40E-03, but the maximum HV of 1.10E-01 (tied with MOPSO and MOMA). On ZDT2 and ZDT3, the proposed algorithm also attains the lowest IGD and GD values and has the highest HV. On the difficult multimodal ZDT4, the Proposed algorithm achieves IGD of 4.87E-03 and GD of 1.63E-03, while three competing algorithms get a zero HV. Conversely,

turnitin Page 155 of 208 - Integrity Submission Submission ID trn:oid:::27535:142293373

turnitin Page 156 of 208 - Integrity Submission Submission ID trn:oid:::27535:142293373

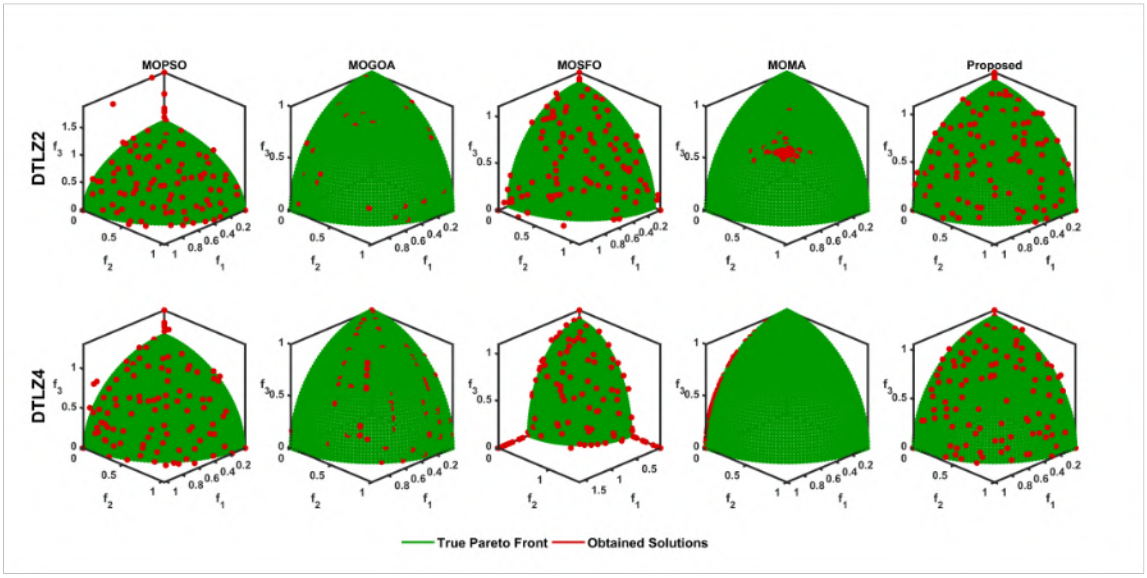


Fig. 6.3: Comparison of true and obtained Pareto front for DTLZ2 and DTLZ4 using different multi-objective optimization algorithms.

the proposed algorithm yields the highest HV of 1.10E-01. On ZDT6, the proposed algorithm achieves the minimum GD of 3.49E-04 and the highest HV of 8.19E-02, while its IGD of 4.45E-03 is very close to the best one (exactly MOMA of 3.84E-03). The Proposed algorithm also achieves the lowest IGD of 8.00E-02 (DTLZ2) and 7.27E-02 (DTLZ4) and the highest HV of 6.78E-01 (DTLZ2) and 6.82E-01 (DTLZ4) in the two three-objective problems, exhibiting the best performance with respect to both convergence and solution coverage.

Figure 6.2 and Figure 6.3 display the Pareto fronts achieved by all five methods on the two-objective benchmark functions (ZDT1–ZDT6) and the three-objective benchmark functions (DTLZ2 and DTLZ4), respectively. From these figures, we can observe that the proposed method is very close to the true Pareto front, whereas the other four methods have some deviations from the front or incomplete coverage of the front, especially in multimodal cases like the ZDT4 function and the complex Pareto front of the DTLZ4 function, indicating that their convergences and distribution performances are relatively weak.

turnitin Page 156 of 208 - Integrity Submission Submission ID trn:oid:::27535:142293373

turnitin Page 157 of 208 - Integrity Submission Submission ID trn:oid:::27535:142293373

6.5.2 Deterministic MOORPD

The proposed method is implemented to address the MOORPD problem. To evaluate its effectiveness and flexibility, six optimization cases are considered on the IEEE-30 and IEEE-57 bus systems as described below. The load flow computations for this research work are carried out using the Matpower-7.1 toolbox.[111]

6.5.2.1 IEEE-30 Bus System

- CASE-1 (P_{Loss} vs. VD)
- CASE-2 (P_{Loss} vs. VSI)
- CASE-3 (P_{Loss} vs. VD vs. VSI)

6.5.2.2 IEEE-57 Bus System

- CASE-4 (P_{Loss} vs. VD)
- CASE-5 (P_{Loss} vs. VSI)
- CASE-6 (P_{Loss} vs. VD vs. VSI)

6.5.2.3 Modified IEEE-30 Bus System

- CASE-7 ($EP_{Loss,sc}$ vs. EVD_{sc})
- CASE-8 ($EP_{Loss,sc}$ vs. $EVSI_{sc}$)
- CASE-9 ($EP_{Loss,sc}$ vs. EVD_{sc} vs. $EVSI_{sc}$)

In the first and fourth cases (CASE-1 and CASE-4), a bi-objective formulation that minimizes P_{Loss} and VD is presented. In the second and fifth cases (CASE-2 and CASE-5), a bi-objective formulation that minimizes P_{Loss} and VSI is discussed. Finally, a tri-objective formulation (CASE-3 and CASE-6) with the minimization of P_{Loss}, VD and VSI is discussed. All of these cases highlight the ability of the proposed algorithm to simultaneously address conflicting and cooperative objectives for reactive power optimization. This work focuses on evaluating the versatility and effectiveness of the proposed algorithm by comparing it with

turnitin Page 157 of 208 - Integrity Submission Submission ID trn:oid:::27535:142293373

turnitin Page 158 of 208 - Integrity Submission Submission ID trn:oid:::27535:142293373

MOPSO, MOMA, MOGOA and MOSFO algorithms. For the IEEE 30 and 57-bus systems, each algorithm is run with 1000 iterations and a population size of 100.

6.5.3 Decision Making in MOORPD problem

In this work, a percentage saving-based decision-making approach combined with the max–min criterion for determining the best compromise solution (BCS) is adopted for the MOORPD problem. The adopted percentage saving-based approach assesses each Pareto solution by the extent to which the objectives can be improved relative to the base and best values, and finally selects the Pareto solution with the best balance among the objectives. The procedure of the adopted decision-making approach is outlined as follows:

Consider a multi-objective optimization problem with m objectives and a Pareto set containing N solutions. The objective vector is defined as

$$F(x) = [f_1(x), f_2(x), \ldots, f_i(x), \ldots, f_m(x)] \tag{6.33}$$

where $f_i(x)$ represents the $i-th$ objective function. A decision-making approach is needed to identify a compromise solution from the Pareto optimal set. [109].

For each objective i, two reference values are considered: the base case value f_i^{base}, representing the system performance without optimization, and the best value f_i^{best}, obtained from single-objective optimization.

The percentage saving associated with ith objective for Pareto solution x_j is calculated as

$$S_{ij}(\%) = \frac{f_i^{base} - f_i(x_j)}{f_i^{base} - f_i^{best}} \times 100 \tag{6.34}$$

where S_{ij} indicates the percentage of maximum achievable improvement from the base value to the best value obtained in the single objective optimization [134].

The minimum savings among all objectives for each Pareto solution is calculated as

$$MS_j = \min_{i=1,\ldots,m} (S_{ij}) \tag{6.35}$$

turnitin Page 158 of 208 - Integrity Submission Submission ID trn:oid:::27535:142293373

turnitin Page 159 of 208 - Integrity Submission Submission ID trn:oid:::27535:142293373

Finally, the BCS is determined using the max–min criterion [135]

$$x^* = \arg \max_{j=1,\ldots,N} (MS_j) \tag{6.36}$$

This approach chooses the Pareto solution, which gives the highest minimum improvement that can be achieved for each objective, resulting in a balanced compromise solution.

6.5.4 IEEE 30-bus system

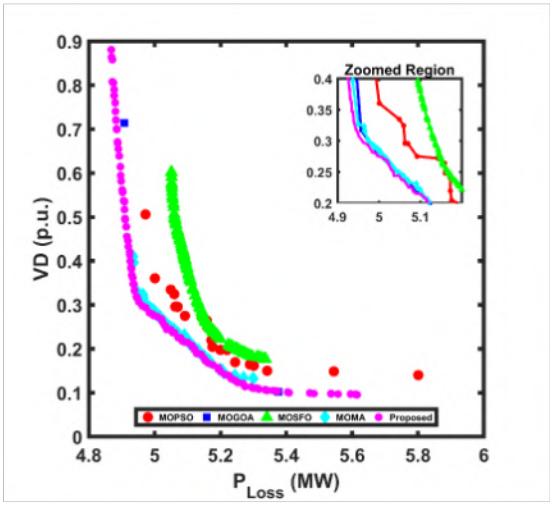
The MOORPD problem is analyzed on the IEEE 30-bus system, which includes six generators, nine shunt VAR compensators, and four tap-changing transformers. The generator data of this system are provided in Table A.2 of Appendix A. The system load is 283.4 MW and 126.2 MVAr. Control variables are considered continuous, with generators' active powers (except the slack bus) held constant. The reactive power output of the shunt VAR compensators is constrained within 0–5 MVAr, while the transformer tap ratios are limited to 0.9–1.1 p.u. The load bus voltages are maintained within 0.95 and 1.05 p.u. to ensure secure system operation.

Figures 6.4 (a), 6.4 (b) and 6.4 (c) illustrate the Pareto fronts obtained by the different methods for the cases considered on the IEEE 30-bus system. The bi-objective case Pareto fronts for the P_{Loss} vs VD (Figure 6.4 (a)) and the P_{Loss} vs VSI (Figure 6.4 (b)) demonstrate the trade-offs between reducing the P_{Loss} and lowering the VD or improving the VSI. It can be seen that the Pareto front obtained by our proposed algorithm dominates the fronts obtained by the other algorithms, since most of its solutions lie in the lower region of the objective space. This verifies the better convergence and optimization ability of our proposed method compared with MOPSO, MOGOA, MOSFO, and MOMA. In addition, the solutions obtained by the proposed method span a broader region of the objective space, reflecting greater diversity and improved exploration capability. For the tri-objective case (P_{Loss} vs VD vs VSI), the non-dominated solutions are shown by a three-dimensional scatter diagram (Figure 6.4 (c)), which displays the correlation among the three objectives. The distribution of the solutions indicates that our

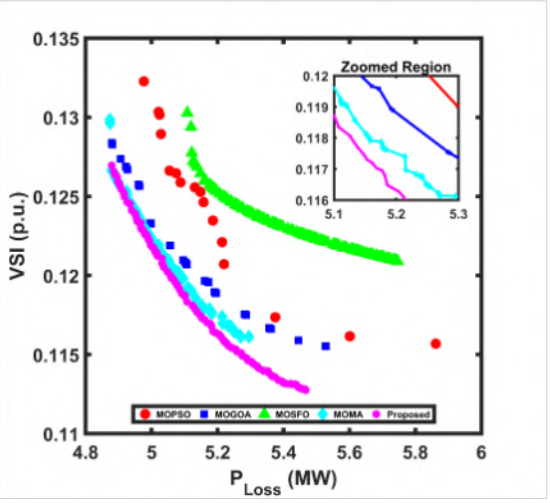
turnitin Page 159 of 208 - Integrity Submission Submission ID trn:oid:::27535:142293373

turnitin Page 160 of 208 - Integrity Submission Submission ID trn:oid:::27535:142293373

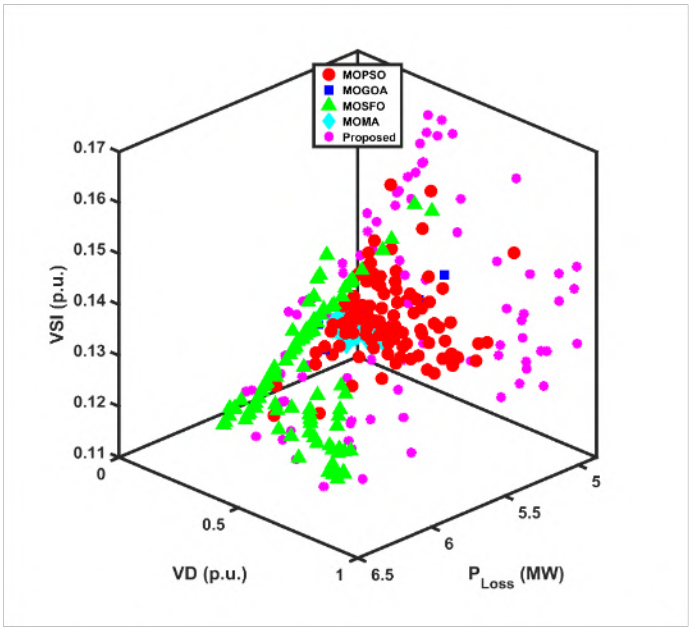
proposed algorithm can maintain good diversity with a thorough search of the search space for the tri-objective MOORPD problem.



(a) P_{Loss} vs. VD



(b) P_{Loss} vs. VSI



(c) P_{Loss} vs. VD vs. VSI

Fig. 6.4: Pareto solutions for the IEEE 30-bus system.

turnitin Page 160 of 208 - Integrity Submission Submission ID trn:oid:::27535:142293373

turnitin Page 161 of 208 - Integrity Submission Submission ID trn:oid:::27535:142293373

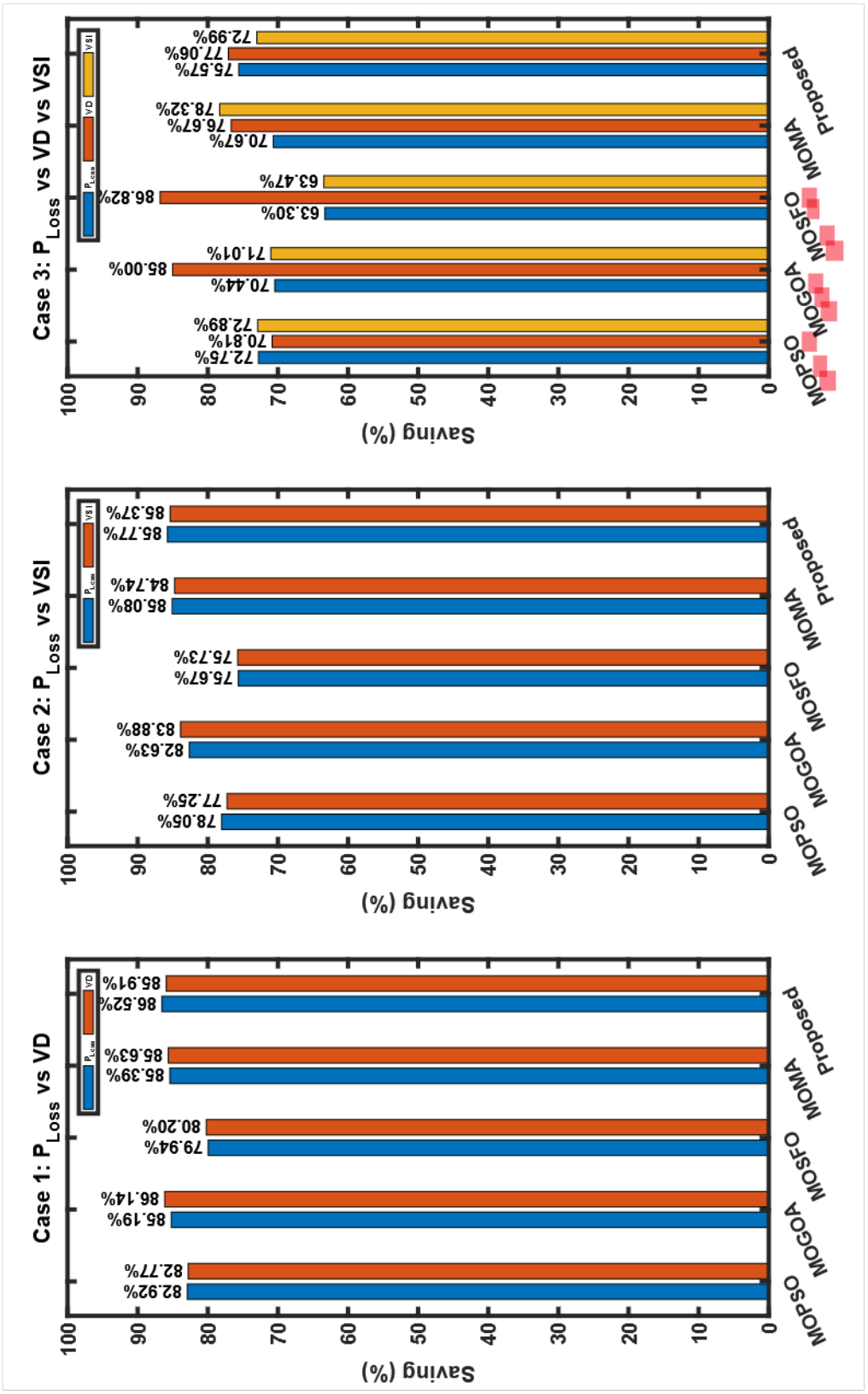


Fig. 6.5: Comparison of saving percentages achieved by different algorithms for the IEEE 30-bus ORPD problem under the multi-objective cases.

turnitin Page 161 of 208 - Integrity Submission Submission ID trn:oid:::27535:142293373

turnitin Page 162 of 208 - Integrity Submission Submission ID trn:oid:::27535:142293373

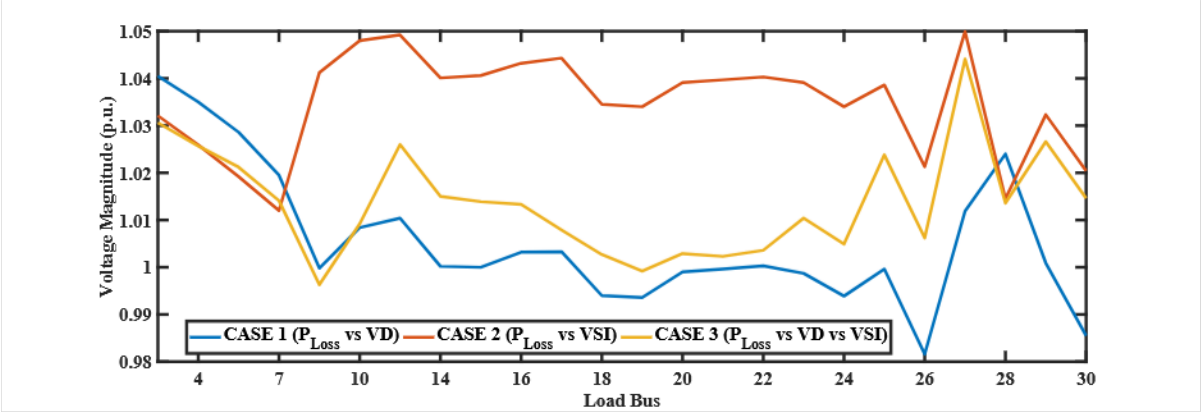


Fig. 6.6: IEEE 30-bus load bus voltage profile corresponding to the BCS obtained for the three cases.

Table 6.3: Comparison of BCS for various cases of the IEEE 30-bus system.

Method	Case 1		Case 2		Case 3		
	P_{Loss} vs VD		P_{Loss} vs VSI		P_{Loss} vs VD vs VSI		
	P_{Loss} (MW)	VD (p.u.)	P_{Loss} (MW)	VSI (p.u.)	P_{Loss} (MW)	VD (p.u.)	VSI (p.u.)
MOPSO	5.0919	0.2751	5.1577	0.1246	5.2293	0.4052	0.1270
MOGOA	5.0612	0.2384	5.0959	0.1210	5.2605	0.2508	0.1281
MOSFO	5.1322	0.3031	5.1899	0.1255	5.3569	0.2311	0.1322
MOMA	5.0585	0.2440	5.0628	0.1205	5.2574	0.3415	0.1241
Proposed	**5.0433**	**0.2410**	**5.0534**	**0.1202**	**5.1912**	**0.3372**	**0.1270**

In the base operating condition (before optimization), the system shows a P_{Loss} of 6.212 MW, a VD of 1.1758 p.u., and a VSI of 0.1672 p.u. The optimal values for the single objective ORPD problem, obtained using the single objective version of the proposed method in Chapter 4, are 4.8612 MW, 0.0876 p.u., and 0.1121 p.u., respectively. The BCS for each case is determined using the proposed decision-making approach on the Pareto optimal solutions obtained by all five algorithms. The associated results are listed in Table 6.3. From the table, it is evident that the proposed method attains the BCS in all three cases relative to the other algorithms. For case 1, the proposed method obtains P_{Loss} of 5.0433 MW, a VD of 0.2410 p.u. For case 2, the proposed method obtains P_{Loss} of 5.0534 MW, a

turnitin Page 162 of 208 - Integrity Submission Submission ID trn:oid:::27535:142293373

turnitin Page 163 of 208 - Integrity Submission Submission ID trn:oid:::27535:142293373

VSI of 0.1202 p.u. For case 3, the proposed method obtains P_{Loss} of 5.1912 MW, a VD of 0.3372 p.u. and VSI of 0.127 p.u.

Table 6.4: Results of the BCS for the IEEE 30-bus system using the proposed method.

Variables	Min	Max	Case 1 P_{Loss} vs VD	Case 2 P_{Loss} vs VSI	Case 3 P_{Loss} vs VD vs VSI
Generator Voltage (p.u.)					
V1	0.95	1.10	1.0636	1.0590	1.0513
V2	0.95	1.10	1.0515	1.0464	1.0450
V5	0.95	1.10	1.0265	1.0220	1.0242
V8	0.95	1.10	1.0263	1.0204	1.0190
V11	0.95	1.10	1.0336	1.0371	1.0198
V13	0.95	1.10	1.0282	1.0534	1.0448
Transformer Tap (p.u.)					
T11	0.90	1.10	1.0803	0.9851	1.0743
T12	0.90	1.10	0.9333	0.9130	0.9542
T15	0.90	1.10	1.0402	0.9824	1.0031
T36	0.90	1.10	0.9946	0.9439	0.9358
Shunt Compensators (MVAr)					
QC10	0	5	4.3533	4.6852	5.0000
QC12	0	5	1.9073	4.8856	0.4298
QC15	0	5	3.2123	4.5828	4.7867
QC17	0	5	3.3224	4.9995	5.0000
QC20	0	5	4.8706	4.3956	3.8780
QC21	0	5	4.9904	4.8956	5.0000
QC23	0	5	4.3506	4.0535	3.4806
QC24	0	5	5.0000	4.7118	4.8251
QC29	0	5	3.0053	0.5394	0.6177
Objective Functions					
P_{Loss} (MW)	6.212		**5.0433**	**5.0534**	**5.1912**

turnitin Page 163 of 208 - Integrity Submission Submission ID trn:oid:::27535:142293373

turnitin Page 164 of 208 - Integrity Submission Submission ID trn:oid:::27535:142293373

Variables	Min	Max	Case 1	Case 2	Case 3
			P_{Loss} vs VD	P_{Loss} vs VSI	P_{Loss} vs VD vs VSI
VD (p.u.)	1.1758		**0.2410**	0.8332	**0.3372**
VSI (p.u.)	0.1672		0.1483	**0.1202**	**0.1270**

Table 6.4 summarizes the values obtained and admissible ranges of all control variables for the IEEE 30-bus system. The values of all objectives are also shown to depict the trade-off achieved for the considered objectives. In addition, the selected compromise solutions in each case and their corresponding percentage savings are also shown in a bar graph (Figure 6.5). In Case 1 (P_{Loss} vs VD), the proposed method attains 86.52% reduction in P_{Loss} and 85.91% improvement in VD, outperforming MOMA (85.39%, 85.63%), MOGOA (85.19%, 86.14%), MOPSO (82.92%, 82.77%), and MOSFO (79.94%, 80.20%). In Case 2 (P_{Loss} vs VSI), the proposed approach achieves an 85.77% reduction in power loss and 85.37% improvement in VSI, providing a better compromise compared to MOMA (85.08%, 84.74%) and MOGOA (82.63%, 83.88%), while MOPSO (78.05%, 77.25%) and MOSFO (75.67%, 75.73%) exhibit comparatively lower performance. In Case 3 (P_{Loss} vs VD vs VSI), the proposed method continues to show consistent and robust behavior by achieving 75.57%, 78.06%, and 72.99% improvements in P_{Loss}, VD, and VSI, respectively, outperforming MOMA (70.67%, 76.67%, 78.32%), MOGOA (70.44%, 85.00%, 71.01%), MOPSO (72.75%, 70.81%, 72.89%), and MOSFO (63.30%, 86.82%, 63.47%) in terms of overall balance. These results confirm that the proposed method ensures improved convergence, enhanced stability, and a well-distributed Pareto-optimal solution across all considered scenarios. These results illustrate that the proposed method achieves a balanced improvement in all objectives in the three cases, which supports its capability to obtain a suitable trade-off solution. The load bus voltage profiles obtained corresponding to the BCS for the IEEE 30-bus system in all three cases are depicted in Figure 6.6, which shows that bus voltage magnitudes lie within permissible limits.

6.5.5 IEEE 57-bus system

This section analyses the MOORPD problem on the IEEE 57-bus system. The generator data of this system are provided in Table A.3 of Appendix A. The

turnitin Page 164 of 208 - Integrity Submission Submission ID trn:oid:::27535:142293373

turnitin Page 165 of 208 - Integrity Submission Submission ID trn:oid:::27535:142293373

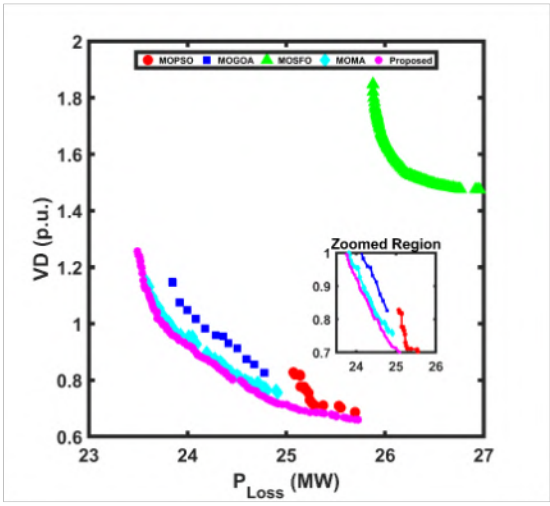
system includes seven generators, three shunt VAR compensators, and seventeen tap-changing transformers. The system load demand is 1250.8 MW and 336.4 MVAr. Control variables are treated as continuous, with generators' active powers (except for the slack bus) held constant. The reactive power output of the shunt VAR compensators is constrained within 0–20 MVAr, while the transformer tap ratios are limited to 0.9–1.1 p.u. The load bus voltages are maintained within 0.94 and 1.06 p.u. to ensure secure system operation.

Figures 6.7 (a), 6.7 (b) and 6.7 (c) illustrate the Pareto fronts obtained by the different methods for the cases considered on the IEEE 57-bus system. For the bi-objective cases, i.e., P_{Loss} vs VD (Figure 6.7 (a)) and P_{Loss} vs VSI (Figure 6.7 (b)), the Pareto fronts of the proposed algorithm dominate the other competing algorithms in the sense that the majority of the solutions are in the lower zone of the objective space. Thus, the proposed algorithm achieves a lower P_{Loss} with better voltage performance. Moreover, the obtained solutions cover a broader region of the objective space, indicating their enhanced diversity. For the tri-objective case, i.e., P_{Loss} vs VD vs VSI, the three-dimensional scatter distribution (Figure 6.7 (c)) indicates that the proposed algorithm generates a well-distributed set of non-dominated solutions across a broader region of the objective space.

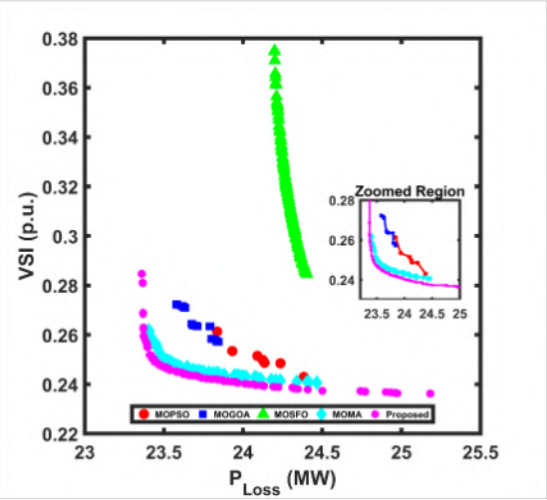
In the base operating condition, the system has a P_{Loss} of 28.462 MW, a VD of 1.5543 p.u. and a VSI of 0.3218 p.u. In the single-objective ORPD problem, the optimal values obtained by the single-objective method version of the method proposed in Chapter 4 are 23.3039 MW, 0.59821 p.u., and 0.19815 p.u., respectively. The BCS for each of the three cases is obtained by applying the proposed decision-making method to the Pareto-optimal solutions generated by all five algorithms. The results are summarized in Table 6.5, which shows that the proposed method reaches the BCS in all three cases relative to the competing algorithms. In case 4, the proposed method achieves a P_{Loss} of 24.4391 MW and a VD of 0.8126 p.u. In case 5, the proposed method achieves a P_{Loss} of 24.4088 MW and a VSI of 0.2377 p.u. In case 6, it achieves a P_{Loss} of 24.5596 MW, a VD of 0.9234 p.u. and a VSI of 0.2458 p.u.

turnitin Page 165 of 208 - Integrity Submission Submission ID trn:oid:::27535:142293373

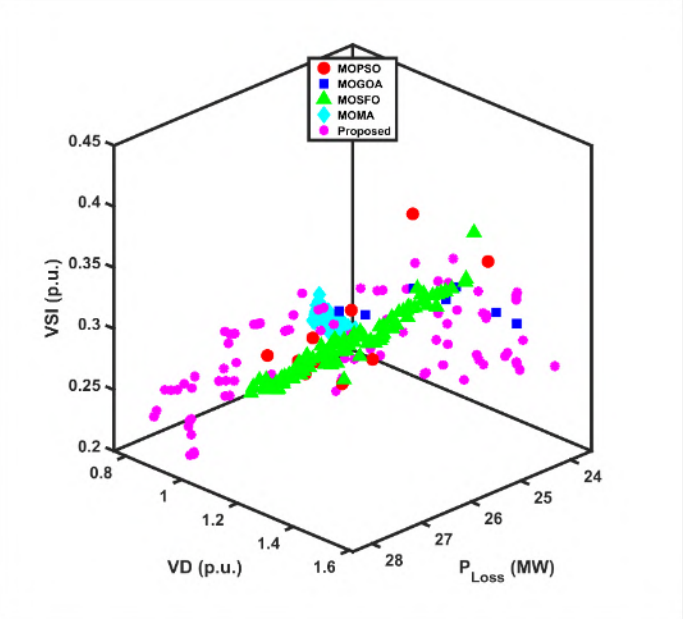
turnitin Page 166 of 208 - Integrity Submission Submission ID trn:oid:::27535:142293373



(a) P_{Loss} vs. VD



(b) P_{Loss} vs. VSI



(c) P_{Loss} vs. VD vs. VSI

Fig. 6.7: Pareto solutions for the IEEE 57-bus system.

turnitin Page 166 of 208 - Integrity Submission Submission ID trn:oid:::27535:142293373

turnitin Page 167 of 208 - Integrity Submission Submission ID trn:oid:::27535:142293373

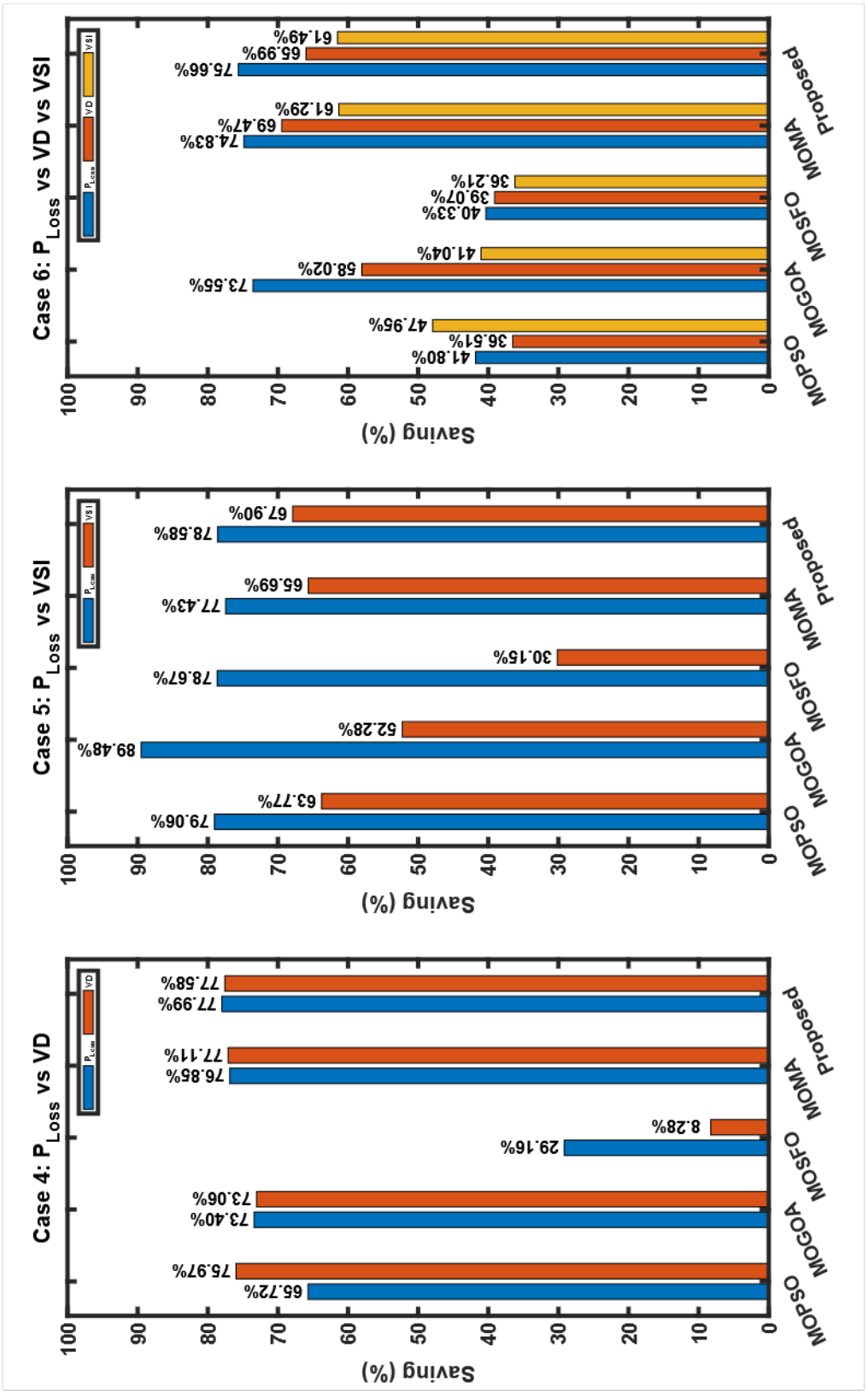


Fig. 6.8: Comparison of saving percentages achieved by different algorithms for the IEEE 57-bus ORPD problem under the multi-objective cases.

turnitin Page 167 of 208 - Integrity Submission Submission ID trn:oid:::27535:142293373

turnitin Page 168 of 208 - Integrity Submission Submission ID trn:oid:::27535:142293373

Table 6.5: Comparison of BCS for various cases of the IEEE 57-bus system.

Method	Case 4		Case 5		Case 6		
	P_{Loss} vs VD		P_{Loss} vs VSI		P_{Loss} vs VD vs VSI		
	P_{Loss} (MW)	VD (p.u.)	P_{Loss} (MW)	VSI (p.u.)	P_{Loss} (MW)	VD (p.u.)	VSI (p.u.)
MOPSO	25.0722	0.8280	24.3839	0.2430	26.3061	1.2052	0.2625
MOGOA	24.6758	0.8558	23.8466	0.2572	24.6786	0.9996	0.2710
MOSFO	26.9580	1.4751	24.4044	0.2845	26.3816	1.1807	0.2770
MOMA	24.4982	0.8171	24.4679	0.2406	24.6024	0.8901	0.2460
Proposed	**24.4391**	**0.8126**	**24.4088**	**0.2377**	**24.5596**	**0.9234**	**0.2458**

Table 6.6 presents the optimal values and admissible ranges for all the control variables of the IEEE 57-bus system. The results shown in the table are the BCS obtained using the proposed decision-making approach for the multi-objective cases. Values of all the objectives are also reported to show the trade-off achieved for the considered objectives. Moreover, the selected compromise solutions in each case and their corresponding percentage savings are also shown in a bar chart (Figure 6.8). In Case 4 (P_{Loss} vs VD), the proposed method achieves 77.99% reduction in P_{Loss} and 77.58% improvement in VD, outperforming MOMA (76.85%, 77.11%), MOGOA (73.40%, 73.06%), and MOPSO (65.72%, 75.97%), while MOSFO shows significantly lower VD improvement (8.28%). In Case 5 (P_{Loss} vs VSI), although MOGOA records the highest P_{Loss} reduction (89.48%), its VSI improvement (52.28%) is comparatively limited, indicating an imbalanced solution; in contrast, the proposed method maintains a better compromise with 78.58% reduction in P_{Loss} and 67.90% enhancement in VSI, outperforming other methods in terms of overall balance. In the three-objective Case 6 (P_{Loss} vs VD vs VSI), the proposed approach continues to exhibit consistent performance by achieving 75.66%, 65.99%, and 61.49% improvements in P_{Loss}, VD, and VSI, respectively, surpassing MOMA (74.83%, 69.47%, 61.29%), MOGOA (73.55%, 58.02%, 41.04%), MOPSO (41.80%, 36.51%, 47.95%), and MOSFO (40.33%, 39.07%, 36.21%). These results clearly indicate that the proposed method has achieved balanced improvements across all objectives in the three cases, confirming its ability to find an appropriate trade-off solution. Figure 6.9 shows the load bus

turnitin Page 168 of 208 - Integrity Submission Submission ID trn:oid:::27535:142293373

turnitin Page 169 of 208 - Integrity Submission Submission ID trn:oid:::27535:142293373

voltage profiles for the BCS of the IEEE 30-bus system under the considered cases, demonstrating that all bus voltages are within specified limits.

Table 6.6: Results of the BCS for the IEEE 57-bus system using the proposed method.

Variables	Min	Max	Case 4	Case 5	Case 6
			P_{Loss} vs VD	P_{Loss} vs VSI	P_{Loss} vs VD vs VSI
Generator Voltage (p.u.)					
V1	0.95	1.10	1.076	1.0872	1.0741
V2	0.95	1.10	1.0621	1.0712	1.0584
V3	0.95	1.10	1.0419	1.0481	1.0372
V6	0.95	1.10	1.0286	1.0310	1.0257
V8	0.95	1.10	1.0467	1.0439	1.0454
V9	0.95	1.10	1.0176	1.0226	1.0141
V12	0.95	1.10	1.0252	1.0459	1.0250
Transformer Tap (p.u.)					
T19	0.90	1.10	0.9194	1.0193	1.0302
T20	0.90	1.10	1.1000	0.9362	0.9908
T31	0.90	1.10	0.9959	1.0383	1.0008
T35	0.90	1.10	1.0081	1.0468	0.9309
T36	0.90	1.10	0.9927	0.9883	0.9931
T37	0.90	1.10	1.0149	1.1000	1.0230
T41	0.90	1.10	1.0101	0.9950	0.9930
T46	0.90	1.10	0.9366	0.9000	0.9132
T54	0.90	1.10	0.9038	0.9026	0.9006
T58	0.90	1.10	0.9798	0.9874	0.9643
T59	0.90	1.10	0.9761	0.9612	0.9676
T65	0.90	1.10	0.9886	0.9749	0.9931
T66	0.90	1.10	0.9365	0.9012	0.9370
T71	0.90	1.10	0.9702	0.9630	0.9760
T73	0.90	1.10	1.0169	1.0243	0.9883
T76	0.90	1.10	0.9144	0.9977	0.9352

turnitin Page 169 of 208 - Integrity Submission Submission ID trn:oid:::27535:142293373

turnitin Page 170 of 208 - Integrity Submission Submission ID trn:oid:::27535:142293373

Variables	Min	Max	Case 4	Case 5	Case 6
			P_{Loss} vs VD	P_{Loss} vs VSI	P_{Loss} vs VD vs VSI
T80	0.90	1.10	1.0093	0.9825	1.0031
Shunt Compensators (MVAr)					
QC18	0	20	12.4553	4.5448	12.8914
QC25	0	20	14.4648	9.6544	9.7947
QC53	0	20	19.9898	11.2363	16.1657
Objective Function					
P_{Loss} (MW)	28.462		**24.4391**	**24.4088**	**24.5596**
VD (p.u.)	1.5543		**0.8126**	1.5645	**0.9234**
VSI (p.u.)	0.3218		0.2704	**0.2377**	**0.2458**

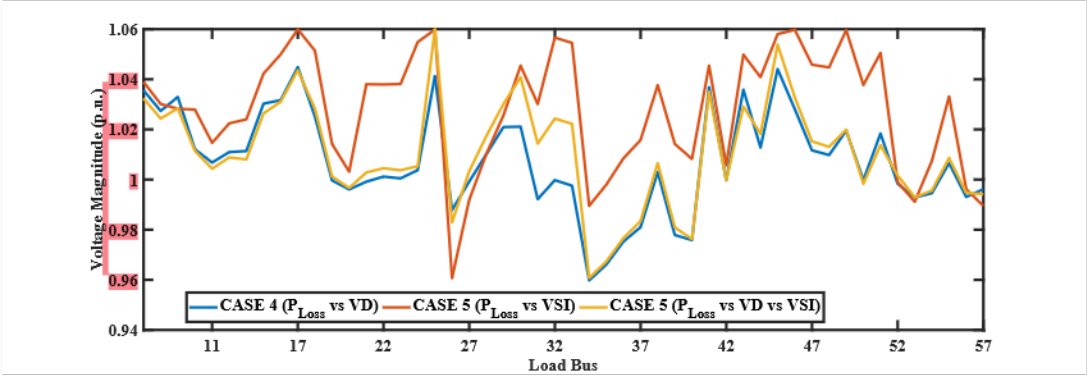


Fig. 6.9: IEEE 57-bus system load bus voltage profiles corresponding to the BCS obtained for the three cases.

6.5.6 Stochastic MOORPD

In the modified IEEE 30-bus system (see Table A.2 of Appendix A), the thermal generators in buses 5, 8, and 13 are replaced by a 75 MW wind generator, a 50 MW PV unit, and a 50 MW hybrid energy system (solar and small hydro), respectively, as shown in Figure 6.10. In different scenarios, the load demand, wind power, PV generation, and hybrid power output are varied according to the stochastic framework introduced in Section 3. The swing generator is used

turnitin Page 170 of 208 - Integrity Submission Submission ID trn:oid:::27535:142293373

turnitin Page 171 of 208 - Integrity Submission Submission ID trn:oid:::27535:142293373

to provide the difference between the system power demand and the sum of power generations from renewable and thermal generators when the real power outputs of the RESs cannot meet the demand. Besides, transformer tap settings and shunt VAR compensators are still considered as continuous control variables as in Cases 7–9. The maximum real power generation of the swing generator is set to 200 MW, which is large enough to meet the system demand in all scenarios. The reduced set of 10 representative scenarios, along with their corresponding probabilities, load demand, and power generation from wind, solar, and hydro sources, is presented in Table 6.7. The expected values of P_{Loss}, VD and VSI of the 10 scenarios are calculated based on Equations 6.23 to 6.25, respectively. These expected values of objective functions are simultaneously optimized in the multi-objective optimization to obtain a set of Pareto-optimal solutions representing trade-offs among the conflicting objectives.

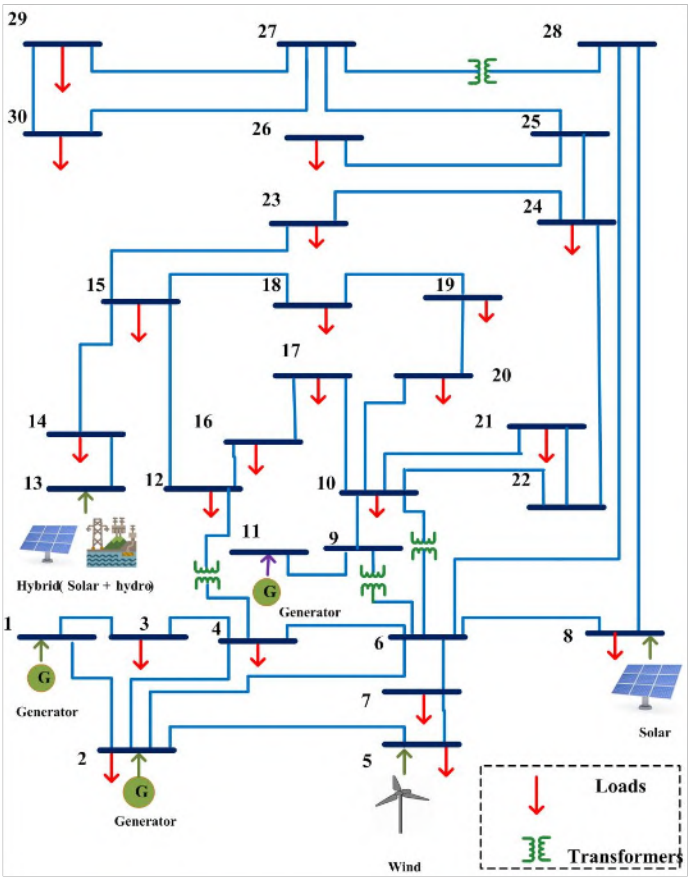


Fig. 6.10: Modified IEEE 30-bus system.

turnitin Page 171 of 208 - Integrity Submission Submission ID trn:oid:::27535:142293373

turnitin Page 172 of 208 - Integrity Submission Submission ID trn:oid:::27535:142293373

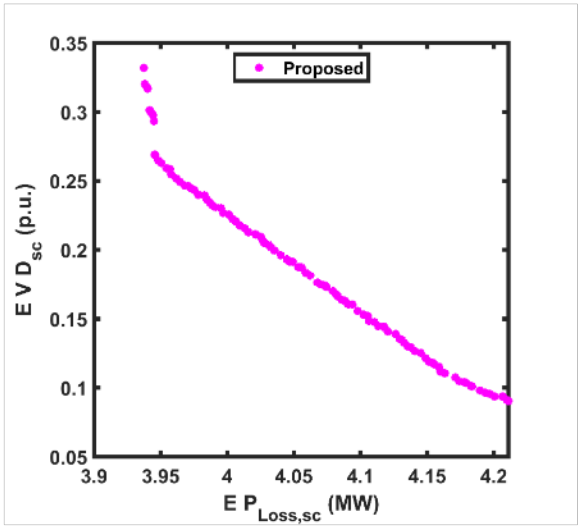
Table 6.7: Representative reduced scenarios and corresponding system parameters used for stochastic ORPD analysis.

Sc. No.	Scenario Probability (Δ_{sc})	Load (%)	wind Speed (V_w) (m/s)	Wind Power (P_w) (MW) Bus 5	Solar irradiance (G_{s1})	Solar Power (P_{s1}) (MW) Bus 8	River Flow rate (Q_w)	Hydro Power (P_H) (MW) Bus 13	Solar Irradiance (G_{s2})	Solar Power (P_{s2}) (MW) Bus 13
1	0.796	71.22	4.78	10.25	0.00	0.00	15.24	3.18	0.00	0.00
2	0.094	62.54	6.17	18.31	336.18	16.81	14.18	2.96	0.00	0.00
3	0.002	68.44	9.37	36.72	786.63	39.33	16.98	3.54	248.83	11.20
4	0.002	64.45	8.76	33.24	498.58	24.93	14.93	3.11	733.23	33.00
5	0.068	66.01	11.64	49.82	382.04	19.10	17.13	3.57	229.16	10.31
6	0.004	74.15	3.37	2.12	668.86	33.44	15.30	3.19	485.87	21.86
7	0.018	67.76	8.62	32.43	601.03	30.05	16.15	3.37	0.00	0.00
8	0.006	56.47	9.22	35.90	816.81	40.84	14.58	3.04	0.00	0.00
9	0.002	86.25	14.32	65.32	1000.00	50.00	14.46	3.01	60.36	1.37
10	0.008	89.39	8.02	28.94	0.00	0.00	18.76	3.91	539.42	24.27

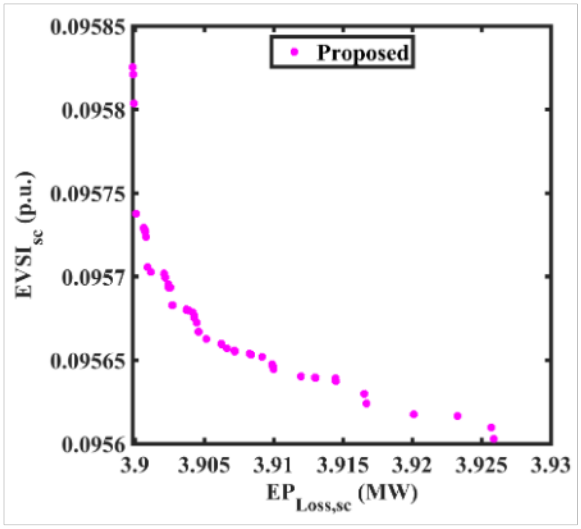
In Chapter 4, stochastic single-objective ORPD was carried out under the same set of ten scenarios, wherein each objective function was optimized independently. The corresponding optimal (expected) values obtained for P_{Loss}, VD and VSI are 3.8425 MW, 0.0592 p.u., and 0.0771 p.u., respectively. These results represent the single-objective optima, with the remaining performance indices evaluated at their respective optimal operating points. Figures 6.11 (a), 6.11 (b) and 6.11 (c) illustrate the Pareto fronts obtained by the proposed method for the cases 7, 8 and 9 considered on the modified IEEE 30-bus system. The BCS for each case is determined using the proposed decision-making approach on the Pareto optimal solutions obtained by the proposed method. The associated results are listed in Table 6.8. For case 7, the proposed method obtains the expected values of P_{Loss} of 4.0791 MW, a VD of 0.1702 p.u. For case 8, the proposed method obtains the expected values of P_{Loss} of 3.9257 MW, a VSI of 0.0956 p.u. For case 9, the proposed method obtains the expected values of P_{Loss} of 4.3745 MW, a VD of 0.2505 p.u. and VSI of 0.0978 p.u.

turnitin Page 172 of 208 - Integrity Submission Submission ID trn:oid:::27535:142293373

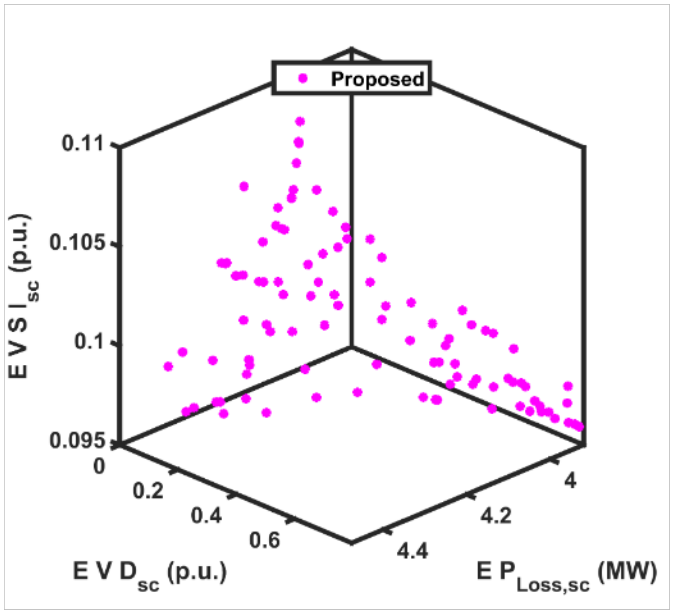
turnitin Page 173 of 208 - Integrity Submission Submission ID trn:oid:::27535:142293373



(a) $EP_{Loss,sc}$ vs. EVD_{sc}



(b) $EP_{Loss,sc}$ vs. $EVSI_{sc}$



(c) $EP_{Loss,sc}$ vs. EVD_{sc} vs. $EVSI_{sc}$

Fig. 6.11: Pareto solutions for the modified IEEE 30-bus system under stochastic operating conditions.

80

turnitin Page 173 of 208 - Integrity Submission Submission ID trn:oid:::27535:142293373

turnitin Page 174 of 208 - Integrity Submission Submission ID trn:oid:::27535:142293373

Table 6.8: Results of the BCS for the modified IEEE 30-bus system using the proposed method.

Variables	Min	Max	Case 7 $EP_{Loss,sc}$ vs. EVD_{sc}	Case 8 $EP_{Loss,sc}$ vs. $EVSI_{sc}$	Case 9 $EP_{Loss,sc}$ vs. EVD_{sc} vs. $EVSI_{sc}$
Generator Voltage (p.u.)					
V1	0.95	1.10	1.0473	1.0655	1.0437
V2	0.95	1.10	1.0396	1.0592	1.0394
V5	0.95	1.10	1.0158	1.0387	1.0117
V8	0.95	1.10	1.0139	1.0358	1.0038
V11	0.95	1.10	1.0311	1.1000	1.0534
V13	0.95	1.10	1.0155	1.0471	0.9951
Transformer Tap (p.u.)					
T11	0.90	1.10	1.0608	1.0991	1.0884
T12	0.90	1.10	0.9830	0.9158	0.9438
T15	0.90	1.10	1.0170	0.9773	0.9388
T36	0.90	1.10	0.9963	0.9894	0.9494
Shunt Compensators (MVAr)					
QC10	0	5	3.5020	0.4796	4.3403
QC12	0	5	1.1819	0.4939	2.2485
QC15	0	5	2.4422	0.4959	1.1539
QC17	0	5	2.2931	3.9586	0.0015
QC20	0	5	4.6136	1.9110	1.6515
QC21	0	5	4.9206	2.9582	3.0579
QC23	0	5	3.3320	0.5339	1.9916
QC24	0	5	4.7450	2.5117	2.3505
QC29	0	5	2.1011	3.0259	3.8667
Objective Function					
$\mathbf{EP_{Loss,sc}}$ (MW)	6.212		**4.0791**	**3.9257**	**4.3475**
$\mathbf{EVD_{sc}}$ (p.u.)	1.1758		**0.1702**	0.8623	**0.2505**

turnitin Page 174 of 208 - Integrity Submission Submission ID trn:oid:::27535:142293373

turnitin Page 175 of 208 - Integrity Submission Submission ID trn:oid:::27535:142293373

Variables	Min Max	Case 7	Case 8	Case 9
		$EP_{Loss,sc}$ vs. EVD_{sc}	$EP_{Loss,sc}$ vs. $EVSI_{sc}$	$EP_{Loss,sc}$ vs. EVD_{sc} vs. $EVSI_{sc}$
$\mathbf{EVSI_{sc}}$ (p.u.)	0.1672	0.1022	**0.0956**	**0.0978**

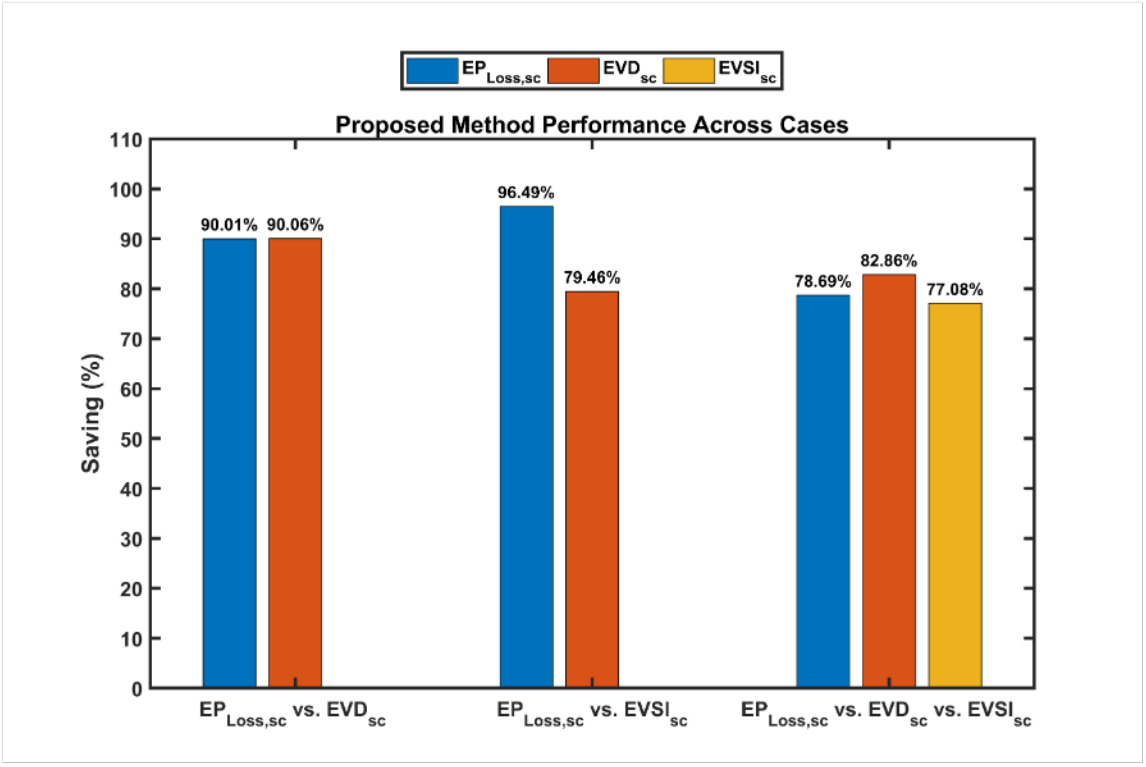


Fig. 6.12: Saving percentages achieved by the proposed method for different cases of the modified IEEE 30 bus.

Table 6.8 summarizes the values obtained and admissible ranges of all control variables for the modified IEEE 30-bus system. The values of all objectives are also shown to depict the trade-off achieved for the considered objectives. In addition, the selected compromise solutions in each case and their corresponding percentage savings are also shown in a bar graph (Figure 6.12). In Case 7, the proposed method achieves a reduction of 90.01% in the expected P_{Loss} and a 90.06% improvement in the expected VD. In Case 8, it achieves a reduction of 96.49% in P_{Loss} along with an improvement of 79.46% in the expected VSI. In the three-objective Case 9, the proposed approach continues to demonstrate consistent performance, achieving improvements of 78.69%, 82.86%, and 77.08% in expected values of P_{Loss}, VD and

turnitin Page 175 of 208 - Integrity Submission Submission ID trn:oid:::27535:142293373

turnitin Page 176 of 208 - Integrity Submission Submission ID trn:oid:::27535:142293373

VSI, respectively. The load bus voltage profiles obtained for each scenario in Cases 7, 8, and 9 are presented in Figures 6.13, 6.14, and 6.15, respectively. From these figures, it can be observed that the voltages at all load buses remain well within the acceptable limits of 0.95 to 1.05 p.u.

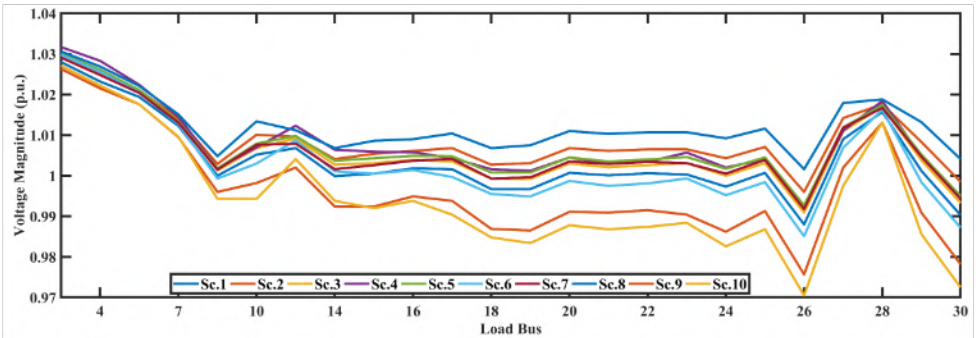


Fig. 6.13: Modified IEEE 30-bus system load bus voltage profiles corresponding to the BCS for ten scenarios (Case 7).

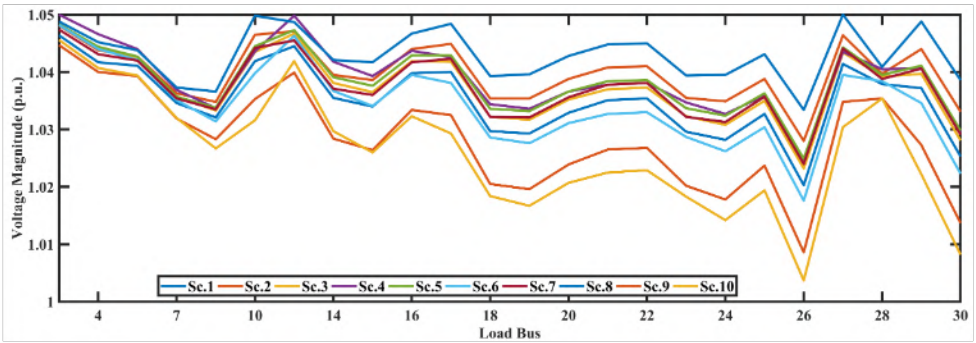


Fig. 6.14: Modified IEEE 30-bus system load bus voltage profiles corresponding to the BCS for ten scenarios (Case 8).

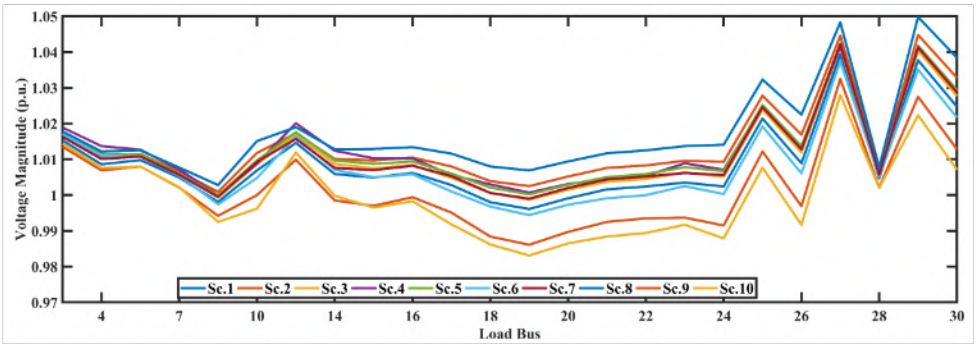


Fig. 6.15: Modified IEEE 30-bus system load bus voltage profiles corresponding to the BCS for ten scenarios (Case 9).

turnitin Page 176 of 208 - Integrity Submission Submission ID trn:oid:::27535:142293373

turnitin Page 177 of 208 - Integrity Submission Submission ID trn:oid:::27535:142293373

6.6 Conclusions

This study proposes a new hybrid multi-objective algorithm that integrates opposition-based strategies with the DE and GPC algorithms, with an NSGA-II selection mechanism to ensure effective convergence and diversity. The effectiveness of the proposed method is examined using standard DTLZ and ZDT benchmark test suites, which are widely used to assess the convergence and diversity of multi-objective optimization algorithms. Performance evaluation is conducted using widely adopted metrics, including Hypervolume (HV), Inverted Generational Distance, Generational Distance, Spacing and Maximum Spread. A statistical comparison is performed with several recently introduced multi-objective optimization algorithms, such as MOPSO, MOMA, MOGOA, and MOSFO. The results show that the proposed algorithm produces well-distributed Pareto solutions while maintaining competitive performance in terms of convergence and diversity.

The proposed algorithm is applied to solve the MOORPD problem to simultaneously minimize P_{Loss}, VD and VSI in different cases of IEEE 30-bus and IEEE 57-bus systems, while satisfying various system constraints. The algorithm is then extended to a stochastic ORPD model on a modified IEEE 30-bus system. This model considers uncertainties in load demand, wind speed, solar irradiance, and small-hydro inflows, representing their natural variability and intermittent characteristics. The results obtained demonstrate that the proposed algorithm generates uniformly distributed, high-quality Pareto-optimal solutions, exhibiting superior convergence and diversity compared to other algorithms. Furthermore, a Best Compromise Solution is obtained for each case using a savings percentage-based decision-making approach, enabling the selection of a suitable operating point. Overall, the findings demonstrate that the proposed algorithm is effective and robust in addressing the challenging multi-objective ORPD problem, with robust search capabilities that enable effective trade-offs among conflicting objectives.

turnitin Page 177 of 208 - Integrity Submission Submission ID trn:oid:::27535:142293373

turnitin Page 179 of 208 - Integrity Submission Submission ID trn:oid:::27535:142293373

Chapter 7

Conclusions, Future Scope and Societal Impact

7.1 Conclusions

The thesis work presents a comprehensive study of single-objective and multi-objective deterministic and stochastic ORPD problems in modern power systems, through the development of advanced optimization approaches. Firstly, a hybrid Opposition-based Differential Evolution-Giza Pyramids Construction (DE-GPC) algorithm was proposed by combining the global exploration ability of Differential Evolution with the constructive search mechanism of the Giza Pyramids Construction algorithm. The proposed approach has been initially validated using standard benchmark functions and it showed superior convergence characteristics, robustness and solution accuracy. The proposed algorithm is tested on the IEEE 30-bus and IEEE 57-bus systems and demonstrates better performance in reducing real P_{Loss} and VD while improving VSI compared to existing optimization techniques.

To address uncertainties in modern power systems, the framework proposed in this work is extended to the stochastic ORPD, accounting for variations in load demand and renewable energy sources, including solar, wind, and small-hydro generation. Probabilistic models were incorporated to reflect the stochastic and intermittent nature of renewable energy resources to develop a more realistic and practical ORPD formulation. Simulation results indicated that the presented stochastic framework is stable and robust under uncertain operating conditions and improved the expected values of the objective functions.

turnitin Page 179 of 208 - Integrity Submission Submission ID trn:oid:::27535:142293373

turnitin Page 180 of 208 - Integrity Submission Submission ID trn:oid:::27535:142293373

Further, a machine learning-based, Improved Evolutionary Algorithm-Self Organized Maps (IEASOM) framework is proposed for solving deterministic and stochastic ORPD problems in electrical power systems. The proposed approach is validated using the IEEE 30-bus and IEEE 118-bus test systems to examine its effectiveness and suitability for both medium- and large-scale power networks. In the stochastic ORPD formulation, uncertainty associated with solar photovoltaic (PV) generation is modeled using real-time meteorological parameters, including solar irradiance, wind velocity, and PV panel temperature, thereby improving the practical applicability of the proposed method in renewable-integrated power systems.

Moreover, a new multi-objective opposition-based hybrid DE-GPC algorithm is developed in combination with the NSGA-II selection method in order to solve complex multi-objective ORPD problems with conflicting objectives. The proposed methodology has successfully generated well-distributed and high-quality Pareto-optimal solutions, which can be utilized for effective trade-off analysis among objectives such as P_{Loss} minimization, VD improvement and VSI enhancement. Additionally, a percentage saving-based decision-making strategy was incorporated to select the most suitable operating solution from the derived Pareto-optimal set, thereby improving the practical applicability of the proposed framework to real-world power system operation and planning.

Overall, the proposed methods exhibited better convergence, robustness, computational efficiency, and solution quality than many recently reported optimization techniques. The developed frameworks provide efficient, reliable and scalable solutions to solve complex ORPD problems under both deterministic and uncertain operating environments. Therefore, this work makes a significant contribution to the advancement of intelligent and hybrid optimization techniques for modern power system operation, planning and control.

7.2 Future Work

Future work can focus on extending the proposed ORPD frameworks to real-time, large-scale smart power systems, where fast decision-making and dynamically changing operating conditions are of great importance. The use of advanced grid components as FACTS devices, energy storage systems, electric vehicles, and

turnitin Page 180 of 208 - Integrity Submission Submission ID trn:oid:::27535:142293373

turnitin Page 181 of 208 - Integrity Submission Submission ID trn:oid:::27535:142293373

distributed energy resources can further improve the controlability, flexibility, and operational performance of the system. In addition, the contingency-constrained ORPD for N-1 and N-k security criteria can be studied to enhance system reliability under fault and outage conditions. More advanced uncertainty modeling and forecasting approaches might also be used to better reflect the unpredictability of renewable energy and load uncertainty. Moreover, the use of distributed and parallel optimization techniques based on artificial intelligence provides promising opportunities for improving computational efficiency and developing adaptive, fast and scalable optimization solutions for future intelligent power systems.

7.3 Societal Impact

This research aligns with the global sustainability framework established by the United Nations through the Sustainable Development Goals (SDGs). The proposed research on deterministic, stochastic, and MOORPD contributes to the development of sustainable, reliable, and energy-efficient modern power systems by improving operational efficiency, supporting renewable energy integration, and enhancing system reliability and stability. The proposed optimization frameworks support several SDGs by promoting clean energy utilization, intelligent power system operation, and environmentally sustainable energy management.

1. **SDG 7: Affordable and Clean Energy:**
   The proposed research strongly supports "Affordable and Clean Energy" by improving the operational efficiency of power systems through optimal reactive power dispatch. The developed optimization frameworks minimize real P_{Loss}, improve voltage stability, and facilitate the efficient integration of RESs such as solar, wind, and small-hydro generation into electrical power systems. These improvements contribute to a more reliable, sustainable, and cost-effective electricity supply while supporting the transition from conventional fossil-fuel-based generation toward clean and renewable energy systems.

2. **SDG 9: Industry, Innovation, and Infrastructure:**
   The research contributes to "Industry, Innovation, and Infrastructure" through the development of advanced hybrid and machine learning-assisted

turnitin Page 181 of 208 - Integrity Submission Submission ID trn:oid:::27535:142293373

turnitin Page 182 of 208 - Integrity Submission Submission ID trn:oid:::27535:142293373

optimization algorithms for modern power system applications. The proposed DE–GPC and IEA–SOM frameworks enhance the operational performance, reliability, and resilience of power networks under both deterministic and uncertain operating conditions. These intelligent optimization approaches support the modernization of electrical infrastructure and promote innovation in smart grid technologies, computational intelligence, and decision-support systems for future energy networks.

3. **SDG 11: Sustainable Cities and Communities:**
   The proposed ORPD frameworks contribute to "Sustainable Cities and Communities" by supporting efficient, reliable, and environmentally sustainable operation of urban power systems. Rapid urbanization and increasing electricity demand place considerable stress on modern power networks. By reducing transmission losses, improving voltage profiles, and enabling efficient renewable energy integration, the proposed methodologies help ensure stable and sustainable electricity supply for urban and industrial applications. This contributes to the development of resilient and energy-efficient smart cities.

4. **SDG 12: Responsible Consumption and Production:**
   The research supports "Responsible Consumption and Production" by promoting efficient utilization of electrical energy resources and reducing unnecessary energy wastage within power systems. Through optimal reactive power management and intelligent optimization techniques, the proposed approaches minimize power losses and improve overall system efficiency. This leads to more sustainable patterns of electricity generation, transmission, and consumption while improving resource utilization in modern power networks.

5. **SDG 13: Climate Action:**
   The proposed research contributes significantly to "Climate Action" by facilitating greater integration of renewable energy resources into electrical power systems and reducing dependence on fossil-fuel-based electricity generation. The reduction in transmission losses and improvement in energy efficiency indirectly decrease greenhouse gas emissions associated with

turnitin Page 182 of 208 - Integrity Submission Submission ID trn:oid:::27535:142293373

turnitin Page 183 of 208 - Integrity Submission Submission ID trn:oid:::27535:142293373

power generation. Furthermore, the stochastic ORPD framework effectively addresses uncertainties associated with renewable energy intermittency, thereby supporting reliable and sustainable low-carbon power system operation. Consequently, the proposed methodologies contribute toward global efforts aimed at mitigating climate change and promoting environmentally sustainable energy systems.

Overall, the proposed optimization frameworks provide significant societal benefits by improving power system efficiency, reliability, sustainability, and renewable energy utilization. The developed methodologies contribute toward the advancement of intelligent and environmentally responsible power system operation and support the global transition toward sustainable and low-carbon energy infrastructures.

turnitin Page 183 of 208 - Integrity Submission Submission ID trn:oid:::27535:142293373

Research Publications

Journals

- G. K. Jaiswal, U. Nangia, and N. K. Jain, "A novel hybrid optimization approach for stochastic reactive power dispatch in hybrid energy systems," *Computers & Electrical Engineering*, vol. 130, p. 110912, 2026.
- G. K. Jaiswal, U. Nangia, and N. K. Jain, "Improved evolutionary algorithm–self organized maps (IEA-SOM) for optimal reactive power dispatch problem," *Journal of Electrical Engineering & Technology*, 2026.
- G. K. Jaiswal, U. Nangia, and N. K. Jain, "A novel hybrid multi-objective optimization approach for deterministic and stochastic reactive power dispatch," *Applied Soft Computing* (Under Review).

Conferences

- G. K. Jaiswal, U. Nangia, and N. K. Jain, "Optimal reactive power dispatch using Honey Badger algorithm (HBA)," in *Proc. IEEE 10th Power India Int. Conf. (PIICON)*, New Delhi, India, 2022, pp. 1–6.
- G. K. Jaiswal, U. Nangia, and N. K. Jain, "Optimal reactive power dispatch using Giza Pyramids Construction algorithm," in *Proc. 2nd Int. Conf. Adv. Electr., Comput., Commun. Sustain. Technol. (ICAECT)*, Bhilai, India, 2022, pp. 1–6.

turnitin Page 187 of 208 - Integrity Submission Submission ID trn:oid:::27535:142293373

References

[1] M. S. Saddique, "Solution to optimal reactive power dispatch in transmission system using meta-heuristic techniques—status and technological review," *Electric Power Systems Research*, vol. 178, 2020. 1

[2] J. Carpentier, "Contribution to the economic dispatch problem," *Bulletin de la Société Française des Électriciens*, vol. 3, no. 8, pp. 431–447, 1962. 1

[3] U. Mittal, U. Nangia, and N. K. Jain, "An in-depth examination of artificial intelligence-based methods for optimal power flow solutions," *Neural Computing and Applications*, vol. 36, no. 29, pp. 17 881–17 929, 2024.

[4] F. Capitanescu, "Critical review of recent advances and further developments needed in ac optimal power flow," *Electric Power Systems Research*, vol. 136, pp. 57–68, 2016. 1

[5] H. Abdi, M. Moradi, R. Asadi, S. Naderi, B. Amiri, and F. Karimi, "Optimal reactive power dispatch problem: A comprehensive study on meta-heuristic algorithms," *Journal of Energy Management and Technology*, vol. 5, no. 3, pp. 67–84, 2021. 2

[6] X. Geng, L. Xie, and D. Obadina, "Chance constrained optimal reactive power dispatch," in *Proc. IEEE Power and Energy Society General Meeting*, 2018. 2

[7] Y. Zhang and L. Wehenkel, "A reliability management system for power grids under uncertainty," *IEEE Transactions on Power Systems*, vol. 25, no. 1, pp. 318–326, 2010. 2

[8] C. Gusain, M. M. Tripathi, and U. Nangia, "Study of meta-heuristic optimization methodologies for design of hybrid renewable energy systems," *Thermal Science and Engineering Progress*, vol. 39, p. 101711, 2023. 2

turnitin Page 187 of 208 - Integrity Submission Submission ID trn:oid:::27535:142293373

turnitin Page 188 of 208 - Integrity Submission Submission ID trn:oid:::27535:142293373

[9] C. Bingane, M. F. Anjos, and S. L. Digabel, "Tight-and-cheap conic relaxation for the optimal reactive power dispatch problem," *arXiv preprint arXiv:1810.03040*, 2022. 2

[10] R. Roy, T. Das, and K. K. Mandal, "Optimal reactive power dispatch for voltage security using jaya algorithm," in *Proc. Int. Conf. on Computational Intelligence and Data Science*, 2020. 3

[11] N. Karthik, A. K. Parvathy, and R. Arul, "Levy interior search algorithm-based multi-objective optimal reactive power dispatch for voltage stability enhancement," in *Recent Trends in Power Systems*. Springer, 2021. 3

[12] B. A. Robbins and A. D. Domínguez-García, "Optimal reactive power dispatch for voltage regulation in unbalanced distribution systems," *IEEE Transactions on Power Systems*, vol. 31, no. 4, pp. 2903–2913, 2016. 3

[13] S. Bhongade and A. Tomar, "Optimal reactive power dispatch optimization using statcom," *J. Inst. Eng. India Ser. B*, 2021. 3

[14] P. Preedavichit and S. C. Srivastava, "Optimal reactive power dispatch considering facts devices," *Electric Power Systems Research*, vol. 46, no. 3, pp. 251–257, 1998. 3

[15] S. B. Pandya and R. Roy, "Particle swarm optimization based optimal reactive power dispatch," in *Proc. Int. Conf. on Electrical, Electronics, Signals, Communication and Optimization*, 2015. 3

[16] T. Das and R. Roy, "Optimal reactive power dispatch using jaya algorithm," in *Proc. Int. Conf. on Emerging Trends in Electronic Devices and Computational Techniques*, 2018. 3

[17] R. Ravisekar and K. Srinivasan, "Optimal reactive power dispatch with series and shunt facts devices using sine cosine algorithm," *Int. J. Adv. Res. Eng. Technol.*, vol. 11, no. 1, 2020. 4

[18] D. Karthikaikannan and G. Ravi, "Optimal reactive power dispatch considering multi-type facts devices using harmony search algorithms," *Automatika*, vol. 59, no. 3–4, pp. 353–362, 2018. 4

turnitin Page 188 of 208 - Integrity Submission Submission ID trn:oid:::27535:142293373

turnitin Page 189 of 208 - Integrity Submission Submission ID trn:oid:::27535:142293373

[19] N. G. Hingorani, "Flexible ac transmission," *IEEE Spectrum*, vol. 30, no. 4, pp. 40–45, April 1993. 4

[20] E. H. Talbi, M. E. Moudden, and F. Baijou, "Robust deterministic optimization approach for optimal reactive energy management in electrical transmission network," in *Advances in Science, Technology and Innovation*. Springer, 2024. 4

[21] T. Sharma, A. Yadav, S. Jamhoria, and R. Chaturvedi, "Comparative study of methods for optimal reactive power dispatch," *Electrical and Electronics Engineering: An International Journal*, vol. 3, no. 3, pp. 53–61, August 2014. 4

[22] M. Y. Ali and K. Raahemifar, "Reactive power optimization based on hybrid particle swarm optimization algorithm," in *Proc. Canadian Conf. on Electrical and Computer Engineering*, 2012. 5

[23] K. Mahadevan and P. S. Kannan, "Comprehensive learning particle swarm optimization for reactive power dispatch," *Applied Soft Computing*, vol. 10, no. 2, pp. 641–652, 2010. 5

[24] S. M. Mohseni-Bonab and A. Rabiee, "Optimal reactive power dispatch: A review, and a new stochastic voltage stability constrained multi-objective model at the presence of uncertain wind power generation," *IET Gener., Transmiss. Distrib.*, vol. 11, no. 4, pp. 815–829, 2017. 5

[25] P. Das, S. Dawn, and S. Gope, "Optimal reactive power dispatch and demand response in electricity market using multi-objective grasshopper optimization algorithm," *Processes*, vol. 12, no. 9, p. 2049, 2024. 6

[26] I. H. Shanono, A. Muhammad, and N. R. H. Abdullah, "Optimal reactive power dispatch: A bibliometric analysis," *Repository Article*, 2024. 6

[27] H. M. Sultan, A. A. Z. Diab, A. S. Menesy, M. Kassas, M. Alqahtani, M. Khalid, and H. I. Abdul-Ghaffar, "Enhancing optimal power flow in power systems: A comparative analysis of recent metaheuristic optimization techniques," *Energy Reports*, vol. 13, pp. 3957–3999, June 2025. 6

turnitin Page 189 of 208 - Integrity Submission Submission ID trn:oid:::27535:142293373

turnitin Page 190 of 208 - Integrity Submission Submission ID trn:oid:::27535:142293373

[28] Y. Zhou, J. Zhang, and X. Yang, "Optimal reactive power dispatch using water wave optimization algorithm," *Operational Research*, vol. 20, no. 2, pp. 1019–1053, 2020. 6

[29] S. A. Adegoke, A. A. Jimoh, and A. Y. Abdelaziz, "A mini review on optimal reactive power dispatch incorporating renewable energy sources and facts devices," *Electrical Engineering*, vol. 106, no. 2, pp. 1547–1565, 2024. 6

[30] C. Gusain, U. Nangia, and M. M. Tripathi, "Optimal sizing of standalone hybrid renewable energy system based on reliability indicator: A case study," *Energy Conversion and Management*, vol. 310, p. 118490, 2024.

[31] S. S. Reddy, P. R. Bijwe, and A. R. Abhyankar, "Real-time economic dispatch considering renewable variability," *IEEE Systems Journal*, vol. 9, no. 4, pp. 1440–1451, 2015. 6, 44

[32] U. Mittal, U. Nangia, N. K. Jain, and S. Gupta, "Optimal power flow solutions for normal and critical loading scenarios using hybrid Rao-2 sine cosine algorithm," *Computers and Electrical Engineering*, vol. 123, p. 110230, 2025. 7

[33] X. Fang, S. Misra, G. Xue, and D. Yang, "Smart grid—the new and improved power grid: A survey," *IEEE Communications Surveys & Tutorials*, vol. 14, no. 4, pp. 944–980, 2012. 7

[34] Z. Yang, A. Bose, H. Zhong, and T. Zheng, "Optimal reactive power dispatch with accurately modeled discrete control devices: A successive linear approximation approach," *IEEE Transactions on Power Systems*, vol. 32, no. 3, pp. 2435–2444, 2017. 7

[35] M. De and S. K. Goswami, "Optimal reactive power procurement with voltage stability consideration in deregulated power system," *IEEE Transactions on Power Systems*, vol. 29, no. 5, pp. 2078–2086, 2014. 7

[36] N. K. Jain, U. Nangia, and I. Singh, "Multiobjective economic load dispatch in 3-d space by genetic algorithm," *Journal of The Institution of Engineers (India): Series B*, vol. 98, no. 5, pp. 495–501, 2017. 7

turnitin Page 190 of 208 - Integrity Submission Submission ID trn:oid:::27535:142293373

turnitin Page 191 of 208 - Integrity Submission Submission ID trn:oid:::27535:142293373

[37] A. Mahate and V. G. Jadhao, "Multi-objective differential evolution algorithm for optimal reactive power dispatch," *International Journal of Electrical Power & Energy Systems*, vol. 118, p. 105784, 2020.

[38] N. K. Jain, U. Nangia, and J. Jain, "Multiobjective economic load dispatch studies in 2-d and 3-d space by particle swarm optimization technique," *Journal of the Institution of Engineers (India): Series B*, vol. 100, no. 3, pp. 233–247, 2019. 7

[39] Y. M. Zhang, C. R. Chen, and C. Y. Lee, "Solution of the optimal reactive power dispatch for power systems by using novel charged system search algorithm," in *Proceedings of the IEEE International Symposium on Next-Generation Electronics (ISNE)*, 2018. 8

[40] K. Vaisakh and P. K. Rao, "Differential evolution based optimal reactive power dispatch for voltage stability enhancement," *International Journal of Electrical Power & Energy Systems*, vol. 30, no. 3, pp. 155–162, 2008. 8

[41] R. M. Jan and N. Chen, "Application of the fast newton-raphson economic dispatch and reactive power/voltage dispatch by sensitivity factors to optimal power flow," *IEEE Transactions on Energy Conversion*, vol. 10, no. 2, pp. 293–301, 1995. 11

[42] S. Granville, "Optimal reactive dispatch through interior point methods," *IEEE Transactions on Power Systems*, vol. 9, no. 1, pp. 136–146, 1994. 11

[43] K. Y. Lee, Y. M. Park, and J. L. Ortiz, "A unified approach to optimal real and reactive power dispatch," *IEEE Transactions on Power Apparatus and Systems*, vol. PAS-104, no. 5, pp. 1147–1153, 1985. 11

[44] N. Deeb and S. M. Shahidehpour, "An efficient technique for reactive power dispatch using a revised linear programming approach," *Electr. Power Syst. Res.*, vol. 15, no. 2, pp. 121–134, 1990. 12

[45] M. Granada, M. J. Rider, J. R. S. Mantovani, and M. Shahidehpour, "A decentralized approach for optimal reactive power dispatch using a lagrangian decomposition method," *Electric Power Systems Research*, vol. 89, pp. 148–156, 2012. 12

turnitin Page 191 of 208 - Integrity Submission Submission ID trn:oid:::27535:142293373

turnitin Page 192 of 208 - Integrity Submission Submission ID trn:oid:::27535:142293373

[46] B. Mahdad and S. Kamel, "Modified salp swarm algorithm for optimal reactive power planning," *IET Generation, Transmission & Distribution*, vol. 13, no. 20, pp. 4523–4540, 2019. 12

[47] C. Dai, W. Chen, Y. Zhu, and X. Zhang, "Reactive power dispatch considering voltage stability with seeker optimization algorithm," *Electric Power Systems Research*, vol. 79, no. 10, pp. 1462–1471, 2009. 12

[48] M. Abdelmoumene, M. Belkacemi, and A. Boubakeur, "Optimal reactive power dispatch using differential evolution algorithm with voltage profile control," *International Journal of Intelligent Systems and Applications*, vol. 5, no. 10, pp. 28–34, 2013. 12

[49] A. A. El-Ela, A. Kinawy, R. El-Sehiemy, and M. Mouwafi, "Optimal reactive power dispatch using ant colony optimization algorithm," *Electrical Engineering*, vol. 93, no. 2, pp. 103–116, 2011. 13

[50] M. Ghasemi, M. Taghizadeh, S. Ghavidel, J. Aghaei, and A. Abbasian, "Solving optimal reactive power dispatch problem using a novel teaching–learning-based optimization algorithm," *Engineering Applications of Artificial Intelligence*, vol. 39, pp. 100–108, 2015. 13

[51] S. K. Gupta, M. K. Kar, L. Kumar, and S. Kumar, "A simplified sine cosine algorithm for the solution of optimal reactive power dispatch," *International Transactions on Electrical Energy Systems*, vol. 2022, 2022. 13

[52] R. Roy, T. Das, and K. K. Mandal, "Optimal reactive power dispatch using a novel optimization algorithm," *Journal of Electrical Systems and Information Technology*, vol. 8, no. 1, 2021. 13

[53] S. Mouassa, T. Bouktir, and A. Salhi, "Ant lion optimizer for solving optimal reactive power dispatch problem in power systems," *Engineering Science and Technology, an International Journal*, vol. 20, no. 3, pp. 885–895, 2017. 13

[54] R. N. S. Mei, M. H. Sulaiman, Z. Mustaffa, and H. Daniyal, "Optimal reactive power dispatch solution by loss minimization using moth-flame optimization technique," *Applied Soft Computing*, vol. 59, pp. 210–222, 2017. 13

turnitin Page 192 of 208 - Integrity Submission Submission ID trn:oid:::27535:142293373

turnitin Page 193 of 208 - Integrity Submission Submission ID trn:oid:::27535:142293373

[55] W. Lai, Q. Song, X. Zheng, and H. Chen, "The study of optimal reactive power dispatch in power systems based on further improved membrane search algorithm," *Applied Energy*, vol. 377, p. 124433, 2025. 13

[56] S. Biswas, N. Chakraborty, and K. K. Mandal, "Differential evolution technique with random localization for tuned reactive power dispatch problem," *Engineering Optimization*, vol. 45, no. 4, pp. 500–518, 2013. 14

[57] B. Shaw, V. Mukherjee, and S. Ghoshal, "Solution of reactive power dispatch of power systems by an opposition-based gravitational search algorithm," *International Journal of Electrical Power & Energy Systems*, vol. 55, pp. 29–40, 2014. 14

[58] H. Yapici, "Solution of optimal reactive power dispatch problem using pathfinder algorithm," *Engineering Optimization*, vol. 53, no. 11, pp. 1946–1963, 2021. 14

[59] M. A. M. Shaheen, "Enhanced transient search optimization algorithm-based optimal reactive power dispatch including electric vehicles," *Energy*, vol. 277, 2023. 14

[60] S. Sarhan, A. Shaheen, R. El-Sehiemy, and M. Gafar, "An augmented social network search algorithm for optimal reactive power dispatch problem," *Mathematics*, vol. 11, no. 5, 2023. 14

[61] A. M. A.-E. Wahab, S. Kamel, M. H. Hassan, M. I. Mosaad, and T. A. Abdulfattah, "Optimal reactive power dispatch using a chaotic turbulent flow of water-based optimization algorithm," *Mathematics*, vol. 10, no. 3, 2022. 14

[62] L. Kanagasabai, "Factual power loss reduction by meadow fritillary butterfly optimization algorithm," in *Proceedings of the Springer Conference Series*, 2022, pp. 737–742. 15

[63] Z. Li, Y. Cao, L. V. Dai, X. Yang, and T. T. Nguyen, "Finding solutions for optimal reactive power dispatch problem by a novel improved antlion optimization algorithm," *Energies*, vol. 12, no. 15, p. 2968, 2019. 15

turnitin Page 193 of 208 - Integrity Submission Submission ID trn:oid:::27535:142293373

[64] B. K. Dora, A. Rajan, S. Mallick, and S. Halder, "Optimal reactive power dispatch problem using exchange market based butterfly optimization algorithm," *Applied Soft Computing*, vol. 147, p. 110833, 2023. 15

[65] Y. Li, Y. Wang, and B. Li, "A hybrid artificial bee colony assisted differential evolution algorithm for optimal reactive power flow," *International Journal of Electrical Power & Energy Systems*, vol. 52, no. 1, pp. 25–33, 2013. 16

[66] S. K. M. Shareef and R. S. Rao, "Optimal reactive power dispatch under unbalanced conditions using hybrid swarm intelligence," *Computers & Electrical Engineering*, vol. 69, pp. 183–193, 2018. 16

[67] S. Padaiyatchi and M. Daniel, "Opf-based reactive power planning and voltage stability limit improvement under single line outage contingency condition through evolutionary algorithms," *Turkish Journal of Electrical Engineering & Computer Sciences*, vol. 21, no. 4, pp. 1092–1106, 2013. 16

[68] C.-M. Huang and Y.-C. Huang, "Combined differential evolution algorithm and ant system for optimal reactive power dispatch," *Energy Procedia*, vol. 14, pp. 1238–1243, 2012. 17

[69] S. Chen, W. Hu, C. Su, X. Zhang, and Z. Chen, "Optimal reactive power and voltage control in distribution networks with distributed generators by fuzzy adaptive hybrid particle swarm optimisation method," *IET Generation, Transmission & Distribution*, vol. 9, no. 11, pp. 1096–1103, 2015. 17

[70] M. Ghasemi, M. M. Ghanbarian, S. Ghavidel, S. Rahmani, and E. M. Moghaddam, "Modified teaching learning algorithm and double differential evolution algorithm for optimal reactive power dispatch problem: A comparative study," *Information Sciences*, vol. 278, pp. 231–249, 2014. 17

[71] E. Naderi, H. Narimani, M. Fathi, and M. R. Narimani, "A novel fuzzy adaptive configuration of particle swarm optimization to solve large-scale optimal reactive power dispatch," *Applied Soft Computing*, vol. 53, pp. 441–456, 2017. 17

turnitin Page 195 of 208 - Integrity Submission Submission ID trn:oid:::27535:142293373

[72] A. Rajan and T. Malakar, "Optimal reactive power dispatch using hybrid nelder-mead simplex based firefly algorithm," *International Journal of Electrical Power & Energy Systems*, vol. 66, pp. 9–24, 2015. 17

[73] A. M. A.-E. Wahab, S. Kamel, H. M. Sultan, M. H. Hassan, and F. J. Ruiz-Rodríguez, "Optimizing reactive power dispatch using hybrid artificial rabbits and gradient-based optimization," *Electrical Engineering*, 2024. 17

[74] S. Jeyadevi, S. Baskar, C. K. Babulal, and M. W. Iruthayarajan, "Solving multiobjective optimal reactive power dispatch using modified nsga-ii," *International Journal of Electrical Power & Energy Systems*, vol. 33, no. 2, pp. 219–228, 2011. 18

[75] T. Niknam, M. R. Narimani, R. Azizipanah-Abarghooee, and B. Bahmani-Firouzi, "Multiobjective optimal reactive power dispatch and voltage control: A new opposition-based self-adaptive modified gravitational search algorithm," *IEEE Systems Journal*, vol. 7, no. 4, pp. 742–753, 2013. 18

[76] Q. Li, M. Liu, and H. Liu, "Piecewise normalized normal constraint method for optimal reactive power dispatch," *IEEE Transactions on Power Systems*, vol. 30, no. 3, pp. 1243–1251, 2015. 18

[77] L. Srivastava and H. Singh, "Hybrid multi-swarm particle swarm optimisation based multi-objective reactive power dispatch," *IET Generation, Transmission & Distribution*, vol. 9, no. 8, pp. 727–739, 2015. 19

[78] K. Nuaekaew, P. Artrit, N. Pholdee, and S. Bureerat, "Optimal reactive power dispatch using multi-objective grey wolf optimizer," *Expert Systems with Applications*, vol. 87, pp. 79–89, 2017. 19

[79] P. Panthagani and R. S. Rao, "Optimal allocation of facts devices for reactive power dispatch using kinetic gas molecule optimization," *International Journal of Advanced Intelligence Paradigms*, vol. 27, no. 3–4, pp. 347–363, 2024. 19

[80] T. M. Aljohani, A. F. Ebrahim, and O. Mohammed, "Hybrid artificial physics-particle swarm optimization for reactive power dispatch," *Energies*, vol. 12, no. 12, p. 2333, 2019. 19

turnitin Page 195 of 208 - Integrity Submission Submission ID trn:oid:::27535:142293373

[81] M. Mahzouni-Sani, A. Hamidi, D. Nazarpour, and S. Golshannavaz, "Multi-objective optimal reactive power dispatch of wind-integrated networks," *IET Generation, Transmission & Distribution*, vol. 13, no. 13, pp. 2686–2696, 2019. 19

[82] M. Zhang and Y. Li, "Multi-objective optimal reactive power dispatch using evolutionary algorithm," *IEEE Access*, vol. 8, pp. 38 198–38 209, 2020. 19

[83] S. Karimi, S. Hosseini-Hemati, and A. Rastgou, "Stochastic multi-objective reactive power dispatch for distribution networks," *Sustainable Energy Technologies and Assessments*, vol. 57, p. 103235, 2023. 19

[84] F. Bhurt, A. Ali, M. U. Keerio, G. Abbas, Z. Ahmed, N. H. Mugheri, and Y.-S. Kim, "Stochastic multi-objective optimal reactive power dispatch with the integration of wind and solar generation," *Energies*, vol. 16, no. 13, p. 4896, 2023. 20

[85] S. Dutta, S. Paul, and P. K. Roy, "Optimal allocation of svc and tcsc using quasi-oppositional chemical reaction optimization for solving multi-objective orpd problem," *Journal of Electrical Systems and Information Technology*, vol. 5, no. 1, pp. 83–98, 2018. 20

[86] G. Gangil, S. K. Goyal, and A. Saraswat, "Multi-objective reactive power dispatch using fuzzy tuned mayfly algorithm," *Expert Systems with Applications*, vol. 249, p. 123819, 2024. 20

[87] M. Ebeed, S. Ali, A. M. Kassem, M. Hashem, S. Kamel, A. G. Hussien, F. Jurado, and E. A. Mohamed, "Solving stochastic optimal reactive power dispatch using an adaptive beluga whale optimization considering uncertainties of renewable energy resources and the load growth," *Ain Shams Engineering Journal*, vol. 15, no. 8, p. 102762, 2024. 20

[88] P. Panthagani and R. S. Rao, "Kgmo for multi-objective optimal allocation of svc and reactive power dispatch," in *Proc. Int. Conf. Power Embedded Drive Control (ICPEDC)*, 2017, pp. 365–369. 20

[89] S. Kamel, S. Abdel-Fatah, M. Ebeed, J. Yu, K. Xie, and C. Zhao, "Solving optimal reactive power dispatch problem considering load uncertainty,"

turnitin Page 197 of 208 - Integrity Submission Submission ID trn:oid:::27535:142293373

in *IEEE PES Innovative Smart Grid Technologies Asia (ISGT-Asia)*, 2019, pp. 1335–1340. 21, 23

[90] T. Das, R. Roy, and K. K. Mandal, "Optimal reactive power dispatch problem integrating probabilistic model of wind power for uncertainties in load using jaya algorithm," *International Journal of Ambient Energy*, vol. 45, no. 1, p. 2304721, 2024. [Online]. Available: https://doi.org/10.1080/01430750.2024.2304721 21, 23

[91] P. P. Biswas, P. N. Suganthan, R. Mallipeddi, and G. A. J. Amaratunga, "Optimal reactive power dispatch with uncertainties in load demand and renewable energy sources," *Applied Soft Computing*, vol. 75, pp. 616–632, 2019. 22, 23

[92] N. H. Khan, Y. Wang, D. Tian, M. A. Z. Raja, R. Jamal, and Y. Muhammad, "Design of fractional particle swarm optimization gravitational search algorithm for optimal reactive power dispatch problems," *IEEE Access*, vol. 8, pp. 146 785–146 806, 2020. 22, 23

[93] M. Ebeed, A. Alhejji, S. Kamel, and F. Jurado, "Solving the optimal reactive power dispatch using marine predators algorithm considering the uncertainties in load and wind-solar generation systems," *Energies*, vol. 13, no. 17, 2020. 22, 23

[94] M. Ebeed, A. Ali, M. I. Mosaad, and S. Kamel, "Improved lightning attachment procedure optimizer for optimal reactive power dispatch with renewable uncertainty," *IEEE Access*, vol. 8, pp. 168 721–168 731, 2020. 22

[95] M. H. Hassan, S. Kamel, M. A. El-Dabah, T. Khurshaid, and J. L. Dominguez-Garcia, "Optimal reactive power dispatch with time-varying demand and renewable uncertainty using rao-3 algorithm," *IEEE Access*, vol. 9, pp. 23 264–23 283, 2021. 22, 23

[96] N. H. Khan, R. Jamal, M. Ebeed, S. Kamel, H. Zeinoddini-Meymand, and H. M. Zawbaa, "Scenario-based optimal reactive power dispatch with wind and solar integration using improved marine predator algorithm," *Ain Shams Engineering Journal*, vol. 13, no. 5, 2022. 22, 24

turnitin Page 197 of 208 - Integrity Submission Submission ID trn:oid:::27535:142293373

turnitin Page 198 of 208 - Integrity Submission Submission ID trn:oid:::27535:142293373

[97] M. Naidji and M. Boudour, "Stochastic multi-objective optimal reactive power dispatch considering load and renewable energy sources uncertainties: A case study of the adrar isolated power system," *International Transactions on Electrical Energy Systems*, vol. 30, no. 6, 2020. 22, 24

[98] N. H. Khan, Y. Wang, R. Jamal, S. Iqbal, M. Ebeed, Y. Y. Ghadi, and Z. M. S. Elbarbary, "Enhanced skill optimization algorithm: Solution to the stochastic reactive power dispatch framework with optimal inclusion of renewable resources using large-scale network," *IET Renewable Power Generation*, vol. 18, no. S1, pp. 4565–4583, 2024. 24

[99] P. Megantoro, S. A. Halim, N. A. M. Kamari, L. J. Awalin, R. Mohamed, and H. M. Rosli, "An enhanced multi-objective reactive power dispatch for hybrid wind-solar power system using Archimedes optimization algorithm," *International Journal of Electrical Power & Energy Systems*, vol. 168, p. 110676, 2025. 24

[100] R. Jamal, J. Zhang, B. Men, N. H. Khan, M. Ebeed, and S. Kamel, "Deterministic and stochastic optimal reactive power dispatch using modified artificial hummingbird algorithm," *Energy Reports*, vol. 9, pp. 4157–4173, 2023. 24

[101] D. H. Wolpert and W. G. Macready, "No free lunch theorems for optimization," *IEEE Transactions on Evolutionary Computation*, vol. 1, no. 1, pp. 67–82, 1997. 25

[102] R. Mallipeddi, S. Jeyadevi, P. N. Suganthan, and S. Baskar, "Efficient constraint handling for optimal reactive power dispatch problems," *Swarm and Evolutionary Computation*, vol. 5, pp. 28–36, 2012. 28

[103] M. Basu, "Quasi-oppositional differential evolution for optimal reactive power dispatch," *Int. J. Electr. Power Energy Syst.*, vol. 78, pp. 29–40, 2016. 29

[104] S. K. Elsayed, S. Kamel, A. Selim, and M. Ahmed, "An improved heap-based optimizer for optimal reactive power dispatch," *IEEE Access*, vol. 9, pp. 62 983–62 998, 2021. 29, 30

turnitin Page 198 of 208 - Integrity Submission Submission ID trn:oid:::27535:142293373

turnitin Page 199 of 208 - Integrity Submission Submission ID trn:oid:::27535:142293373

[105] P. Kessel and H. Glavitsch, "Estimating the voltage stability of a power system," *IEEE Trans. Power Del.*, vol. 1, no. 3, pp. 346–354, 1986. 30

[106] Q. H. Wu and J. T. Ma, "Power system optimal reactive power dispatch using evolutionary programming," *IEEE Trans. Power Syst.*, vol. 10, no. 3, pp. 1243–1249, 1995. 30

[107] M. Abido, "Multiobjective optimal var dispatch using strength pareto evolutionary algorithm," in *2006 IEEE International Conference on Evolutionary Computation*, 2006, pp. 730–736. 30

[108] C. A. C. Coello, "Theoretical and numerical constraint-handling techniques used with evolutionary algorithms: A survey of the state of the art," *Computer Methods in Applied Mechanics and Engineering*, vol. 191, no. 11–12, pp. 1245–1287, 2002. 32

[109] K. Deb, *Multi-Objective Optimization Using Evolutionary Algorithms*. Chichester, England: John Wiley & Sons, 2001. 33, 122

[110] C. L. Wadhwa, *Electrical Power Systems*, 7th ed. New Delhi, India: New Age International Publishers, 2017. 34

[111] R. D. Zimmerman, C. E. Murillo-Sánchez, and R. J. Thomas, "Matpower: Steady-state operations, planning, and analysis tools for power systems research and education," *IEEE Transactions on Power Systems*, vol. 26, no. 1, pp. 12–19, 2011. 34, 35, 121

[112] O. Alsac and B. Stott, "Optimal load flow with steady-state security," *IEEE Trans. Power Appar. Syst.*, no. 3, pp. 745–751, 1974. 34

[113] P. P. Biswas, P. N. Suganthan, R. Mallipeddi, and G. A. J. Amaratunga, "Optimal power flow solutions using differential evolution algorithm integrated with effective constraint handling techniques," *Eng. Appl. Artif. Intell.*, vol. 68, pp. 81–100, 2018. 35

[114] H. R. Tizhoosh, "Opposition-based learning: A new scheme for machine intelligence," in *Proceedings of the International Conference on Computational Intelligence for Modelling, Control and Automation*, vol. 1, 2005, pp. 695–701. 37, 40

turnitin Page 199 of 208 - Integrity Submission Submission ID trn:oid:::27535:142293373

turnitin Page 200 of 208 - Integrity Submission Submission ID trn:oid:::27535:142293373

[115] R. Storn and K. Price, "Differential evolution for global optimization," *Journal of Global Optimization*, vol. 11, no. 4, pp. 341–359, 1997. 37, 40

[116] S. Harifi, J. Mohammadzadeh, M. Khalilian, and S. Ebrahimnejad, "Giza pyramids construction: An ancient-inspired metaheuristic algorithm for optimization," *Evolutionary Intelligence*, vol. 14, no. 4, pp. 1743–1761, 2021. 37, 38, 51

[117] A. Ibraheemi, A. Tally, A. Nadweh, A. A. Sayed, R. Tawfeq, H. Gheni, N. Shah, and R. Sekhar, "A cognitive energy-driven routing strategy for ultra-efficient data transfer in wireless sensor networks," *Applied Data Science and Analysis*, vol. 2025, pp. 131–143, Apr. 2025. 40

[118] P. P. Biswas, P. N. Suganthan, B. Y. Qu, and G. A. J. Amaratunga, "Multiobjective economic-environmental power dispatch with stochastic renewable sources," *Energy*, vol. 150, pp. 1039–1057, 2018. 43

[119] S. M. Mohseni-Bonab, A. Rabiee, and B. Mohammadi-Ivatloo, "Voltage stability constrained optimal reactive power dispatch under uncertainty," *Renewable Energy*, vol. 85, pp. 598–609, 2016. 47

[120] N. Gröwe-Kuska, H. Heitsch, and W. Römisch, "Scenario reduction and scenario tree construction for power management problems," in *IEEE PowerTech Conference*, 2003, vol. 3, pp. 152–158. 49

[121] I. Naruei and F. Keynia, "A new optimization method based on coot bird natural life model," *Expert Systems with Applications*, vol. 183, 2021. 51, 75

[122] F. A. Hashim, E. H. Houssein, K. Hussain, M. S. Mabrouk, and W. Al-Atabany, "Honey badger algorithm: A new metaheuristic algorithm for optimization," *Mathematics and Computers in Simulation*, vol. 192, pp. 84–110, 2022. 51

[123] E. Cuevas and J. Gálvez, "An optimization algorithm guided by a machine learning approach," *International Journal of Machine Learning and Cybernetics*, vol. 10, pp. 2963–2991, 2019. 75, 76, 86

[124] M. Dehghani, E. Trojovská, and P. Trojovský, "A new human-based metaheuristic algorithm for solving optimization problems on the base of

turnitin Page 200 of 208 - Integrity Submission Submission ID trn:oid:::27535:142293373

turnitin Page 201 of 208 - Integrity Submission Submission ID trn:oid:::27535:142293373

simulation of driving training process," *Scientific Reports*, vol. 12, no. 1, 2022. 75

[125] Solcast, "Historical time series data toolkit," 2024, [Accessed: 2024]. [Online]. Available: https://toolkit.solcast.com.au/historical/timeseries/request 82

[126] R. Aman, M. Rizwan, and A. Kumar, "A novel hybrid intelligent approach for solar photovoltaic power prediction considering uv index and cloud cover," *Electrical Engineering*, 2024. 82

[127] C. A. C. Coello, G. T. Pulido, and M. S. Lechuga, "Handling multiple objectives with particle swarm optimization," *IEEE Transactions on Evolutionary Computation*, vol. 8, no. 3, pp. 256–279, 2004. 108

[128] S. Z. Mirjalili, S. Mirjalili, S. Saremi, H. Faris, and I. Aljarah, "Grasshopper optimization algorithm for multi-objective optimization problems," *Applied Intelligence*, vol. 48, no. 4, pp. 805–820, 2018. 108

[129] K. Zervoudakis and S. Tsafarakis, "Mayfly optimization algorithm," *Computers & Industrial Engineering*, vol. 145, p. 106559, 2020. 108

[130] J. L. J. Pereira and G. F. Gomes, "Multi-objective sunflower optimization: A new hypercubic meta-heuristic for constrained engineering problems," *Expert Systems*, 2023. 108

[131] K. Deb, A. Pratap, S. Agarwal, and T. Meyarivan, "A fast and elitist multiobjective genetic algorithm: Nsga-ii," *IEEE Transactions on Evolutionary Computation*, vol. 6, no. 2, pp. 182–197, 2002. 114

[132] K. Deb, L. Thiele, M. Laumanns, and E. Zitzler, "Scalable test problems for evolutionary multiobjective optimization," in *Evolutionary Multiobjective Optimization: Theoretical Advances and Applications*. Springer, 2005, pp. 105–145. 114

[133] C. A. C. Coello, G. B. Lamont, and D. A. V. Veldhuizen, *Evolutionary Algorithms for Solving Multi-Objective Problems*. Springer, 2007. 114

[134] N. K. Jain, U. Nangia, and A. Jain, "Pso for multiobjective economic load dispatch (meld) for minimizing generation cost and transmission losses,"

turnitin Page 201 of 208 - Integrity Submission Submission ID trn:oid:::27535:142293373

Journal of The Institution of Engineers (India): Series B, vol. 97, pp. 185–191, 2016. 122

[135] M. Zeleny, *Multiple Criteria Decision Making*. New York: McGraw-Hill, 1982. 123

turnitin Page 203 of 208 - Integrity Submission Submission ID trn:oid:::27535:142293373

Appendix A

Supplementary Data

Table A.1: Benchmark functions considered for performance evaluation.

Mathematical Expression	Range	Dimension	$F_{\min}$
Unimodal Functions			
$f_1(x) = \sum_{i=1}^{d} x_i^2$	$[-100, 100]$	30	0
$f_2(x) = \sum_{i=1}^{d} \lvert x_i \rvert + \prod_{i=1}^{d} \lvert x_i \rvert$	$[-10, 10]$	30	0
$f_3(x) = \sum_{i=1}^{d} \left(\sum_{j=1}^{i} x_j \right)^2$	$[-100, 100]$	30	0
$f_4(x) = \max \{ \lvert x_i \rvert, 1 \leq i \leq d \}$	$[-100, 100]$	30	0
$f_5(x) = \sum_{i=1}^{d-1} \left[100(x_{i+1} - x_i^2)^2 + (x_i - 1)^2 \right]$	$[-30, 30]$	30	0
$f_6(x) = \sum_{i=1}^{d} (\lvert x_i + 0.5 \rvert)^2$	$[-100, 100]$	30	0
$f_7(x) = \sum_{i=1}^{d} i x_i^4 + \text{rand}$	$[-1.28, 1.28]$	30	0
Multimodal Functions			
$f_8(x) = \sum_{i=1}^{d} -x_i \sin \left(\sqrt{\lvert x_i \rvert} \right)$	$[-500, 500]$	30	-12569.5
$f_9(x) = \sum_{i=1}^{d} \left[x_i^2 - 10 \cos(2\pi x_i) + 10 \right]$	$[-5.12, 5.12]$	30	0
$f_{10}(x) = -20 \exp \left(-0.2 \sqrt{\frac{1}{d} \sum_{i=1}^{d} x_i^2} \right) - \exp \left(\frac{1}{d} \sum_{i=1}^{d} \cos(2\pi x_i) \right) + 20 + e$	$[-32, 32]$	30	0
$f_{11}(x) = \frac{1}{4000} \sum_{i=1}^{d} x_i^2 - \prod_{i=1}^{d} \cos \left(\frac{x_i}{\sqrt{i}} \right) + 1$	$[-600, 600]$	30	0

turnitin Page 203 of 208 - Integrity Submission Submission ID trn:oid:::27535:142293373

Mathematical Expression	Range	Dimension	$F_{\min}$
$f_{12}(x) = \frac{\pi}{d}\left\{10\sin^2(\pi y_1) + \sum_{i=1}^{d-1}(y_i-1)^2 \times \left[1+10\sin^2(\pi y_{i+1})\right] + (y_d-1)^2\right\} + \sum_{i=1}^{d} u(x_i,5,100,4)$	$[-50,50]$	30	0
Where, $y_i = 1+\frac{x_i+1}{4}$, $u(x_i,a,k,m) = \begin{cases} k(x_i-a)^m, & x_i > a \\ 0, & -a < x_i < a \\ k(-x_i-a)^m, & x_i < -a \end{cases}$ $f_{13}(x) = \sin^2(3\pi x_1) + \sum_{i=1}^{d-1}(x_i-1)^2 \times \left[1+\sin^2(3\pi x_i+1)\right] + (x_d-1)^2\left[1+\sin^2(2\pi x_d)\right] + \sum_{i=1}^{d} u(x_i,5,100,4)$	$[-50,50]$	30	0

Table A.2: IEEE 30 bus system generator data for various cases (Including solar, wind & hybrid).

Bus No.	P_{Max} (MW)	P_{Min} (MW)	Q_{Max} (MVAr)	Q_{Min} (MVAr)	P_G (Case 1,2,3) (MW)	P_G (Case 7,8,9) (MW)
1	200	50	150	-20	Swing	Swing
2	80	20	60	-20	80	80
5	50	15	62.5	-15	50	50
5 (Wind)	75	0	35	-30	–	Variable
8	35	10	48.7	-15	20	20
8 (Solar)	50	0	25	-20	–	Variable
11	30	10	40	-10	20	20
13	40	12	44.7	-15	20	20
13 (Hybrid)	50	0	25	-20	–	Variable

turnitin Page 205 of 208 - Integrity Submission Submission ID trn:oid:::27535:142293373

Table A.3: IEEE 57 bus system generator data for various cases.

Bus No.	P_{Max} (MW)	P_{Min} (MW)	Q_{Max} (MVAr)	Q_{Min} (MVAr)	P_G (Case 4,5,6) (MW)
1	576	0	200	-140	Swing
2	100	30	50	-17	0
3	140	40	60	-10	40
6	100	30	25	-8	0
8	550	100	200	-140	450
9	100	30	9	-3	0
12	410	100	155	-150	310

Table A.4: IEEE 30 bus system generator data for various cases (Including solar).

Bus No.	P_{Max} (MW)	P_{Min} (MW)	Q_{Max} (MVAr)	Q_{Min} (MVAr)	P_G (Case 1,2,3) (MW)	P_G (Case 4,5,6) (MW)
1	200	50	150	-20	Swing	Swing
2	80	20	60	-20	80	80
5	50	15	62.5	-15	50	50
8	35	10	48.7	-15	20	20
8 (Solar)	50	0	25	-20	–	Variable
11	30	10	40	-10	20	20
13	40	12	44.7	-15	20	20

Table A.5: IEEE 118 bus system generator data.

Bus No.	P_{Max} (MW)	P_{Min} (MW)	Q_{Max} (MVAr)	Q_{Min} (MVAr)	P_G (Case 7,8,9) (MW)
1	100	0	15	-5	0
4	100	0	300	-300	0
6	100	0	50	-13	0
8	100	0	300	-300	0
10	550	0	200	-147	450
12	185	0	120	-35	85
15	100	0	30	-10	0
18	100	0	50	-16	0
19	100	0	24	-8	0

22

turnitin Page 205 of 208 - Integrity Submission Submission ID trn:oid:::27535:142293373

170

Bus No.	P_{Max} (MW)	P_{Min} (MW)	Q_{Max} (MVAr)	Q_{Min} (MVAr)	P_G (Case 7,8,9) (MW)
24	100	0	300	-300	0
25	320	0	140	-47	220
26	414	0	1000	-1000	314
27	100	0	300	-300	0
31	107	0	300	-300	7
32	100	0	42	-14	0
34	100	0	24	-8	0
36	100	0	24	-8	0
40	100	0	300	-300	0
42	100	0	300	-300	0
46	119	0	100	-100	19
49	304	0	210	-85	204
54	148	0	300	-300	48
55	100	0	23	-8	0
56	100	0	15	-8	0
59	255	0	180	-60	155
61	260	0	300	-100	160
62	100	0	20	-20	0
65	491	0	200	-67	391
66	492	0	200	-67	392
69	805.2	0	300	-300	Swing
70	100	0	32	-10	0
72	100	0	100	-100	0
73	100	0	100	-100	0
74	100	0	9	-6	0
76	100	0	23	-8	0
77	100	0	70	-20	0
80	577	0	280	-165	477
85	100	0	23	-8	0
87	104	0	1000	-100	4
89	707	0	300	-210	607
90	100	0	300	-300	0
91	100	0	100	-100	0
92	100	0	9	-3	0
99	100	0	100	-100	0

turnitin Page 207 of 208 - Integrity Submission Submission ID trn:oid:::27535:142293373

Bus No.	P_{Max} (MW)	P_{Min} (MW)	Q_{Max} (MVAr)	Q_{Min} (MVAr)	P_G (Case 7,8,9) (MW)
100	352	0	155	-50	252
103	140	0	40	-15	40
104	100	0	23	-8	0
105	100	0	23	-8	0
107	100	0	200	-200	0
110	100	0	23	-8	0
111	136	0	1000	-100	36
112	100	0	1000	-100	0
113	100	0	200	-100	0
116	100	0	1000	-1000	0

Table A.6: Mathematical formulation of multi-objective benchmark test functions.

Function	Mathematical Formulation	Dim	Range
ZDT1	$F_1 = x_1$ $F_2 = g(x)\left(1 - \sqrt{\frac{F_1}{g(x)}}\right)$ $g(x) = 1 + \frac{9}{D-1}\sum_{i=2}^{D} x_i$	30	$x_i \in [0,1]$
ZDT2	$F_1 = x_1$ $F_2 = g(x)\left(1 - \left(\frac{F_1}{g(x)}\right)^2\right)$ $g(x) = 1 + \frac{9}{D-1}\sum_{i=2}^{D} x_i$	30	$x_i \in [0,1]$
ZDT3	$F_1 = x_1$ $F_2 = g(x)\left(1 - \sqrt{\frac{F_1}{g(x)}} - \frac{F_1}{g(x)}\sin(10\pi F_1)\right)$ $g(x) = 1 + \frac{9}{D-1}\sum_{i=2}^{D} x_i$	30	$x_i \in [0,1]$

turnitin Page 207 of 208 - Integrity Submission Submission ID trn:oid:::27535:142293373

172

Function	Mathematical Formulation	Dim	Range
ZDT4	$F_1 = x_1$ $F_2 = g(x)\left(1-\sqrt{\frac{F_1}{g(x)}}\right)$ $g(x) = 1+10(D-1)$ $+\sum_{i=2}^{D}\left[x_i^2 - 10\cos(4\pi x_i)\right]$	10	$x_1 \in [0,1]$ $x_i \in [-5,5]$
ZDT6	$F_1 = 1-\exp(-4x_1)\sin^6(6\pi x_1)$ $F_2 = g(x)\left(1-\left(\frac{F_1}{g(x)}\right)^2\right)$ $g(x) = 1+9\left(\frac{1}{D-1}\sum_{i=2}^{D}x_i\right)^{0.25}$	10	$x_i \in [0,1]$
DTLZ2	$F_1 = (1+g)\cos\left(\frac{\pi}{2}x_1\right)\cos\left(\frac{\pi}{2}x_2\right)$ $F_2 = (1+g)\cos\left(\frac{\pi}{2}x_1\right)\sin\left(\frac{\pi}{2}x_2\right)$ $F_3 = (1+g)\sin\left(\frac{\pi}{2}x_1\right)$ $g(x) = \sum_{i=3}^{D}(x_i-0.5)^2$	12	$x_i \in [0,1]$
DTLZ4	$F_1 = (1+g)\cos\left(\frac{\pi}{2}x_1^{\alpha}\right)\cos\left(\frac{\pi}{2}x_2^{\alpha}\right)$ $F_2 = (1+g)\cos\left(\frac{\pi}{2}x_1^{\alpha}\right)\sin\left(\frac{\pi}{2}x_2^{\alpha}\right)$ $F_3 = (1+g)\sin\left(\frac{\pi}{2}x_1^{\alpha}\right)$ $g(x) = \sum_{i=3}^{D}(x_i-0.5)^2$	12	$x_i \in [0,1]$